

Exploring the diversity and productivity of clonal Chinese hamster ovary host cell lines derived from a non-clonal population

A thesis submitted to the University of Manchester for the degree of
Doctor of Philosophy in the Faculty of Life Sciences

2015

Andrew Richard Jeavons

Table of contents

| | |
|--|-----------|
| TABLE OF CONTENTS | 2 |
| LIST OF FIGURES | 7 |
| LIST OF TABLES | 10 |
| ABSTRACT | 11 |
| DECLARATION | 12 |
| COPYRIGHT STATEMENT | 12 |
| ACKNOWLEDGEMENTS | 13 |
| DEDICATION | 13 |
| ABBREVIATIONS | 14 |
| 1. INTRODUCTION | 18 |
| 1.1 Biopharmaceuticals | 19 |
| 1.1.1 Biopharmaceuticals: Today and tomorrow | 19 |
| 1.1.1.1 Recombinant proteins | 20 |
| 1.1.1.2 Monoclonal antibodies..... | 20 |
| 1.1.1.3 Hybrids and novel-format antibodies | 24 |
| 1.2 Expression systems for biopharmaceutical production | 26 |
| 1.2.1 History of the CHO cell line..... | 28 |
| 1.2.2 Generation of clonal recombinant transfectants | 29 |
| 1.2.3 Selection system..... | 31 |
| 1.3 Cell line variability | 33 |
| 1.3.1 Effects of phenotype and culture environment | 33 |
| 1.3.2 Phenotypic drift..... | 36 |
| 1.3.3 Mutator phenotype..... | 38 |
| 1.4 The use of metabolic profiling to define phenotype | 41 |
| 1.4.1 Metabolomic techniques | 41 |
| 1.4.2 The metabolic phenotype | 43 |
| 1.5 Aims and objectives | 46 |
| 2. MATERIALS AND METHODS | 48 |
| 2.1 Materials and equipment | 49 |
| 2.1.1 Sources of chemicals, reagents and equipment..... | 49 |
| 2.1.2 Preparation and sterilisation of solutions | 49 |
| 2.1.3 pH measurements | 49 |

| | |
|---|-----------|
| 2.2 Generation and purification of plasmids in bacterial cells | 49 |
| 2.2.1 Bacterial growth medium | 49 |
| 2.2.2 Transformation of Z-competent <i>E. coli</i> cells | 49 |
| 2.2.3 Extraction of plasmid DNA..... | 50 |
| 2.2.4 Linearisation, phase lock gel extraction (PLG) and ethanol precipitation of plasmid DNA | 50 |
| 2.2.5 Determination of nucleic acid concentration | 51 |
| 2.2.6 Preparation of glycerol stocks..... | 51 |
| 2.3 Mammalian cell culture | 51 |
| 2.3.1 Revival from liquid nitrogen | 51 |
| 2.3.2 Maintenance of cell lines | 51 |
| 2.3.3 Batch and fed-batch culture..... | 52 |
| 2.3.4 Determination of cell number and viability | 52 |
| 2.3.5 Sonata cell culture | 52 |
| 2.3.6 Cryopreservation of cells | 52 |
| 2.3.7 Nucleofection of host cell lines | 53 |
| 2.3.8 Generation of polyclonal pools | 53 |
| 2.3.9 Generation of clonal transfectants | 53 |
| 2.4 Metabolite analysis | 54 |
| 2.4.1 Glucose, lactate, glutamine and glutamate analysis..... | 54 |
| 2.4.2 Gas chromatography-mass spectrometry (GC-MS) | 54 |
| 2.4.2.1 Sample preparation and derivitisation | 54 |
| 2.4.2.2 Sample injection | 55 |
| 2.4.2.3 Gas chromatography..... | 55 |
| 2.4.2.4 Mass spectrometry | 55 |
| 2.4.2.5 Data processing | 55 |
| 2.5 Protein analysis | 56 |
| 2.5.1 Analysis of mAb titre | 56 |
| 2.5.2 Western blot analysis..... | 56 |
| 2.5.2.1 Protein extraction | 56 |
| 2.5.2.2 Bradford assay | 56 |
| 2.5.2.3 SDS-PAGE..... | 57 |
| 2.5.2.4 Protein transfer..... | 57 |
| 2.5.2.5 Antibody probing and detection..... | 57 |
| 2.5.2.6 Densitometric analysis | 58 |
| 2.5.3 GS activity assay | 58 |
| 2.6 Isolation, handling and analysis of RNA/DNA..... | 59 |

| | |
|---|------------|
| 2.6.1 mRNA analysis | 59 |
| 2.6.1.1 Trizol mRNA extraction | 59 |
| 2.6.1.2 DNase treatment of mRNA..... | 59 |
| 2.6.1.3 Qiagen RNeasy Plus Mini Kit mRNA extraction | 60 |
| 2.6.1.4 cDNA synthesis | 60 |
| 2.6.1.5 PCR to verify primer design | 61 |
| 2.6.1.6 Agarose gel electrophoresis..... | 61 |
| 2.6.1.7 qRT-PCR for mRNA analysis | 62 |
| 2.6.2 Recombinant gene copy number analysis..... | 63 |
| 2.6.2.1 Genomic DNA extraction..... | 63 |
| 2.6.2.2 qRT-PCR for gene copy number analysis..... | 63 |
| 2.7 Flow cytometry..... | 64 |
| 2.7.1 Molecular probe labelling..... | 64 |
| 2.7.2 Flow cytometric analysis..... | 65 |
| 2.8 Microscopy | 65 |
| 2.8.1 Preparation of metaphase spreads..... | 65 |
| 2.8.2 Metaphase staining..... | 66 |
| 2.8.3 Image acquisition and analysis..... | 66 |
| 2.9 Statistical methods | 66 |
| 2.10 Calculations..... | 67 |
| 2.10.1 Calculation of average cell growth day^{-1} | 67 |
| 2.10.2 Calculation of cumulative cell time (CCT)..... | 68 |
| 2.10.3 Calculation of cell doubling time | 68 |
| 2.10.4 Calculation of specific productivity (Q_p) and rates of metabolite production and utilisation..... | 69 |
| 3. ANALYSIS OF THE PHENOTYPIC VARIABILITY OF CLONAL HOST CELL LINES DERIVED FROM A NON-CLONAL POPULATION | 70 |
| 3.1 Introductory remarks..... | 71 |
| 3.2 Analysis of growth characteristics of the clonal host cell lines | 71 |
| 3.2.1 Analysis of growth characteristics during long-term culture..... | 71 |
| 3.2.2 Analysis of early and late generation host cell line growth characteristics during batch culture | 81 |
| 3.3 Analysis of nutrient utilisation | 87 |
| 3.4 Analysis of endogenous glutamine synthetase..... | 100 |
| 3.4.1 Analysis of variability in endogenous glutamine synthetase..... | 100 |

| | |
|--|------------|
| 3.4.2 The effect of glutamine-free culture on growth and endogenous glutamine synthetase | 104 |
| 3.5 Analysis of mitochondrial membrane potential..... | 110 |
| 3.6 Summary..... | 114 |
| 4. DETERMINATION OF PHENOTYPIC VARIABILITY AND HERITABILITY OF TRANSFECTANTS DERIVED FROM CLONAL HOST CELL LINES..... | 115 |
| 4.1 Introductory remarks..... | 116 |
| 4.2 Transfection with mAb-109 plasmid and generation of stable transfectants ... | 118 |
| 4.2.1 Round 1: Analysis of growth and productivity characteristics of polyclonal pools in batch and fed-batch culture | 118 |
| 4.2.2 Round 2: Analysis of growth and productivity characteristics of polyclonal pools in batch and fed-batch culture | 128 |
| 4.2.3 Generation and productivity analysis of clonal transfectants..... | 134 |
| 4.3 Characterisation of clonal transfectants derived from clonal host cell line 15 and 19 | 139 |
| 4.3.1 Analysis of transfectant growth characteristics during long-term culture..... | 139 |
| 4.3.2 Analysis of early and late generation transfectant growth and productivity during fed-batch culture | 143 |
| 4.3.3 Analysis of recombinant mAb-109 mRNA expression | 149 |
| 4.3.4 Analysis of nutrient utilisation by early and late generation transfectants | 152 |
| 4.3.5 Analysis of early and late generation transfectant glutamine synthetase | 157 |
| 4.4 Summary..... | 159 |
| 5. MOLECULAR AND METABOLIC PROFILING TO IDENTIFY INDICATORS OF HIGH PRODUCTIVITY | 160 |
| 5.1 Introductory remarks..... | 161 |
| 5.2 Characterisation of high and low producing transfectants | 162 |
| 5.2.1 Growth and mAb titre analysis of high and low producing transfectants | 162 |
| 5.2.2 Chromosome numbers of high and low producing transfectants..... | 168 |
| 5.2.3 Recombinant gene copy number analysis of high and low producing transfectants | 171 |
| 5.2.4 Analysis of mitochondrial membrane potential in high and low producing transfectants | 174 |
| 5.3 Metabolite profiling of high and low producing transfectants | 176 |
| 5.3.1 Glycolysis..... | 180 |
| 5.3.2 Citric acid cycle intermediates | 188 |
| 5.3.3 Amino acids and derivatives | 194 |

| | |
|---|------------|
| 5.3.4 Lipid synthesis | 201 |
| 5.4 Summary..... | 206 |
| 6. OVERALL DISCUSSION | 207 |
| 6.1 Overall Discussion..... | 208 |
| 6.2 Phenotypic variability of clonally derived host cell lines. | 210 |
| 6.2.1 Do clonally derived CHO host cell lines display inter-clonal variability? | 211 |
| 6.2.2 Do clonal host cell lines give rise to transfectants that display less phenotypic variability than the non-clonal host cell line? | 213 |
| 6.2.3 What defines the phenotype of a cell line and is it stable? | 213 |
| 6.3 Are phenotypic features of the host cell line heritable? | 215 |
| 6.4 Can metabolic markers be identified that relate to productivity? | 218 |
| 6.5 Future work | 219 |
| REFERENCES | 221 |
| APPENDICES | 238 |
| Appendix A – List of materials, equipment and suppliers..... | 239 |
| Appendix B – Host cell line lactate:glucose ratio..... | 252 |
| Appendix C – Analysis of transfection round 2 pool kill curves..... | 253 |
| Appendix D – Linear regression analysis of clonal transfectant mAb production from 96-well and 24-well static plate culture | 255 |
| Appendix E – Verification of primer specificity and efficiency | 257 |
| Appendix F – Comparison of enzymatic and GC-MS metabolite data..... | 260 |

Word count: 60,784

List of figures

| | |
|--|-----|
| Figure 1.1 The structure of immunoglobulin G (IgG) | 23 |
| Figure 1.2 The CHO cell lineage..... | 29 |
| Figure 1.3 The enzyme reactions used as selection systems in CHO cell culture | 32 |
| Figure 1.4 Accumulation of genetic error in CHO cell lineages in relation to a mutator phenotype | 40 |
| Figure 1.5 Derivatisation and ionisation of metabolites during GC-MS analysis | 43 |
| Figure 3.1 Analysis of host cell line growth during continuous LTC..... | 74 |
| Figure 3.2 Analysis of host cell line diameter during continuous LTC | 78 |
| Figure 3.3 Comparison of early and late generation host cell line growth parameters in batch culture | 84 |
| Figure 3.4 Analysis of glucose and lactate concentrations during batch culture in response to LTC | 89 |
| Figure 3.5 Analysis of glucose and lactate utilisation rates during batch culture in response to LTC | 91 |
| Figure 3.6 Analysis of glutamine and glutamate concentrations during batch culture in response to LTC | 96 |
| Figure 3.7 Analysis of glutamine and glutamate utilisation rates during batch culture in response to LTC | 98 |
| Figure 3.8 Analysis of glutamine synthetase in host cell lines during continuous LTC... | 102 |
| Figure 3.9 Effect of glutamine-free culture on host cell line growth | 106 |
| Figure 3.10 Host cell lines upregulate glutamine synthetase protein expression in response to glutamine-free culture | 108 |
| Figure 3.11 Analysis of mitochondrial membrane potential using rhodamine-123 and MitoTracker Green FM..... | 112 |
| Figure 4.1 Flow diagram of transfection process | 117 |
| Figure 4.2 Growth parameters of pools from transfection round 1 in batch culture | 121 |
| Figure 4.3 Growth parameters of pools from transfection round 1 in fed-batch culture.. | 123 |
| Figure 4.4 Analysis of mAb production of pools from transfection round 1 in batch and fed-batch culture | 125 |
| Figure 4.5 Growth parameters and mAb production of pools from transfection round 2 grown in batch and fed-batch culture..... | 131 |
| Figure 4.6 Analysis of clonal transfectant mAb production from 96-well and 24-well plates | 136 |
| Figure 4.7 Analysis of transfectant growth rate and diameter during LTC..... | 141 |

| | |
|---|-----|
| Figure 4.8 Comparison of early and late generation transfectant growth parameters in fed-batch culture | 145 |
| Figure 4.9 Comparison of early and late generation transfectant mAb production in fed-batch culture | 147 |
| Figure 4.10 Analysis of mAb mRNA expression in early generation transfectants..... | 150 |
| Figure 4.11 Analysis of glucose and lactate utilisation rates in early and late generation transfectants during fed-batch culture..... | 154 |
| Figure 4.11 Analysis of glutamine and glutamate utilisation rates in early and late generation transfectants during fed-batch culture..... | 156 |
| Figure 4.12 Analysis of glutamine synthetase activity and mRNA expression in early and late generation transfectants..... | 158 |
| Figure 5.1 Analysis of growth of host cell lines, high and low producing transfectants growth parameters in batch and fed-batch culture..... | 164 |
| Figure 5.2 Analysis of mAb production from high and low producing transfectants in fed-batch culture | 166 |
| Figure 5.3 Metaphase spreads of host cell lines and transfectants | 169 |
| Figure 5.4 Recombinant gene copy number analysis of high and low producing transfectants | 173 |
| Figure 5.5 Analysis of mitochondrial membrane potential in high and low producing transfectants | 175 |
| Figure 5.6 Manual correction of compound identification in Chemstation | 177 |
| Figure 5.7 Central carbon metabolism of CHO cells..... | 179 |
| Figure 5.8 Analysis of extracellular glycolysis-associated metabolites for early generation cell line 15 transfectants during fed-batch culture..... | 184 |
| Figure 5.9 Analysis of extracellular glycolysis-associated metabolites for late generation cell line 15 transfectants during fed-batch culture..... | 185 |
| Figure 5.10 Analysis of extracellular glycolysis-associated metabolites for early generation cell line 19 transfectants during fed-batch culture..... | 186 |
| Figure 5.11 Analysis of intracellular glycolysis-associated metabolites for early and late generation cell line 15 and 19 transfectants during fed-batch culture..... | 187 |
| Figure 5.12 Analysis of extracellular citric acid cycle intermediates for early generation cell line 15 transfectants during fed-batch culture | 190 |
| Figure 5.13 Analysis of extracellular citric acid cycle intermediates for late generation cell line 15 transfectants during fed-batch culture | 191 |
| Figure 5.14 Analysis of extracellular citric acid cycle intermediates for early generation cell line 19 transfectants during fed-batch culture | 192 |

| | |
|---|-----|
| Figure 5.15 Analysis of intracellular citric acid cycle intermediates for early and late generation cell line 15 and 19 transfectants during fed-batch culture..... | 193 |
| Figure 5.16 Analysis of extracellular amino acids and derivatives for early generation cell line 15 transfectants during fed-batch culture | 197 |
| Figure 5.17 Analysis of extracellular amino acids and derivatives for late generation cell line 15 transfectants during fed-batch culture | 198 |
| Figure 5.18 Analysis of extracellular amino acids and derivatives for early generation cell line 19 transfectants during fed-batch culture | 199 |
| Figure 5.19 Analysis of intracellular amino acids and derivatives for early and late generation cell line 15 and 19 transfectants during fed-batch culture..... | 200 |
| Figure 5.20 Analysis of extracellular lipid-associated metabolites for early generation cell line 15 transfectants during fed-batch culture | 202 |
| Figure 5.21 Analysis of extracellular lipid-associated metabolites for late generation cell line 15 transfectants during fed-batch culture | 203 |
| Figure 5.22 Analysis of extracellular lipid-associated metabolites for early generation cell line 19 transfectants during fed-batch culture | 204 |
| Figure 5.23 Analysis of intracellular lipid-associated metabolites for early and late generation cell line 15 and 19 transfectants during fed-batch culture..... | 205 |
| Figure AB.1 – Ratio of lactate production rate to glucose consumption rate during batch culture in response to LTC..... | 252 |
| Figure AC.1 Analysis of transfection round 2 pool kill curves..... | 253 |
| Figure AD.1 Linear regression analysis of clonal transfectant mAb production from 96-well and 24-well static plate culture..... | 255 |
| Figure AE.1 Agarose gel electrophoresis of PCR products from mAb-109 primers | 257 |
| Figure AE.2 Agarose gel electrophoresis of PCR products from gene copy number analysis primers | 258 |
| Figure AF.1 Comparison of enzymatic and GC-MS glucose data from high and low producing transfectants..... | 260 |
| Figure AF.2 Comparison of enzymatic and GC-MS lactate data from high and low producing transfectants..... | 262 |
| Figure AF.3 Comparison of enzymatic and GC-MS glutamine data from high and low producing transfectants..... | 264 |
| Figure AF.4 Comparison of enzymatic and GC-MS glutamate data from high and low producing transfectants..... | 266 |

List of tables

| | |
|--|-----|
| Table 1.1 Antibody and hybrid biopharmaceuticals approved between 1986 and 2014... | 25 |
| Table 2.1 Antibodies used for Western blot | 58 |
| Table 2.2 Primers used for mRNA analysis | 62 |
| Table 2.3 Primers used for gene copy number analysis..... | 64 |
| Table 3.1 Analysis of host cell line growth during continuous LTC..... | 76 |
| Table 3.2 Analysis of host cell line diameter during continuous LTC..... | 80 |
| Table 3.3 Analysis of early and late generation host cell line growth parameters in batch culture | 86 |
| Table 3.4 Ratio of lactate production rate to glucose consumption rate during batch culture in response to LTC..... | 93 |
| Table 4.1 Analysis of growth parameters and specific productivity of pools from transfection round 1 grown in batch and fed-batch culture | 127 |
| Table 4.2 Analysis of growth parameters and specific productivity of pools from transfection round 2 grown in batch and fed-batch culture | 133 |
| Table 4.3 24-well plate, day 11 static titre of transfectants adapted to shake culture..... | 138 |
| Table 4.4 Analysis of early and late generation transfectant growth parameters and specific productivity in fed-batch culture | 148 |
| Table 4.5 Ratio of lactate production rate to glucose consumption rate in early and late generation transfectants during fed-batch culture..... | 155 |
| Table 5.1 Analysis of growth and specific productivity of host cell lines, high and low producing transfectants in batch and fed-batch culture | 167 |
| Table 5.2 Analysis of chromosome number of host cell lines, high and low producing transfectants | 170 |
| Table AE.1 Efficiency of PCR primers for qRT-PCR analysis of mAb-109 mRNA expression..... | 257 |
| Table AE.2 Efficiency of PCR primers for qRT-PCR analysis of gene copy number..... | 259 |

Abstract

Abstract for a PhD in Biotechnology thesis submitted in September 2015 at the University of Manchester by Andrew Richard Jeavons titled “Exploring the diversity and productivity of clonal Chinese hamster ovary host cell lines derived from a non-clonal population”

Chinese hamster ovary (CHO) cell lines are the most frequently used mammalian host for commercial production of recombinant protein-based biopharmaceuticals. Heterogeneity and phenotypic drift in CHO populations is well established, thus production cell lines must be clonally derived to help ensure product purity and homogeneity. A vast range of engineering strategies has been employed to improve the bioprocessing capabilities of CHO cell lines and decrease production costs, although these strategies have yielded mixed results. The use of clonally derived host CHO cell lines, may allow exploitation of the genetic and phenotypic variability in parental populations for the discovery of new hosts with desirable, heritable characteristics. Furthermore, in-depth characterisation of phenotypic diversity may assist in the development of tools and molecular markers to rapidly identify a desirable cell line.

A panel of clonally derived host CHO cell lines and the non-clonal parental population were investigated to determine their phenotypic variability, and their ability to produce transfectants with predictable characteristics. Significant differences were identified in the growth profiles and proliferative capacity of the host cell lines, in addition to their nutrient utilisation, endogenous protein expression and mitochondrial membrane potential. Transfection of the host cell lines did not suggest that the use of clonal host cell lines produces transfectants with less phenotypic variability than transfectants derived from a non-clonal population. However, transfectant population averages suggested that a ‘toolbox’ of host cell lines could be developed, in which specific hosts may improve the probability of isolating transfectants with a desired phenotype.

Rhodamine-123 (Rh-123) staining and flow cytometric analysis of host cell lines identified interclonal variability in mitochondrial membrane potential. Extending this approach to transfectants suggested this is a heritable property of CHO cell lines, which correlates with growth rate, and the glucose and lactate utilisation of the host cell line. Rh-123 could serve as a tool for rapid screening of prospective host cell lines, without the need for scale-up and batch culture. Furthermore, gas chromatography-mass spectrometry (GC-MS) metabolomic analysis of transfectants, with high productivity and low productivity, identified novel metabolites which may be linked to the productivity phenotype.

This study has shown that the diversity of CHO populations can be utilised to isolate novel host cell lines with different phenotypes that are desirable for biopharmaceutical production. This approach has the potential to increase production yields and decrease biopharmaceutical production costs without the need for cell line engineering.

Declaration

No portion of the work referred to in the thesis has been submitted in support of an application for another degree or qualification of this or any other university or other institute of learning.

Copyright statement

- I. The author of this thesis (including any appendices and/or schedules to this thesis) owns certain copyright or related rights in it (the "Copyright") and s/he has given The University of Manchester certain rights to use such Copyright, including for administrative purposes.
- II. Copies of this thesis, either in full or in extracts and whether in hard or electronic copy, may be made **only** in accordance with the Copyright, Designs and Patents Act 1988 (as amended) and regulations issued under it or, where appropriate, in accordance with licensing agreements which the University has from time to time. This page must form part of any such copies made.
- III. The ownership of certain Copyright, patents, designs, trade marks and other intellectual property (the "Intellectual Property") and any reproductions of copyright works in the thesis, for example graphs and tables ("Reproductions"), which may be described in this thesis, may not be owned by the author and may be owned by third parties. Such Intellectual Property and Reproductions cannot and must not be made available for use without the prior written permission of the owner(s) of the relevant Intellectual Property and/or Reproductions.
- IV. Further information on the conditions under which disclosure, publication and commercialisation of this thesis, the Copyright and any Intellectual Property and/or Reproductions described in it may take place is available in the University IP Policy (see <http://documents.manchester.ac.uk/DocuInfo.aspx?DocID=487>), in any relevant Thesis restriction declarations deposited in the University Library, The University Library's regulations (see <http://www.manchester.ac.uk/library/aboutus/regulations>) and in The University's policy on Presentation of Theses

Acknowledgements

I would like to thank the many people who have helped me during the course of my PhD. Foremost, I'd like to thank my supervisors Alan Dickson, Diane Hatton and Sarah Milne for their support and guidance. Their continuous advice during my research, motivation and patience during writing were invaluable.

I would like to acknowledge my colleagues at MedImmune, in particular Amanda Lewis who offered great advice and support. I'm grateful for help from Gareth Lewis, Rahul Pradhan for their help and support. Also, I would like to show appreciation to Colin Glover for his valuable assistance with qRT-PCR.

I wish to express my gratitude to my advisor Mark Ashe for his encouragement and insightful comments. I am thankful to all the members of lab B.2075 for their support and friendship. I am grateful for help from Annes Lambert with automated cell culture and Mark Elvin for his assistance with GC-MS. I would also like to thank Eric Chang for his friendship and "Corner".

I am very grateful for funding from the BBSRC and MedImmune.

Dedication

I would like to dedicate my thesis to my family, who have always been there with love and support.

Abbreviations

| | |
|-------------------------------|------------------------------------|
| ANOVA | analysis of variance |
| B2M | β_2 microglobulin |
| BHK | baby hamster kidney |
| BSA | bovine serum albumin |
| <i>C. griseus</i> | <i>Cricetulus griseus</i> |
| CCT | cumulative cell line |
| cDNA | complementary DNA |
| CDR | complementarity-determining region |
| C_H^1 , C_H^2 and C_H^3 | heavy chain – constant domains |
| CHO | Chinese hamster ovary |
| C_L | light chain – constant domain |
| DAPI | 4',6-diamidino-2-phenylindole |
| DEPC | diethylpyrocarbonate |
| DHFR | dihydrofolate reductase |
| DMSO | dimethylsulphoxide |
| DNA | deoxyribonucleic acid |
| E | early (generation cell line) |
| <i>E. coli</i> | <i>Escherichia coli</i> |
| EDTA | ethylenediaminetetraacetic acid |
| EI | electron impact |

| | |
|-------|---|
| ESI | electrospray ionisation |
| Fab | fragment antibody binding |
| Fc | fraction crystallisable |
| G3P | glycerol-3-phosphate |
| GAP | glyceraldehyde 3-phosphate |
| GC-MS | gas chromatography-mass spectrometry |
| gDNA | genomic DNA |
| GS | glutamine synthetase |
| HACA | human anti-chimeric antibody |
| HAHA | human anti-human antibody |
| HAMA | human anti-mouse antibody |
| HC | heavy chain |
| hPC | human pyruvate carboxylase |
| HSP | heat shock protein |
| IgG | immunoglobulin G |
| L | late (generation cell line) |
| L | molecular weight marker |
| LC | light chain |
| LC-MS | liquid chromatography-mass spectrometry |
| LDH-A | lactate dehydrogenase-A |
| LTC | long-term culture |

| | |
|-------|---|
| M | medium |
| mAb | monoclonal antibody |
| MFI | median fluorescence intensity |
| MOX | methoxyamine hydrochloride |
| MPER | Mammalian Protein Extraction Reagent |
| mRNA | messenger RNA |
| MSTFA | N-methyl-N-(trimethylsilyl)trifluoroacetamide |
| MSX | methionine sulfoximine |
| mtDNA | mitochondrial DNA |
| MTG | MitoTracker Green FM |
| MTX | methotrexate |
| NC | non-clonal |
| NMR | nuclear magnetic resonance |
| NTC | no template control |
| PBS | phosphate buffered saline |
| PCR | polymerase chain reaction |
| PI | propidium iodide |
| PLG | phase lock gel |
| PTM | post-translational modification |
| Q | quarter |
| Qp | specific productivity |

| | |
|----------------------|--|
| qRT-PCR | quantitative real-time polymerase chain reaction |
| r | correlation coefficient |
| r ² | coefficient of determination |
| Rh-123 | rhodamine-123 |
| RNA | ribonucleic acid |
| RT | reverse transcriptase |
| <i>S. cerevisiae</i> | <i>Saccharomyces cerevisiae</i> |
| SD | standard deviation |
| SEM | standard error of the mean |
| siRNA | small interfering RNA |
| TCMS | trichloromethylsilane |
| TNF | tumour necrosis factor |
| tPA | tissue plasminogen activator |
| UCOE | ubiquitous chromatin opening element |
| VCD | viable cell density |
| VCD _{max} | maximum viable cell density |
| V _H | heavy chain – variable domain |
| V _L | light chain – variable domain |

1. Introduction

1.1 Biopharmaceuticals

1.1.1 Biopharmaceuticals: Today and tomorrow

What are biopharmaceuticals? In 2002 Gary Walsh provided a definition of that a biopharmaceutical was “a protein- or nucleic acid-based pharmaceutical substance used for therapeutic or in vivo diagnostic purposes, which is produced by means other than direct extraction from a native (non-engineered) biological source” (Walsh 2002).

Protein-based biopharmaceuticals are either first-generation or second-generation. First-generation biopharmaceuticals include recombinant proteins, with an amino acid sequence identical to a native human protein, which are administered for the purpose of replacement or augmentation of the protein in patients. Additionally, first-generation monoclonal antibodies (mAbs) are produced using murine hybridoma technology without the need for protein engineering (Walsh 2004). Second-generation biopharmaceuticals are recombinant proteins or mAbs that have been designed using protein-engineering techniques to create a product with desirable properties (Walsh 2004). The concept of protein engineering was conceived at the beginning of the 1980's. One of the first uses of protein-engineering, was site-directed mutagenesis to mutate tyrosyl-transfer RNA synthetase, causing a decrease in enzymatic activity (Winter et al. 1982). Since this initial work, protein-engineering technologies have been extending beyond alteration of one or two amino acids of a protein, to generate insertion or deletion of extensive sections of amino acid sequence (Neuberger et al. 1984). In addition, novel polypeptides have been designed from the fusion of multiple sequences (Moreland et al. 1997). These technologies generate an amazing degree of control over the structure and function of engineered proteins (Winter et al. 1982; Brannigan & Wilkinson 2002).

The first biopharmaceutical that was made available to patients was a recombinant insulin (Humulin), which gained marketing approval in 1982 (Johnson 1983). Following the success of Humulin, the biopharmaceutical industry experienced tremendous growth and in 2013 the global market was valued at \$140 billion, up from \$99 billion in 2009 (Walsh 2010; Walsh 2014). Approximately 250 biopharmaceutical products are now available to treat many diseases including (but not limited to) anaemia, growth disorders, infectious diseases, cancers and inflammatory disorders (Nicolaidis et al. 2010; Walsh 2014).

Protein-based biopharmaceuticals can be classified into several categories, including recombinant proteins, antibodies and hybrids.

1.1.1.1 Recombinant proteins

Recombinant therapeutic proteins were brought to market following the production of recombinant insulin. In 1982, Humulin was the first recombinant insulin, produced using an *Escherichia coli* (*E. coli*) expression system, to be taken to market (Johnson 1983). Recombinant insulin was not only a breakthrough for insulin-dependent diabetics, but also the research conducted during its development paved the way for future biopharmaceuticals. In 1991, the first recombinant human insulin produced in *Saccharomyces cerevisiae* (*S. cerevisiae*) received marketing approval (Walsh 2005). Early insulin products are examples of first-generation biopharmaceuticals.

Second-generation biopharmaceuticals were brought to market in the mid 1990's (Walsh 2004). Second-generation biopharmaceutical proteins are often designed to include more desirable properties than the first-generation alternative, thrombolytic biopharmaceuticals provide an example of this. Thrombolytic therapy is used in the treatment of myocardial infarction and thromboembolic strokes (Lapchak 2002; Dundar 2003). In humans blood clots are degraded, but slowly through the action of a 527 amino acid serine protease known as tissue plasminogen activator (tPA) (Walsh 2004). Alteplase is a first-generation tPA with an amino acid sequence identical to native human tPA (Genentech, Inc 2015). In 1987, Alteplase became the first biopharmaceutical product, manufactured in CHO cells, to receive US FDA approval (Walsh 2004). More recently, several second-generation tPAs have been brought to market. For example, Reteplase is an engineered form of tPA that consists of only two of the 5 protein domains that make up the native human tPA. As this product is manufactured using an *E. coli* expression system, the protein is non-glycosylated (EKR Therapeutics 2009). The lack of glycosylation decreased renal and hepatic clearance and consequently, Reteplase has a 3.3-fold greater plasma half-life than Alteplase (Martin et al. 1992; Llevadot et al. 2001). Tenecteplase is a further example of a second-generation tPA, that differs from native human tPA by amino acid substitutions at three sites; the resultant protein has a greater plasma half-life than native human tPA or Alteplase (Genentech, Inc 2011).

1.1.1.2 Monoclonal antibodies

Therapeutic antibodies produced by the biopharmaceutical industry are a form of recombinant protein. However, they can be distinguished from the proteins discussed in the previous section as they are designed to bind and antagonise soluble factors or cell surface proteins. Rather than simply replacing endogenous proteins, antibodies can

interact with the immune system very specifically sites of disease (Nicolaidis et al. 2010). There are five classes of endogenous antibodies, IgA, IgD, IgE, IgG and IgM. The classes have different characteristics and properties (Brekke & Sandlie 2003). IgG is the most abundant immunoglobulin found in the human body. There are four subclasses of IgG, which are named in order of the concentration that is usually found in serum. The subclasses are known as IgG1, IgG2, IgG3 and IgG4, they have serum concentrations of 9, 3, 1 and 0.5 mg ml⁻¹ respectively (Wood 2001; Jefferis 2007). The four subclasses differ slightly in structure and function, however they are closely related (Wood 2001). IgG is commonly used as a basis for recombinant monoclonal antibody therapeutics as this class is capable of immune protection by antibody-dependent cell-mediated cytotoxicity and complement-dependent cytotoxicity (Clynes et al. 2000). In the work to be described in this thesis, all transfected cell lines produced a model IgG1 class antibody.

In 1986, Muromonab-CD3, which targets the CD3 receptor on T cells, was approved for therapeutic use making it the first mAb to reach the clinic. The mAb was approved for the prevention of acute rejection in organ transplantation (Yoon et al. 2010). Muromonab-CD3 was effective in patients, although its therapeutic potential was limited because of its murine origin. In subsequent years, additional first-generation, murine mAbs gained approval as human therapeutics (Walsh 2004). All these murine mAbs shared the similar limitations of short serum half-life, relative to endogenous human IgG antibodies; and development of a human anti-mouse antibody (HAMA) immunogenic response, following a single exposure to a murine mAb in 50-100% of patients (Hwang & Foote 2005).

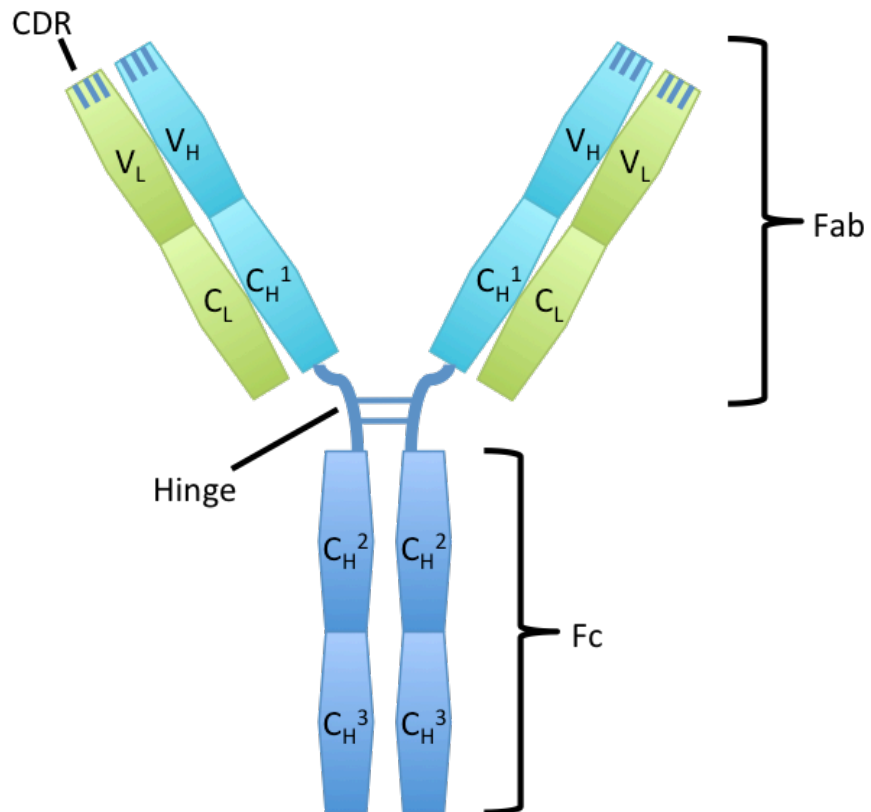
In order to overcome the disadvantages of first-generation mAbs, genetic/protein engineering strategies were developed. This approach led to the production of second-generation chimeric mAbs. The structure of IgG antibodies consists of four polypeptide chains, two heavy and two light chains arranged in a Y-shape (Figure 1.1). Chimeric antibodies are engineered gene products, and are comprised of the variable regions of a murine antibody and the constant regions of a human antibody (Boulianne et al. 1984; Shin 1991). As a result of limiting the murine component of chimeric mAbs, the immunogenic response seen in humans was typically much less than that seen with first-generation mAbs (Yoon et al. 2010). The first chimeric mAb to be granted market approval was abciximab in 1994 (Yoon et al. 2010). The mAb was highly efficacious for the prevention of thrombus formation during and after angioplasty, although a degree of immunogenic response was still observed despite the decreased murine content. After an initial administration, human anti-chimeric antibodies (HACA) were found in 5% of patients and this increased to 19% of patients after re-administration (Tcheng et al. 2001). Whilst

the presence of a HACA response is common for chimeric antibodies, the percentage of patients that show immunogenicity was markedly lower when compared to murine antibodies (Hwang & Foote 2005).

A further decrease in the murine component of second-generation antibodies was achieved with the development of humanized antibodies. Humanized antibodies require more complex protein engineering than the chimeric predecessors. The variable domains of the immunoglobulin polypeptide chains each contain three hypervariable regions or complementarity-determining regions (CDRs) (Figure 1.1). In order to create a humanized antibody, the CRDs from a murine antibody are grafted into the variable domain of an appropriate human immunoglobulin gene (Jones et al. 1986). The anti-VEGF humanised mAb bevacizumab (as later reported for several other humanised mAbs) showed no human anti-human antibody (HAHA) response in patients (Hwang & Foote 2005).

Continued development of monoclonal antibody technology now enables the production of fully human mAbs. Murine mAbs have been available for over two decades, however, an ethical barrier prevents the production of human mAbs via the same technology. It is not ethical to immunise humans against antigens in order to harvest B cells for the generation of hybridoma cell lines. Phage display technology allows generation of fully human mAb generation but bypasses the ethical considerations of human immunization *in vivo* (McCafferty et al. 1990; Kim et al. 2005).

Figure 1.1 The structure of immunoglobulin G (IgG)



Depicted here is the typical IgG structure. The molecule is comprised of four polypeptide chains. Two light chains containing one variable domain (V_L) and one constant domain (C_L), the heavy chains include one variable domain (V_H) and three constant domains (C_H¹, C_H² and C_H³). In addition, the heavy chains contain a flexible hinge region. Disulphide bridges link the two heavy chains at the hinge region, the light chains are attached to the heavy chains by further disulphide bridges. Each of the variable domains contains three complementarity-determining regions (CDR), which are important for antibody specificity. The molecules can be enzymatically cleaved into fragments: fragment antibody binding (Fab) containing the variable regions, and fragment crystallisable (Fc) containing C_H² and C_H³.

1.1.1.3 Hybrids and novel-format antibodies

Hybrid biopharmaceuticals are products of protein engineering. Such products can be created by the fusion of two or more proteins/protein fragments (Krueger & Callis 2003; Litzinger et al. 2007). Alternatively, toxins (Vitetta et al. 1983; Siegall et al. 1988) or radionuclides (Witzig 2002) can be conjugated to proteins. This technology allows for the generation of powerful biopharmaceutical agents that have an intrinsic biological action that can be targeted against specific biological targets, for example cancer cells (Vitetta et al. 1983; Siegall et al. 1988; Witzig 2002). Protein engineering has also been used to design novel-format antibodies. These include minibodies and bispecific antibodies and may present new challenges for bioprocessing (Nelson & Reichert 2009).

An example of a hybrid biopharmaceutical is Etanercept. Etanercept is used in treatment of rheumatoid arthritis, due to its ability to bind and sequester tumour necrosis factor (TNF), which is thought to be a causal factor in rheumatoid arthritis (Moreland et al. 1997). Etanercept consists of the ligand-binding region of the human TNF receptor, p75, joined to the Fc region of IgG. The drug competes with cellular TNF receptor and thus helps neutralise free TNF in the patients circulation (Moreland et al. 1997).

A summary of antibody and hybrid biopharmaceuticals approved by the FDA is presented in Table 1.

Table 1.1 Antibody and hybrid biopharmaceuticals approved between 1986 and 2014

| Name | Target | Production Host | Antibody Type | Indication | Company | Year |
|------------------------------|----------------------|----------------------------|---------------------|--|---------------------------|------|
| Muromonab-CD3 | CD3 | Murine hybridoma cell line | Murine | Acute kidney transplant rejection | Ortho Biotech | 1986 |
| Abciximab | Platelet GB IIb/IIIa | Sp2/0 cell line | Chimeric | Prevention of blood clots | Centocor | 1994 |
| Edrecolomab | 17-1A | Murine hybridoma cell line | Murine | Colorectal cancer | GlaxoSmithKline | 1995 |
| Rituximab | CD20 | CHO cell line | Chimeric | Non-Hodgkin's lymphoma | Genentech/Biogen-Idec | 1997 |
| Daclizumab | IL-2Ra (CD25) | NS0 cell line | Humanized | Acute kidney transplant rejection | Hoffman-LaRoche | 1997 |
| Trastuzumab | Her2 | Murine cell line | Humanized | Metastatic breast cancer | Genentech | 1998 |
| Basiliximab | IL-2R | Sp2/0 cell line | Chimeric | Prophylaxis of acute organ rejection | Novartis | 1998 |
| Palivizumab | RSV | NS0 cell line | Humanized | Respiratory syncytial virus | MedImmune | 1998 |
| Gemtuzumab | CD33 | NS0 cell line | Humanized | Acute myelogenous lymphoma | Wyeth-Ayerst | 2000 |
| Alemtuzumab | CD52 | CHO cell line | Humanized | B cell chronic lymphocytic leukaemia | Takeda | 2001 |
| Adalimumab | TNF α | CHO cell line | Human | Rheumatoid arthritis | Abbott | 2002 |
| Ibritumomab | CD20 | CHO cell line | Murine | Non-Hodgkin's lymphoma | Biogen-Idec | 2002 |
| Alefacept | CD2 | CHO cell line | LFA3 fused IgG1 Fc | Psoriasis | Biogen-Idec | 2003 |
| Tositumomab | CD20 | Murine hybridoma cell line | Murine | Non-Hodgkin's lymphoma | Corixa/GSK | 2003 |
| Bevacizumab | VEGF | CHO cell line | Humanized | Colorectal cancer | Genentech | 2004 |
| Natalizumab | A4 integrin | NS0 cell line | Humanized | Multiple sclerosis | Biogen-Idec/Elan | 2004 |
| Abatacept | CD80/86 | Murine cell line | CTLA4 fused IgG1 Fc | Rheumatoid arthritis | Bristol-Myers Squibb | 2005 |
| Ranibizumab | VEGF-A | <i>E. coli</i> cell line | Fab | Age related macular degeneration | Genentech | 2006 |
| Panitumumab | EGFR | CHO cell line | Human | Colorectal cancer | Amgen | 2006 |
| Rilonacept | IL-1 | CHO cell line | IL-1R fused IgG1 Fc | Cryopyrin associated periodic syndrome | Regeneron | 2007 |
| Certolizumab | TNF α | <i>E. coli</i> cell line | PEGylated Fab | Crohn's disease | UCB | 2008 |
| Golimumab | TNF α | Sp2/0 cell line | Human | Rheumatoid arthritis | Centocor | 2008 |
| Tocilizumab | IL-6 | CHO cell line | Humanized | Rheumatoid arthritis | Roche | 2009 |
| Denosumab | RANK ligand | CHO cell line | Human | Osteoporosis in postmenopausal women | Amgen | 2010 |
| Ipilimumab | CTLA-4 | CHO cell line | Human | Melanoma | Bristol-Myers Squibb | 2011 |
| Raxibacumab | Bacillus anthracis | NS0 cell line | Human | Inhalational anthrax | GSK/Human Genome Sciences | 2012 |
| Trastuzumab emtansine | HER-2 | CHO cell line | Humanised fusion | Breast cancer | Roche/Genentech | 2013 |
| Obinutuzumab | VEGF-2 receptor | CHO cell line | Human | Gastric cancer | Ely Lilly | 2014 |

The name, target, production host, antibody type, indication, manufacturing company and year of US approval is summarised for examples of antibody-based biopharmaceuticals approved between 1986 and 2014. Adapted from Shukla & Thömmes (2010) and Walsh (2014).

1.2 Expression systems for biopharmaceutical production

Production of recombinant biopharmaceuticals requires use of an expression system, a host cell line that can take up and express genes delivered on a DNA vector (Birch & Racher 2006). Host cells of bacterial, yeast, insect and mammalian origin have all been used to make various types of recombinant biopharmaceuticals. Each of these has different culture conditions and production costs as well as more specific advantages and disadvantages (Bhopale & Nanda 2005; Birch & Racher 2006; Sekhon 2010). Mammalian and *E. coli* expression systems account for the majority of industry manufactured and approved biopharmaceuticals on the market between 1982 and 2014; 56% were produced in mammalian systems and 19% were produced in *E. coli* systems (Walsh 2014).

Bacterial expression systems have been used since the production of recombinant insulin in 1982. *E. coli* is a very well characterised prokaryote, and strains of *E. coli* are the most abundantly used bacterial expression system (Terpe 2006; Ferrer-Miralles et al. 2009). Advantages of using *E. coli* as an expression system include the fast growth rate of *E. coli* leading to the rapid production of recombinant proteins. *E. coli* are also relatively easy to transform with low quantities of vector DNA and cell culture is relatively inexpensive (Verma et al. 1998). Despite the advantages of *E. coli* as an expression system, the prokaryotic system does include several features that are not favourable to the production of some biopharmaceuticals. Following the successful synthesis of recombinant proteins in *E. coli*, specific proteins accumulate as an inactive, insoluble form in the bacterial cytosol in inclusion bodies (Verma et al. 1998). This feature of the system calls for more complicated downstream processing than if the proteins were to be secreted directly into the growth medium (Verma et al. 1998). A final, major disadvantage of prokaryotic expression systems is the lack of required cellular machinery needed to perform many post-translational modifications (PTMs). Common PTMs include glycosylation, disulphide bond formation, phosphorylation and proteolytic processing. PTMs are important for the correct function of many proteins *in vivo*, disulphide bond for example are crucial for antibody structure (Kim et al. 2005), whereas glycosylation is crucial for antibody effector functions (Jefferis 2009). Some PTMs can be applied synthetically (Ferrer-Miralles et al. 2009), however other, eukaryotic, expression systems can avoid this complication altogether.

Yeast is also used as a eukaryotic expression system, the species *S. cerevisiae* and *P. pastoris* are exploited for biopharmaceutical production (Walsh 2010). Between 2006 and

2010, several vaccine and hormone-based products produced using *S. cerevisiae* were approved by the FDA (Walsh 2010). Some of the benefits of bacterial systems are also true of yeast expression systems. Yeast are fast growing, cost effective and will achieve high cell densities in bioreactors (Ferrer-Miralles et al. 2009). The major advantage of using a yeast system rather than a bacterial system is the ability of yeast to perform a wider range of PTMs. However N-linked glycosylation patterns created by yeast can cause immunogenic responses and short serum half-life in the final product (Verma et al. 1998; Ferrer-Miralles et al. 2009). GlycoFi have developed an engineered strain of *P. pastoris* that is capable of performing complex N-glycosylation modifications, similar in structure to human modifications, which is capable of biopharmaceutical production (Beck et al. 2010).

Two other systems that can be used for recombinant protein expression are baculovirus infected insect cells and plant cell systems. The vaccine Cervarix is produced using an insect cell system, however this is one of just three products manufactured using insect cell lines (Walsh 2014). The use of baculovirus is considered a “safe” vector as it is unable to infect mammalian cells (Verma et al. 1998). Plant cell expression systems are yet to realise their potential in the biopharmaceutical industry. In 2012, Pfizer brought taliglucerase alfa to the US market. Expressed in carrot root cells, this became the first biopharmaceutical approved from a plant-based expression system (Walsh 2014). The 2014 West African Ebola outbreak saw ZMapp brought to mainstream media attention. This cocktail of three mAbs, whilst not yet approved, has been used in man as an experimental treatment for Ebola virus disease. Produced in transgenic tobacco plant cells, ZMapp has shown curative effects in non-human primates following an Ebola viral challenge (Olinger et al. 2012; Qiu et al. 2014; Walsh 2014).

As previously mentioned 56% of the biopharmaceuticals approved by the FDA between 1982 and 2014 were produced using a mammalian expression system. The majority of these expression systems were a derivation of the Chinese hamster ovary (CHO) cell line, although some other mammalian cell lines such as baby hamster kidney (BHK) and NS0 hybridoma are also used (Walsh 2010; Walsh 2014). The use of mammalian systems has various benefits, for example, the PTMs produced are very similar to those added by human cell lines. Various mammalian cell lines have now been adapted to grow in chemically defined, serum-free medium as suspension cultures. These culture media improve the biosafety of products as they carry a much lower risk of contamination from disease causing agents such as viruses and prions (Ferrer-Miralles et al. 2009).

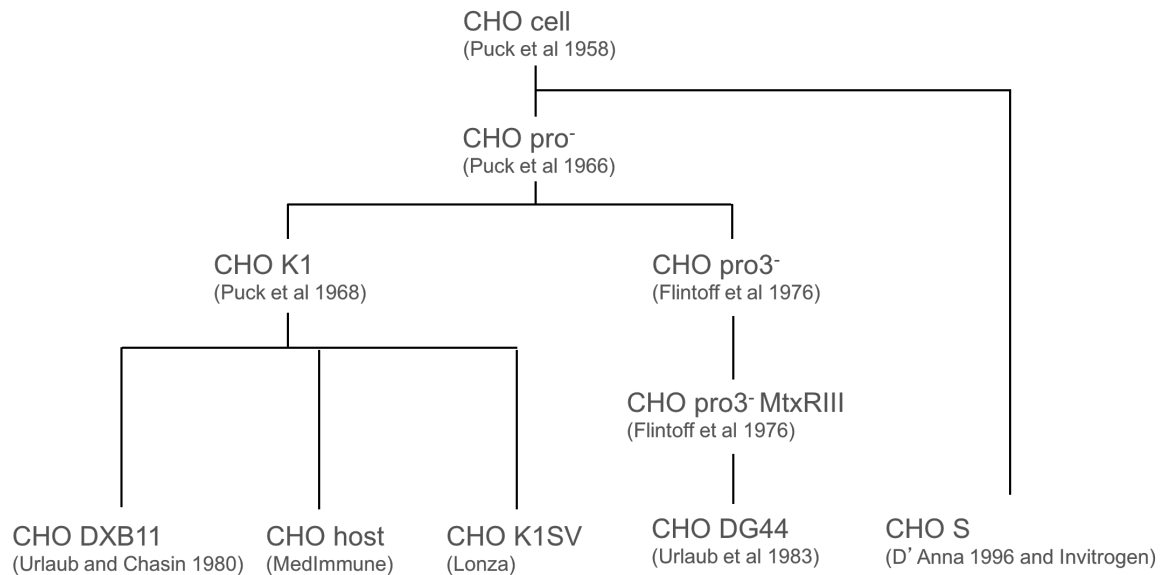
1.2.1 History of the CHO cell line

Puck et al. created the original CHO cell line from partially inbred, adult female Chinese hamsters (*Cricetulus griseus*). The group also cultivated cell lines from other organs of *C. griseus* such as lung and spleen, but, they observed that the ovary cells were particularly suitable for long-term cell culture (Puck et al. 1958). Various daughter cell lines of the progenitor CHO cell line now exist (Figure 1.2) which have varying industrial relevance. The first daughter cell line required proline for growth and thus was named CHO pro⁻ (Kao & Puck 1967). Derived from this cell line was the CHO K1 cell line (Kao & Puck 1967). The CHO K1 cell line has been used extensively in industry, particularly the CHO K1SV variant developed by Lonza Biologics (Edmonds et al. 2006). Similarly, the suspension adapted MedImmune CHO cell lines used in this research have been derived from the ancestral CHO K1 cell line and are based on the glutamine synthetase (GS) selection system (Section 1.2.3). In addition to CHO K1, two cell lines were created that are deficient in dihydrofolate reductase (DHFR), these are known as DXB11 (Urlaub & Chasin 1980) and DG44 (Urlaub et al. 1983). DG44 are one of the most commonly used CHO cells in the biopharmaceutical industry, they are deficient in both alleles for DHFR and this makes the gene an excellent selection marker (Derouazi et al. 2006). The DHFR gene in the DBX11 cell line is deleted at one locus, and the second locus has a missense mutation (Urlaub & Chasin 1980; Wurm 2013)

Primary diploid cells of the Chinese hamster have 22 chromosomes (Wurm & Hacker 2011). The diverse CHO cell lineage exhibit various mutations and chromosomal rearrangements, consequently there is a large degree of clonal variability between the CHO variants. Differences in modal chromosome number have been reported for CHO variants. CHO K1 has 21 chromosomes and DG44 has only 20 chromosomes, however these figures are a modal representation of a broad range observed (Deaven & Petersen 1973; Derouazi et al. 2006; Wurm 2013). A major development in CHO genomics arrived in August 2011 when Xu et al. published the draft sequence of a CHO K1 cell line, obtained from the American Type Culture Collection, genome. The published genome comprised 2.45 Gb of genomic sequence and was predicted to define 24,383 genes. The CHO genome database, which is publically available, will help to facilitate analysis of future CHO 'omics based studies. An important caveat of the database is that the sequence may not be fully representative of cell lines derived from the CHO K1 lineage, due to genetic changes that may have accumulated (Xu et al. 2011). Subsequent update

papers have confirmed this, and sequencing of further CHO variants has revealed single-nucleotide polymorphisms, indels and copy-number variations across the cell lines analysed (Lewis et al. 2013; Brinkrolf et al. 2013).

Figure 1.2 The CHO cell lineage



Puck et al. first created the CHO cell lineage in 1958. The cell line was subjected to multiple rounds of mutagenesis, and over time daughter cell lines have been created which have unique genotypic and phenotypic properties.

1.2.2 Generation of clonal recombinant transfectants

Generation of stable recombinant CHO cell lines requires a method of introducing extracellular transgenes into the host cell nucleus.

Electroporation is a commonly used rapid method of gene delivery. This method involves the application of an electric pulse to a suspension of host cell lines and plasmid DNA. The electric pulse opens pores in the plasma membrane of host cell lines, thus allowing the DNA to enter the cell. Carefully optimised conditions of the electric waveform are required to balance DNA transfer efficiency with the adverse effects of the pulse on cell viability (Canatella et al. 2001; Costa et al. 2010).

Chemical methods of transfection are also available. Calcium phosphate can be co-precipitated with a DNA vector prior to application to host cell lines. This allows the host cells to take-up the DNA via endocytosis (Jordan et al. 1996). Liposomes are also effective for transgene delivery. Several commercial lipid-based transfection reagents are available. Combined with plasmid DNA, these reagents form complexes which transport the DNA into the cytoplasm of the host cells (Hui et al. 1996). Cationic polymers such as polyethyleneimine can also form complexes with DNA. These polyplexes form due to electrostatic interactions with the positively charged polymer and the negatively charged DNA. The net positive charge on these polyplexes triggers endocytosis into the host cells, and subsequently deliver the plasmid DNA to the nucleus of the cells (Godbey et al. 1999).

Standard transfection techniques do not allow control over the site of transgene insertion into host cell genomic DNA (Derouazi et al. 2006). However, transgene localisation can impact on expression. DNA in the cell is typically organised as transcriptionally repressed heterochromatin, or transcriptionally active euchromatin. These two states are altered by various epigenetic modifications (Kouzarides 2007). When plasmids integrate in regions of heterochromatin, transcription of the transgene can be silenced by subsequent chromatin organisation (Pikaart et al. 1998; Matasci et al. 2011). Epigenetic modifications, including DNA methylation and covalent histone modification (Jones & Baylin 2007), are a source of phenotypic variability (Neildez-Nguyen et al. 2008). Additionally, these modifications have been shown to affect the stability of recombinant protein production in CHO cell lines (Kim et al. 2011). Studies have also found that gene integration near the telomeric regions of chromosomes can result in increased stability and productivity of the cell line (Yoshikawa et al. 2000).

Several tools to negate the effects of site of integration and gene silencing effects of chromatin organisation have been developed. Ubiquitous chromatin opening elements (UCOE) can confer resistance to epigenetic gene silencing mechanisms such as DNA methylation (Zhang et al. 2010). Incorporation of UCOE into transgene vectors has been shown to increase transgene mRNA expression, increase the specific productivity of recombinant production and maintain the stability of production in CHO cell lines (Kim et al. 2011; Betts & Dickson 2015). Also, transposable elements such as *piggyBac* have been used with promising results. This method of transgene integration has been used to generate cell lines that show increased stability and productivity when compared to cell lines produced using standard transfection methods (Matasci et al. 2011). Furthermore,

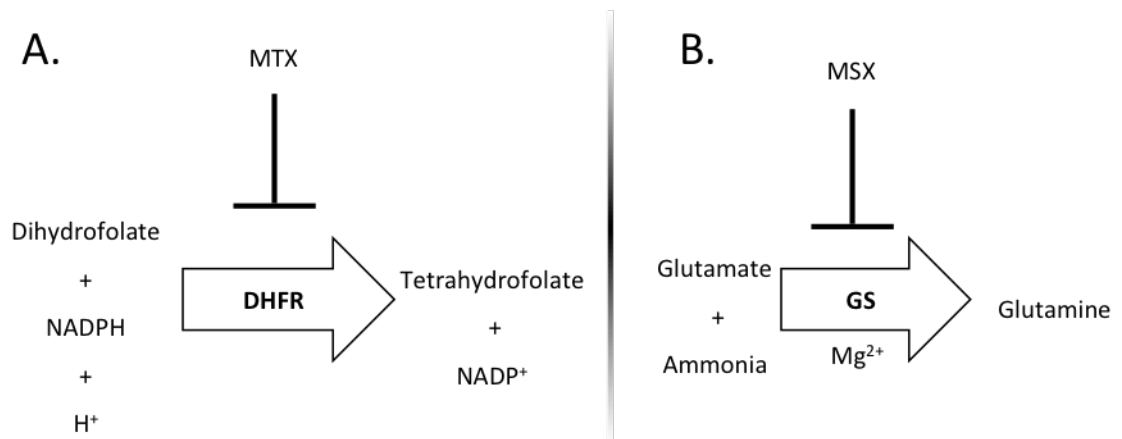
Artificial Chromosome Expression technology has been developed, which enables strict control over transgene copy number and genomic environment (Kennard et al. 2009).

1.2.3 Selection system

When transfecting a host cell line with a gene of interest, it is important that a second gene, which confers a selectable attribute, is included in the expression vector. CHO cell expression systems typically use one of two genes: DHFR and GS.

The CHO DG44 and DXB11 cell lines, as previously mentioned, are deficient in the DHFR gene (Urlaub & Chasin 1980; Urlaub et al. 1983). DHFR catalyses the reduction of dihydrofolate to tetrahydrofolate (Figure 1.3 A). Tetrahydrofolate is a crucial molecule for the function of several cellular pathways, including those for the synthesis of glycine, thymidine and purine. DG44 and DXB11 host cell lines cannot grow in culture medium that is deficient of glycine, thymidine and hypoxanthine. Thus exposing a pool of transfected cells to such a medium, will lead to the selection of cells that successfully integrated the DNA vector (Jayapal et al. 2007). DHFR not only enables the selection of successful transfectants, but the gene can also be exploited to cause amplification of the DHFR gene and the gene of interest in terms of gene copy number (Yoshikawa et al. 2000; Kotsopoulou et al. 2010). In order to induce amplification, cells are treated with increasing concentrations of methotrexate (MTX), which is a competitive inhibitor of DHFR (Figure 1.3 A) (Kaufman et al. 1985; Kotsopoulou et al. 2010). Amplification can result in hundreds to thousands of copies of transfected genes (Wurm et al. 1986). Increasing gene copy number may increase expression of recombinant protein, however the process can take months to successfully select a high producing clone (Wurm et al. 1986).

Figure 1.3 The enzyme reactions used as selection systems in CHO cell culture



A. Dihydrofolate reductase (DHFR) catalyses tetrahydrofolate production from dihydrofolate. The enzyme can be inhibited by the presence of methotrexate (MTX). B. Glutamine synthetase catalyses glutamine production from glutamate and ammonia. The enzyme can be inhibited by the presence of methionine sulphoximine (MSX).

Glutamine synthetase is another commonly used enzyme that is used for the selection of successful transfectants, and is the selection system used in this research. The enzyme is essential for cells cultured in the absence of glutamine as GS is the only pathway for glutamine synthesis (Bebbington et al. 1992). The pathway requires glutamate, ammonia and a presence of Mg²⁺ to synthesise glutamine (Figure 1.3 B) (Brown et al. 1992). Some cell lines, such as NS0 cells are deficient of GS and inclusion of the gene in a transfection vector is sufficient for selection. However, CHO cell lines do express endogenous GS. Successful selection can still be achieved if the selection medium is supplemented with methionine sulphoximine (MSX), an inhibitor of GS (Brown et al. 1992; Bebbington et al. 1992). As with the DHFR method of selection, GS system can (if required) be used to amplify gene copy number. Brown et al. found that a single round of amplification was sufficient when using the GS system. This could result in shorter time scales compared to when using the DHFR system for amplification (Brown et al. 1992). A further advantage of the GS system is that the accumulation of toxic ammonia is avoided as it is converted to glutamine (Dietmair et al. 2011). The GS System is currently marketed by Lonza Biologics, who supply over 100 companies with their technology, and to date, 10 products have been brought to market using this platform (Lonza Group Ltd. 2015). Zinc finger nuclease technology has been employed to advance the GS system, creating glutamine synthetase knockout host cell lines (Fan et al. 2011). This resulted in improved selection efficiency, and improved productivity.

1.3 Cell line variability

As previously stated, the majority of biopharmaceuticals are produced using mammalian expression systems (Walsh 2014). Unlike bacterial and yeast culture, working with mammalian cells is time consuming and there are associated high costs. Unfortunately for patients and healthcare systems, high production costs and cell line variability translates to very high treatment costs (Dietmair et al. 2011). Herceptin and Avastin can cost between \$40,000-60,000 per patient, per annum for the treatment of cancer (Dietmair et al. 2011). There is currently a great research effort towards increasing productivities of CHO and other mammalian cultures with the aim of lowering production costs.

1.3.1 Effects of phenotype and culture environment

There are various factors that are thought to be desirable of a production cell line. Ideally CHO production cell lines should have relatively rapid rates of proliferation, be able to achieve a high cell density, maintain high viability, maintain a high specific production rate and produce proteins with acceptable product quality. If these criteria are met by a production cell line, in theory high production titres should be achieved more rapidly than with cell lines that do not meet the criteria (Dietmair et al. 2011). Efforts to engineer the phenotype CHO cells to have improved 'vitality' characteristics have had mixed results.

Ifandi and Al-Rubeai investigated the effect of c-Myc overexpression in CHO K1 cells. The c-Myc gene is associated with cellular proliferation. The group did observe a positive effect on proliferation and viable cell density. However, in static, serum-free batch culture apoptosis was 6% more prevalent in the c-Myc overexpressing cells, than in the control cell line by day 9 of culture (Ifandi & Al-Rubeai 2003). As c-Myc can influence increased apoptosis, the group conducted a further study to investigate the effect of overexpressing the anti-apoptotic Bcl-2 in addition to c-Myc. Dual expression resulted in prolonged cell viability and a reduction of apoptosis. This was observed in both serum-containing and serum-free, static batch culture conditions (Ifandi & Al-Rubeai 2005). Unfortunately this study did not include suspension cultures and no data was collected for cultures with dual expression of c-Myc and Bcl-2 in addition to an industrially relevant protein such as an antibody. More recently, Majors et al. overexpressed the cell cycle transcription factor E2F-1, in serum-free suspension cultures of CHO DG44 cells. The cell lines used were expressing a humanised monoclonal antibody. Although the group did observe a 20% increase in viable cell density, this was not reflected by an increase in titre (Majors et al. 2008). In the Majors study, clonal cell lines were created from pools of transfectants, the

data show variation in the maximum viable cell density (VCD_{max}) achieved by these clonal cell lines. This is indicative of clonal variability, which could be a consequence of the site of integration of the expression vector. However, it is also possible that variability in the host cell lines result in some clones having an inherent propensity to achieve high viable cell density (VCD).

The production of biopharmaceutical proteins in a bioreactor is a terminal process, the onset of apoptosis therefore presents as a limiting factor of protein production (Dietmair et al. 2011). A number of factors can have an influence on apoptosis in the bioreactor environment including nutrient limitation, shear stress, oxygen availability and the accumulation of toxic products such as ammonia (Singh et al. 1994; Al-Rubeai & Singh 1998). Further to the study of cells overexpressing c-Myc and Bcl-2 carried out by Ifandi and Al-Rubeai, research has been undertaken by others to delay apoptosis.

Mastrangelo et al. found that adherent CHO K1 cells infected with an alphaviral vector would die within four days of infection. The group then overexpressed the anti-apoptotic Bcl-x_L in the CHO K1 cells. They observed that the cells could then recover from infection and resume exponential growth. The overexpressing cells were also able to secrete twice the amount of recombinant IL-12 as the parental cell line (Mastrangelo et al. 2000).

Chiang and Sisk have conducted further investigation into the promising effects of Bcl-x_L overexpression. They overexpressed Bcl-x_L in CHO DG44 cells that were secreting a humanised mAb. The overexpression of Bcl-x_L caused an increase in product titre and specific productivity in small-scale (50-100 ml) fed-batch culture. Importantly, this was reflected following scale-up to 2 L bioreactor culture. At this scale, the overexpressing cells had roughly 60% increased titre and a 2-fold increase in specific productivity when compare to the control cells (Chiang & Sisk 2005).

Heat shock protein (HSP) 27 and HSP70 are regulators of apoptotic pathways and cause inhibition at multiple stages of these pathways (Lee et al. 2009). Lee et al. used an industrially relevant CHO cell line expressing recombinant human interferon- γ to investigate the result of HSP27 and HSP70 overexpression. When overexpressed individually, both proteins gave rise to desirable effects. However, co-overexpression of the two proteins in 2 L bioreactor fed-batch culture produced the best improvement in cell line characteristics. The co-expressing cultures demonstrated improved growth and viability when compared to control cultures, and this produced a 2.8-fold improvement in interferon- γ yield (Lee et al. 2009).

Biopharmaceutical expression systems, like all industrial production systems, have a requirement for raw materials (nutrients) and they generate waste products. Environment and medium optimisation has been studied as a means of improving product titres (Dietmair et al. 2011).

Ammonia is a by-product of glutamine metabolism and is toxic to mammalian cells. In order to decrease the build-up of ammonia in cultures, cells can be transfected with the GS gene. This can be sufficient to enable cell growth in glutamine-free medium and decrease build-up of ammonia (Bell et al. 1995). Lonza Biologics have had great success marketing cell lines and vectors based on this technology. An alternative approach for limiting ammonia build-up was investigated by Park et al. They transfected hybridoma cells with two enzymes from the urea cycle, this caused waste ammonia to be converted into citrulline. The transfected enzymes resulted in up to 33% less ammonia accumulation than in the control cells (Park et al. 2000).

Another toxic waste product that can accumulate and inhibit growth during cell culture is lactate. Kim and Lee investigated two methods of cell line engineering in an attempt to moderate lactate accumulation and improve the growth profiles of CHO cell cultures. In one study, the group used a small interfering RNA (siRNA) approach to knockdown lactate dehydrogenase-A (LDH-A) in order to down-regulate pyruvate-to-lactate conversion. This study used a recombinant CHO cell line that was producing human thrombopoietin. The knockdown resulted in a 75-89% decrease in LDH-A activity from the control group enzyme activity. Although the growth characteristics of the siRNA knockdown and control cells were similar, the knockdown of LDH-A enabled up to a 2.2-fold increase in product titre (Kim & Lee 2007a). The group commented that although the parental cell line used in this study was clonally derived, it might have been heterogeneous regarding productivity and metabolism. A consequence of a heterogeneous population may be that some cells (and therefore some transfectants) within that population will produce more product than other cells of the same population. Based on this, they studied multiple clones to ensure that their observations were a result of LDH-A knockdown and not a consequence of clonal variability. An alternative approach to regulating lactate production from the same group, was to express human pyruvate carboxylase (hPC) in a CHO DG44 cell line. This enzyme catalyses the production of oxaloacetate from pyruvate, downstream products of oxaloacetate are components of the mitochondrial citric acid cycle. Again the group commented on the need to consider clonal variability in this type of study. The group saw an improvement in cell viability and specific

lactate production was decreased in the clones studied by 21-39% as a result of hPC expression (Kim & Lee 2007b).

These studies aimed at decreasing ammonia and lactate production have focussed on altering CHO cell metabolism in order to improve culture characteristics and boost productivity. In contrast, Sellick et al. studied CHO LB01 cell metabolism in order to design, a “simple inexpensive” feed that complemented the metabolism of the culture. The group used a gas chromatography-mass spectrometry (GC-MS) approach to collect intra and extracellular metabolism data from the cell line, which was expressing a chimeric IgG4 antibody. The metabolomics data was used to produce a timeline indicating when metabolites were depleted or accumulated in the culture medium. Using this data, the group designed a feed to replenish key nutrients in order to promote sustained growth and productivity. The addition of feed at the correct time point influenced a 35% increase in viable cell density, sustained the stationary phase for one additional day and boosted antibody titre by 100% (Sellick et al. 2011). This study has a direct industrial impact as the theory can be applied to any culture process.

An additional example of environmental optimisation comes from Yoon et al. They designed a study to build on previous reports that lowering culture temperature can enhance productivity of CHO cells. By simply lowering the culture temperature of an erythropoietin expressing cell line from 37°C to 32.5°C, the group observed an increase in titre, however the culture duration was increased by seven days due to slow cell growth. The group then introduced a biphasic culture approach. When cultures were maintained at 37°C for two days for optimal growth, followed by culture at 32.5°C for optimal production, a 1.4 fold increase in productivity was observed compared to monophasic culture at 32.5°C (Yoon et al. 2006).

1.3.2 Phenotypic drift

One of the criteria for mammalian cell lines used for the production of biopharmaceuticals is that they are clonal. The term ‘clonal’ indicates that a cell line was derived from one parent cell (Barnes et al. 2006). Unfortunately, mammalian cells display an inherent instability and display phenotypic drift during long-term culture (Barnes et al. 2006; Dorai et al. 2012; Wurm 2013). As a result of this, clonal CHO cell lines can be considered to be a heterogeneous population after fairly short periods of time in culture (Kim & Lee 2007b). Barnes et al., found that after three rounds of limited dilution cloning of NS0 myeloma cells, they could not obtain cell lines with similar growth phenotypes. It was observed that

the divergence in growth only had about 7% variability, this could indicate that cell line variability is at least in part regulated by competitive advantages of the mean phenotype (Barnes et al. 2006). This inherent instability has important implications when considering cell lines developed for industrial protein production.

Cell line instability has been reported to cause significant decreases in protein titres in hybridoma (Frame & Hu 1990), DHFR-CHO (Fann et al. 2000) and CHOK1SV cells (Kim et al. 2011; Dorai et al. 2012; Davies et al. 2013). Unstable clones can cause huge problems in the biopharmaceutical industry due to loss of titre during production scale-up, and also it can cause problems in gaining regulatory approval of the product. Strategies for selecting stable clones involve extended culture and analysis of multiple potential clones for 55-60 population doublings. This number of doublings is considered to occur during the period from cell line creation to bioreactor culture (Dorai et al. 2012). These experiments take 2-3 months, which is an undesirable feature in a development timeline. Due to demand on resources, candidate cell lines are usually selected from a large number of possible clones based on early growth and titre data. Davies et al. have suggested that (epi)genetic drift in clonal CHO cell lines created functional diversity, they found that this diversity caused mAb production to cluster around the population average observed in the non-clonal host cell line (Davies et al. 2013). In a study aimed at improving early screening of candidate cell lines, Dorai et al. observed that a population of unproductive cells would spontaneously arise in unstable cell lines from as early as passage three. They suggested that screening cell lines for caspase 3 activity from as early as passage one could highlight unstable cell lines. They had observed that unstable cell lines had greater caspase 3 activity and conclude that using cell lines engineered to be apoptosis resistant could help decrease instability (Dorai et al. 2012).

Whilst phenotypic drift can cause problems during long-term manufacturing processes, it can also be manipulated as a tool during cell line development. CHO cells have proven to be highly adaptable. Early studies of CHO cells used them in anchorage and serum-dependent platforms. Phenotypic drift and genetic instability of the cells has been exploited to adapt CHO cell lines to the suspension and serum-free conditions typically used for biopharmaceutical manufacture (Sinacore et al. 2000). In addition to this, variability observed in clonally derived transfectants can be exploited for the selection of the transfectants with the “best” growth and productivity characteristics (Porter et al. 2010; Porter et al. 2010; Davies et al. 2013). Additionally, the “best” clonal host cell line for producing a mAb may not be the “best” host for the production of a more complex molecule. O’Callaghan et al. found that clonal hosts cell lines could out perform the non-

clonal parental cell line in mAb production, but could not replicate this result in the production of an Fc-fusion protein (O'Callaghan et al. 2015). Despite this, transfectant selection based on growth and productivity is a relatively simple approach. A greater understanding of the biologic determinants of these traits will be critical for future development of optimal, stable transfectants.

1.3.3 Mutator phenotype

A cause of phenotypic drift is that CHO cells have a high tendency to mutate (Davies et al. 2013; Wurm 2013). Genome sequencing of CHO cell lines has identified millions of mutations across multiple lineages in addition to missing hamster genes

(Xu et al. 2011; Lewis et al. 2013). In addition to sequence-level heterogeneity, CHO cells are heterogeneous at the chromosome-level (Derouazi et al. 2006; Cao et al. 2011; Wurm 2013). A “mutator phenotype” has been described as a precursor to cancer cells (Loeb 1991). The diversity and frequency of mutations and chromosome rearrangements that have been observed in CHO cell lines, suggests a similarity to the cancer cell mutator phenotype.

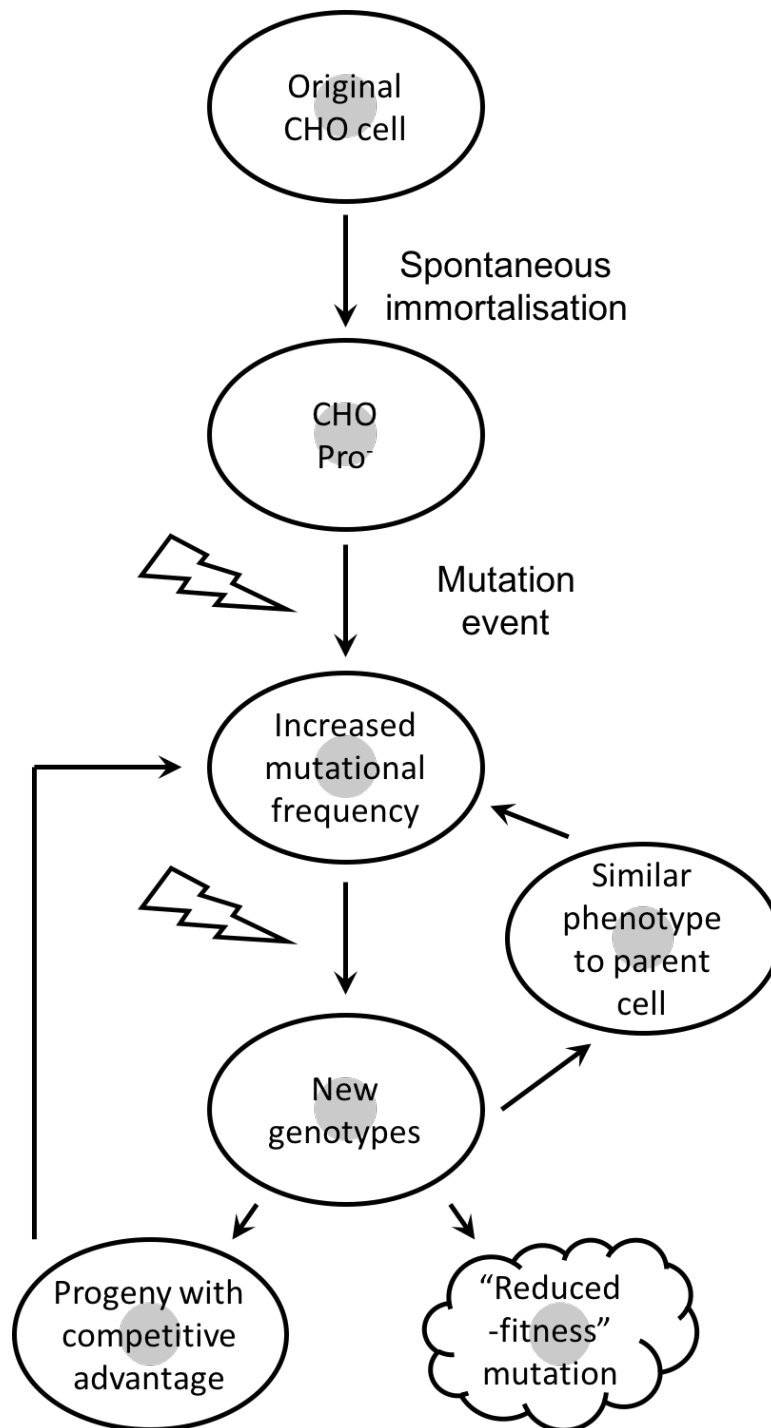
It is believed that in somatic human cells, the occurrence of mutations is relatively low, with an approximate rate of $2\text{-}30 \times 10^{-7}$ mutations per cell division (Araten 2005). The mutator phenotype is characterised by a high rate of mutation and genetic instability (Loeb 2001; Prindle et al. 2010). Loeb et al. have suggested that the low rate of mutation in normal cells is not sufficient to explain the high number of mutations found in cancer cells (Loeb et al. 1974). Thus, they hypothesised that a mutator phenotype can arise from mutations in genes that have a role in genomic stability (Prindle et al. 2010). Loss of function events, such as mutation, epigenetic modification and chromosomal aberrations, in genes involved in DNA polymerase, DNA mismatch repair and DNA excision repair can all contribute to the mutator phenotype (Venkatesan et al. 2007; Jones & Baylin 2007; Prindle et al. 2010).

It is thought that a spontaneous immortalisation event occurred during the development of the original, ancestral, CHO cell line. The details of this are not clear, however it is likely that this involved genetic modifications (mutations) (Wurm 2013). Additionally, it was reported in 1977 that CHO cell lines were unable to synthesize proline (Hamilton & Ham 1977; Wurm 2013). Clonal expansion of CHO cell lines will likely have caused a cumulative effect on the accumulation of genetic modifications throughout the history of

the lineage. These modifications will all contribute to the “mutator phenotype” observed in CHO cells today.

In opposition to the mutator phenotype, it has been suggested that a mutator phenotype would be deleterious to cancer progression, as “reduced-fitness” mutations would occur alongside “beneficial” mutations. Thus implying that a mutator phenotype would be selected against (Beckman & Loeb 2005; Attolini & Michor 2009). Beckman and Loeb have contradicted this, suggesting that although reduced-fitness mutations are likely to occur, they will be selected against and eliminated from the population. As such, the cells lacking reduced-fitness mutations will continue to proliferate (Beckman & Loeb 2005). Extending this theory to CHO cells, implies that routine cell culture, would select and expand mutant variants that have evolved phenotypes that promote survival and/or growth. Figure 1.4 depicts how the mutator phenotype could apply to CHO cell lineages.

Figure 1.4 Accumulation of genetic error in CHO cell lineages in relation to a mutator phenotype



The original CHO cell line is thought to have undergone spontaneous immortalisation and given rise to cells deficient in proline synthesis (CHO Pro⁻). The development of a “mutator” mutation results in an increased frequency of developing further mutations. The resultant genotypes may manifest as “reduced-fitness” or provide a competitive advantage. Cells with “reduced-fitness” mutations would typically be eliminated from the population. (Loeb et al. 1974; Beckman & Loeb 2005; Wurm 2013)

1.4 The use of metabolic profiling to define phenotype

It is common to monitor a subset of metabolites, e.g. glucose, lactate, glutamine, glutamate and ammonium, during biopharmaceutical production processes. However, typically, the number of metabolites monitored is low, most commonly including glucose, lactate, glutamine, glutamate and ammonia (Ma et al. 2009; Tsao et al. 2005; Porter et al. 2010; Dietmair et al. 2011; Gilbert et al. 2013). These analyses can be rapidly performed on cell culture medium samples using enzymatic assays and bioanalysis instruments from companies such as Nova Biomedical and YSI. Whilst these metabolites do provide insight into the phenotype of a cell culture, the metabolome is extensive and more in-depth techniques may enable a better understanding of CHO metabolism. Increased understanding of CHO metabolism has the potential to identify the 'best' host cell lines and resultant transfectants. Additionally, metabolic analysis has the potential to guide ongoing refinement of culture media and nutrient feeds, which are supportive of high quality and high yield production processes.

1.4.1 Metabolomic techniques

Metabolomic techniques revolve around highly sensitive instruments, which are capable of detecting hundreds of different metabolite compounds contained within a sample. Nuclear magnetic resonance (NMR) spectroscopy, liquid chromatography mass spectrometry (LC-MS) and gas chromatography mass spectrometry (GC-MS) techniques have all been applied to analyse intracellular and extracellular metabolism (Aranibar et al. 2011; Chong et al. 2011; Chong et al. 2012; Selvarasu et al. 2012; Ma et al. 2009; Sellick et al. 2011).

GC-MS is a powerful tool for metabolic profiling and has been applied to plants (Fiehn et al. 2000), prokaryotes (Wang et al. 2014) and eukaryotes such as CHO cell cultures (Sellick et al. 2011; Ma et al. 2009; Dietmair et al. 2012; Dean & Reddy 2013). GC-MS has greater sensitivity when compared to NMR (Pan & Rafferty 2006), making it more suitable for the detection of metabolites with low abundance. LC-MS is superior for the detection of large, polar molecules, however, GC-MS is highly suited to smaller, volatile, molecules. Additionally, the high-purity gas used as a mobile phase in GC-MS does not result in batch-to-batch retention time shifts that can present in LC-MS analysis (Büscher et al. 2009). A further disadvantage of LC-MS stems from the ionisation process. LC-MS typically relies on electrospray ionisation (ESI). ESI causes very little fragmentation of the molecules entering the mass spectrometer. GC-MS, instead, uses electron impact (EI) ionisation, standardised to 70 eV. EI is capable of ionising neutral molecules and causes

fragmentation. The resultant mass spectra are reproducible and specific to each metabolite (Kind et al. 2009). This enables comparison of GC-MS spectra to metabolite mass spectral and retention time indexed libraries, such as the Fiehn library for metabolite identification. The Fiehn library contains the mass spectra of over 1000 metabolite derivatives (Kind et al. 2009) and was chosen for metabolite analysis in this research.

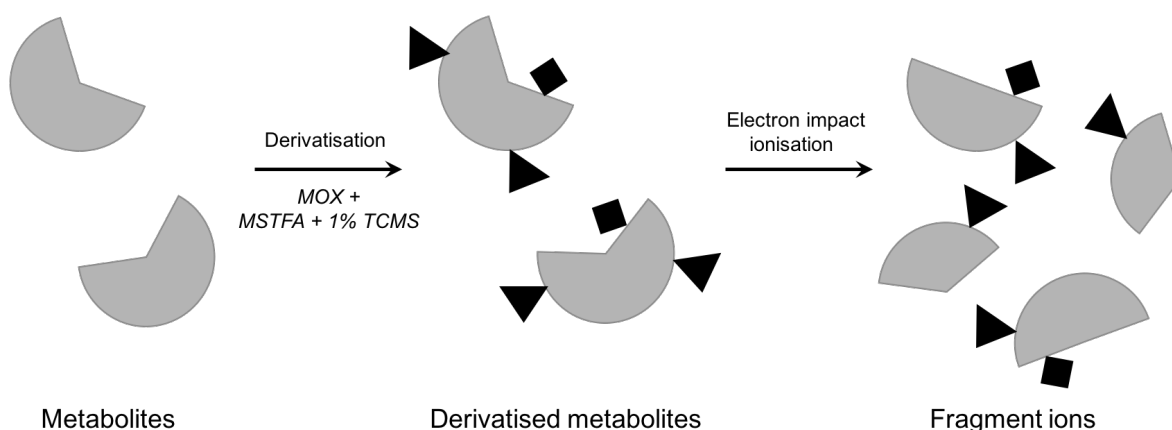
Sample preparation is critical for metabolomic analysis. Extracellular metabolite preparation is relatively simple. The culture medium can be separated from the cells by centrifugation prior to preparation and analysis of the sample. Greater complexity is involved in the preparation of intracellular metabolite samples. The turnover of some highly labile metabolites can be less than 2 seconds (Weibel et al. 1974), thus metabolism must be quenched rapidly upon sampling ensure accuracy of analysis (Sellick et al. 2010). Sellick et al. evaluated several methods of quenching and extraction of intracellular metabolites, and developed a two-step process that was found to recover the greatest range and quantity of intracellular metabolites from suspension cultures (Sellick et al. 2009; Sellick et al. 2010; Sellick et al. 2011). This technique is based on a cold (-40 °C) buffered, methanol-based quenching procedure, which decreases the turnover of intracellular enzymes and minimises metabolite leakage from the cells.

Before metabolite samples can be analysed by GC-MS they must be derivatised. Derivatisation chemically modifies compound to produce derivative compounds that are suitable for GC-MS analysis. This step in sample preparation has several important implications for analysis (Regis Technologies 2000):

- Increases volatility by elimination of polar groups.
- Increases the detectability of steroid molecules e.g. cholesterol.
- Increases the stability of compounds prone to thermal decomposition.
- Decreases volatility of molecules with low molecular weight.

There are a large number of derivatisation reagents available for GC-MS. In this research, metabolites were derivatised using a two-step process using methoxyamine hydrochloride (MOX) prior to N-methyl-N-(trimethylsilyl)trifluoroacetamide + 1% (v/v) trichloromethylsilane (MSTFA + 1% TCMS) (Figure 1.5).

Figure 1.5 Derivatisation and ionisation of metabolites during GC-MS analysis



Derivatisation reagents are used to produce derivative compounds of metabolites prior to GC-MS analysis. In this example, methoxyamine hydrochloride (MOX) (black triangle) and N-methyl-N-(trimethylsilyl)trifluoroacetamide + 1% (v/v) trichloromethylsilane (MSTFA + 1% TCMS) (black diamond) are used to derivatise metabolite compounds. Derivatised metabolites are separated using gas chromatography. Prior to mass spectrometry, the derivatised metabolites are ionised by electron impact, this process causes the derivatised metabolites to fragment into fragment ions.

1.4.2 The metabolic phenotype

Cell line engineering has been used to influence the metabolism of cell lines to improve growth or productivity characteristic (Section 1.3.1). These approaches have had mixed results and were focused on specific enzymes. Optimisation of cell culture medium and nutrient feeds has been a key driver for the increases in product yield that has been documented over the last few decades (Wurm 2004). Medium optimisation involves alterations in metabolite availability and concentration, this has been shown to have a significant influence on the phenotype of CHO cell cultures (Sellick et al. 2011; Gilbert et al. 2013). Statistical methods have been used to optimise cell culture medium (Lee et al. 1999; Castro et al. 1992; Kim & Lee 2009), however these approaches require a large number of variables to be screened to identify the optimal conditions. The use of metabolomic approaches, enables the extracellular environment to be rationally modified, based on the individual needs of a specific cell line (Sellick et al. 2011).

Metabolomics can be used as a powerful tool for medium and feed development, but in addition to this it can be used to determine the metabolic phenotype of cell lines. Metabolism incorporates every chemical reaction that occurs within a cell, and metabolomic technologies enable a more detailed understanding of what determines a

“good” metabolic phenotype. In addition to the routinely monitored metabolites, metabolomic research has identified metabolites that were previously unknown to be of significance.

It has been observed that sorbitol and glycerol accumulate both intracellularly and in the cell culture medium during batch culture processes (Luo et al. 2011; Sellick et al. 2011). The production of these metabolites is linked to the redox state of the cells (Tomlinson & Gardiner 2008). Additionally, the production of sorbitol could indicate that glucose is not efficiently channelled into glycolysis, and may represent a means for cells to deal with high glucose concentrations (Luo et al. 2011).

Metabolic shifts in citric acid cycle metabolites have been observed in relation to the phases of CHO batch culture. Citrate, isocitrate, fumarate, succinate and malate have all been shown to accumulate in the during exponential growth phases of culture (Ma et al. 2009; Sellick et al. 2011). However during the stationary phase, these metabolites shift from net production, to net consumption. Additionally, the high concentration of citrate that has been observed to accumulate in the extracellular medium, may be representative of a truncated citric acid cycle (Ma et al. 2009).

Metabolomic techniques have been applied to CHO transfectants with distinct phenotypic traits, specifically growth rate and specific productivity. Dietmair et al., using three different culture medium formulations, known to affect growth rates, identified 37 metabolites that could be associated with growth rate. In particular, they highlighted that metabolism of the nucleotides, CTP and UTP, as being important for growth rate (Dietmair et al. 2012). They commented that interpretation of the differences in these metabolites was complicated by the interconnectivity of intracellular metabolic pathways. An LC-MS based study has identified 7 metabolites that may be associated with specific productivity. CHO DG44 clones, producing an IgG mAb, and classified as high and low producers were studied. The high producing clones were determined to have a larger pool of electron carriers and a larger glutathione pool. Additionally, greater quantities of nucleotide-activated sugar precursors were identified in the high producing clones. The authors concluded that the high producing clones had a greater metabolic capacity for energy generation, glycosylation and were better suited to handle oxidative stress, than the low producing clones (Chong et al. 2012). Supportive of this, Dean and Reddy have suggested that high performing clones had a more active citric acid cycle than low performing clones, and that robust oxidative phosphorylation pathways are essential to high performing clones (Dean & Reddy 2013).

A greater understanding of CHO cell metabolism will enable the refinement of metabolic models (Ahn & Antoniewicz 2013). The use of such models may one day enable metabolomic screening of CHO transfectants, early in development processes, in order to select the most desirable clones for the production of biopharmaceuticals.

1.5 Aims and objectives

Cell line development is a time consuming and costly facet of biopharmaceutical production. Efforts to improve product yield through cell line engineering has shown mixed results, whilst environmental optimisation has seen some successes. Phenotypic drift in CHO cell populations can be problematic during cell line development. However, this inherent variability, can also lead to beneficial phenotypes that can be exploited for biopharmaceutical production. Defining a beneficial phenotype is complex and many cellular parameters must be considered, including proliferation, maximum cell density, transcription, translation and the metabolic state of the cells. The balance of such parameters will influence specific productivity and overall product yields.

MedImmune have developed a panel of in-house suspension CHO clonal host cell lines that, along with the non-clonal parent population, were cultured for 40-50 generations prior to cell bank creation. It is hypothesised that within a population, there are some cells that would be the 'best' or have the maximum potential in a cell line development process. An in-depth characterisation and understanding of the phenotype and variation within and between clonal cell lines, will enable the generation of a set of "rules" and markers that can be used to identify desirable cell lines for the expression of protein-based biopharmaceuticals.

The overall aim of this project was to gain an improved understanding of CHO cell phenotypic variability and identify metabolic parameters that relate to productivity. There are many published works that have investigated the variability in clonally derived CHO transfectants. However, an improved understanding of the relationship between the host cell line phenotype and the characteristics of progeny transfectants, has the potential to streamline cell line development processes. Additionally, metabolomic techniques have the potential to identify metabolic markers that may be predictive of the most productive cell phenotypes. A greater understanding of CHO cell metabolic parameters could allow further optimisation of cell line development processes.

The main objectives of this project are:

- To analyse phenotypic variability of a panel of clonal host cell lines derived from a non-clonal population.
- To determine the variability of transfectants derived from clonal host cell lines in relation to a non-clonal host cell line.

- To determine the response of transfectants to feed.
- To assess the heritability of host cell line phenotype in transfectant populations.
- To identify metabolic markers that are related to productivity.

2. Materials and Methods

2.1 Materials and equipment

2.1.1 Sources of chemicals, reagents and equipment

A full list of the suppliers for all reagents and equipment used can be found in Appendix A.

2.1.2 Preparation and sterilisation of solutions

All aqueous solutions were prepared using Type 1 water, unless otherwise stated. Phosphate buffered saline (PBS) solution was prepared using PBS tablets according to the manufacturer's instructions. Solutions were sterilised using a Prestige Medical Classic Media autoclave. Alternatively, where autoclaving was inappropriate, solutions were filtered using a 0.22 μm membrane syringe filter. Solutions were stored at room temperature or according to the manufacturer's instructions.

2.1.3 pH measurements

Measurements of pH were made using Mettler Toledo SevenEasy pH meter (calibrated according to the manufacturer's instructions), unless otherwise stated. pH was adjusted using 1M hydrochloric acid and/or 1M sodium hydroxide, unless otherwise stated.

2.2 Generation and purification of plasmids in bacterial cells

2.2.1 Bacterial growth medium

For bacterial growth 2xTY medium (1.6% [w/v] tryptone, 1% [w/v] yeast extract, 0.5% [w/v] sodium chloride, pH 7.0, supplemented with 100 $\mu\text{g ml}^{-1}$ ampicillin, was used. Solid medium was prepared as 2xTY medium with the addition of 1.5% [w/v] agar. 100 $\mu\text{g ml}^{-1}$ ampicillin was added whilst the 2xTY agar medium was liquid, but had cooled to $<55\text{ }^{\circ}\text{C}$. Approximately 20 ml of this medium was poured into 90 mm, sterile Petri dishes and allowed to cool. The Petri dishes were then stored, inverted, at $4\text{ }^{\circ}\text{C}$ until required.

2.2.2 Transformation of Z-competent *E. coli* cells

Z-competent DH5 α cells (100 μl) were thawed on ice. 100 ng plasmid DNA was added to the thawed cells, gently mixed and incubated on ice for 10 minutes. 20 μl of transformed cells were mixed with 80 μl of 2xTY medium and spread on 2xTY agar plates (Section

2.2.1) with an L-shaped spreader. Plates were incubated overnight in a static incubator at 37 °C for colonies to form.

2.2.3 Extraction of plasmid DNA

Starter cultures were prepared by the inoculation of 5 ml 2xTY medium, supplemented with 100 µg ml⁻¹ ampicillin, with a single colony of transformed *E. coli* from a plate culture (Section 2.2.2), or by taking a sample with an inoculation loop from a glycerol stock (Section 2.2.6). Starter cultures were incubated at 37 °C, 300 rpm in a shaking incubator for approximately 6 hours. Maxi prep cultures of 100 ml 2xTY medium, supplemented with 100 µg ml⁻¹ ampicillin, were inoculated with 1 ml starter culture and incubated at 37 °C, 300 rpm in a shaking incubator overnight (approximately 15 hours). Cells were harvested by centrifugation at 3,600 x g, at 4 °C for 30 minutes. The supernatant was discarded and plasmid was prepared from the pellet using a Qiagen HiSpeed Plasmid Maxi kit. The manufacturer's instructions were followed when harvesting high-copy number plasmids.

2.2.4 Linearisation, phase lock gel extraction (PLG) and ethanol precipitation of plasmid DNA

120 µg plasmid DNA was combined with 30 µl Pvu I restriction endonuclease, 45 µl Buffer H and tissue culture grade water up to a final volume of 450 µl. The reaction was incubated overnight at 37°C in a dry block heater. The plasmid DNA was cleaned using 2 ml PLG heavy tubes according to the manufacturer's instructions. Recovered DNA was precipitated in (relative to the initial digest volume) 2 volumes, ice-cold ethanol and 0.1 volumes, 3 M sodium acetate (relative to the initial PLG volume). The material was mixed by rapid inversion and incubated at -20 °C for 30 minutes. The material then was centrifuged at 12,000 x g, 4 °C for 30 minutes. The supernatant was discarded and the DNA pellet was suspended in ice-cold 70% ethanol, briefly vortexed and centrifuged at 12,000 x g, 4 °C for 10 minutes. The supernatant was removed and the pellet air-dried for 10 minutes. The pellet was resuspended in 100 µl tissue culture grade water. The DNA was analysed for complete digestion by agarose gel electrophoresis (Section 2.6.1.6) and the concentration determined using a NanoDrop UV/Vis spectrophotometer (Section 2.2.5).

2.2.5 Determination of nucleic acid concentration

Nucleic acid concentrations were determined using a NanoDrop ND-1000 UV/Vis spectrophotometer, according to manufacturer's instructions. Purity was assessed by the A260 nm/A280 nm ratio, a ratio of 1.6-2.0 was considered pure.

2.2.6 Preparation of glycerol stocks

In a 2 ml cryovial, 500 μ l 50% glycerol [v/v] was combined with 1000 μ l *E. coli* culture following overnight incubation (Section 2.2.3) and gently mixed by pipetting. The preparation was stored at -80 °C.

2.3 Mammalian cell culture

2.3.1 Revival from liquid nitrogen

Vials of cryopreserved cells (Section 2.3.6) were thawed briefly (1-2 minutes) in a 37°C water bath before the content was transferred into 30 ml of fresh cell culture medium. A 1 ml sample of the suspension was taken for cell counting (Section 2.3.4). The remaining cell suspension was then used to produce a 30 ml culture at 0.3×10^6 cells ml^{-1} in a 125 ml vented-cap Erlenmeyer flask, by further dilution with culture medium. Following this, flasks were transferred to a cell culture incubator and subcultured after 3 days as described in Section 2.3.2.

2.3.2 Maintenance of cell lines

CHO host cell lines, derived from CHO-K1, were cultured in CD CHO medium supplemented with 6 mM L-glutamine, unless otherwise stated. Transfected cells were cultured in CD CHO medium supplemented with 50 μ M methionine sulfoximine (MSX). All cultures were incubated in an orbital shaking incubator set at 140 rpm, \varnothing 25 mm, 37 °C, 5% [v/v] CO₂ and 70% humidity unless otherwise stated. Host cells were routinely subcultured in 30 ml or 50 ml medium in 125 ml or 250 ml vented-cap Erlenmeyer flasks, respectively. Cells were subcultured with a seeding density of 0.2×10^6 cells ml^{-1} on a rolling 3-day/4-day cycle unless otherwise stated. All solutions were sterilised by the manufacturer or as described in Section 2.1.2.

2.3.3 Batch and fed-batch culture

Batch cultures of host cell lines were seeded into 250 ml vented-cap Erlenmeyer flasks at a density of 0.2×10^6 cells ml^{-1} in 50 ml CD CHO medium supplemented with 6 mM L-glutamine, unless otherwise stated. Batch cultures of transfected cells were seeded into 125 ml vented-cap Erlenmeyer flasks at 0.5×10^6 cells ml^{-1} in 35 ml CD CHO medium supplemented with 50 μM MSX. Fed-batch cultures of transfected cells were seeded into 250 ml vented-cap Erlenmeyer flasks at 0.5×10^6 cells ml^{-1} in 35 ml growth medium. During fed-batch culture, 3.5 ml of a proprietary feed (supplied by MedImmune) was added on days 3, 5, 7, 9 and 11 of culture. All flasks were incubated as stated in Section 2.3.2.

2.3.4 Determination of cell number and viability

Methods of cell viability testing were based on trypan blue dye exclusion. During Sonata cell culture (Section 2.3.5), cell density, viability and cell diameter was determined using an Innovatis Cedex cell counter according to the manufacturer's instructions. During manual cell culture, cell density and viability were determined using a Beckman Coulter Vi-CELL XR or Invitrogen Countess Automated Cell Counter according to the manufacturer's instructions. Cell diameter data was also acquired using the Vi-CELL XR system. Where appropriate, dilutions were prepared using PBS solution.

2.3.5 Sonata cell culture

In addition to manual cell culture, some cell culture was performed using a TAP Biosystems Sonata system. This system was used to culture cells in a manner that closely reflects manual techniques. The Sonata was programmed to follow the routines set out in Sections 2.3.2 and 2.3.3. Counting of cells in the Sonata was performed using the online Cedex cell counter described in Section 2.3.4. The Sonata includes a built-in humidified incubator which was set to 113 rpm, \varnothing 25 mm, 37 °C, 5% CO_2 .

2.3.6 Cryopreservation of cells

Cells were centrifuged at 130 x g for 5 minutes at room temperature and the supernatant was discarded. The cell pellet was resuspended in CD CHO medium supplemented with 7.5% [v/v] dimethylsulphoxide (DMSO) to give 1×10^7 cells ml^{-1} . 1 ml aliquots were distributed into 1.8ml cryovials, and the vials placed into Mr Frosty pots. When filled, Mr

Frosty pots containing isopropanol were cooled at -80°C overnight. Subsequently, the vials were transferred to vapour phase liquid nitrogen storage.

2.3.7 Nucleofection of host cell lines

All CD CHO medium used for transfection was equilibrated with 5% [v/v] CO_2 in air, and warmed to 37°C prior to use. Linearized plasmid DNA (Section 2.2.4) was diluted to $0.4\ \mu\text{g}\ \mu\text{l}^{-1}$ to standardise the volume of DNA added per nucleofection event. For the generation of clonal transfectants, $2\ \mu\text{g}$ DNA was used per transfection. For stable pool generation, $6\ \mu\text{g}$ DNA was used per transfection. 1×10^7 cells were harvested from maintenance flasks on day 2 of routine subculture and centrifuged at $130 \times g$ for 5 minutes at room temperature. The supernatant was discarded and the cell pellet was resuspended in $100\ \mu\text{l}$ Amaxa Nucleofector solution. The cell suspension and DNA were transferred to Amaxa Nucleofector cuvettes. An Amaxa Nucleofector 2b Device was used to complete the nucleofection. Following nucleofection either Section 2.3.8, for stable pools, or Section 2.3.9, for clonal transfectants, was followed.

2.3.8 Generation of polyclonal pools

Following nucleofection (Section 2.3.7), the cells from two cuvettes (i.e. two independent nucleofection events) were combined and transferred to $40\ \text{ml}$ CD CHO medium in a $250\ \text{ml}$ vented-cap Erlenmeyer flask. The flasks were incubated as stated in Section 2.3.2. After 24 hours, $6\ \text{ml}$ CD CHO medium supplemented with $383\ \mu\text{M}$ MSX was added to each flask to achieve a final concentration of $50\ \mu\text{M}$ MSX.

2.3.9 Generation of clonal transfectants

Following each nucleofection event (Section 2.3.7), cells from a single cuvette were diluted in $192\ \text{ml}$ CD CHO medium. The suspension was distributed over 20 96-well plates at $50\ \mu\text{l}\ \text{well}^{-1}$. The cells were incubated in a humidified static incubator set at 37°C and 5% [v/v] CO_2 . After 24 hours, $150\ \mu\text{l}$ CD CHO medium supplemented with $66.6\ \mu\text{M}$ MSX was added to each well to achieve a final concentration of $50\ \mu\text{M}$ MSX. The cells were returned to the incubator for 3 weeks to allow colonies to grow. Single colonies were identified by eye and $150\ \mu\text{l}$ supernatant was sampled from these wells for mAb titre analysis (Section 2.5.1). The cells from these wells were then transferred to 24-well plates in $1\ \text{ml}$ CD CHO supplemented with $50\ \mu\text{M}$ MSX and returned to the static incubator. In 24-well plate format, the cells were subcultured every 7 days, by adding $200\ \mu\text{l}$ cell

suspension to fresh 24-well plates containing 800 μl growth medium. To adapt transfectants to shake culture, 750 μl aliquots of cell suspension were transferred from the 24-well plates to T25 flasks containing 3.5 ml growth medium and incubated under static conditions. After 6 days, 2 ml growth medium was added to each flask and the flasks were then transferred (upright) to an orbital shaking incubator (Section 2.3.2). After 24 hours, the transfectants were counted and subcultured to 125 ml vented-cap Erlenmeyer flasks at 3×10^5 cells ml^{-1} in a 20 ml volume. The transfectants were then maintained according to standard conditions (Section 2.3.2) and cryopreserved (Section 2.3.6).

2.4 Metabolite analysis

2.4.1 Glucose, lactate, glutamine and glutamate analysis

1 ml samples were taken from batch and fed-batch cultures and centrifuged at $130 \times g$ for 5 minutes. 200 μl aliquots were transferred to a 96-well plate and analysed for glucose, lactate, glutamine and glutamate using YSI 2900 Biochemistry Analyzers according to the manufacturer's instructions.

2.4.2 Gas chromatography-mass spectrometry (GC-MS)

2.4.2.1 Sample preparation and derivitisation

Samples were collected as described in Section 2.4.1, 700 μl of the sample supernatant was transferred to a clean 1.5 ml microcentrifuge tube and stored at $-80\text{ }^\circ\text{C}$ until required. 20 μl of cell culture supernatant was mixed with 5 μl internal standard myristic- d_{27} acid (3 mg ml^{-1} [w/v] in 2:5:2 water/methanol/isopropanol) in 1.5 ml microcentrifuge tubes, 200 μl of methanol was then added to precipitate any protein present. The samples were centrifuged at $12,000 \times g$ for 2 minutes and the supernatants transferred to clean microcentrifuge tubes. The material was dried using an Eppendorf Concentrator plus vacuum centrifuge at $30\text{ }^\circ\text{C}$ prior to storage at $-80\text{ }^\circ\text{C}$. Samples were dried for 5 minutes using a vacuum centrifuge at $30\text{ }^\circ\text{C}$ and derivitised in 10 μl methoxyamine hydrochloride (MOX, 40 mg ml^{-1} [w/v] in pyridine) at $30\text{ }^\circ\text{C}$, 120 rpm in a shaking incubator for 90 minutes. Next, 90 μl N-methyl-N-(trimethylsilyl)trifluoroacetamide + 1% (v/v) trichloromethylsilane (MSTFA + 1% TCMS) was added and the samples incubated at $37\text{ }^\circ\text{C}$ for 30 minutes. Derivitised samples were centrifuged at $12,000 \times g$ for 2 minutes, the supernatant was transferred to silanized glass vials immediately prior to GC-MS analysis.

Intracellular metabolite samples were prepared from 1×10^7 viable cells according to Sellick (2011). Following metabolite extraction, 5 μl internal standard myristic- d_{27} acid (3 mg ml^{-1} [w/v] in 2:5:2 water/methanol/isopropanol) was added and the samples were dried and derivitised as described for the culture supernatant samples (above).

2.4.2.2 Sample injection

Samples were randomized and loaded onto an Agilent 7685B series autosampler, the sequence was programmed into the operating software running on the control PC (MSD Chemstation E.02.00.493, Agilent Technologies). Samples were injected into the GC inlet using a 7685B series injector fitted with a 10 μl Agilent Gold Standard Syringe. The syringe was washed with pyridine (4 x 10 μl washes) immediately prior to each 1 μl sample injection.

2.4.2.3 Gas chromatography

Gas chromatography was performed using an Agilent 7890A GC System on a DB-5ms (30 m, 0.25 mm, 0.25 μm) + DuraGuard (10 m) column using helium carrier gas (1.2 ml/minute flow rate). The system was retention time-locked to myristic- d_{27} acid. Components were separated by isothermal chromatography for 1 min at 60°C, followed by an increase to 325°C at a rate of 10°C/min then 10 min at 325°C.

2.4.2.4 Mass spectrometry

An Agilent 5975C Inert XL MSD with Triple-Axis Detector was used for mass spectrometry. Prior to use, the mass spectrometer was tuned using perfluorotributylamine as a calibration compound. The instrument was used in positive ion mode using an electron impact source and mass spectra were scanned from 50 to 600 mass units. The source temperature was 250 °C and the quadrupole temperature was 150 °C.

2.4.2.5 Data processing

Metabolite peaks from the raw chromatograms were identified using MSD Chemstation. The software compared the observed mass spectra against the Fiehn mass spectral library. Peak identifications were based on retention time and fragmentation pattern matching. The software used one representative fragment ion (quantification ion) from each peak for quantification, and a further two fragment ions (qualification ions) were

quantified and used for qualification. For a successful identification, the observed ratio of the qualification ions to the quantification ion were required to be within 20% of the expected ratio from the Fiehn mass spectral library. Data were exported from Chemstation as a custom report into Microsoft Excel for analysis. The data were normalized to the internal standard (myristic-d₂₇ acid). The data processing protocol was developed by Dr David Knight (Biomolecular Analysis Core Facility, University of Manchester).

2.5 Protein analysis

2.5.1 Analysis of mAb titre

Samples were taken from batch and fed-batch cultures and centrifuged at 130 x g for 5 minutes. The supernatant was analysed using a FortéBIO Octet 384QK according to the manufacturer's instructions.

2.5.2 Western blot analysis

2.5.2.1 Protein extraction

Protein samples were prepared from cell cultures to provide material for Western blot and GS activity assays. 2.5×10^7 cells were harvested and centrifuged for 5 minutes at 130 x g at room temperature. Culture supernatant was then discarded and the cells were resuspended in 1 ml PBS and transferred to a 1.5 ml microfuge tube. The samples were centrifuged for 5 minutes at 130 x g, the supernatant was discarded and the pellets were then placed on ice. The pellets were resuspended in 500 μ l Mammalian Protein Extraction Reagent (MPER) containing 1 x Halt protease inhibitor. The samples were incubated on ice for 10 minutes with occasional inversion to mix. Following the incubation, the samples were centrifuged for 5 minutes at 16,000 x g at 4 °C. The lysate (supernatant) was transferred to clean 1.5 ml microcentrifuge tubes and stored at -80 °C.

2.5.2.2 Bradford assay

Bovine serum albumin (BSA, 100 μ g ml⁻¹ [w/v] in water) was used to generate a 9-point standard curve (0-66.7 μ g ml⁻¹ [w/v]). Protein samples (Section 2.5.2.1) were diluted (typically 1:200 in water) and 1 μ l standard/sample was added to a 96-well plate in triplicate. Bio-Rad Protein Assay Dye Reagent Concentrate was diluted 1:2 [v/v] in water and 60 μ l of reagent was added to each well. The samples were incubated for 5 minutes

at room temperature and the absorbance was measured at 570 nm using a PowerWave microplate spectrophotometer. Protein concentration of the samples was determined by interpolation of the standard curve.

2.5.2.3 SDS-PAGE

The XCell SureLock gel apparatus was used with Novex NuPAGE 4-12% bis-tris, 15-well gels for SDS-PAGE. 10 µg protein was added to each gel lane. Protein samples of known concentration (Section 2.5.2.2) were mixed with 4x sample buffer (40% [v/v] glycerol, 240 mM Tris-HCl pH 6.8, 8% [w/v] SDS, 0.04% [w/v] bromophenol blue), 10% [v/v] β-mercaptoethanol and water to achieve 10 µg protein per 15 µl. Samples were incubated at 95 °C for 1 minute, briefly vortexed and centrifuged at 1,000 x g for <1 minute. The XCell SureLock gel apparatus was assembled according to the manufacturer's instructions and the upper and outer reservoirs were filled with 1x MES running buffer. 10 µl pre-stained protein marker and 15 µl protein samples were loaded into duplicate gels and electrophoresed at 200 V until the dye front reached the bottom of the gel (approximately 40 minutes).

2.5.2.4 Protein transfer

Immediately following SDS-PAGE (Section 2.5.2.3) separated proteins were transferred to nitrocellulose membranes. Membranes and thick filter papers were pre-soaked for 5 minutes in blotting buffer (25mM Tris base, 190mM glycine, 20% [v/v] methanol, pH 7.4). Proteins were transferred on a Bio-Rad Trans-Blot SD Semi-Dry Transfer Cell at 15 V for 45 minutes. Successful transfer was determined by incubation of the membrane with Ponceau-S solution (0.1% [w/v] in 5% acetic acid). Ponceau-S staining was removed by 3 washes for 2 minutes each with PBS-Tween (1% [v/v] Tween-20).

2.5.2.5 Antibody probing and detection

Membranes (Section 2.5.2.4) were incubated in blocking buffer (5% [w/v] skimmed milk powder in PBS-Tween (1% [v/v] Tween-20)) at 4 °C overnight on an orbital platform. The primary antibodies were diluted, as described in Table 2.1, in Ab incubation buffer (2.5% [w/v] skimmed milk powder in PBS-Tween). 10 ml diluted antibody solution was added to each membrane and incubated for 1 hour at room temperature on an orbital shaking platform, then washed 4 times with 30 ml PBS-Tween. The secondary antibodies were diluted, as described in Table 2.1, in Ab incubation buffer; 10 ml was added to the

membranes prior to 1 hour incubation at room temperature on an orbital shaking platform. Following incubation, membranes were washed 4 times with 30 ml PBS-Tween and the proteins were detected using a LI-COR Odyssey Imaging System. Protein band detection was confirmed by comparison to the molecular weight markers and the intensity was determined using ImageJ for densitometric analysis.

Table 2.1 Antibodies used for Western blot

| Protein | Primary antibody | Dilution | Secondary antibody | Dilution |
|-------------------------|-----------------------------------|----------|--------------------------------------|----------|
| ERK 2 | ERK2 (6H3) mouse monoclonal | 1:5,000 | IRDye 800CW donkey anti- mouse | 1:10,000 |
| Glutamine synthetase | GS rabbit monoclonal | 1:10,000 | IRDye 800CW donkey anti-rabbit | 1:10,000 |

2.5.2.6 Densitometric analysis

The positions of protein bands were compared to that of the molecular weight markers. The intensity of bands was determined by densitometric analysis using ImageJ software.

2.5.3 GS activity assay

Protein samples were prepared as in Section 2.5.2.1 and protein concentration determined as in Section 2.5.2.2. Protein samples were diluted in MPER to fix the protein concentration at 2 mg ml⁻¹ and stored on ice until needed. L-glutamic acid γ -monohydroxamate (100 mM stock solution) was diluted in assay buffer (25 mM manganese (II) chloride, 25 mM hydroxylamine, 100 mM glutamine, 0.32 mM ADP, 50 mM imidazole, 25 mM sodium arsenate) to prepare a 12-point standard curve (0-20 mM). 30 μ l standard/sample was added to a 96-well plate in triplicate and mixed with 50 μ l assay buffer. The plates were sealed and incubated at 37 °C for 1 hour. 133.3 μ l stop solution (2.42% [w/v] ferric (III) chloride, 18.1 mM hydrochloric acid, 12.5 mM trichloroacetic acid) was added to each well and the absorbance was measured at 540 nm, using a Polarstar OPTIMA microplate reader. γ -glutamyl-hydroxamate concentration was determined by interpolation of the standard curve.

2.6 Isolation, handling and analysis of RNA/DNA

For all procedures involving RNA and/or DNA, solutions were prepared using 0.05% [v/v] diethyl pyrocarbonate (DEPC)-treated water. DEPC was added to Type 1 water and incubated overnight at room temperature, the solution was then autoclaved before use.

2.6.1 mRNA analysis

2.6.1.1 Trizol mRNA extraction

5×10^6 cells were harvested from culture and centrifuged at $130 \times g$ for 5 minutes at room temperature. The supernatant was discarded and the pellet was resuspended in 1 ml TRIzol reagent. Samples were stored at -80°C until required. Samples were thawed and incubated for 5 minutes at room temperature. 300 μl of chloroform was added to each sample then tubes were shaken vigorously for 15 seconds. After incubation for 15 minutes at room temperature the material was centrifuged at $12,000 \times g$ for 15 minutes at 4°C . The aqueous phase was transferred to a 1.5 ml microcentrifuge tube and 600 μl isopropanol was added to precipitate the RNA. The material was incubated for 10 minutes at room temperature, and then centrifuged at $12,000 \times g$ for 10 minutes at 4°C . The supernatant was discarded and the RNA pellet was washed with 1 ml 75% [v/v] ethanol by vortex mixing. Extracts were centrifuged at $7,500 \times g$ for 5 minutes at 4°C , the supernatant was discarded and the pellet was air-dried for 5-10 minutes. The pellet was dissolved in 30 μl water and incubated for 10 minutes at $55-60^\circ\text{C}$. RNA extracts were stored at -80°C until required.

2.6.1.2 DNase treatment of mRNA

RNA was treated with DNase I to remove any contaminating DNA. The nucleic acid concentration of samples was determined using a NanoDrop UV/Vis Spectrophotometer (Section 2.2.5). In a 1.5 ml microcentrifuge tube, 1 μg of RNA, 1 μl 10 x reaction buffer, and 1 μl DNase I were combined and the solution was made up to a final volume of 10 μl with water. After mixing gently, the tubes were incubated for 60 minutes at 37°C , and then 1 μl stop solution was added. Samples were heated for 10 minutes at 70°C . Samples were cooled on ice and stored at -80°C for storage until required.

2.6.1.3 Qiagen RNeasy Plus Mini Kit mRNA extraction

1.5 x10⁶ cells were harvested from culture and centrifuged at 2,000 x g for 5 minutes at 4 °C. The supernatant was discarded and the pellet was resuspended in 600 µl Qiagen buffer RLT Plus, supplemented with 1% [v/v] β-mercaptoethanol. This material was stored at -80 °C until required. The samples were thawed on ice and the RNA was extracted using a Qiagen RNeasy Plus Mini kit according to the manufacturer's instructions using a Qiagen QIAcube instrument. Extracted RNA was stored at -80 °C until required.

2.6.1.4 cDNA synthesis

For host cell line glutamine synthetase (Section 3.4) and mAb-109 (Section 4.3.3) analysis, cDNA was generated using a Bioron Tetro cDNA synthesis kit. Samples of DNase-treated RNA (Section 2.6.1.2) were thawed, quantified (Section 2.2.5) and stored on ice until required. A reaction master mix was prepared (according to the manufacturer's instructions) in a microcentrifuge tube on ice, for each sample 1 µl oligo (dT)₁₈ primer, 1 µl 10 mM dNTP mix, 4 µl 5 x RT buffer, 1 µl Ribosafe RNase inhibitor and 1 µl Tetro reverse transcriptase was added and mixed. In clean 0.2 ml PCR tubes, 1 µg RNA was combined with 8 µl master mix and the total volume was adjusted to 20 µl with water. The material was incubated at 45 °C for 30 minutes and the reaction was terminated by incubation at 85 °C for 5 minutes followed by a final hold at 4 °C, using a TC-3000 thermal cycler. Reverse transcriptase negative control samples were prepared identically, however the Tetro reverse transcriptase was substituted with water. Samples were chilled on ice for 2 minutes, and then stored at -20°C until used in further analytical procedures.

For transfectant GS (Section 4.3.5) analysis, cDNA was generated using a Life Technologies SuperScript VILO MasterMix kit. Samples of RNA (Section 2.6.1.3) were quantitated (Section 2.2.5) and stored on ice until required. In clean 0.2 ml PCR tubes, 500 ng RNA (Section 2.6.1.3) was combined with 4 µl SuperScript VILO MasterMix and the total volume was adjusted to 20 µl with water. The material was incubated at 25 °C for 10 minutes, 42 °C for 30 minutes and the reaction was terminated by incubation at 85 °C for 5 minutes followed by a final hold at 4 °C, using a Mastercycler Pro thermal cycler. Reverse transcriptase negative control samples were prepared identically, however they used SuperScript VILO MasterMix that had been heat inactivated by incubation at 65 °C for 20 minutes. Following the reaction, each sample was diluted using 80 µl water ready for subsequent use. Samples were chilled on ice for 2 minutes, and then stored at -20°C until required.

2.6.1.5 PCR to verify primer design

Primers were designed using the web-based primer design tool Primer3 (Koressaar & Remm 2007; Untergasser et al. 2012). Primers were supplied by Eurofins MWG Operon. A list of PCR primers used is shown in Table 2.2 and 2.3 (Section 2.6.1.7 and 2.6.2.2).

PCR reactions were performed using Bioline BIOTAQ DNA polymerase and Bioline 100 mM dNTP mix. A reaction master mix was prepared in a microcentrifuge tube on ice, for each sample 5 μ l 10 x NH_4 reaction buffer, 2.5 μ l MgCl_2 , 1 μ l 100 mM dNTP mix, 2 μ l 10 μ M sense primer, 2 μ l 10 μ M antisense primer, 36 μ l water and 0.5 μ l DNA polymerase was added and mixed. For each reaction, 49 μ l master mix was added to a 0.2 ml PCR tube containing 1 μ l cDNA template (Section 2.6.1.4). The tubes were briefly vortex-mixed and centrifuged before placing into a TC-3000 thermal cycler.

The following thermal profile was used for standard PCR: Denaturation for 5 minutes at 94 °C, then 30 cycles of denaturation for 30 seconds at 94 °C, annealing for 30 seconds at 58 °C, and extension for 30 seconds at 72 °C. After the 30 cycles there was a final extension step for 10 minutes at 72 °C. The completed reactions were stored at 4 °C until required.

2.6.1.6 Agarose gel electrophoresis

Agarose powder was added to 1x TBE buffer (89 mM Tris base, 89 mM boric acid, and 2 mM EDTA) to achieve a final concentration of 2% [w/v]. This mixture was heated to dissolve the agarose and then allowed to cool to ~55 °C, before 10 μ l per 100 ml gel solution SafeView nucleic acid stain was added. The solution was poured into a prepared horizontal gel tank and allowed to solidify. 16 μ l PCR products (Section 2.6.1.5) were mixed with 4 μ l 5x sample loading buffer (supplied with HyperLadder 25bp) and the mixture was loaded into wells on the agarose gel. HyperLadder 25bp molecular weight marker was used for size determination of PCR products. Electrophoresis was performed in 1x TBE buffer for approximately 60 minutes at 100 V, until the dye front had migrated sufficiently to visualise PCR products with ultraviolet transillumination. Images were acquired using a BioRad ChemiDoc MP system.

To resolve DNA plasmids, separation was performed with a 1% [w/v] agarose gel. This was prepared following the same methodology as for a 2% gel.

2.6.1.7 qRT-PCR for mRNA analysis

Primers were designed as described previously (Section 2.6.1.5) or provided by MedImmune. A list of qRT-PCR primers used is shown in Table 2.2.

Glutamine synthetase mRNA expression was determined using TaqMan technology. The following reagents were added to a translucent 96-well PCR plate: 10 μ l TaqMan Gene Expression MasterMix, 1 μ l 18s ribosomal TaqMan probe/primers (VIC), 1 μ l GS probe/primers (FAM), 3 μ l water, 5 μ l template cDNA (Section 2.6.1.4). Plates were sealed and centrifuged for 1 minute at 1000 x g. The PCR reaction was performed using an Applied Biosystems ABI7000MBI instrument using the following thermal profile: DNA polymerase activation for 10 minutes at 95 °C, then 30 cycles of denaturation for 15 seconds at 95 °C, annealing/extension for 60 seconds at 60 °C.

mAb-109 mRNA expression was determined using SYBR green technology. The following reagents were added to each well of a translucent 96-well plate: 10 μ l 2x SensiFast SYBR Hi-ROX, 0.8 μ l 10 μ M sense primer, 0.8 μ l 10 μ M antisense primer, 8.4 μ l cDNA (Section 2.6.1.4). The plate was sealed and centrifuged for 1 minute at 1000 x g. The PCR reaction was performed using a Life Technologies StepOne Plus instrument with the following thermal profile: DNA polymerase activation for 2 minutes at 95 °C, followed by 30 cycles of denaturation for 5 seconds at 95 °C, annealing for 10 seconds at 58 °C, extension for 20 seconds at 72 °C. A melting curve was generated to check the quality of the amplified product.

All qRT-PCR data was analysed using the $\Delta\Delta$ Ct method (Livak & Schmittgen 2001).

Table 2.2 Primers used for mRNA analysis

| Target gene | Sense primer* | Anti-sense primer* | Probe* |
|-------------------------|-----------------------|----------------------|----------------------|
| mAb-109 heavy chain | CGGCAAGGAATACAAGTGCA | TTCTTGGTCATCTCCTCCCG | - |
| mAb-109 light chain | CTCACCGTCCTTGACACGAA | TCATCTGGATGTCCGAGTGC | - |
| β_2 microglobulin | ACGGAGTTTACACCCACTGC | CAGACCTCCATGATGCTTGA | - |
| Glutamine synthetase | AGCCTATGGCAGGGATATCGT | TTGACCCAGCATACAAGCA | Proprietary sequence |

* All primers are written 5'-3'.

2.6.2 Recombinant gene copy number analysis

2.6.2.1 Genomic DNA extraction

Genomic DNA (gDNA) was extracted using a Life Technologies PureLink Genomic DNA kit. Cells were cultured as described in Section 2.3.3. On day 3 of culture, medium containing 5×10^6 cells was transferred to a microcentrifuge tube and centrifuged at $250 \times g$ for 5 minutes. The supernatant was discarded and the cells were resuspended in 200 μ l PBS. 20 μ l of Proteinase K, followed by 20 μ l RNase A was added to the cells. The suspension was briefly vortexed and incubated for 2 minutes at room temperature. 200 μ l PureLink Genomic Lysis/Binding Buffer was added to the cells, the samples were vortexed to achieve a homogeneous solution. The samples were incubated for 10 minutes at 55 °C, following which 200 μ l 100% ethanol was added prior to vortex mixing for 5 seconds. The lysed samples were transferred to PureLink Spin Columns and centrifuged at $10,000 \times g$ for 1 minute at room temperature. The collection tubes were removed from the Spin Columns, discarded and replaced with clean collection tubes. 500 μ l Wash Buffer 1 was added to each Spin Column prior to centrifugation at $10,000 \times g$ for 1 minute. The collection tubes were discarded and replaced with clean collection tubes. 500 μ l Wash Buffer 2 was added to each Spin Column prior to centrifugation at $13,000 \times g$ for 3 minutes. The collection tubes were replaced with 1.5 ml microcentrifuge tubes. 50 μ l water was added to each Spin Column prior to incubation for 1 minute at room temperature. The Spin Columns were then centrifuged at $13,000 \times g$ for 1 minute to elute the purified gDNA. The gDNA samples were stored at -20 °C until required.

2.6.2.2 qRT-PCR for gene copy number analysis

Recombinant gene copy number was determined using SYBR green technology. Plasmid DNA was prepared as described in Section 2.2.3. The stock plasmid was quantified (Section 2.2.5) and diluted in water to achieve 300,000 copies per 8.4 μ l. Serial dilutions were then prepared to create a 5 point standard curve (30, 300, 3,000, 30,000 and 300,000 copies per 8.4 μ l). Purified gDNA (Section 2.6.2.1) was diluted in water to achieve 3000 genomes per 8.4 μ l, this calculation was based upon the average CHO genome size of 3.41 pg (Gregory 2014). All plasmid/gDNA solutions were stored on ice until required on the day.

The following reagents were added to each well of a translucent 96-well plate: 10 µl 2x SensiFast SYBR Hi-ROX, 0.8 µl 10 µM sense primer, 0.8 µl 10 µM antisense primer, 8.4 µl plasmid or gDNA template. The plate was sealed and centrifuged for 1 minute at 1000 x g. The PCR reaction was performed using a Life Technologies StepOne Plus instrument with the following thermal profile: DNA polymerase activation for 3 minutes at 95 °C, followed by 30 cycles of denaturation for 5 seconds at 95 °C, annealing for 10 seconds at 58 °C, extension for 15 seconds at 72 °C. A melting curve was generated to check the quality of the amplified product.

Gene copy number was calculated by interpolation of the standard curve.

Table 2.3 Primers used for gene copy number analysis

| Target gene | Sense primer* | Anti-sense primer* |
|---------------------|-------------------------|------------------------|
| GS 1 | TTAAGCTGCAGAAGTTGGTCGT | TGCCTATCAGAAACGCAAGAGT |
| GS 2 | CACTGGGCAGGTAAGTATCAAGG | GGTGCCTATCAGAAACGCAAGA |
| mAb-109 heavy chain | AGGAGGTCAATCTACGGTGGT | GAGGTTCCAGCGTCCAGTGTC |
| mAb-109 light chain | CGCTTCTTGGTCTCCTTGCT | CCCTTGGGTGTGTTGTTTGC |

* All primers are written 5'-3'.

Two GS primer sets were used for analysis, as only the sense primer could be designed to be specific to the recombinant GS sequence

2.7 Flow cytometry

2.7.1 Molecular probe labelling

Cells were cultured as described in Section 2.3.3. When required, 2×10^6 cells were transferred to a microcentrifuge tube and centrifuged for 5 minutes at 300 x g. The supernatant was discarded and the cells were resuspended in 1 ml pre-warmed (37 °C) CD-CHO medium, supplemented with either 10 nM MitoTracker Green FM (MTG) or 10 µg ml⁻¹ rhodamine-123 (Rh-123). The cells were incubated for 15 minutes at 37 °C, prior to centrifugation for 5 minutes at 300 x g. The supernatant was discarded and the cells

were resuspended in PBS supplemented with $1 \mu\text{g ml}^{-1}$ propidium iodide (PI). Controls were prepared following the same procedure with the subsequent amendments. Unstained controls were prepared using CD-CHO (no supplement) and PBS (no supplement). Non-viable controls were prepared using CD-CHO (no supplement) plus $200 \mu\text{l}$ 70% ethanol and PBS supplemented with $1 \mu\text{g ml}^{-1}$ PI. Single stain, molecular probe only controls were prepared using PBS (no supplement). Samples were analysed immediately as described in Section 2.7.2.

2.7.2 Flow cytometric analysis

Samples (Section 2.7.1) were analysed using a BD Accuri C6 flow cytometer with CSampler. MTG and Rh-123 fluorescence was detected using a 530/30 filter, PI fluorescence was detected using a 670/LP filter. Data for 10,000 events on the pre-set slow flow rate were collected for each sample. This data were gated to exclude debris and cell aggregates from the recorded population based on forward and side scatter parameters. The non-viable control was used to gate and therefore exclude dead cells from analysis. The single stain controls were used to apply colour compensation to the data. Data was exported as the median fluorescence intensity (MFI) of the population and normalised against the unstained control.

2.8 Microscopy

2.8.1 Preparation of metaphase spreads

On day 3 of culture (Section 2.3.2), 5 ml of CHO cell suspension was transferred to T25 cell culture flasks and treated with 150 ng ml^{-1} [w/v] of colcemid overnight. The flasks were incubated upright under conditions described in Section 2.3.2. The treated cell suspension was transferred to centrifuge tubes and centrifuged for 5 minutes at $130 \times g$. The supernatant was discarded and the cells were resuspended by agitation in approximately $100 \mu\text{l}$ of supernatant. 10ml of hypotonic solution (75 mM potassium chloride) was added drop-wise with continuous gentle mixing. The cell suspension was incubated for 20 minutes at $37 \text{ }^\circ\text{C}$ prior to centrifugation at $220 \times g$ for 5 min. The supernatant was discarded and the cells were resuspended in $100 \mu\text{l}$ of hypotonic solution. 5ml ice-cold fixative solution (3:1 methanol:acetic acid) was added drop-wise with continuous gentle mixing. This suspension was centrifuged for 5 minutes at $220 \times g$ and the supernatant was discarded. The process of fixative addition and centrifugation was repeated 3x in total. After the final centrifugation, the cells were resuspended in a $500 \mu\text{l}$ ice-cold fixative

solution and stored at -20 °C until required. Approximately 10 µl of cell suspension was dropped, from a height of approximately 10 cm, onto humidified glass slides that had been wiped with fixative solution. Slides were incubated overnight at room temperature.

2.8.2 Metaphase staining

Slides were stained with approximately 10 µl ProLong Gold Antifade Mountant (with DAPI). Coverslips were applied to the specimens and sealed with clear nail varnish. The slides were stored protected from light until images were acquired as described in Section 2.8.3.

2.8.3 Image acquisition and analysis

Images of the metaphase spreads (Section 2.8.2) were collected using an Olympus BX51 upright microscope using a Coolsnap HQ camera (Photometrics) through MetaVue Software (Molecular Devices). Slides were viewed using a 100 x/1.30 UPlanFLN oil immersion objective with a DAPI band pass filter. Images were processed and analysed using ImageJ Software (Schneider et al. 2012).

2.9 Statistical methods

Data presented is represented as a mean ± the standard error of mean (SEM), unless otherwise stated.

$$\text{Standard deviation (SD)} = \left(\sqrt{[\Sigma\{x - m\}^2]/[n - 1]} \right)$$

Where:

x = observed value

m = mean of n observations

n-1 = degrees of freedom

$$SEM = (SD/\sqrt{n})$$

Where:

n = number of independent observations

The independent sample t-test was used to determine whether the difference between data was statistically significant. The independent samples t-test was performed using GraphPad Prism (v6.0). Data was considered significant if $p < 0.05$. Additionally the one-way analysis of variance (ANOVA) test was used to determine whether significant variance was observed between groups. Where appropriate the Tukey post-hoc test was applied to identify where significant differences arose. ANOVA and Tukey tests were performed using GraphPad Prism (v6.0). Data was considered significant if $p < 0.05$. The GraphPad Prism (v6.0) software was also used for correlation analysis and interpolation of standard curves.

2.10 Calculations

2.10.1 Calculation of average cell growth day⁻¹

Average cell growth day⁻¹ during maintenance culture of cells was calculated with the following formula:

$$\text{Average cell growth day}^{-1} = \frac{(X_1 - X_0)}{(T_1 - T_0)}$$

Where:

X_0 = viable cell density ($\times 10^6$ cells ml⁻¹) by first point of analysis i.e. seeding density

X_1 = viable cell density ($\times 10^6$ cells ml⁻¹) by second point of analysis

T_0 = day of first point of analysis i.e. day seeded

T_1 = day of second point of analysis

2.10.2 Calculation of cumulative cell time (CCT)

Cumulative cell time (CCT) was calculated between two points during batch culture using the following formula (N.B. the cumulative (sum) values are used in this report):

$$CCT = \left(\frac{X_1 + X_0}{2} \right) \times (T_1 - T_0)$$

Where:

X_0 = viable cell density ($\times 10^6$ cells ml^{-1}) by first point of analysis

X_1 = viable cell density ($\times 10^6$ cells ml^{-1}) by second point of analysis

T_0 = day of first point of analysis

T_1 = day of second point of analysis

2.10.3 Calculation of cell doubling time

Cell doubling time was calculated using the following formula:

$$\text{Doubling time} = \left[\frac{\ln(2)}{\ln \left\{ \frac{X_1}{X_0} \right\}} \right] \times T \times 24$$

Where:

X_0 = viable cell density ($\times 10^6$ cells ml^{-1}) by first point of analysis

X_1 = viable cell density ($\times 10^6$ cells ml^{-1}) by second point of analysis

T = Time between analysis points (days)

2.10.4 Calculation of specific productivity (Qp) and rates of metabolite production and utilisation

Rates of metabolite production and utilisation were calculated between two points during batch culture using the following formula:

$$Q_p \text{ or rate of production or utilisation} = \frac{\left[\frac{P_1 - P_0}{\left\{ \frac{X_1 + X_0}{2} \right\}} \right]}{T_1 - T_0}$$

Where:

P_0 = antibody titre or metabolite concentration by first point of analysis

P_1 = antibody titre or metabolite concentration by second point of analysis

X_0 = viable cell density ($\times 10^6$ cells ml^{-1}) by first point of analysis

X_1 = viable cell density ($\times 10^6$ cells ml^{-1}) by second point of analysis

T_0 = day of first point of analysis

T_1 = day of second point of analysis

3. Analysis of the phenotypic variability of clonal host cell lines derived from a non-clonal population

3.1 Introductory remarks

A large volume of research has been conducted to increase productivity in mammalian cell cultures. Research typically falls into three main approaches: improvement of expression vectors, medium and process optimisation and host cell line engineering (Dietmair et al. 2011; Birch & Racher 2006). In this chapter, a panel of clonal host cell lines have been characterised as natural genetic variation may result in phenotypic advantages for biopharmaceutical production. The clonal host cell lines were isolated from a non-clonal population, by limiting dilution cloning, then cultured for 40-50 generations prior to the creation of cryopreserved cell banks (Section 1.2.1 and 1.5).

The aim of this Chapter was to analyse variability in the phenotype of a panel of clonally derived, non-producing, host cell lines. In many instances, the non-clonal host cell line (cell line NC), from which the others were derived, is treated as a control. The cells were subjected to a period of long-term culture (LTC); this was performed to investigate growth properties of the cell lines, during an industrially relevant number of generations. The nutrient (glucose, lactate, glutamine and glutamate) utilisation of the cell lines was analysed, as this could indicate metabolic variation between the different hosts. The endogenous GS content of the host cell lines, at an early and late generation, was investigated as GS was used as the selection system following transfection of these host cell lines (Chapter 4). Subsequently, the host cell lines were screened for their mitochondrial membrane potential using a rhodamine-123 fluorescence assay.

3.2 Analysis of growth characteristics of the clonal host cell lines

3.2.1 Analysis of growth characteristics during long-term culture

To investigate the phenotype and variability in clonal host cell lines, seven clonal and non-clonal host cell lines (cell line NC, 10, 15, 16, 19, 20 and 21) were cultured for 81 days using a Sonata cell culture robot (Section 2.3.5). During this period, the growth characteristics were examined. The viable cell density (VCD) and viability of the cultures was monitored at each passage, this enabled the production of a sawtooth-like plot for VCD (Figure 3.1). Initially during the study (first 21 days), cell line NC achieved approximately 5×10^6 cells ml^{-1} VCD by day 4. As the study progressed, the day 4 measurements of VCD for this cell line decreased. At the beginning of the study, cell line 10 followed a similar pattern of growth to cell line NC with day 4 VCD values of

approximately 5×10^6 cells ml^{-1} . Cell lines 15, 20 and 21 achieved greater VCD than cell line NC, day 4 cell counts during the initial 21 days were consistently above 6×10^6 cells ml^{-1} . Cell line 20 demonstrated the greatest VCD of all, with one culture reaching 7.5×10^6 cells ml^{-1} . Conversely, cell lines 16 and 19 both achieved poor day 4 densities compared to cell line NC. Day 4 cell counts for cell line 16 peaked below 4×10^6 cells ml^{-1} , and cell line 19 peaked slightly above 4×10^6 cells ml^{-1} .

As the study progressed past 21 days, the sawtooth growth patterns started to change. A decrease in the day 4 VCD values was observed for all of the cell lines, whilst the opposite became apparent for the day 3 VCD values. This change in the pattern of growth could be an effect of cell age, however it is important to note that the batch of CD-CHO medium was changed at the day 21 passages. CD-CHO is a chemically defined medium, thus the composition should be consistent, however any variation between the batches could have introduced a confounding variable into this experiment.

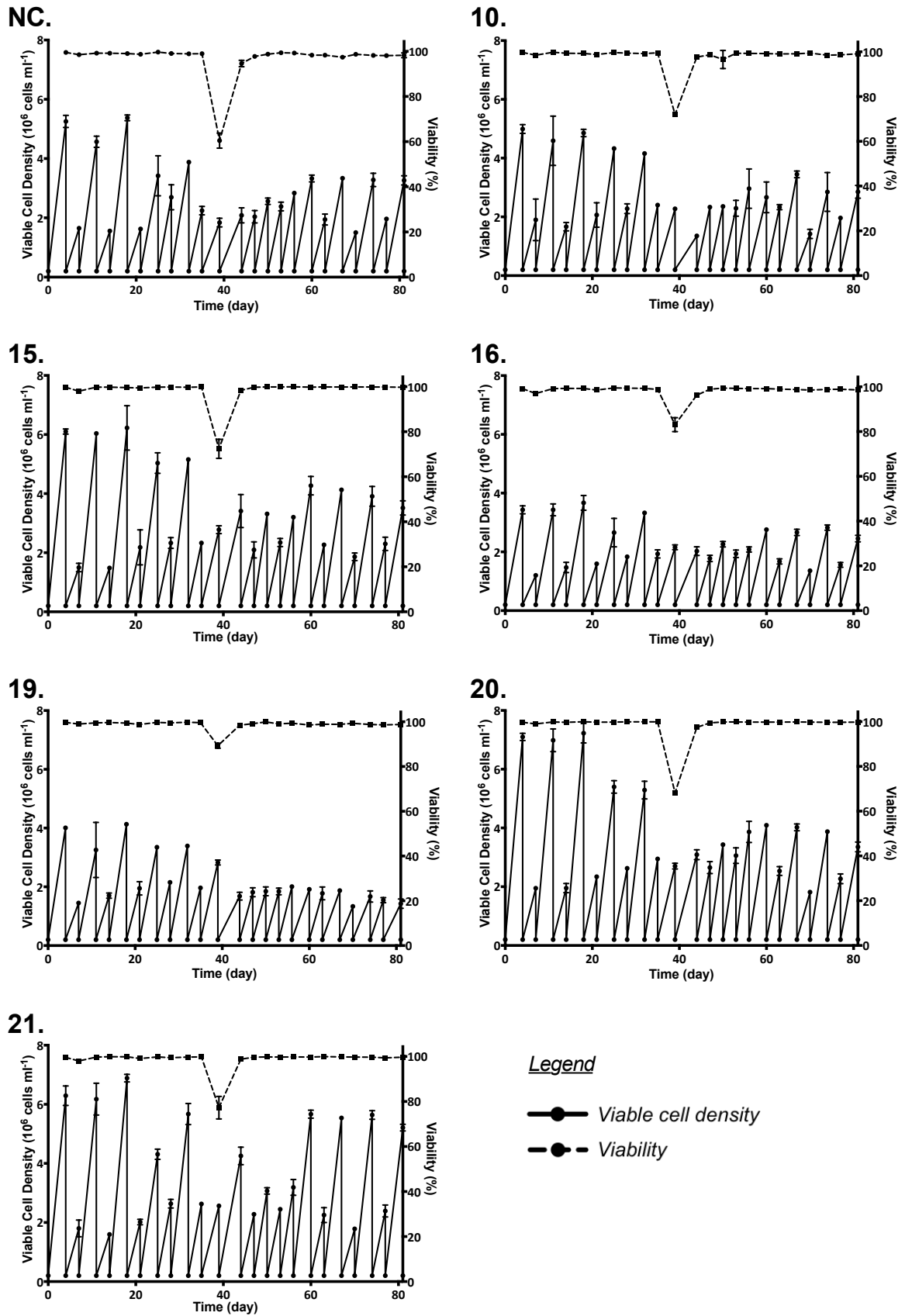
The viability of all cultures remained high (above 95%) for the duration of the study, with the exception of one event at day 39. This was caused by a fault with the shaking incubator; this caused the cultures to remain static for several hours. Following this event, the subculture routine was altered to rescue the cultures and to bring the Sonata back onto schedule.

To assess changes in growth rate, the LTC period was divided into quarters and the average growth rate was calculated for each quarter (Table 3.1). The data show that the growth rate decreased for each cell line during the study. To assess the significance of this change, the growth rate for each passage was used in a one-way ANOVA test (Section 2.9). As highlighted in Table 3.1, only cell line 19 was determined to show a significant decrease in growth rate during the LTC period. The growth rate in the fourth quarter of the study was significantly slower than the growth rate in quarter 1 and 2.

Considering the design of the 3-day, 4-day design of the study, and also the alteration to the passage schedule following the incubator fault, the ANOVA test described previously takes into account a great deal of experimental noise. This will have had an impact on the power of the test. A second one-way ANOVA was performed on the data using only the rate of growth from day 4 cell counts. Quarter 3 data had to be excluded from this test. This second test found that the average growth rate was significantly slower in quarter 4 than in quarter 1 for all cell lines except cell line 21. The post-hoc test also highlighted that cell line 19 was the only cell line to show a significant decrease in growth rate when comparing quarter 2 and 4, this supports the finding of the test highlighted in Table 3.1.

The LTC period equated to at least 78 generations for each cell line. This period covers the typical industrial time scale from a working cell bank to final production culture (Brown et al. 1992). The data show that there was inter-clonal variability in growth rate between the clonal and non-clonal host cell lines, inter-clonal variability in clonal host cell line growth has been previously reported for other GS-CHO clonal host cell lines (Davies et al. 2013). Three of the clonal host cell lines maintained a consistently greater growth rate than cell line NC (Table 3.1). Engineering strategies in CHO cell lines have previously enhanced proliferation rates (Dreesen & Fussenegger 2011), however these results show that enhanced rates of proliferation can be achieved by using clonal host cell lines. The growth rate of the host cell lines was not consistent throughout the LTC study. The growth rate of cell line 19 was found to decrease significantly during the study when analysing day 3 and day 4 growth rates. Additionally, the growth rate of all host cell lines, except cell line 21, decreased significantly when the analysis was restricted to day 4 growth rates. The observed decrease in growth rate was not expected, as published findings of long-term clonal host cell line culture has found that subculture processes select for any faster growing subpopulations (Davies et al. 2013). The decrease in growth rate observed in this study, could be interpreted as an indicator of instability, however the study was confounded by a medium batch change and a mechanical fault in the incubator. A related observation from the data in Figure 3.1 was that the cell lines all responded differently to the drop in viability caused by the incubator malfunction. For example the growth of cell line 19 following the malfunction remained consistently low. Contrastingly, the growth of cell line 21 recovered and the growth profile showed a similarity to the day 0-21 growth profile. This observation suggested that the cell lines respond differently to stress encountered during cell culture. It has previously been shown that unstable clonal recombinant cell lines had greater Annexin V and caspase 3 activity than stable cell lines (Dorai et al. 2012). Similar variations in apoptosis related proteins may be related to the response to stress observed here.

Figure 3.1 Analysis of host cell line growth during continuous LTC



Seven clonal and non-clonal host cell lines were subject to LTC in suspension using CD-CHO medium supplemented with 6 mM L-glutamine. Each host was grown in duplicate flasks for 81 days and passaged on a 3-/4-day schedule using a TAP Biosystems Sonata cell culture automation system. Cultures were maintained and subcultured as described in Section 2.3.2. Cell counts were determined using an Innovatis Cedex cell counter integrated with the Sonata (Section 2.3.4), this is based on the trypan blue exclusion method. The charts show the viable cell densities and viability of the non-clonal host cell line NC and clonal host cell lines 10, 15, 16, 19, 20 and 21. Error bars represent the SD for two biological replicates.

Table 3.1 Analysis of host cell line growth during continuous LTC

| Cell Line | Average growth rate ($\times 10^5$ cells ml^{-1} day^{-1}) | | | |
|-----------|--|---------|-------|-------|
| | Q 1 | Q 2 | Q 3 | Q 4 |
| NC | 0.917 | 0.687 | 0.694 | 0.654 |
| 10 | 0.903 | 0.765 | 0.649 | 0.640 |
| 15 | 1.060 | 0.862 | 0.841 | 0.780 |
| 16 | 0.648 | 0.579 | 0.571 | 0.528 |
| 19 | 0.723 * | 0.677 * | 0.494 | 0.408 |
| 20 | 1.269 | 0.939 | 0.937 | 0.778 |
| 21 | 1.137 | 0.869 | 0.929 | 0.982 |

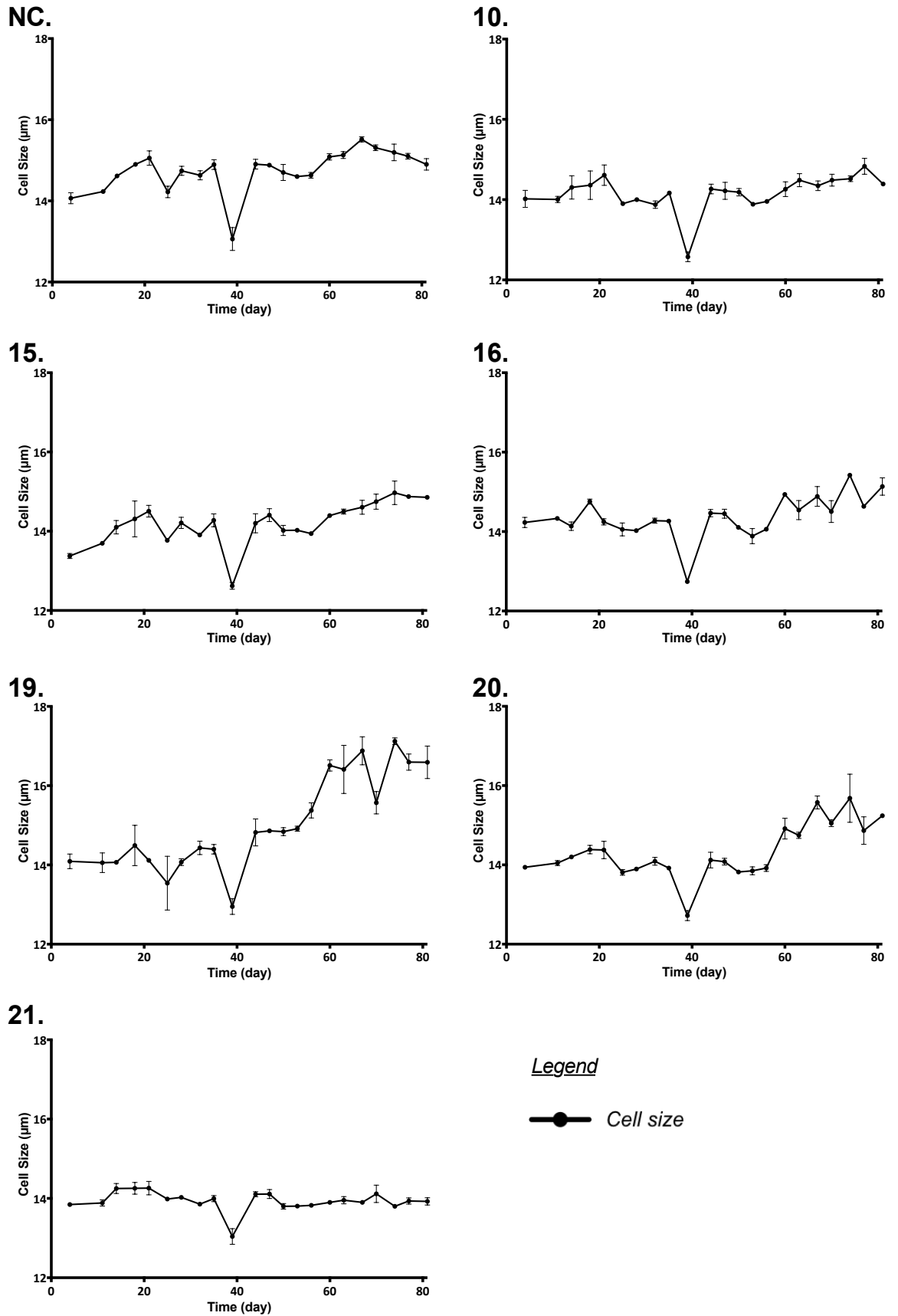
Seven clonal and non-clonal host cell lines were subject to LTC in suspension using CD-CHO medium supplemented with 6 mM L-glutamine. Each host was grown in duplicate flasks for 81 days and passaged on a 3-/4-day schedule using a TAP Biosystems Sonata cell culture automation system. Cultures were maintained and subcultured as described in Section 2.3.2. Cell counts were determined using an Innovatis Cedex cell counter integrated with the Sonata (Section 2.3.4), this is based on the trypan blue exclusion method. The LTC period was divided into quarters (Q), and the cell count data from each quarter was used to calculate the average growth rate of each cell line throughout the LTC period. * indicates $p < 0.05$, compared to Q4 growth rate using one-way ANOVA with the Tukey post-hoc test to analyse variance between the quarters for each cell line.

In addition to the cell count data collected during the LTC study, cell diameter data was exported from the Cedex cell counter to assess size variation between the host cell lines (Figure 3.2). At the beginning of the study, all of the cell lines had an average diameter of approximately 14 μm . This value is similar to previously published values for adherent CHO K1 and DHFR mutant cell lines (Kim et al. 2001; Kuystermans & Al-Rubeai 2009). Analysis of the cell diameter data from each cell count up to day 35 (thus, not taking into account the period following the incubator fault), shows that cell diameter is not consistent between the host cell lines. Using the Students T-test, all of the host cell lines were found to significantly differ in diameter when compared to cell line NC ($p < 0.01$).

Figure 3.2 shows fluctuation in the cell diameter throughout the period of LTC. To analyse this further, the study was divided into quarters (as done for Table 3.1), the average cell diameter was then calculated per quarter (Table 3.2). One-way ANOVA found that all of the cell lines, with the exception of cell line 10 and 21, showed a significant degree of variance in diameter over the duration of the study. The trends in the data (Figure 3.2, Table 3.2) show that this variance is predominantly an increase in diameter as the study progressed.

Significant variation in inter-clonal cell diameter was observed, however it is unclear whether the differences were related to other phenotypic parameters. Further to this, Table 3.2 highlights that a significant increase in cell diameter was observed over the duration of the study, in all cell lines except cell line cell line 10 and 21. The increase in diameter becomes evident following the incubator malfunction on day 39 (Figure 3.2). As previously discussed, growth rates decreased as the study progressed, this could indicate that more cells were in the G_0/G_1 phase of the cell cycle and may explain the increase in cell size (Kuystermans et al. 2010). It is unclear whether this increase in size would be beneficial or detrimental to cell line productivity following transfection with a recombinant protein gene, although a positive correlation between cell size and productivity has been observed in NS0 myeloma cells (Khoo & Al-Rubeai 2009). CHO cell lines have been described to show phenotypic drift (Section 1.3.2), the increased size could indicate that the incubator malfunction selected for a subset of cells with different phenotypic characteristics (Dorai et al. 2012).

Figure 3.2 Analysis of host cell line diameter during continuous LTC



Seven clonal and non-clonal host cell lines were subject to LTC in suspension using CD-CHO medium supplemented with 6 mM L-glutamine. Each host was grown in duplicate flasks for 81 days and passaged on a 3-/4-day schedule using a TAP Biosystems Sonata cell culture automation system. Cultures were maintained and subcultured as described in Section 2.3.2. Cell size was determined using an Innovatis Cedex cell counter integrated with the Sonata (Section 2.3.4). The charts show the average diameter of the non-clonal host cell line NC and the clonal host cell lines 10, 15, 16, 19, 20 and 21. Error bars represent the SD for two biological replicates.

Table 3.2 Analysis of host cell line diameter during continuous LTC

| Cell Line | Average cell size (μm) | | | |
|-----------|-------------------------------------|-------|-------|-------|
| | Q 1 | Q 2 | Q 3 | Q 4 |
| NC * | 14.42 | 14.44 | 14.81 | 15.20 |
| 10 | 14.16 | 13.86 | 14.13 | 14.51 |
| 15 * | 13.83 | 13.89 | 14.17 | 14.76 |
| 16 * | 14.32 | 13.94 | 14.32 | 14.86 |
| 19 * | 14.13 | 13.92 | 15.22 | 16.53 |
| 20 * | 14.14 | 13.80 | 14.12 | 15.20 |
| 21 | 14.09 | 13.86 | 13.93 | 13.94 |

Seven clonal and non-clonal host cell lines were subject to LTC in suspension using CD-CHO medium supplemented with 6 mM L-glutamine. Each host was grown in duplicate flasks for 81 days and passaged on a 3-/4-day schedule using a TAP Biosystems Sonata cell culture automation system. Cultures were maintained and subcultured as described in Section 2.3.2. Cell size was determined using an Innovatis Cedex cell counter integrated with the Sonata (Section 2.3.4). The LTC period was divided into quarters (Q), and the cell size data from each quarter was used to calculate the average size of each cell line throughout the LTC period. * indicates $p < 0.05$, using one-way ANOVA to analyse variance over the duration of the LTC period.

3.2.2 Analysis of early and late generation host cell line growth characteristics during batch culture

The design of the LTC study (Section 3.2.1) included batch cultures that were created at an early generation (between generations 18-22) and late generation (between generations 66-78). These batch cultures were included to enable a more in-depth analysis of cell line growth characteristics. As mentioned in the previous Section, the LTC study was affected by a change in the CD-CHO medium batch and an incubator malfunction. It was assumed that these issues would have impacted the batch culture data. At the point of batch culture creation, aliquots of cells were cryopreserved (Section 2.3.6); these stocks were revived in the same batch of medium to repeat the batch cultures (Figure 3.3). Cell line 10 was not included in the study from this point, further work in the project had found the cells had a tendency to aggregate and poor growth made the host impractical to work with.

Inter-clonal variability in the growth profile of the host cell lines was observed in batch culture (Figure 3.3). The initial pattern of growth between the early and late generation of cell line NC, 16 and 21 was similar, and did not support the decline in growth rate suggested in Section 3.2.1. The late generation batch cultures for cell line 15, 19 and 20 showed a lower VCD on day 4 of culture, and this was also apparent at day 3 for cell line 19. The growth pattern for cell line 19 supported the statistically decreased growth rate observed in the previous Section.

Table 3.3 includes additional data that was generated from the batch cultures and highlights variance between the different host cell lines. Cell line NC had a maximum viable cell density (VCD_{max}) of 4.80×10^6 cell ml^{-1} in the early generation batch culture, this value increased in the late generation batch culture. The cumulative cell time (CCT) was 22.95×10^6 cells ml^{-1} day^{-1} in the early generation batch culture, this also increased in the late generation batch culture. Despite these increases, the doubling time of cell line NC was greater for the late generation cells compared with the early generation.

In terms of growth, cell line 16 performed the poorest. Table 3.3 shows that at both early and late generation the VCD_{max} , CCT and doubling time was significantly different from the comparable cell line NC batch cultures. At both generations, cell line 16 achieved the lowest VCD_{max} and CCT of the host cell lines. The doubling time was also greater than any other cell line. This contrasts the average growth rates seen in Table 3.1, which suggested that the late generation cell line 19 had the slowest growth rate. Cell line 19

did, however grow poorly when compared to cell line NC. The VCD_{max} of cell line 19 was significantly less than the VCD_{max} of cell line NC at both generations. Despite this, only the late generation batch cultures of cell line 19 were significantly different when considering the CCT and doubling time.

The doubling time of cell line 15, 20 and 21 was shorter than the doubling time of cell line NC at both generations, although the difference was not significant. The early generation batch cultures of cell line 15 and 20 achieved a significantly greater VCD_{max} than cell line NC. In the late generation, the VCD_{max} of these two cell lines decreased and was not significantly greater than the VCD_{max} of cell line NC. The CCT of the cell line 15 and 20 batch cultures was significantly greater than the CCT of cell line NC, with the exception of the late generation cell line 20 batch cultures. Table 3.3 suggests that cell line 21 is the best performing clonal cell line in batch culture; this cell line achieved the greatest VCD_{max} and CCT of all the clonal host cell lines and these were consistently significantly greater than the comparative values for host cell line NC.

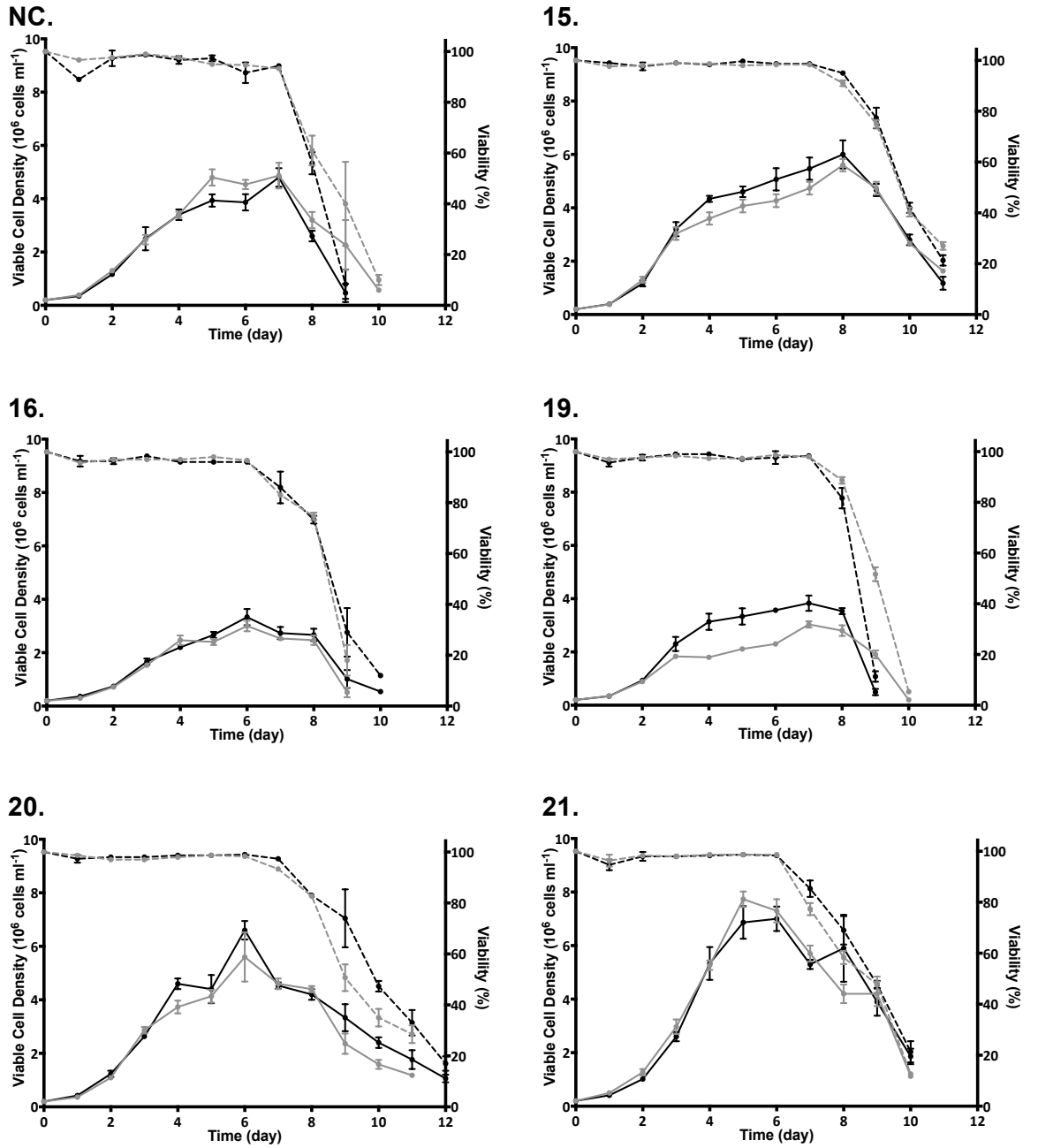
Cell line 15 and 19 had stationary phases that lasted approximately 3-4 days, whereas cell line 21 had a short stationary phase lasting approximately 1 day. This indicates that the high VCD_{max} of cell line 21, depletes available nutrients and/or toxic waste products accumulate to detrimental concentrations. Variation was also observed in the decline phase of the batch cultures. The cell line 19 batch cultures showed a decrease in viability over 2-3 days, whilst the cell line 20 batch cultures showed a gradual decrease in viability over 5-6 days. The total duration of the batch culture was also different between the cell lines.

The average growth rate variability shown in Table 3.1 was reflected in the batch culture profiles. The data in Table 3.3 show that there was significant variation in VCD_{max} , CCT and doubling time when compared to cell line NC. In addition to this, it was apparent that the duration of cell culture phases was different between the cell lines. This could be of particular importance for a production host cell line, as stationary phase has been associated with high specific productivity (Templeton et al. 2013). The VCD_{max} , CCT and doubling time values of cell line NC were in-between the comparable values of the clonal host cell lines; this is not surprising as the clonal host cell lines were derived from cell line NC.

Variation in the growth parameters was observed between the early and late generation batch cultures. The data in Section 3.2.1 suggested that the late generation batch cultures would perform poorly compared to the early generation batch cultures. The data in this

Section does not fully support this, as clone-specific variation in the growth parameters shifted in both directions. Similarly, there have been previous reports where growth parameters have altered in both a positive and negative fashion in response to LTC (Bailey et al. 2012; Beckmann et al. 2012). The variation observed in response to LTC could be due to changes in proliferation and apoptosis rates (Arden & Betenbaugh 2006). However, it has also been suggested that LTC can cause cells to adapt to alterations in culture pH caused by lactate production, this may explain some of the variation observed between the early and late generations (Beckmann et al. 2012).

Figure 3.3 Comparison of early and late generation host cell line growth parameters in batch culture



Legend

- Early Viable cell density
- Late Viable cell density
- - Early Viability
- - Late Viability

Clonal and non-clonal host cell lines were cryopreserved at day 18 (Early) and day 67 (Late) during the LTC study (Figure 3.1). These cryopreserved cells were later revived for the assessment of host cell line performance in batch culture. Early and Late generation cultures of each host were maintained for three passages in suspension using CD-CHO medium supplemented with 6 mM L-glutamine. At the fourth passage, batch cultures were created from each maintenance culture. Batch cultures prepared and maintained as described in Section 2.3.3. Cell counts were taken daily using an Invitrogen Countess Automated Cell Counter (Section 2.3.4), this is based on the trypan blue exclusion method. Cultures were monitored until the viability was $\leq 30\%$. The charts show the early and late generation viable cell densities and viability of the non-clonal host cell line NC and the clonal host cell lines 15, 16, 19, 20 and 21. Error bars represent the SEM for three biological replicates.

Table 3.3 Analysis of early and late generation host cell line growth parameters in batch culture

| Cell line | NC | 15 | 16 | 19 | 20 | 21 |
|--|-------|---------|---------|---------|---------|---------|
| Early VCD _{max} (x10 ⁶ cells ml ⁻¹) | 4.80 | 6.07 * | 3.33 * | 3.87 * | 6.60 * | 7.13 * |
| Late VCD _{max} (x10 ⁶ cells ml ⁻¹) | 5.07 | 5.60 | 3.00 * | 3.10 * | 5.80 | 7.83 * |
| Early CCT (x10 ⁶ cells ml ⁻¹ day ⁻¹) | 22.95 | 38.38 * | 16.98 * | 21.32 | 35.34 * | 39.35 * |
| Late CCT (x10 ⁶ cells ml ⁻¹ day ⁻¹) | 26.72 | 35.30 * | 15.77 * | 17.22 * | 30.04 | 39.79 * |
| Early doubling time (hours) | 19.89 | 18.03 | 23.57 * | 20.51 | 19.36 | 19.48 |
| Late doubling time (hours) | 19.94 | 18.42 | 24.55 * | 22.57 * | 18.76 | 18.60 |

Six clonal and non-clonal host cell lines were cultured as previously described (Figure legend 3.3). VCD_{max} for each host cell line in batch culture was determined from cell count data. CCT was calculated from the summation of the integral of viable cell density, which was determined at daily intervals from cell count data. Doubling time was calculated between day 0 and day 3, this time period falls within the exponential growth phase for all of the host cell lines. The data represent mean values for three biological replicates. * indicates $p < 0.05$, using independent samples t-test to compare clonal cell lines to cell line NC at the respective generation.

3.3 Analysis of nutrient utilisation

On each day of the batch cultures described in Figure 3.3 medium samples were collected for nutrient analysis. The samples were analysed for glucose, lactate, glutamine and glutamate concentration. The glucose concentration in the culture medium decreased as the batch cultures progressed for all cell lines (Figure 3.4). Cell line 15, 20 and 21, which achieved the highest VCD_{max} values (Table 3.3) during batch culture completely depleted the available glucose by day 7 of culture. In contrast, 0.33 mM glucose was present at day 9 in the early generation cell line NC batch cultures, whilst all glucose was depleted at day 8 for the corresponding late generation cultures. Both early and late generation batch cultures of cell line 16 and 19 had glucose available in the culture medium at termination. This was particularly striking in early and late generation cell line 16 cultures where the glucose concentration was approximately 4.06 mM and 5.75 mM respectively at termination.

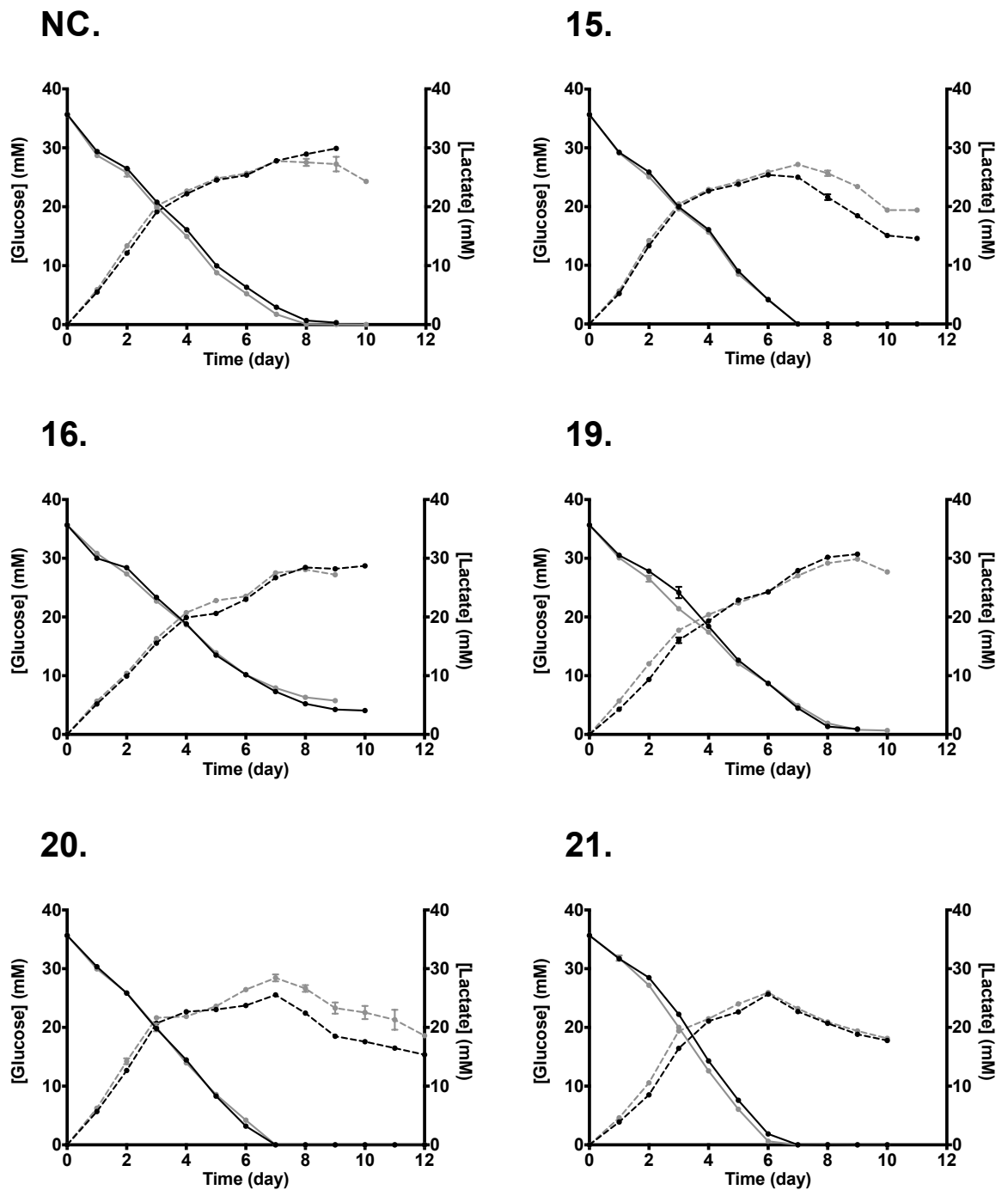
Lactate was observed to accumulate in all batch cultures from culture inoculation (Figure 3.4). The maximum lactate concentration observed for each cell line was within a range of approximately 25-30 mM. Variance was observed in the lactate profile of the host cell lines. Lactate concentration decreased during the batch cultures of cell line 15, 20, 21 and late generation cell line NC. This decrease in lactate concentration coincided with the depletion of glucose in the culture medium. Cell line 16, 19 and early generation cell line NC did not (or showed limited evidence) consume lactate before the cultures were terminated.

Cell line NC consumed glucose at a rate of approximately $2 \text{ pmol cell}^{-1} \text{ day}^{-1}$ (Figure 3.5). All of the clonal host cell lines used glucose at a significantly different rate to cell line NC in one or both generations. Cell line 16 and 19, which have previously been shown to display the poorest growth, consumed the most glucose per cell. The rate of lactate production showed a similar pattern to the rate of glucose consumption, for example the host cell lines with the greatest glucose consumption rates, also had the greatest lactate production rates. As glucose carbon skeletons progress through the glycolytic pathway, they can be converted to either pyruvate or lactate. Complete conversion to lactate would have an approximate molar ratio of 1:2, glucose:lactate (Tsao et al. 2005). The ratio of lactate production rate to glucose consumption rate can be used to indicate the efficiency of glucose conversion to lactate (Table 3.4, Appendix B). These ratios suggest that not only did cell line 16 and 19 use the most glucose per cell, they also produced more lactate per glucose consumed. In contrast, cell line 21, consumed less glucose per cell, the

lactate:glucose ratio suggests that more of the carbon is directed into the citric acid cycle rather than to lactate production.

The cell lines that completely depleted available glucose showed evidence of lactate consumption in the late stages of culture. Similar consumption of lactate has been observed in other CHO cell studies (Tsao et al. 2005; Ma et al. 2009). There was little or no evidence of lactate consumption in the batch cultures where glucose was not depleted by the end of culture. An explanation could be that the depletion of glucose availability triggers a switch to lactate consumption, or simply that when glucose remains present in the medium, excess intracellular pyruvate continues to be converted to lactate. The rate of glucose consumption and lactate production varied significantly between the host cell lines. The cell lines that had the poorest growth consumed the most glucose per cell and also produced the most lactate per cell (Figure 3.5). Ratios of these nutrient utilisation rates suggest that cell line 16 and 19 are inefficient in terms of glucose utilisation. This could be due to low pyruvate carboxylase activity causing a low flux of pyruvate into the citric acid cycle, a finding supported by other research (Kim & Lee 2007b; Wilkens & Gerdtzen 2011).

Figure 3.4 Analysis of glucose and lactate concentrations during batch culture in response to LTC

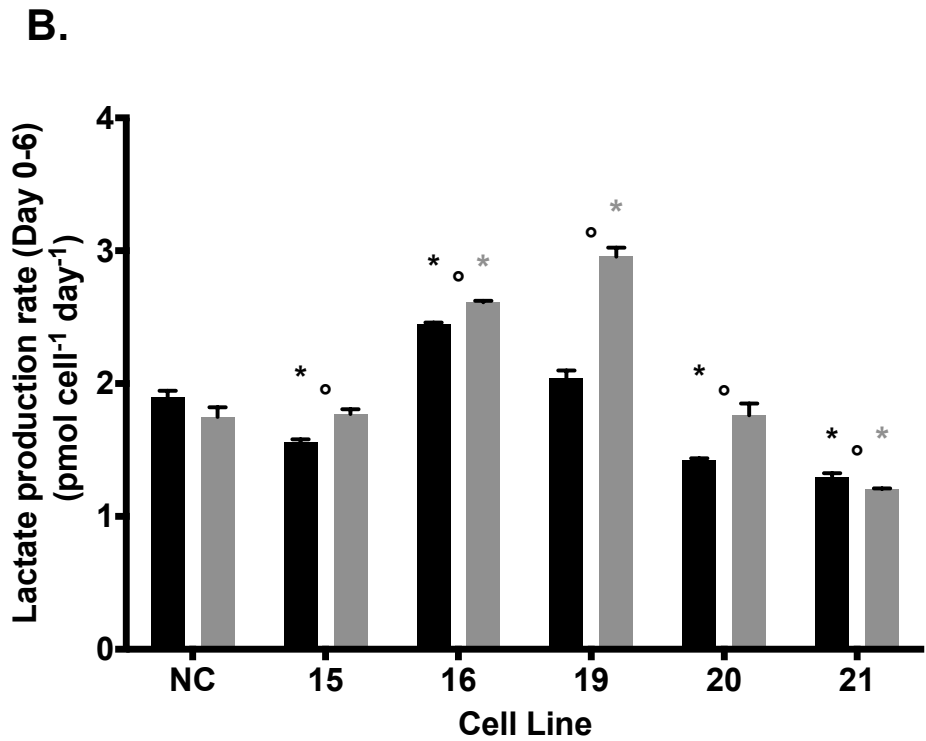
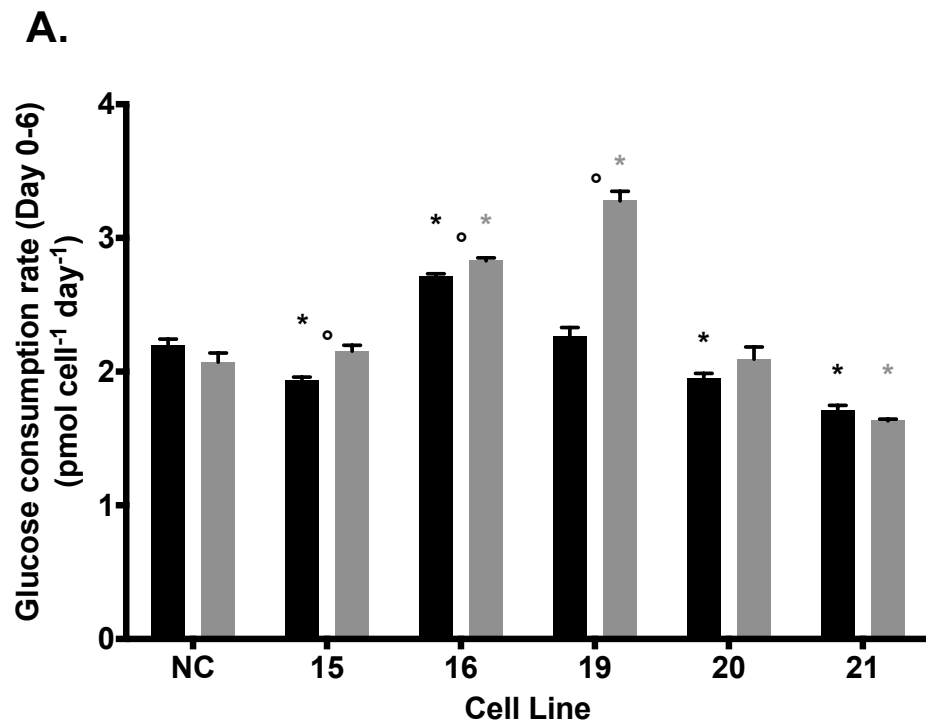


Legend

- Early generation [glucose]
- Late generation [glucose]
- -●- - Early generation [lactate]
- -●- - Late generation [lactate]

During the batch cultures described in Figure 3.3, cell culture medium samples were collected daily for metabolite analysis. The medium samples were analysed using a YSI 2900 Biochemistry Analyzer for glucose and lactate concentration as described in Section 2.4.1. The charts show the early and late generation glucose and lactate concentrations of the non-clonal host cell line NC and the clonal host cell lines 15, 16, 19, 20 and 21. Error bars represent SEM for three biological replicates.

Figure 3.5 Analysis of glucose and lactate utilisation rates during batch culture in response to LTC



Legend

- Early generation
- Late generation

*As described in Figure 3.4, early and late generation clonal and non-clonal host cell lines were monitored in batch culture for glucose and lactate concentration. The cell counts and metabolite analyses were used to determine the rates of utilisation of these metabolites during the growth phase of culture. (A) shows the early and late generation glucose utilisation rates, (B) shows the early and late generation lactate utilisation rates. Error bars represent SEM for three biological replicates. * indicates $p < 0.05$, using independent samples t-test to compare clonal host cell lines to the non-clonal host cell line NC at the respective generation. ° indicates $p < 0.05$, using independent samples t-test to compare early and late generation of each cell line.*

Table 3.4 Ratio of lactate production rate to glucose consumption rate during batch culture in response to LTC

| Cell Line | Lactate:glucose ratio | |
|-----------|-----------------------|-----------------|
| | Early generation | Late generation |
| NC | 0.87 | 0.85 |
| 15 | 0.81 | 0.82 |
| 16 | 0.90 | 0.92 |
| 19 | 0.90 | 0.90 |
| 20 | 0.73 | 0.84 |
| 21 | 0.76 | 0.74 |

Ratios were calculated from the lactate production rate and glucose consumption rates described in Figure 3.5. Considering an approximate molar exchange that 1 glucose molecule can be converted into 2 lactate molecules, a ratio of 1 would imply that 50% of the glucose consumed was converted to lactate. Lower ratio values imply that more carbon enters the citric acid cycle as pyruvate, this represents a more efficient metabolic state. For bar chart see Appendix B.

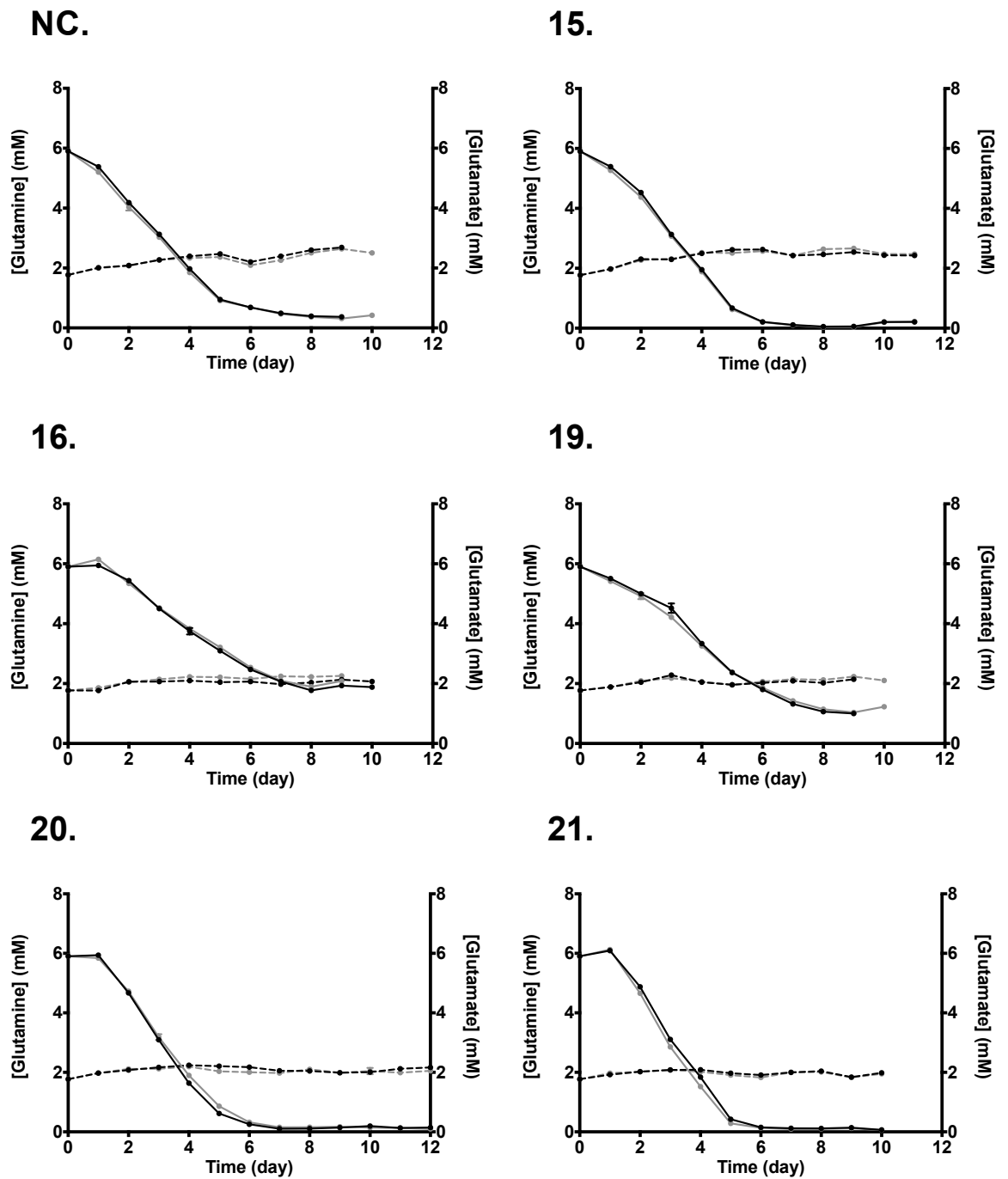
The host cell lines were cultured in medium that was supplemented with 6 mM L-glutamine. Analysis of culture supernatant during the batch cultures provided evidence that the cell lines consumed glutamine during culture (Figure 3.6). The profile of glutamine consumption demonstrated similarity to the profile of glucose usage. Clonal host cell lines 15, 20 and 21 consumed all available glutamine by day 7 of culture. Trace amounts of glutamine were detected after day 7, however this could be a result of endogenous GS activity. Cell line NC consumed glutamine until day 5 of culture, however the cell line did not consume all available glutamine. Additionally, neither clonal host cell lines 16 or 19 consumed all of the available glutamine, the concentration of glutamine was approximately 2 mM and 1 mM at the end of culture, respectively. This could be linked to the poor growth of these cell lines (Table 3.3), however evidence that these cell lines have high relative endogenous GS activity/expression (Section 3.4) could also be a factor. The data in Figure 3.6 also showed that all of the cell lines produced glutamate during batch culture. The increase in glutamate concentration did not change much from the initial concentration in the medium for any cell line.

All of the clonal host cell lines showed a significant variation in the rate of glutamine consumption compared to cell line NC, with the exception of clonal host cell line 16 (Figure 3.7 A). Clonal host cell line 21 consumed the least glutamine per cell. The late generation cultures of clonal host cell line 19 showed the greatest variation in glutamine consumption, and consumed the most glutamine per cell. The rates of glutamate production also showed variation between the host cell lines (Figure 3.7 B). However, the range of glutamate concentration and the range of production rates are small. This could indicate that the glutamate produced could not be accurately detected in the culture supernatant by the methodology used.

The host cell lines in batch culture all consumed glutamine from the culture medium, however the cell lines with poor growth did not use all of the glutamine available (Figure 3.6). Dean and Reddy found that glutamine is used by CHO cells to fuel the citric acid cycle during exponential growth (Dean & Reddy 2013). This could explain why the cell lines that achieved high cell densities depleted the available glutamine. The rate of glutamine uptake did vary between the cell lines (Figure 3.7 A), however the variation did not show a pattern that could explain the variation in cell growth properties. The data showed that the glutamine consumption rate increased in the late generation clonal host cell line 19 culture compared to the early generation. This supports the suggestion that the metabolism of this cell line became more inefficient in response to LTC. The glutamate data (Figure 3.6 and Figure 3.7 B) show that glutamate accumulates in the medium during

batch culture. The rate of production varied between the cell lines, however the production rates are small and intracellular metabolomic techniques could be a better method to investigate glutamate utilisation. As data discussed previously suggested that the cell lines vary in their metabolic efficiency, a low glutamate production rate, as indicated for clonal host cell line 21 may indicate that this clonal host is more efficient at assimilating glutamate into the citric acid cycle.

Figure 3.6 Analysis of glutamine and glutamate concentrations during batch culture in response to LTC

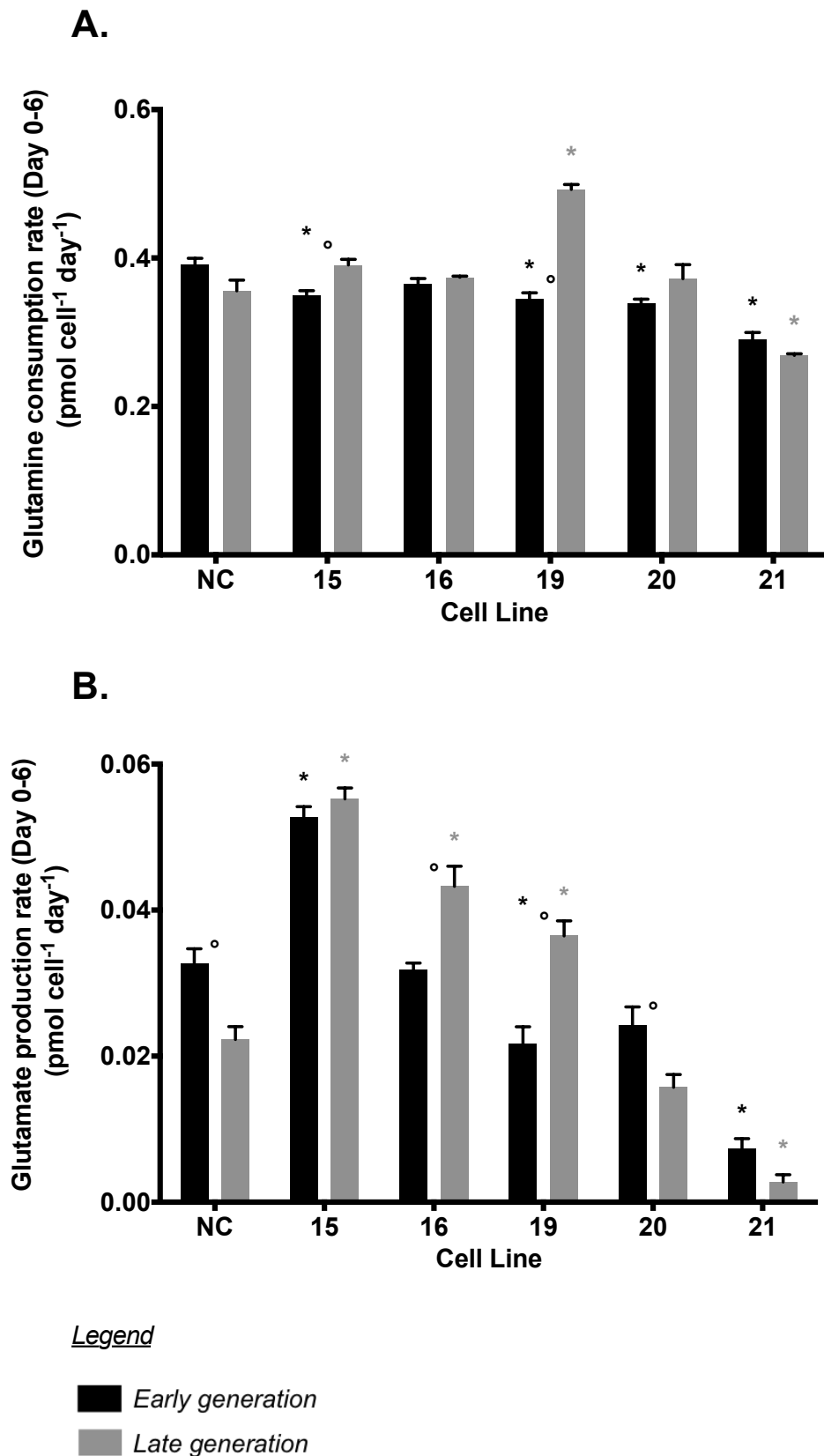


Legend

- Early generation [glutamine]
- Late generation [glutamine]
- - Early generation [glutamate]
- - Late generation [glutamate]

During the batch cultures described in Figure 3.3, cell culture medium samples were collected daily for metabolite analysis. The medium samples were analysed using a YSI 2900 Biochemistry Analyzer for glutamine and glutamate concentration as described in Section 2.4.1. The charts show the early and late generation glutamine and glutamate concentrations of the non-clonal host cell line NC and the clonal host cell lines 15, 16, 19, 20 and 21. Error bars represent SEM for three biological replicates.

Figure 3.7 Analysis of glutamine and glutamate utilisation rates during batch culture in response to LTC



*As described in Figure 3.6, early and late generation clonal and non-clonal host cell lines were monitored in batch culture for glutamine and glutamate concentration. The cell counts and metabolite analyses were used to determine the rates of utilisation of these metabolites during the growth phase of culture. (A) shows the early and late generation glutamine utilisation rates, (B) shows the early and late generation glutamate utilisation rates. Error bars represent SEM for three biological replicates. * indicates $p < 0.05$, using independent samples t-test to compare clonal cell lines to the non-clonal host cell line NC at the respective generation. ° indicates $p < 0.05$, using independent samples t-test to compare early and late generation of each cell line.*

3.4 Analysis of endogenous glutamine synthetase

3.4.1 Analysis of variability in endogenous glutamine synthetase

Expression of endogenous GS protein was determined using Western blots and densitometry (Section 2.5.2) (Figure 3.8 A & B). The relative GS protein expression determined for cell line NC was 0.158 (arbitrary unit) in the early generation batch culture (Figure 3.8 B). The GS expression in the late generation remained stable and no significant difference was observed. The results showed that the relative GS expression for clonal host cell lines 15 and 20 is similar to host cell line NC, no significant difference was observed in either the early or late generation when compared to cell line NC. In contrast, the densitometry indicated that clonal host cell lines 16, 19 and 21 expressed significantly more GS protein at the early generation when compared to host cell line NC. However, in the late generation, protein expression was not found to be significantly greater than host cell line NC for any clonal host cell line. Comparison of early and late generation GS protein expression for each host cell line individually, found GS protein expression decreased significantly in the late generation of clonal host cell lines 16 and 19.

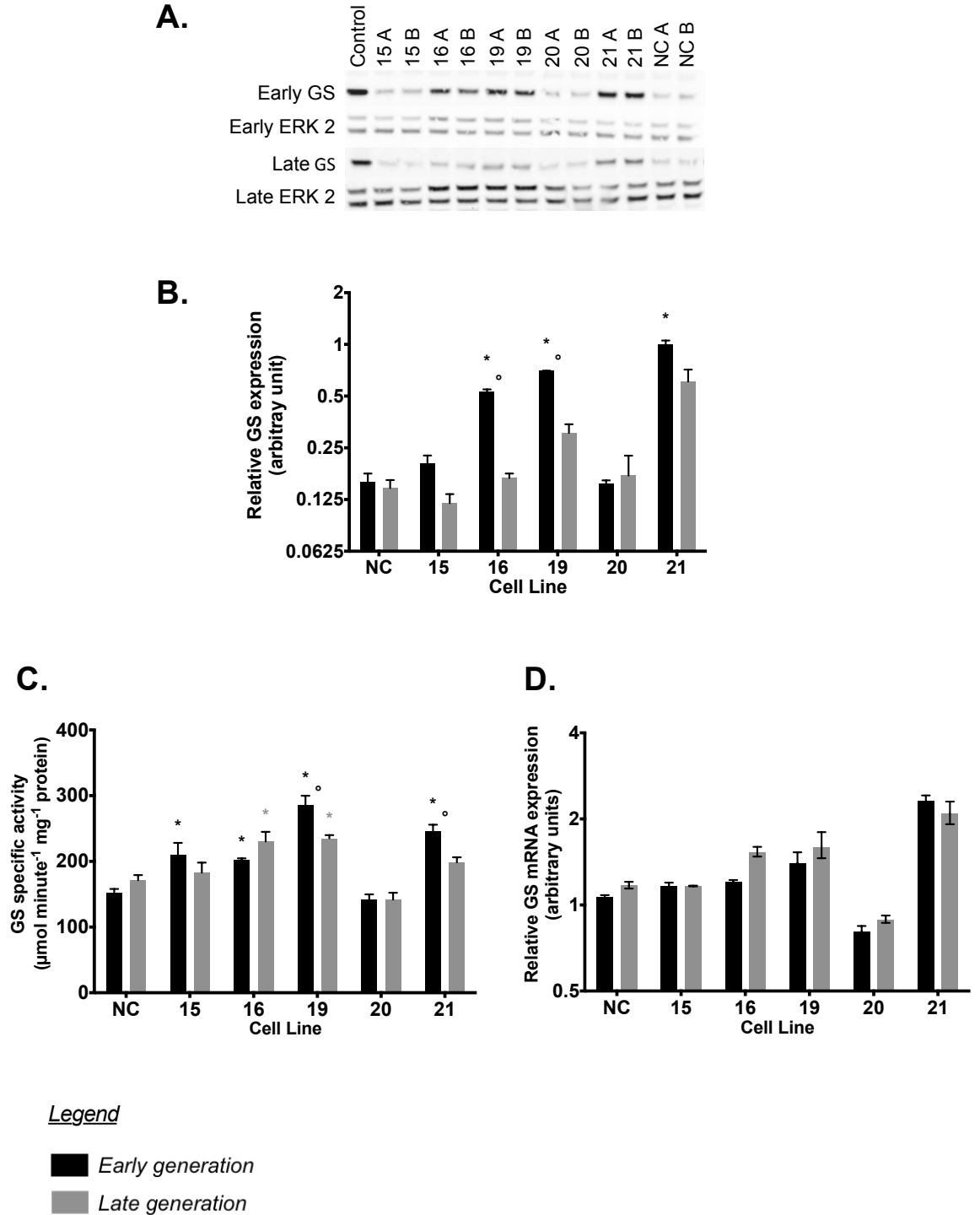
Considering the disadvantages of Western blot and densitometry analysis (Gassmann et al. 2009), GS protein activity in protein lysates was also measured. Glutamine synthetase, in its physiological state, catalyses a synthetase reaction which converts glutamate to glutamine (Section 1.2.3). The GS enzyme can also catalyse a transferase reaction, and this converts glutamine to glutamate. The GS activity assay used in this study exploits this reaction and available glutamine is irreversibly converted to L- γ -glutamyl-hydroxamate. The overall trend in GS activity data (Figure 3.8 C) complemented the trend observed from the densitometry data (Figure 3.8 B). The GS specific activity of early generation cell line NC lysate was $152.7 \mu\text{mol minute}^{-1} \text{mg}^{-1} \text{protein}$, an increase (not significant) in activity was observed in the late generation. With the exception of cell line 20, all of the early generation clonal host cell lines were found to have significantly greater GS activity when compared to the non-clonal host, cell line NC. This observation was also true in the late generation lysates of the clonal host cell lines 16 and 19. Comparison between the early and late generation of each host cell line, found a significant decrease in GS activity between the two generations of clonal host cell lines 19 and 21.

mRNA samples taken from the batch cultures were used in a qRT-PCR assay to investigate the endogenous GS mRNA expression in the host cell lines (Figure 3.8 D).

The observed pattern in GS mRNA expression shows similarity to the pattern of relative GS protein expression and GS activity. Correlation analysis of mean GS activity and mean relative mRNA expression suggested that the two data sets correlate ($r = 0.63$). The coefficient of determination (r^2) for the correlation was 0.40. The r^2 implies that, despite the data showing a positive correlation, only 40% of the variance was shared between the two variables.

Analysis of the GS protein from batch cultures found evidence of variation in the abundance and activity of this enzyme between the clonal and non-clonal host cell lines. The pattern of this data does not provide evidence of a strong relationship to the growth of the cell lines (Figure 3.8). There is also little evidence that the patterns of GS expression explain the rates of nutrient usage. However GS was observed to significantly decline in abundance and activity in the late generation of clonal host cell line 19. This could explain the significant increase observed in glutamine uptake rate in the late generation batch culture (Figure 3.7 A). Analysis of GS mRNA (Figure 3.8 D) positively correlated with GS activity. Interpretation of these data indicated that mRNA expression does influence endogenous GS activity (and this can be extrapolated to GS protein abundance), however it is likely that other cellular mechanisms influence the protein as discussed in Section 3.4.2 and Section 6.2.1.

Figure 3.8 Analysis of glutamine synthetase in host cell lines during continuous LTC



In addition to the batch cultures previously described (Figure 3.3), a batch culture was created for each duplicate maintenance flask during the LTC study (Figure 3.1) on days 18 and 67. Protein was extracted on day 4 of these batch cultures in order to determine GS protein expression. 10 µg of protein was separated by SDS-PAGE as described in Section 2.5.2, this was transferred to nitrocellulose membranes, duplicate blots were prepared. Blots were probed with antibodies against GS and ERK 2 (endogenous loading control). A LICOR Odyssey was used to detect the bands (A). Image J software was used to quantify the relative protein expression of GS (B), normalized against a control sample (taken from clonal host cell line 10). Error bars represent SEM for two biological replicates.

During the batch cultures described in Figure 3.3, protein was extracted on day 4 in order to determine GS activity. The protein extracts were analysed for specific GS activity as described in Section 2.5.3, the data are shown in (C). Also, cells were lysed in Trizol on day 4 to prepare mRNA extracts as described in Section 2.6.1. mRNA was analysed by qRT-PCR for GS expression using TaqMan probes and primers. GS expression was normalized against a calibrator sample (cell line NC, early generation, replicate 2) and 18s ribosomal RNA was used as an endogenous control, the data are displayed in (D). Error bars represent SEM for three biological replicates, additionally, in the qRT-PCR assay each biological replicate was assayed as a technical duplicate.

** indicates $p < 0.05$, using independent samples t-test to compare clonal cell lines to cell line NC at the respective generation.*

° indicates $p < 0.05$, using independent samples t-test to compare early and late generation of each cell line.

3.4.2 The effect of glutamine-free culture on growth and endogenous glutamine synthetase

The clonal and non-clonal host cell lines were revived into CD-CHO medium supplemented with 6 mM L-glutamine, after three days the cultures were subcultured. Two daughter flasks were created, one supplemented with 6 mM L-glutamine and one containing 0 mM L-glutamine. The average growth rate during maintenance culture of the hosts in the presence of glutamine (Figure 3.9 A) approximated to the rates observed in Table 3.1. The host cell lines were able to grow in the absence of glutamine, however the rate of growth decreased (Figure 3.9 A).

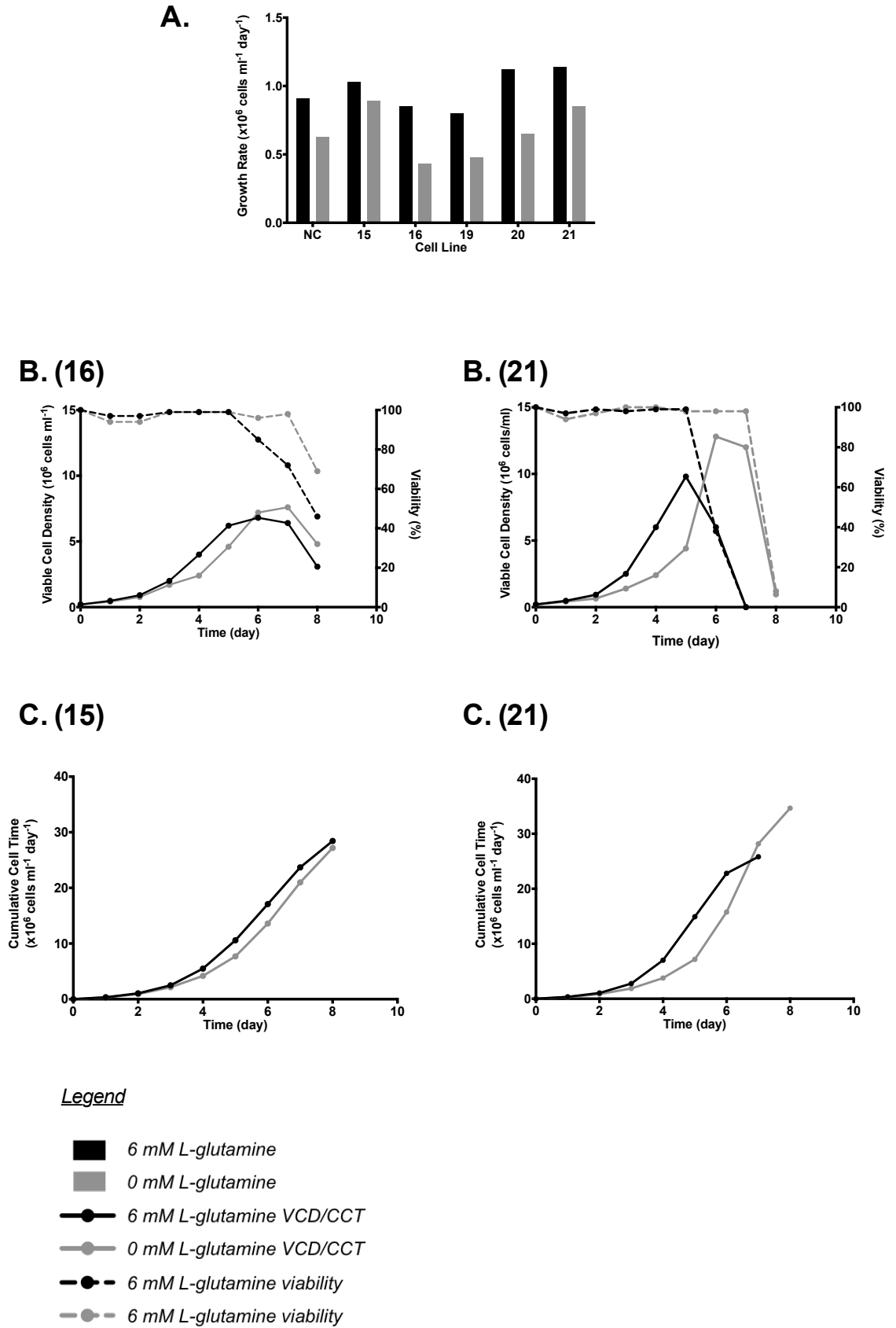
Batch cultures were inoculated for two of the clonal host cell lines (16 and 21), after 6 passages in the appropriate medium to determine how the growth profile is affected by the absence of glutamine. These cell lines were selected as they demonstrated slow growth rates (cell line 16) and more rapid growth rates (cell line 21) in Table 3.1. The data showed that the peak VCD achieved by the cell lines is delayed by one day in the glutamine-free condition (Figure 3.9 B (16)(21)). Both clonal cell lines achieved greater cell densities in the absence of glutamine. In addition, the viability of the glutamine-free cultures remained high ($\geq 98\%$) for two days longer than the cultures supplemented with L-glutamine. It is possible that this was due to a delayed exhaustion of nutrients or delayed accumulation of waste products as a result of slower growth rates. The observed differences in the growth profile had minimal effect on the CCT of cell line 16 (Figure 3.9 C (16)). However, the absence of glutamine with clonal host cell line 21, caused an increase in CCT from 25.8 to 34.7 $\times 10^6$ cells $\text{ml}^{-1} \text{day}^{-1}$ (Figure 3.9 C (21)).

In addition to investigating the effect of glutamine-free culture on host cell line growth, protein lysates were prepared from all of the clonal and non-clonal host cell lines on day 4 of culture in both the 6 mM L-glutamine and 0 mM L-glutamine conditions. The samples were analysed by Western blot and densitometry to determine the effect of glutamine-free culture on GS protein expression (Figure 3.10). The trend of relative GS expression in the 6 mM glutamine condition is supported the trend of Figure 3.8 A. The data showed that in the absence of glutamine, GS protein expression was upregulated when compared to the 6 mM L-glutamine condition. Additionally a greater degree of variability between the cell lines was observed in the 6 mM glutamine condition.

The regulation of endogenous GS expression has not been studied in detail in CHO cells. However, studies in Chinese hamster lung and other cell types have indicated that the

protein is regulated by both pre- and post-translational mechanisms (Tiemeier & Milman 1972; Labow et al. 2001; Huang et al. 2007). These studies indicated that GS is downregulated in the presence of glutamine. It is common for host CHO cell lines to be grown in the presence of glutamine prior to transfection. In this study, cells that had been adapted to grow in glutamine-free medium had a slower growth rate than the cell lines grown with glutamine. This decrease in growth rate is supported by previous findings that glutamine is used as a major source of energy in CHO cell metabolism (Hinterkörner et al. 2007). Glutamine has been found to be important during exponential growth (Dean & Reddy 2013), this supports the right-shift in the growth profile of glutamine-free batch cultures. All of the clonal and non-clonal host cell lines upregulated GS expression in the absence of glutamine (Figure 3.10), this effect of glutamine concentration has been previously observed in Chinese hamster lung cells (Tiemeier & Milman 1972). Less variation was observed in GS protein abundance when the cell lines were grown in glutamine-free medium compared with the 6 mM L-glutamine condition. As transcriptional regulation may only account for 40% of the variability in 6 mM L-glutamine (Section 3.4.1), this data suggests that the cell lines vary in their capacity for proteasomal degradation of GS when extracellular glutamine is present (Huang et al. 2007).

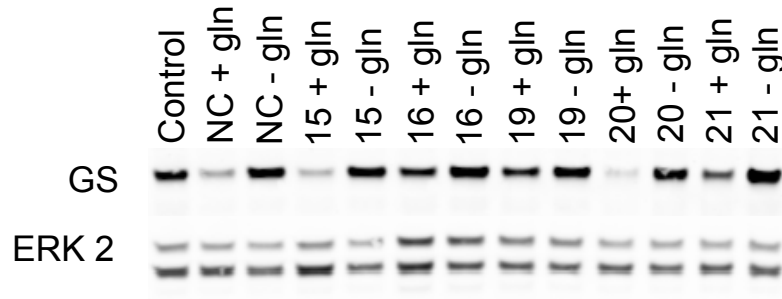
Figure 3.9 Effect of glutamine-free culture on host cell line growth



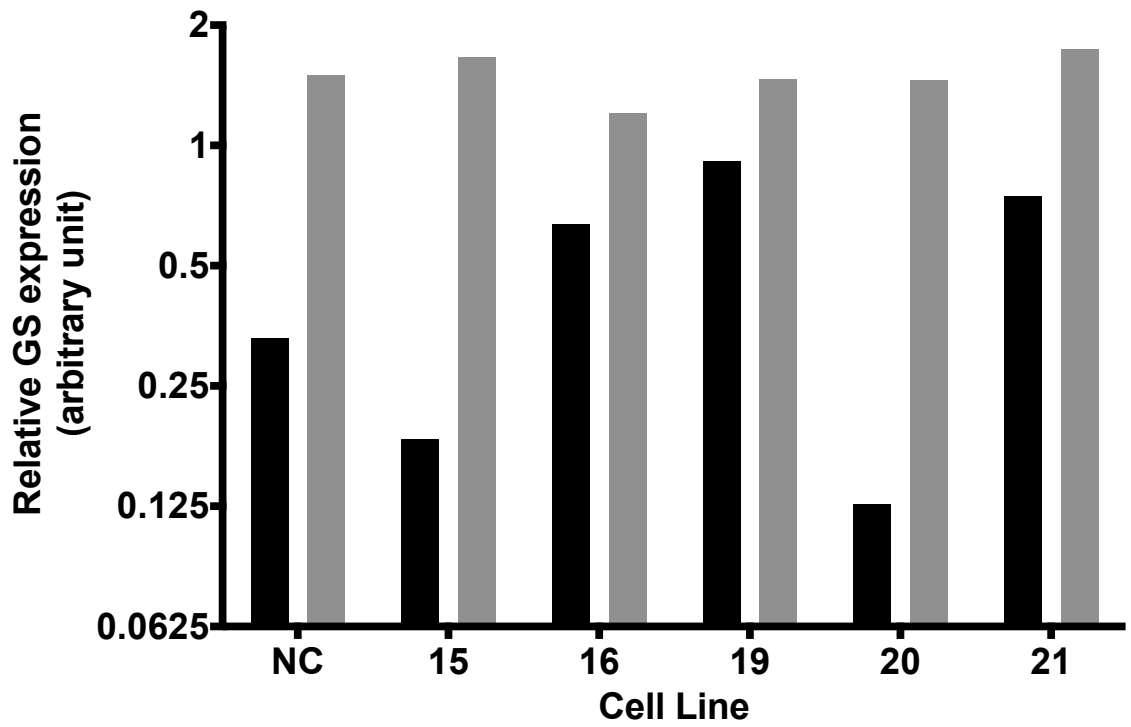
Six clonal and non-clonal host cell lines were grown in the presence and absence of L-glutamine to determine the effect of glutamine-free culture on host performance. The cells were maintained and subcultured as described in Section 2.3.2. Culture medium was CD-CHO containing 6 mM L-glutamine or 0 mM L-glutamine. Cell counts were determined using an Invitrogen Countess Automated Cell Counter as described in Section 2.3.4, this is based on the trypan blue exclusion method. (A) shows the average growth rate of the hosts in maintenance culture. (B) To investigate the effect of glutamine-free culture in batch culture, clonal host cell lines 16 and 21 were seeded at 0.2×10^6 cells ml^{-1} in both the 6 mM and 0 mM conditions. Batch cultures (Section 2.3.3) were monitored daily for up to 8 days. (C) The cell counts from the batch cultures were used to determine the CCT, this is shown for clonal host cell lines 16 and 21. Biological replicates were not included in this experiment.

Figure 3.10 Host cell lines upregulate glutamine synthetase protein expression in response to glutamine-free culture

A.



B.



Legend

- 6 mM L-glutamine
- 0 mM L-glutamine

To determine the effect of glutamine-free culture on GS expression, protein was extracted on day 4 from the maintenance cultures described previously (Figure 3.9). 10 µg of protein was separated by SDS-PAGE as described in Section 2.5.2, this was transferred to nitrocellulose membranes, and duplicate blots were prepared. Blots were probed with antibodies against GS and ERK 2 (endogenous loading control). A LICOR Odyssey was used to detect the bands (A). Image J software was used to quantify the relative protein expression of GS (B), normalized against a control sample (taken from cell line 10).

3.5 Analysis of mitochondrial membrane potential

Previous research found a correlation between mitochondrial membrane potential, measured using the dye rhodamine-123 (Rh-123), and specific glucose uptake rate in hybridoma cells (Borth et al. 1993). A more recent study found that CHO cells with high Rh-123 fluorescence intensity exhibited rapid growth rates, high VCD_{max} and low specific glucose consumption/lactate production rates. CHO cells with low Rh-123 fluorescence intensity displayed the opposite characteristics (Hinterkörner et al. 2007). Rh-123 staining and flow cytometry can be used to rapidly assess mitochondrial membrane potential. This approach was used to determine whether the previously published findings related to mitochondrial membrane potential were consistent with the early generation clonal and non-clonal host cell lines. In addition to Rh-123 staining (Figure 3.11 A), the mitochondrial mass stain MitoTracker Green FM (MTG) was used to identify any variance in the mitochondrial mass per cell (Figure 3.11 B).

The Rh-123 data showed that the mitochondrial membrane potential varied between the host cell lines. With the exception of cell line 20, all clonal host cell lines had significantly different median Rh-123 fluorescence intensity when compared to the non-clonal host, cell line NC. There was no significant variance detected in the MTG fluorescence (Figure 3.11 B). This suggested that the total mitochondrial mass per cell did not significantly vary between the host cell lines. This is an important control for the interpretation of the Rh-123 data.

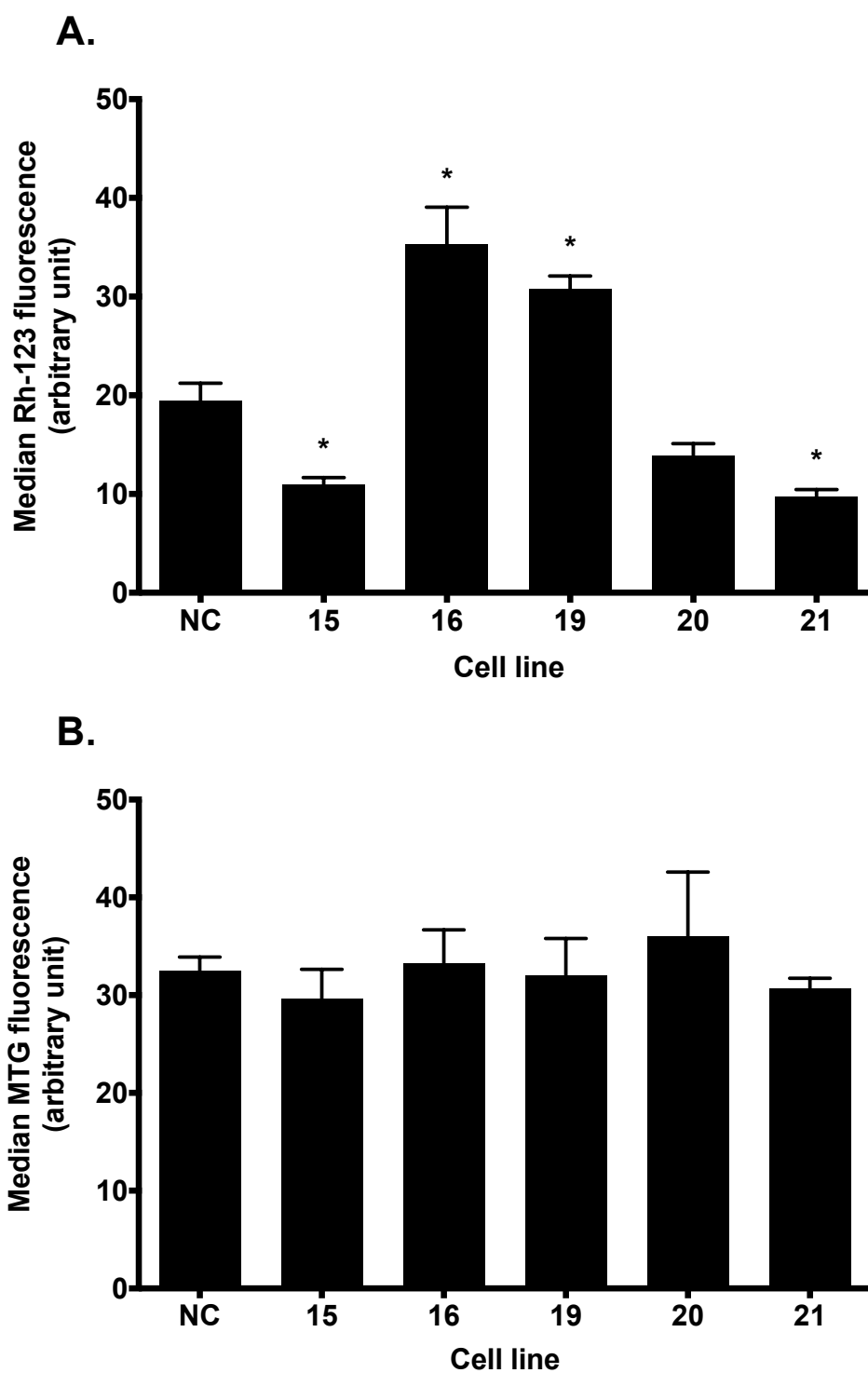
Comparison of the Rh-123 data to the quarter 1 growth rate in Table 3.1 showed that there was a relationship between Rh-123 fluorescence and growth rate. Clonal host cell lines 16 and 19, which had the slowest growth rate, had the strongest Rh-123 fluorescence intensity. Conversely, clonal host cell line 21, which had a faster rate of growth, had the weakest Rh-123 fluorescence intensity. However, clonal host cell line 20, which had the fastest rate of growth, had greater Rh-123 fluorescence intensity than the clonal host cell lines 15 and 21. A similar relationship was apparent when comparing the Rh-123 data to the VCD_{max} and CCT data in Table 3.3.

Early generation lactate production rate to glucose consumption rate ratios (Table 3.4) also correlated with the Rh-123 data (Figure 3.11). This suggested that Rh-123 staining could be a useful tool to identify clonal host cell lines that have a metabolically efficient phenotype. These findings are supported by other studies that have previously used Rh-

123 staining to assay for mitochondrial membrane potential (Borth et al. 1993; Hinterkörner et al. 2007).

Rh-123 can be used in both quenching and non-quenching mode, depending on the concentration used (Perry et al. 2011). The concentration of Rh-123 used in this study falls under quenching mode, in which Rh-123 fluorescence is quenched as more dye accumulates in hyperpolarised mitochondria. This implies that cell lines with low Rh-123 fluorescence have a more negative mitochondrial membrane potential than cell lines with high Rh-123 fluorescence. Mitochondrial membrane potential is critical for the synthesis of ATP via oxidative phosphorylation (Baracca et al. 2003), which explains why cells with weak Rh-123 fluorescence were observed to be more metabolically efficient (Section 3.3). Whilst the study by Hinterkörner is supportive of the findings presented in this thesis, the authors failed to acknowledge the quenching nature of the Rh-123 concentration used in their work, as such their interpretation of mitochondrial membrane potential may be incorrect (Hinterkörner et al. 2007). Quenching is a non-linear event (Perry et al. 2011), thus future experiments using Rh-123 with similar methodology to this study may benefit from decreased Rh-123 concentrations appropriate for non-quenching mode.

Figure 3.11 Analysis of mitochondrial membrane potential using rhodamine-123 and MitoTracker Green FM



*Six clonal and non-clonal host cell lines were cultured as described in Section 2.3.2. Cell counts were determined using an Invitrogen Countess Automated Cell Counter as described in Section 2.3.4, this is based on the trypan blue exclusion method. Cells were sampled on day 4 of culture from 3 consecutive maintenance flasks and assayed for rhodamine-123 fluorescence (A) and MitoTracker Green FM fluorescence (B) as described in Section 2.7. Error bars represent SEM for three biological replicates. * indicates $p < 0.05$, using independent samples t-test to compare clonal cell lines to cell line NC.*

3.6 Summary

The objectives of this chapter were:

- To determine the phenotypic variability of clonal host cell lines during long-term culture
- To assess variability in endogenous glutamine synthetase and determine the effects of glutamine-free culture on glutamine synthetase regulation
- To determine the mitochondrial activity of host cell lines

Study of a panel of host cell lines found variation to be present across a range of phenotypic properties. In many of the properties examined the non-clonal cell line was observed to have relatively average characteristics when compared to the clonal cell lines. This is perhaps to be expected as the clonal cell lines were derived from cell line NC. The experiments in this chapter demonstrate that the characterisation of clonal cell lines can identify phenotypic advantages in comparison to non-clonal cell lines. Cell lines that demonstrated rapid growth and high VCD_{max} were observed to utilise nutrients with greater efficiency than cell lines with inferior growth characteristics. Analysis of endogenous GS did indicate variance amongst the cell lines, however this was not strongly associated with growth. Study of the cell lines in the absence of glutamine suggest that all of the cell lines had similar capacity for maximum GS activity, but differ in their ability to downregulate the protein. Analysis of mitochondrial activity via the uptake of Rh-123 was found to reflect the growth and metabolic efficiency of the cell lines. Thus Rh-123 assays could be used as a rapid assay to identify host cell lines with desirable phenotypes. Transfection of these cell lines, as discussed in Chapter 4, with a vector containing a recombinant gene of interest enabled further study into heritability and advantages of the phenotypic variation observed in this chapter.

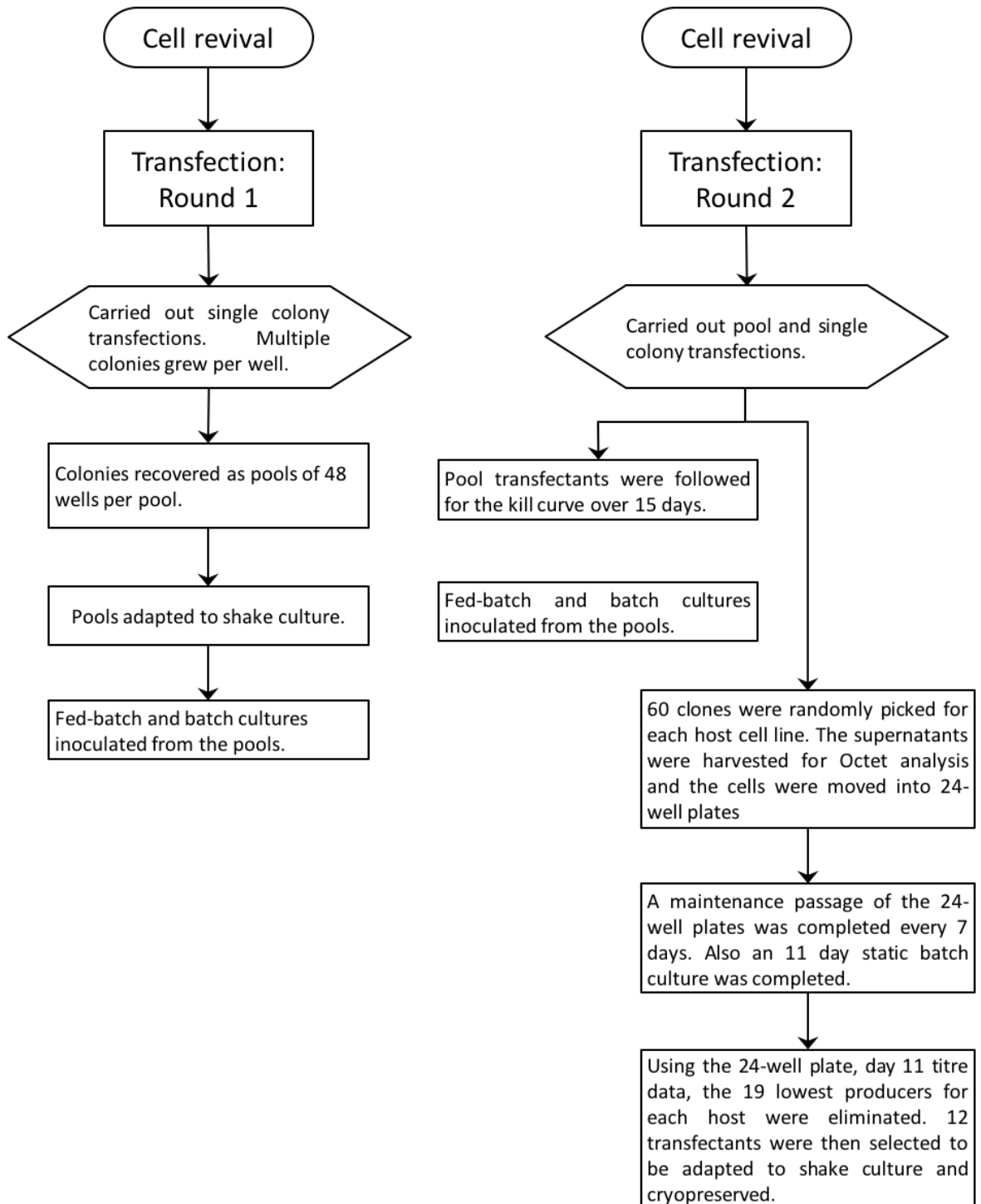
4. Determination of phenotypic variability and heritability of transfectants derived from clonal host cell lines

4.1 Introductory remarks

Previous work had identified that CHO cell lines exhibited considerable variability in growth and metabolite usage. It was inferred from this data that isolation of clonal host cell lines could select for host cell lines with desirable properties in advance of transfection. The aim of this Chapter was to determine whether the use of clonal host cell lines would give rise to transfectants that displayed less phenotypic variability than the non-clonal host cell line. In addition, it was hypothesised that transfectants would inherit the favourable characteristics of the host cell line.

The non-clonal host cell line NC and clonal host cell lines 15, 16, 19, 20 and 21 were revived from a working cell bank and transfected with a plasmid vector containing a gene for an IgG1 antibody, mAb-109. A Ubiquitous Chromatin Opening Element (UCOE) was included in the mAb-109 plasmid to alleviate any potential effects of the site of insertion of the plasmid, by limiting epigenetic silencing of the recombinant DNA (Saunders et al. 2015). Transfection round 1 generated polyclonal pools that were used for initial characterisation. Transfection round 2 generated an additional set of polyclonal pools and clonal transfectants for each of the host cell lines. Figure 4.1 outlines the transfections and generation of the pools/clonal transfectants.

Figure 4.1 Flow diagram of transfection process



Generation of stable, clonal transfectants was required for further study of the host cell lines. This figure outlines the transfection process that was followed whilst generating these transfectants. Polyclonal pools were also generated during this process.

4.2 Transfection with mAb-109 plasmid and generation of stable transfectants

Two sets of polyclonal pools and a panel of clonal transfectants were generated for each of the host cell lines (Figure 4.1), by transfecting with plasmid DNA encoding mAb-109. This Section illustrates, interprets and discusses each set of pools and the clonal transfectants separately.

4.2.1 Round 1: Analysis of growth and productivity characteristics of polyclonal pools in batch and fed-batch culture

Up to 10 pools were created and adapted to shake culture for each host cell line from transfection round 1. Some of the pools had very poor growth in shake culture and were not progressed. Then, in parallel, the pools were analysed in batch (Figure 4.2) and fed-batch culture (Figure 4.3) to determine growth characteristics and monoclonal antibody (mAb) production (Figure 4.4) in response to feed addition.

All batch and fed-batch cultures of transfected cells were inoculated with a greater cell density (0.5×10^6 cell ml^{-1}) than the host cell line batch cultures (Section 3.2.2). This resulted in the transfectants achieving greater cell densities than the host cell lines during the culture. However, the glutamine-free culture and methionine sulfoximine (MSX) may also have affected cell growth. In batch culture, the pools from host cell lines NC, 15, 20 and 21 displayed a similar pattern of growth (Figure 4.2). The pools from clonal host cell lines 16 and 19, which had lower growth as host cell lines (Section 3.2.2), achieved lower cell densities than the other pools and had a longer stationary phase. In fed-batch culture, the addition of feed had the effect of prolonging the growth, stationary and decline phases of culture (Figure 4.3). Variability in the growth profiles of the pools was observed. A greater standard deviation was typically observed in the fed-batch condition compared to the batch condition. The variability in growth was relatively low in the pools from host cell lines 15, 19 and 20 in contrast to the pools from host cell lines NC, 16 and 21.

Samples of culture supernatant collected over the course of culture were analysed for mAb titre (Figure 4.4). When grown in batch culture, the pools produced relatively low amounts of mAb-109 with an average titre of 251 mg l^{-1} . In the fed-batch condition, all of the pools had average titres in excess of 1000 mg l^{-1} with the exception of the pools from clonal host cell line 20. mAb titres were similar in both the batch and fed batch cultures up to day 6 whilst the cells were in growth phase. After day 6, an increase in titre in response

to feed addition was evident. From day 6, the majority of batch cultures were entering decline phase and the VCD decreased (Figure 4.2), and further increase in titre was limited. However, in the fed-batch conditions, the pools transitioned into a prolonged stationary phase (Figure 4.3), and in this phase further increase in mAb titre was observed. The mean harvest (day 14, or final day of culture) titre of the batch cell line 15 pools was significantly less than the cell line NC pools. In the fed-batch condition, the cell line 19 pools had a significantly greater mean harvest titre than the cell line NC pools, and the cell line 20 pools had a significantly lower mean harvest titre than the cell line NC pools. Variability in mAb titre was most evident in the fed-batch condition (Figure 4.4). The harvest titre of the fed-batch pools from host cell lines NC and 16 were the most variable. The fed-batch pools generated from clonal host cell line 15 were the least variable with respect to harvest titre.

The cell count and titre data were used to calculate additional average growth and productivity parameters (Table 4.1). Variation in VCD_{max} was evident in both the batch and fed-batch cultures. The pools from host cell line NC had the highest average VCD_{max} in the batch cultures and only the pools from clonal host cell line 21 grew to a higher average VCD_{max} in the fed-batch cultures. This contrasts with data from the clonal and non-clonal host cell lines (Table 3.3), in which cell line NC cultures achieved a mid-range VCD_{max} . However, the poor growth of clonal host cell lines 16 and 19, was reflected in the batch and fed-batch cultures of the pools. In response to feed addition, all of the fed-batch pools showed increased average VCD_{max} when compared to the batch cultures. However, the pools from host cell lines NC and 20 only demonstrated a mild increase in VCD_{max} , whereas the other pools showed an increase in VCD_{max} in excess of 2×10^6 cells ml^{-1} . Significant variation was observed in the average CCT between the pools in batch and fed-batch culture. Additionally, the average CCT increased in response to fed-batch culture, this reflects the increases in VCD_{max} and also the prolonged phases of cell culture.

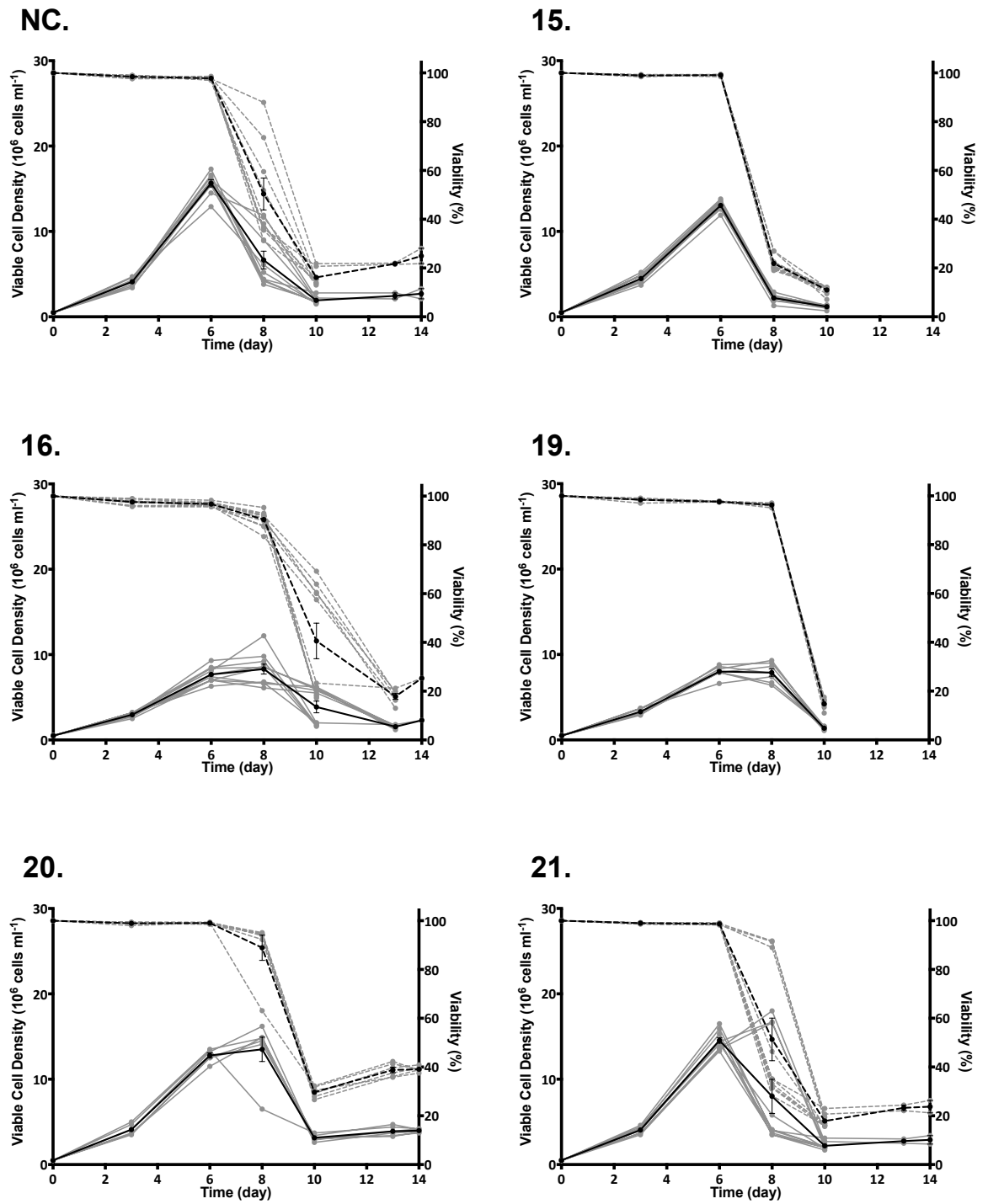
The average doubling time of the pools in batch culture was greater than those of the clonal and non-clonal host cell lines (Table 3.3). The pools from clonal host cell lines 16 and 19 had significantly average greater doubling times than the cell line NC pools. This was consistent with the trend observed in the clonal and non-clonal host cell lines (Table 3.3). The doubling time of the fed-batch pools was greater than that observed with the equivalent batch cultures. Doubling time was calculated between days 0-3 of culture, during this time all cultures were treated equally with the exception of flask size. Batch cultures were cultured in 125 ml Erlenmeyer flasks, whilst fed-batch cultures were cultured

in 250 ml Erlenmeyer flasks. This could have influenced the oxygen transfer rate to the cultures, and affected the doubling time (Maier et al. 2004).

The specific productivity (Q_p) was calculated for the pools over the duration of culture. In the batch condition the pools from clonal host cell line 19 had a statistically greater average Q_p when compared to the cell line NC pools. The pools from clonal host cell line 20, which had the lowest titres (Figure 4.4) also had the lowest Q_p in batch culture. In fed-batch culture, the Q_p increased for all of the pools. The pools from clonal host cell lines 16 and 19 had the greatest Q_p , this was significant when compared to the cell line NC pools. The high Q_p of the cell line 16 and 19 pools accounts for the high harvest titres achieved by these cell lines despite their poor growth properties.

Growth of polyclonal pools generated from transfection round 1 demonstrated that variability was present in the growth profiles and parameters of pools derived from host cell line NC and the clonally derived host cell lines. In addition to variability in growth, variability in mAb production of the cultures was observed. Where applicable, variation was assessed by the standard deviation of parameters measured for the pools from each host cell line. Analysis of VCD_{max} , CCT and harvest titre suggested that the pools derived from clonal host cell lines 15, 19 and 20 displayed less variability than the pools derived from cell line NC. However the pools derived from cell line NC were the least variable in doubling time in the fed-batch condition, and only the cell line 15 and 20 pools were less variable than the cell line NC pools in fed-batch Q_p . Variability in clonally derived cell lines is not surprising, genetic fluidity has been observed in immortalised cell lines since the 1960's (Hsu 1961; Wurm 2013). Karyotype analysis of CHO K1 and CHO DG44 cell lines has previously shown marked differences in chromosome structure and few of the structures are thought to be stable (Deaven & Petersen 1973; Cao et al. 2011). CHO cell clonal variability has been observed in published works (Kim et al. 1998; Davies et al. 2013), however work in NS0 host cells provided evidence that the generation of clonally derived cell lines can decrease the observed variability (Barnes et al. 2006).

Figure 4.2 Growth parameters of pools from transfection round 1 in batch culture



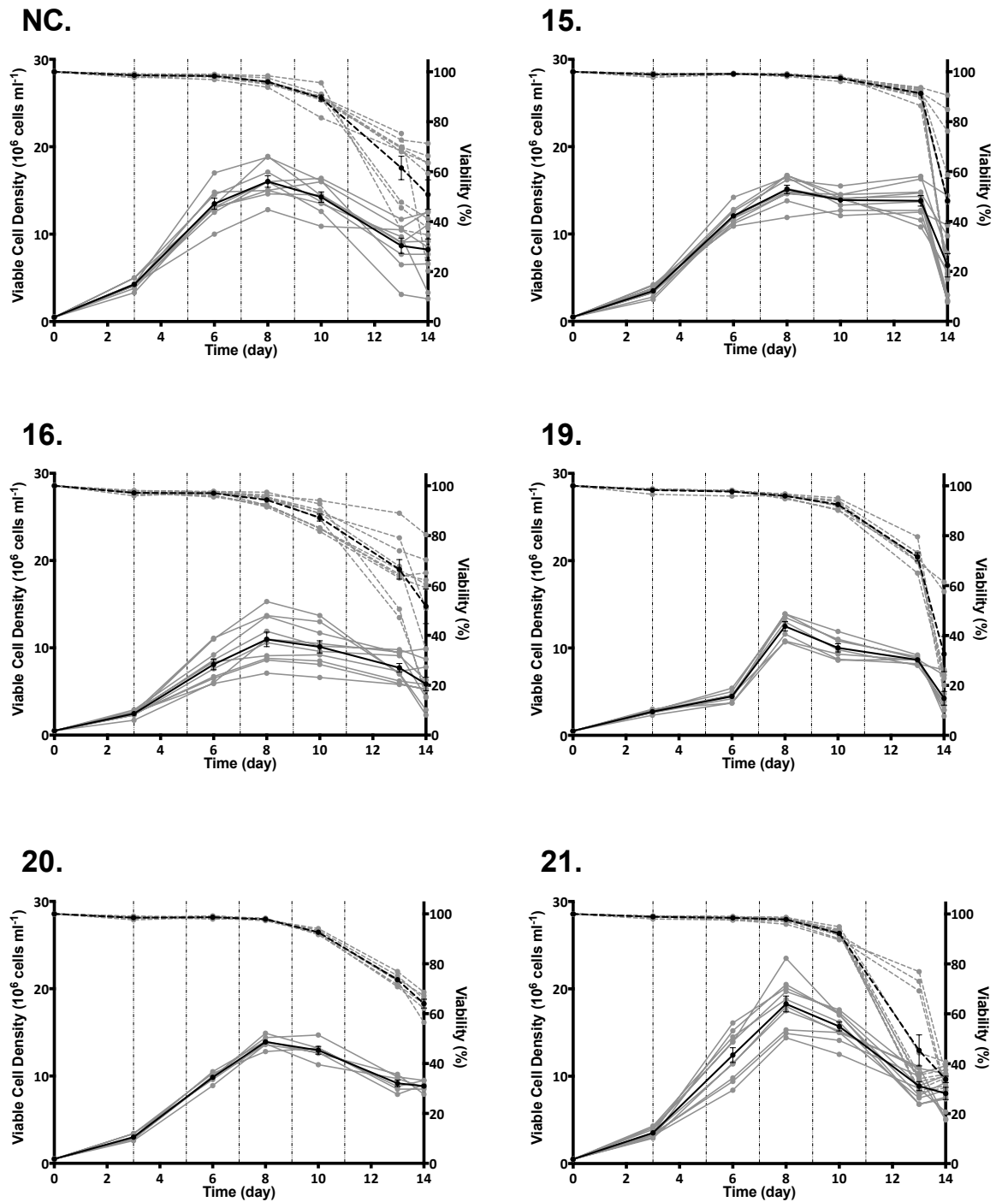
Legend

- Viable cell density
- -●- - Viability
- Mean viable cell density
- -●- - Mean viability

Six clonal and non-clonal host cell lines were transfected with a plasmid vector containing a glutamine synthetase, IgG heavy and IgG light chain genes (Section 2.3.7). The transfected cells were subsequently diluted in CD-CHO media and 50 μ l well⁻¹ was transferred to 96-well. After 24 hours, 150 μ l of CD-CHO containing 66.7 μ M MSX was added to each well to achieve a final MSX concentration of 50 μ M. The plates were maintained at 37 °C, with 5% CO₂ in a humidified static incubator. The cells were left to grow under these conditions for 28 days. Upon inspection, the cells had not been diluted sufficiently to achieve single colonies, thus 10 polyclonal pools were created for each host by combining the cells in 48 wells per pool and adapting to shake culture.

From the pools that successfully adapted to shake culture, batch cultures were created. Batch cultures were initiated and maintained as described in Section 2.3.3. Cell counts were taken using a Beckman Coulter Vi-CELL XR (Section 2.3.4), this is based on the trypan blue exclusion method. Cultures were monitored for up to 14 days. The charts show the viable cell densities and viability of the pools generated from non-clonal host cell line NC and clonal host cell lines 15, 16, 19, 20 and 21. The error bars represent the SEM.

Figure 4.3 Growth parameters of pools from transfection round 1 in fed-batch culture

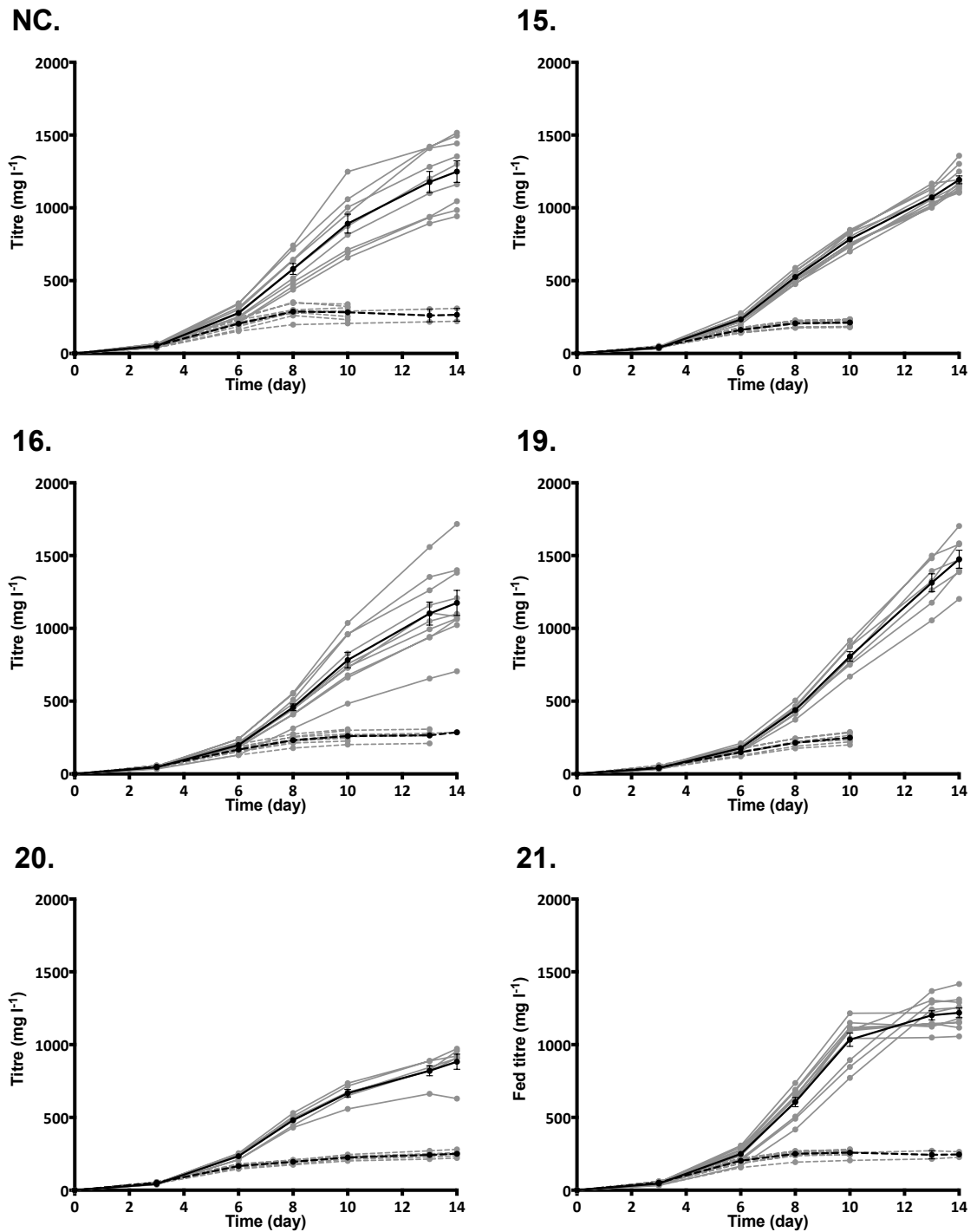


Legend

- Viable cell density
- Viability
- Mean viable cell density
- Mean viability

Pools from Transfection 1 were created as described in Figure 4.2. In addition to the batch cultures described in Figure 4.2, fed-batch cultures were initiated and maintained as described in Section 2.3.3. The cultures were fed with 3.5 ml of a proprietary feed on days 3, 5, 7, 9 and 11, as indicated by vertical dashed lines. Cell counts were taken using a Beckman Coulter Vi-CELL XR (Section 2.3.4), this is based on the trypan blue exclusion method. Cultures were monitored until the viability was $\leq 30\%$. The charts show the viable cell densities and viability of the pools generated from non-clonal host cell line NC, and clonal host cell lines 15, 16, 19, 20 and 21. The error bars represent the SEM.

Figure 4.4 Analysis of mAb production of pools from transfection round 1 in batch and fed-batch culture



Legend

- Fed-batch titre
- Mean fed-batch titre
- -●- - Batch titre
- -●- - Mean batch titre

As described in Figure 4.2 and 4.3, batch and fed-batch cultures were created for the pools derived from Transfection 1. On days 3, 6, 8, 10, 13 and 14, media samples were taken from each culture for antibody titre analysis. 900 µl media samples were removed from the cultures and centrifuged at 130 g for 5 minutes at room temperature. The supernatant was then frozen at -80 °C and subsequently analysed for antibody titre using a FortéBio Octet system (Section 2.5.1). The charts show the antibody titre of the pools generated from the non-clonal host cell line NC, and the clonal host cell lines 15, 16, 19, 20 and 21. Titre data was not included after day 10 for some pools in batch culture, as cultures were terminated after day 10 if viability was below 20% (Figure 4.2). The error bars represent the SEM.

Table 4.1 Analysis of growth parameters and specific productivity of pools from transfection round 1 grown in batch and fed-batch culture

| Cell line | NC | 15 | 16 | 19 | 20 | 21 |
|--|--------------------------|-------------------------|--------------------------|---------------------------|--------------------------|--------------------------|
| Batch VCD_{max} (x10 ⁶ cells ml ⁻¹) | 15.64 1.31 | 13.05* 0.53 | 8.31* 1.66 | 8.03* 0.67 | 13.51 0.92 | 14.55 1.44 |
| Fed-batch VCD_{max} (x10 ⁶ cells ml ⁻¹) | 16.03 1.94 | 15.09 1.40 | 10.98* 2.64 | 12.47* 1.42 | 13.89* 0.65 | 18.26 2.68 |
| Batch CCT (x10 ⁶ cells ml ⁻¹ day ⁻¹) | 69.64 7.9 | 52.40* 3.36 | 55.65* 4.31 | 47.84* 3.25 | 89.59* 5.54 | 69.71 13.69 |
| Fed-batch CCT (x10 ⁶ cells ml ⁻¹ day ⁻¹) | 136.29 11.58 | 137.14 8.96 | 93.89* 16.08 | 89.40* 7.01 | 117.34* 4.88 | 139.85 16.15 |
| Batch doubling time (hours) | 23.77 1.25 | 22.87 1.20 | 28.17* 1.32 | 26.57* 1.47 | 23.90 1.59 | 23.90 0.96 |
| Fed-batch doubling time (hours) | 23.50 1.49 | 26.00* 2.35 | 31.77* 3.34 | 29.63* 1.64 | 27.99* 1.55 | 25.76* 1.64 |
| Batch Titre (mg l ⁻¹) | 265.50 41.47 | 212.44* 22.33 | 285.90 31.68 | 248.80 32.57 | 250.13 20.05 | 245.35 17.37 |
| Fed-batch Titre (mg l ⁻¹) | 1249.02 222.56 | 1192.85 84.70 | 1174.75 272.91 | 1474.90* 164.49 | 882.58* 126.88 | 1218.56 106.50 |
| Batch Qp (pg cell ⁻¹ day ⁻¹) | 4.19 0.94 | 4.09 0.62 | 4.81 0.82 | 5.23* 0.88 | 2.80* 0.24 | 3.89 0.84 |
| Fed-batch Qp (pg cell ⁻¹ day ⁻¹) | 9.20 1.66 | 8.73 0.80 | 12.65* 2.62 | 16.55* 1.93 | 7.54 1.18 | 8.88 1.68 |

Polyclonal pools generated from six clonal and non-clonal host cell lines were grown in batch and fed-batch culture conditions as previously described (Figure 4.2 and 4.3). VCD_{max} for the pools from each host cell line was determined from cell count data. CCT was calculated from the summation of the integral of viable cell density, which was determined between each cell count cell count time point. Doubling time was calculated between day 0 and day 3, this time period falls within the exponential growth phase for all of the pools. The titre represents the harvest titre, determined from the culture supernatant on day 14, or last day of culture if least than 14 days. The Qp represents the Qp final and was calculated from the harvest titre and CCT data. The data represent the mean values for each respective group of cultures. * indicates p<0.05, using

independent samples t-test to compare clonal cell line pools to cell line NC pools of the respective culture conditions. The standard deviation of each value is included in italic font.

4.2.2 Round 2: Analysis of growth and productivity characteristics of polyclonal pools in batch and fed-batch culture

The pools discussed in the previous Section were generated via an unconventional method, however they provided beneficial information regarding how the host cell lines respond to transfection. As the transfection round 1 pools were first grown in static plates, before several colonies were combined, the selective pressures will have differed to the transfection round 2 pools. Additionally, the degree of heterogeneity in the transfection round 1 pools was likely limited by this process of pool creation compared to the transfection round 2 pool methodology. The pools in this Section were generated as described in Section 2.3.8, then monitored for 15 days to assess the kill curve (Appendix C). The kill curve analysis found pool 15 and 20 retained the highest viability. Pool 16, NC, 19 and 21 demonstrated the lowest percentage of viable cells. All of the pools showed an increase in viability from day 8, with the exception of pool 16 which declined until day 11.

Following the recovery and kill curve analysis, the pools were subcultured at least twice prior to initiation of batch and fed-batch cultures (Figure 4.5). In batch culture (Figure 4.5 A), the stationary phase was observed to span 2 days. This duration was increased when compared to the stationary phase of some of the pools from transfection round 1 (Figure 4.2). Analysis of mAb production (Figure 4.5 C) found the average titre to be 262 mg l⁻¹, which was an increase (not significant) when compared to the pools from transfection round 1 (Section 4.2.1).

Fed-batch culture of the pools demonstrated that the feed prolonged the growth and stationary phases of growth (Figure 4.5 B), this was also observed in the transfection round 1 pools (Figure 4.2 and 4.3). Pool NC responded poorly to feed and viability rapidly declined. Poor response to feed was also observed in the mAb production of pool NC, the harvest titre was 539 mg l⁻¹, which was less than the average titre of the transfection round 1 cell line NC pools (1249 mg l⁻¹). Pool 16 was the only fed-batch culture that had a harvest titre greater than the corresponding average reported in the previous Section. The harvest titre of all of the transfection round 2 pools was within the range observed in Figure 4.4, with the exception of pool NC.

Additional parameters calculated from the transfection round 2 pools' culture data are presented in Table 4.2. Variation was apparent between the pools in the VCD_{max} data, which had been observed previously (Table 3.3 and 4.1). In batch culture, comparative to the host cell line data (Table 3.3), pools 16 and 19 had the lowest VCD_{max} . Pool NC had a relatively mid-range VCD_{max} , whilst pool 21 displayed the greatest VCD_{max} . In terms of VCD_{max} , the response to feed differed to that observed in the transfection round 1 pools, where all cell lines displayed an increased VCD_{max} . Only the transfection round 2 pools 16 and 19 displayed an increase in VCD_{max} in response to feed. In support of the transfection round 1 pools data, all of the transfection round 2 pools did show an increase in CCT, in response to feed. Considerable variation was observed in the doubling time of the pools. In the case of pool 16 and 20, a difference of approximately 10 hours was observed in the doubling time between the batch and fed-batch condition. The batch cultures were performed in 125 ml Erlenmeyer flasks and the fed-batch cultures were performed in 250 ml Erlenmeyer flasks; this may have had an effect on the oxygen transfer rate as discussed in Section 4.2.1. However, the impact on doubling time was opposite of that observed in the previous section, this suggests that flask size should be consistent between conditions. Consistent with previous data, variation was observed in the Q_p of the pools. Pool 16 and 19 had the greatest Q_p in the fed-batch condition, this was also observed in the transfection round 1 pools.

The polyclonal pools generated during this work were cultured in both batch and fed-batch conditions, this enabled the response to feed to be analysed. Feed addition prolonged the growth and stationary phases of the transfection round 1 pools (Figure 4.2 and 4.3) and caused an increase in mAb production (Figure 4.4). This response to feed was confirmed by the transfection round 2 pools (Figure 4.5). The addition of feed to the transfection round 1 pools caused an increase in VCD_{max} , this was not supported by pools NC, 15 and 20 from transfection round 2. However, increases in CCT and Q_p were observed in both sets of pools. The response to feed observed in the study, increased CCT and mAb production, is consistent with previous mammalian cell line studies (Ma et al. 2009; Sellick et al. 2011; Mahboudi et al. 2013) which suggests that the application of feed, alleviates some metabolic bottlenecks/nutrient limitations. The metabolic profiles of clonal transfectants will be addressed in greater detail in Chapter 5.

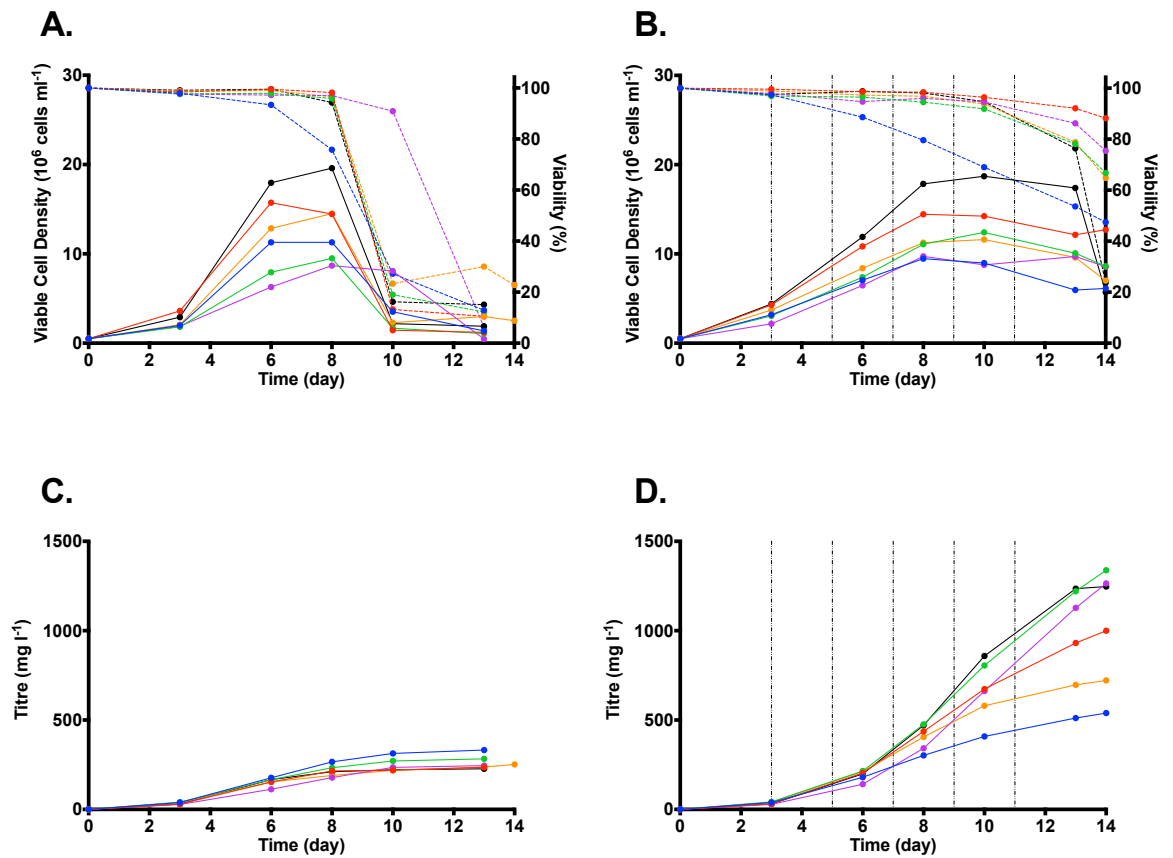
Isolation of clonal transfectants in industry, that are suitable for production processes typically exploit transfectant variability to select the "best" transfectants for recombinant protein production (O'Callaghan et al. 2010; Porter et al. 2010; Porter et al. 2010). However, a consequence of this variability is the large number of transfectants that must

be screened. The work presented in Chapter 3, indicated that clonal host cell lines possess potential phenotypic advantages compared to a non-clonal population. Heritability of these phenotypes in transfectants could enrich resultant transfectant populations with desirable production clones. It also possible that clonal host cell lines could be selected, based on their phenotype, for a specific production platform.

Relationships between the growth parameters of the Transfection 1 pools (Table 4.1) and the clonal host cell lines (Table 3.3) were observed. As hosts, cell line 15, 20 and 21 demonstrated the greatest VCD_{max} and CCT. Host cell line 16 and 19 performed poorly with respect to these properties. A similar pattern was evident in these properties in the transfection round 1 pools. The relationship was also observed in the doubling time data i.e. cell line 16 and 19 had the longest doubling times as both hosts and transfectants. These observations are supported by previous work that determined proliferation rate to be heritable in some CHO clones (Konrad et al. 1977; Davies et al. 2013). Average doubling time was greater for all of the transfection round 1 pools, when compared to their respective hosts. This could be a consequence of glutamine-free culture, the growth rate of the hosts had previously been found to decrease under glutamine-free conditions (Figure 3.9).

Evidence of growth phenotype heritability was also observed in the data VCD_{max} data for the transfection round 2 pools grown in batch culture (Table 4.2). However, comparison to the transfection round 1 data (Table 4.1) also highlights variability in this parameter. It is of interest that pool 16 and pool 19 had the greatest Q_p in fed-batch culture in both data sets. Previous research has found Q_p not to be a heritable functionality of CHO cells (Davies et al. 2013), and subject to stochastic variation (Pilbrough et al. 2009). The pool data presented here suggest that Q_p is subject to variation but is also heritable (at least temporarily (Pichler et al. 2010)). Previous work has suggested a relationship between cell growth and Q_p , in which low rates of growth were linked with greater Q_p . (Gòdia & Cairó 2001; Fussenegger & Betenbaugh 2002; Khoo & Al-Rubeai 2009). The pool data support this, thus heritability of Q_p may be partially explained by the heritability of growth phenotype.

Figure 4.5 Growth parameters and mAb production of pools from transfection round 2 grown in batch and fed-batch culture



Legend

- | | |
|---|---|
| ● Pool NC viable cell density/titre | - - ● - - Pool NC viability |
| ● Pool 15 viable cell density/titre | - - ● - - Pool 15 viability |
| ● Pool 16 viable cell density/titre | - - ● - - Pool 16 viability |
| ● Pool 19 viable cell density/titre | - - ● - - Pool 19 viability |
| ● Pool 20 viable cell density/titre | - - ● - - Pool 20 viability |
| ● Pool 21 viable cell density/titre | - - ● - - Pool 21 viability |

Pools generated during transfection round 2 were allowed to recover from the transfection and the kill curves were monitored for 15 days. Following the recovery period, the pools were used to inoculate batch and fed-batch cultures. All batch and fed-batch cultures were initiated and maintained as described in Section 2.3.3. The fed-batch cultures were fed with 3.5 ml of a proprietary feed on days 3, 5, 7, 9 and 11 as indicated by the dashed vertical lines. Cell counts were taken using a Beckman Coulter Vi-CELL XR, this is based on the trypan blue exclusion method. Samples were taken from the cultures for antibody titre analysis as described in Figure 4.4. Cultures were monitored for up to 14 days. The charts show the viable cell densities and viability of the batch cultures (A), fed-batch cultures (B) and antibody titre of the batch cultures (C), fed-batch cultures (D) of the pools.

Table 4.2 Analysis of growth parameters and specific productivity of pools from transfection round 2 grown in batch and fed-batch culture

| Cell line | NC | 15 | 16 | 19 | 20 | 21 |
|---|--------|--------|---------|---------|--------|---------|
| Batch VCD_{max} ($\times 10^6$ cells ml^{-1}) | 11.29 | 15.73 | 9.50 | 8.68 | 14.50 | 19.60 |
| Fed-batch VCD_{max} ($\times 10^6$ cells ml^{-1}) | 9.47 | 14.44 | 12.41 | 9.73 | 11.61 | 18.70 |
| Batch CCT ($\times 10^6$ cells ml^{-1} day $^{-1}$) | 68.34 | 85.26 | 50.90 | 60.35 | 81.00 | 101.85 |
| Fed-batch CCT ($\times 10^6$ cells ml^{-1} day $^{-1}$) | 84.35 | 135.77 | 106.06 | 88.50 | 107.16 | 163.79 |
| Batch doubling time (hours) | 36.18 | 25.23 | 38.47 | 37.55 | 35.27 | 28.35 |
| Fed-batch doubling time (hours) | 26.91 | 23.25 | 27.53 | 34.02 | 24.86 | 22.97 |
| Batch titre ($mg\ l^{-1}$) | 332.10 | 235.40 | 282.90 | 245.10 | 251.30 | 227.30 |
| Fed-batch titre ($mg\ l^{-1}$) | 539.20 | 999.80 | 1338.20 | 1264.60 | 721.50 | 1246.90 |
| Batch Qp ($pg\ cell^{-1}\ day^{-1}$) | 4.86 | 2.76 | 5.56 | 4.06 | 3.10 | 2.23 |
| Fed-batch Qp ($pg\ cell^{-1}\ day^{-1}$) | 6.39 | 7.36 | 12.62 | 14.29 | 6.73 | 7.61 |

Polyclonal pools generated from six clonal and non-clonal host cell lines were grown in fed-batch and batch culture conditions as previously described (Figure 4.5). VCD_{max} for each pool was determined from cell count data. CCT was calculated from the summation of the integral of viable cell density, which was determined between each cell count time point. Doubling time was calculated between day 0 and day 3, this time period falls within the exponential growth phase for all of the cultures. The titre represents the harvest titre, determined from the culture supernatant on day 14, or last day of culture if least than 14 days. The Qp represents the Qp final and was calculated from the harvest titre and CCT data.

4.2.3 Generation and productivity analysis of clonal transfectants

Clonal transfectants were generated as described in Section 2.3.9. Sixty of the single colony transfectants were picked and moved from 96-well plates to 24-well plates. During the subculture to 24-well plates, samples of cell culture supernatant were collected for mAb titre analysis (Figure 4.6 A). The transfectants were maintained and subcultured in 24-well plate format. In addition to this, a set of plates was used to harvest cell culture supernatant for mAb titre analysis on day 11 of culture (Figure 4.6 B). Mean titres for cell line 20 and 21 transfectants were significantly greater than the mean titre of the transfectants from cell line NC. Analysis of titres from transfectants at 24-well plate stage, showed cell lines 16, 19, 20 and 21 transfectants to have significantly greater mean titres than transfectants from cell line NC. Variability was determined by the standard deviation of the mean titre. The 96-well plate data suggested that transfectants from cell line 19 and 20 were less variable than the transfectants from cell line NC. This was supportive of the transfection round 1 pool data (Section 4.2.1). Conversely, the 24-well plate data suggest that transfectants from cell line NC were the least variable. Linear regression analysis indicated a relatively strong relationship between titre data from 96-well and 24-well plates (Appendix D) for the data for the clonal cell line 15, 16, 20 and 21 transfectants. The relationship was weaker for transfectants generated from cell lines NC and 19. This may indicate that the transfectants generated from cell lines NC and 19 are less likely to be stable in long-term culture.

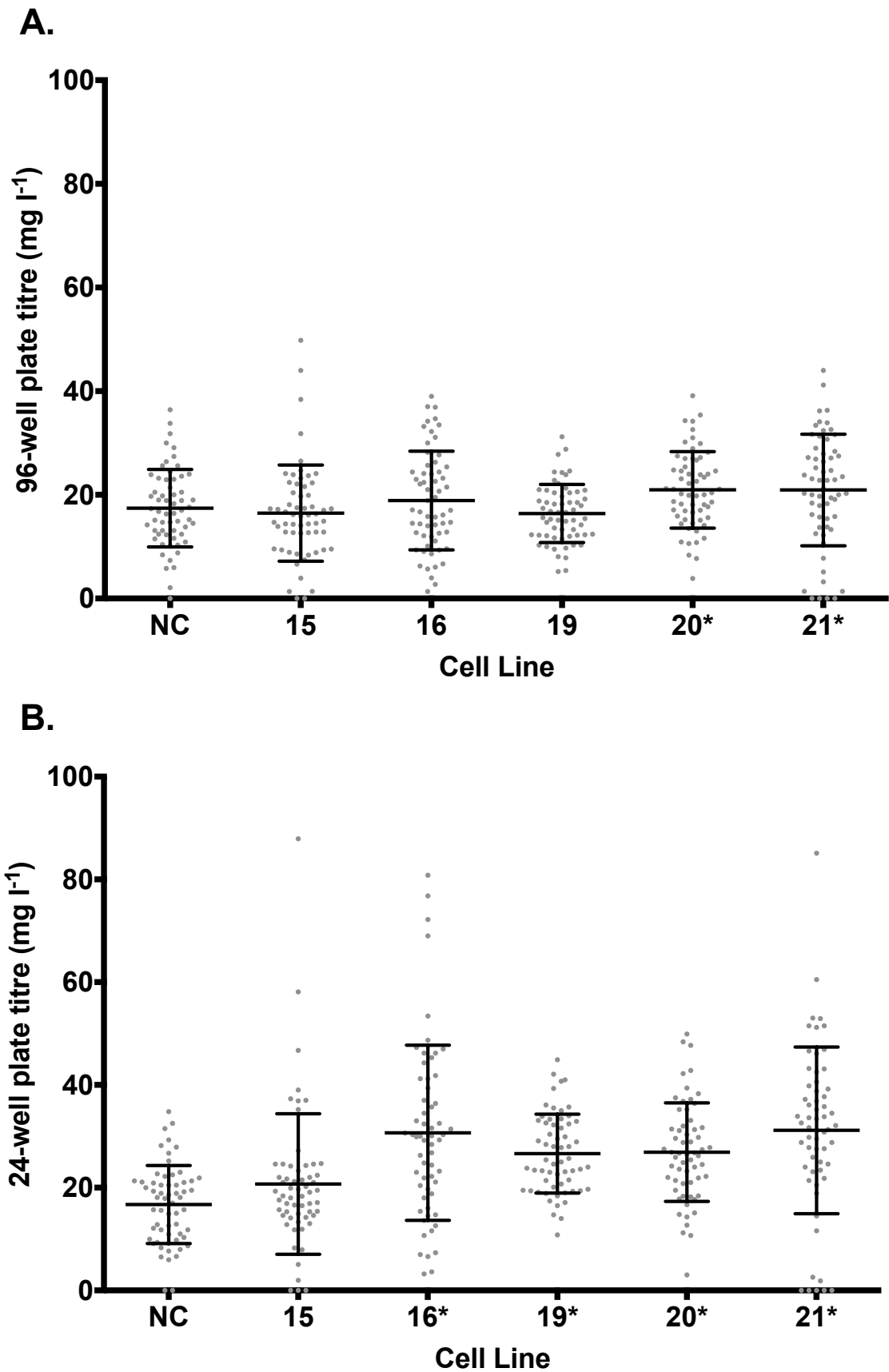
Analysis of the transfection round 1 pool data provided some support to the hypothesis, that the use of clonal host cell lines would give rise to transfectants that displayed less phenotypic variability than a non-clonal host cell line. However, the mAb titre analysis of the clonal transfectants was mostly in favour of the null hypothesis, that the use of clonal host cell lines does not produce transfectants that display less variability than a non-clonal host cell line. Although, it is important to consider that this, single colony, data does not account for cell number, a fed-batch experiment with controlled seeding density would have been preferable, but not practically feasible with this number of transfectants. Gene copy number could also contribute to variability in mAb expression, this was investigated for select high and low productivity clonal transfectants (Section 5.2.3). CHO cell cultures are heterogeneous (Pilbrough et al. 2009), and it has been suggested that they follow a “mutator phenotype” (Davies et al. 2013) and undergo substantial genetic drift during culture (Wurm 2013). Additionally, differences in cellular pathways, which may be affected by epigenetic regulation (Neildez-Nguyen et al. 2008) can affect phenotype. It is possible that “freshly” cloned host cell lines could decrease variability and may have improved the

experimental design (Barnes et al. 2006; Pichler et al. 2010), whereas (epi)genetic variability may have accumulated in the host cell lines prior to transfection or during scale-up post transfection.

The clonal transfectants studied here were generated by one round of limited dilution cloning, and following colony formation care was taken to pick single colonies. More precise automated systems, e.g. Molecular Devices ClonePix System, exist that increase the probability of single colony selection. Selection of any non-clonal colonies could account for a portion of the observed variability, however as double and irregular shaped colonies were not picked this is improbable.

For further study, it was necessary to focus on a smaller number of transfectants, due to incubator space constraints. The transfectants were ranked according to the 24-well plate titre, and the 19 lowest expressers were then excluded. Following this, 12 transfectants for each host cell line were adapted to shake culture and cryopreserved. The transfectants selected covered the range of titres observed (Table 4.3).

Figure 4.6 Analysis of clonal transfectant mAb production from 96-well and 24-well plates



*As described in Section 2.3.7 six clonal and non-clonal host cell lines were transfected with a plasmid vector containing a glutamine synthetase, IgG heavy and IgG light chain gene. The transfected cells were grown in 96-well plates; following this 60 single colonies were moved into 24-well plates (Section 2.3.9). As the cells were been moved into the 24-well plates, 150 µl of the conditioned media was harvested for antibody titre analysis. During the 24-well plate stage, a set of plates were allowed to grow for 11 days as a static batch culture. At day 11, 200 µl of culture media was harvested for antibody titre analysis. The cells were maintained in CD-CHO medium supplemented with 50 µl MSX at 37 °C, with 5% CO₂ in a humidified static incubator. The cell culture media samples were stored at -80 °C and subsequently analysed for antibody titre using a FortéBio Octet system (Section 2.5.1). The charts show 96-well plate titre (A) and 24-well plate titre (B). The mean titre and error bars are shown in black, the error bars represent the SD of the mean. * indicates $p < 0.05$, using independent samples t-test to compare transfectants from clonal host cell lines to transfectants from non-clonal host cell line NC.*

Table 4.3 24-well plate, day 11 static titre of transfectants adapted to shake culture

| Cell line | NC | 15 | 16 | 19 | 20 | 21 |
|-----------------|-----------------------------|------|------|------|------|------|
| | Titre (mg l ⁻¹) | | | | | |
| Transfectant 1 | 34.8 | 87.9 | 80.8 | 44.9 | 49.9 | 85.1 |
| Transfectant 2 | 32.5 | 58.1 | 76.8 | 42.1 | 48.4 | 60.5 |
| Transfectant 3 | 28.2 | 37.3 | 53.4 | 39.3 | 42.2 | 51.5 |
| Transfectant 4 | 23.0 | 27.2 | 46.2 | 35.0 | 37.2 | 46.6 |
| Transfectant 5 | 21.9 | 24.6 | 41.8 | 33.3 | 35.2 | 42.5 |
| Transfectant 6 | 21.0 | 22.4 | 37 | 32.4 | 31.4 | 38.8 |
| Transfectant 7 | 20.5 | 21.5 | 33 | 29.2 | 29.8 | 36.1 |
| Transfectant 8 | 19.2 | 20.2 | 31.4 | 28.4 | 27.8 | 33.9 |
| Transfectant 9 | 18.1 | 19.3 | 30.1 | 25.7 | 26.8 | 32.6 |
| Transfectant 10 | 15.7 | 18.0 | 29.2 | 24.0 | 25.9 | 31.1 |
| Transfectant 11 | 14.9 | 16.9 | 24.8 | 23.3 | 24.2 | 28.8 |
| Transfectant 12 | 12.1 | 15.4 | 22.2 | 22.6 | 22.2 | 27.5 |

As described in Figure 4.6 single colony transfectants were generated from six clonal and non-clonal host cell lines. Twelve transfectants derived from each clonal host cell line were adapted to shake culture. This table shows the range of the transfectant titres determined from the 24-well plate batch culture described in Figure 4.6. For each cell line, transfectant 1 represents the top titre transfectant.

4.3 Characterisation of clonal transfectants derived from clonal host cell line 15 and 19

Clonal transfectants derived from clonal host cell lines 15 and 19 were selected as the pool experiments found relatively limited variation, with respect to VCD_{max} and CCT, in the transfectants compared with transfectants derived from the other clonal and non-clonal host cell lines (Section 4.2). Also, these clonal host cell lines appeared to give rise to transfectant pools that showed inter-clonal differences with respect to growth and Qp (Table 4.1 and 4.2).

4.3.1 Analysis of transfectant growth characteristics during long-term culture

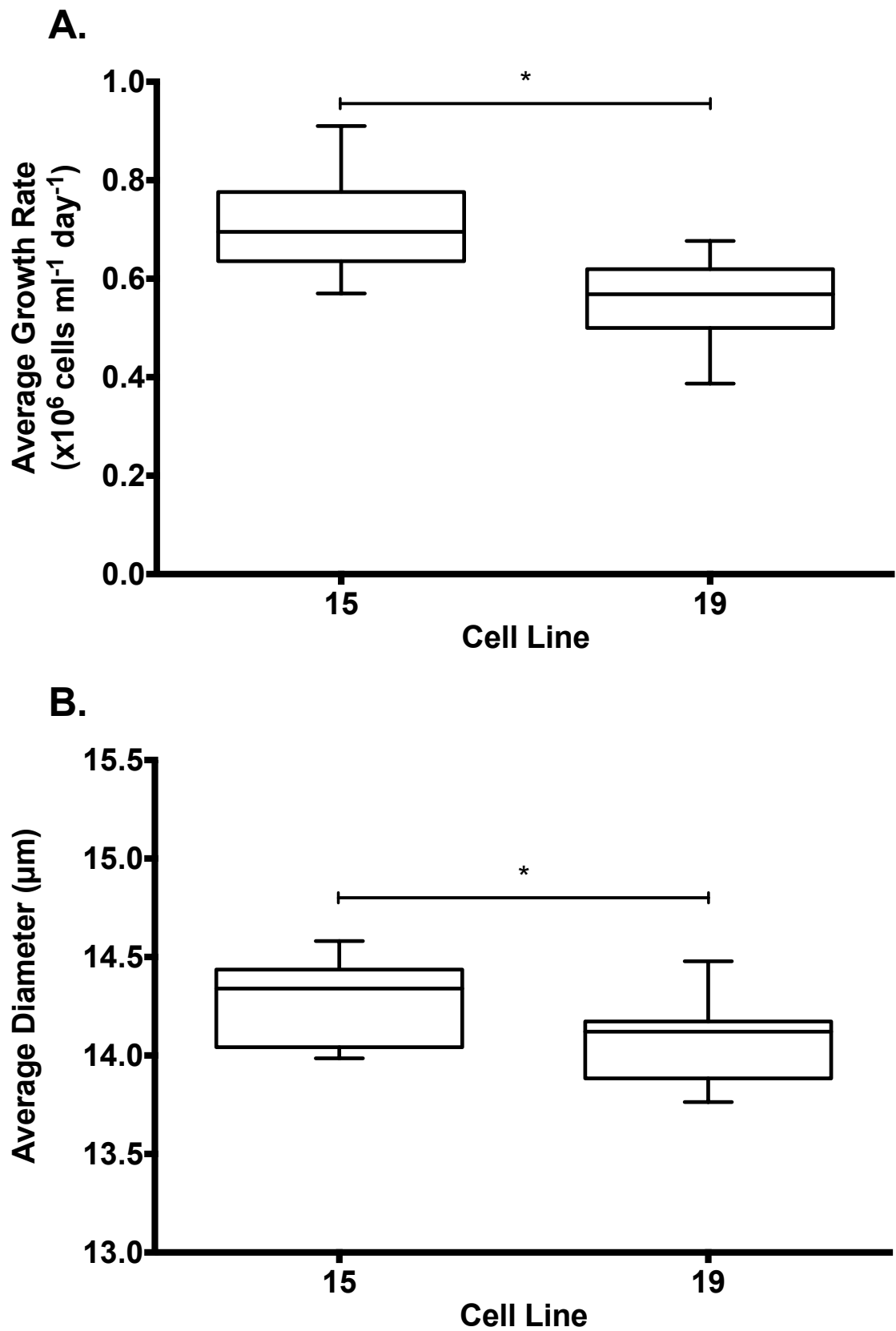
The clonal transfectants derived from host cell lines 15 and 19 were cultured for 55 days as described in Section 2.3.2. During subculture, the average growth rate of the cell line 19 transfectants was significantly ($p < 0.05$) slower than the average growth rate of the cell line 15 transfectants (Figure 4.7 A). A similar difference was observed between the growth rates of the untransfected host cell lines during long-term culture (LTC) (Table 3.1). The transfectants had slower growth rates when compared to the host cell lines during the first quarter of LTC.

The average diameter of the cell line 15 transfectants was significantly greater than the cell line 19 transfectants (Figure 4.7 B). When compared to their respective clonal host cell line (Table 3.2), the cell line 15 transfectants had a greater average diameter than the clonal host 15 during the first half of the host LTC. The cell line 19 transfectants also had a greater average diameter than clonal host cell line 19 during the first half of LTC, although the average diameter of clonal host cell line 19 was within the range observed in the transfectants.

In LTC, the average growth rate of both groups of transfectants (Figure 4.7 A) was less than the growth rate of their respective hosts (Table 3.1 Q1). As discussed in Section 5.2.1, this could be due to the glutamine-free culture of transfectants. The average growth rate of the cell line 19 transfectants was significantly slower than that of cell line 15 transfectants. This is in support of the host data (Table 3.1) and further supports the hypothesis of heritable characteristics. However the observed difference in cell diameter (Figure 4.7 B) was not consistent with the host data (Table 3.2) and also is not supported by previous works that suggest growth rate is inversely proportional to cell size

(Kuystermans et al. 2010; Davies et al. 2013). It is possible that the Q_p of the transfectants is related to cell diameter.

Figure 4.7 Analysis of transfectant growth rate and diameter during LTC



*Twelve transfectants derived from clonal host cell line 15 and 19 were subject to LTC for 55 days as described in Section 2.3.2. The charts show the average growth rate (A) and average diameter (B) during LTC. The boxes show the 25th and 75th percentile of the data and the central line represents the median, the whiskers represent the minimum and maximum values. * indicates $p < 0.05$, using independent samples t-test to compare the cell line 15 transfectants to the cell line 19 transfectants.*

4.3.2 Analysis of early and late generation transfectant growth and productivity during fed-batch culture

The clonal transfectants described in Section 4.3.1 were examined in fed-batch culture at an early (between generations 7-12) and late (between generations 38-54) generation of LTC. Although all transfectants were cultured under identical conditions (Section 2.3.3), variability was observed in the growth of the transfectants (Figure 4.8). The average VCD_{max} of the early generation cell line 15 transfectants was significantly ($p < 0.05$) greater than the VCD_{max} of the cell line 19 transfectants (Table 4.4). Additionally, as determined by the standard deviation, less variance was observed in VCD_{max} for the cell line 15 transfectants than for the cell line 19 transfectants. The average VCD_{max} of the transfectants increased by approximately 2×10^6 cells ml^{-1} for both groups in the late generation cultures, and this was equivalent to a percentage increase of 21.8% for the cell line 15 transfectants and 22.5% for the cell line 19 transfectants. The variance was greater in the late generation cultures compared to the early generation, although the cell line 15 transfectants remained the least variable group throughout the LTC.

The average CCT of the cell line 15 transfectants was significantly greater than the CCT of the cell line 19 transfectants at early and late generations (Table 4.4). An increase in average CCT and CCT variance was observed in the late generation cultures when compared to the early generation for both groups of transfectants. The cell line 15 transfectants were observed to be less variable in CCT than the cell line 19 transfectants.

The average doubling time of the cell line 15 transfectants was significantly less than the average doubling time of the cell line 19 transfectants at both generations. The average doubling time decreased for both groups of transfectants in the late generation. Less variance in the doubling time was observed in the cell line 15 transfectants than the cell line 19 transfectants at both generations. Variance in doubling time decreased for the late generation cell line 15 transfectants, while it increased for the cell line 19 transfectants.

Analysis of mAb production (Section 2.5.1) (Figure 4.9) showed that the average harvest (day 14) titre of the cell line 15 transfectants was greater than the average harvest titre of the cell line 19 transfectants at both generations. The average harvest titre was greater for both groups in the late generation condition, this increase was statistically significant for the cell line 15 and 19 transfectants. Although the cell line 15 transfectants produced the greatest average mAb titre (not significant, $p < 0.05$), the average Q_p of the cell line 19 transfectants was greater than the average Q_p of the cell line 15 transfectants at both

generations (Table 4.4). The variance in the Qp increased between the two generations for the cell line 15 transfectants. Conversely, the variance in Qp decreased for the cell line 19 transfectants between the early and late generations. In the late generation fed-batch cultures, less variance was observed in the Qp for the cell line 19 transfectants when compared to the cell line 15 transfectants.

Correlation analysis of the data discussed in this section was used to identify relationships between:

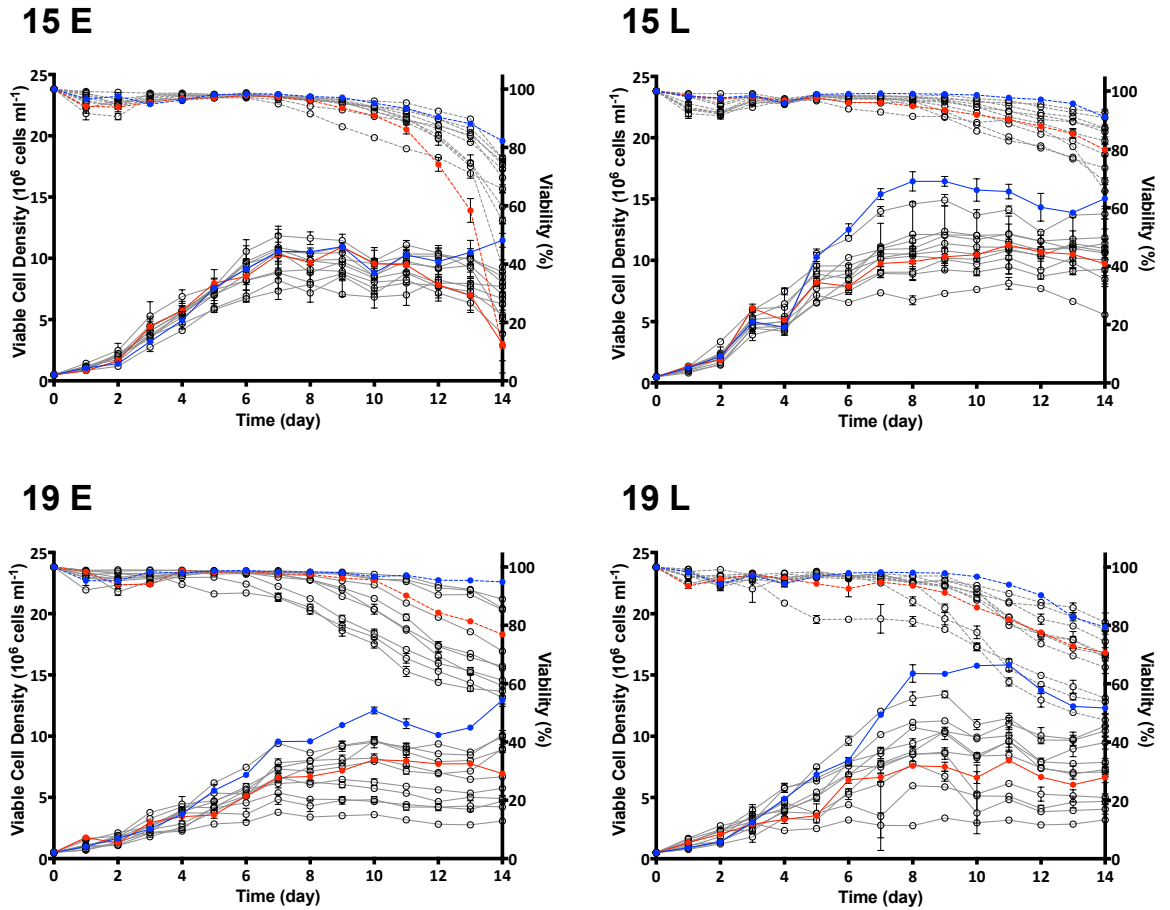
- VCD_{max} and harvest titre
- CCT and harvest titre
- VCD_{max} and Qp
- CCT and Qp

No significant correlation was observed for any of the aforementioned analyses in the early generation fed-batch cultures. In the late generation fed-batch cultures, a positive correlation was found in all of the analyses for the cell line 15 transfectants. As determined by the coefficient of determination (r^2) approximately 60% of the variance between VCD_{max} and CCT was shared with the harvest titre. A weaker correlation was found between VCD_{max} , CCT and Qp, in these analyses approximately 35% of the variance was shared. A correlation was identified between VCD_{max} , CCT and harvest titre for the late generation cell line 19 transfectants and approximately 45% of the variance was shared between the variables. No significant correlation to Qp was identified for the late generation cell line 19 transfectants.

Growth of the transfectants in fed-batch culture highlighted variability between the transfectants (Table 4.4). This was expected as variation was observed during LTC (Figure 4.7). The variability increased in the late generation cultures, with the exception of Qp for the cell line 19 transfectants. This supports previously discussed observations of (epi)genetic drift in mammalian cell cultures (Neildez-Nguyen et al. 2008; Pilbrough et al. 2009; Davies et al. 2013; Wurm 2013). The data also reflect patterns observed for the pool transfectants (Table 4.2), that cell line 19 transfectants have poor growth properties (VCD_{max} , CCT and doubling time) in comparison to cell line 15 transfectants, but have superior Qp. This supports the phenotype heritability hypothesis. Positive correlation of the data from the late generation transfectants suggested a weak relationship between growth and mAb production. However, the absence of correlation in the early generation

data and the relatively weak r^2 of the late generation correlations, indicates that growth is not a major contributing factor in productivity.

Figure 4.8 Comparison of early and late generation transfectant growth parameters in fed-batch culture

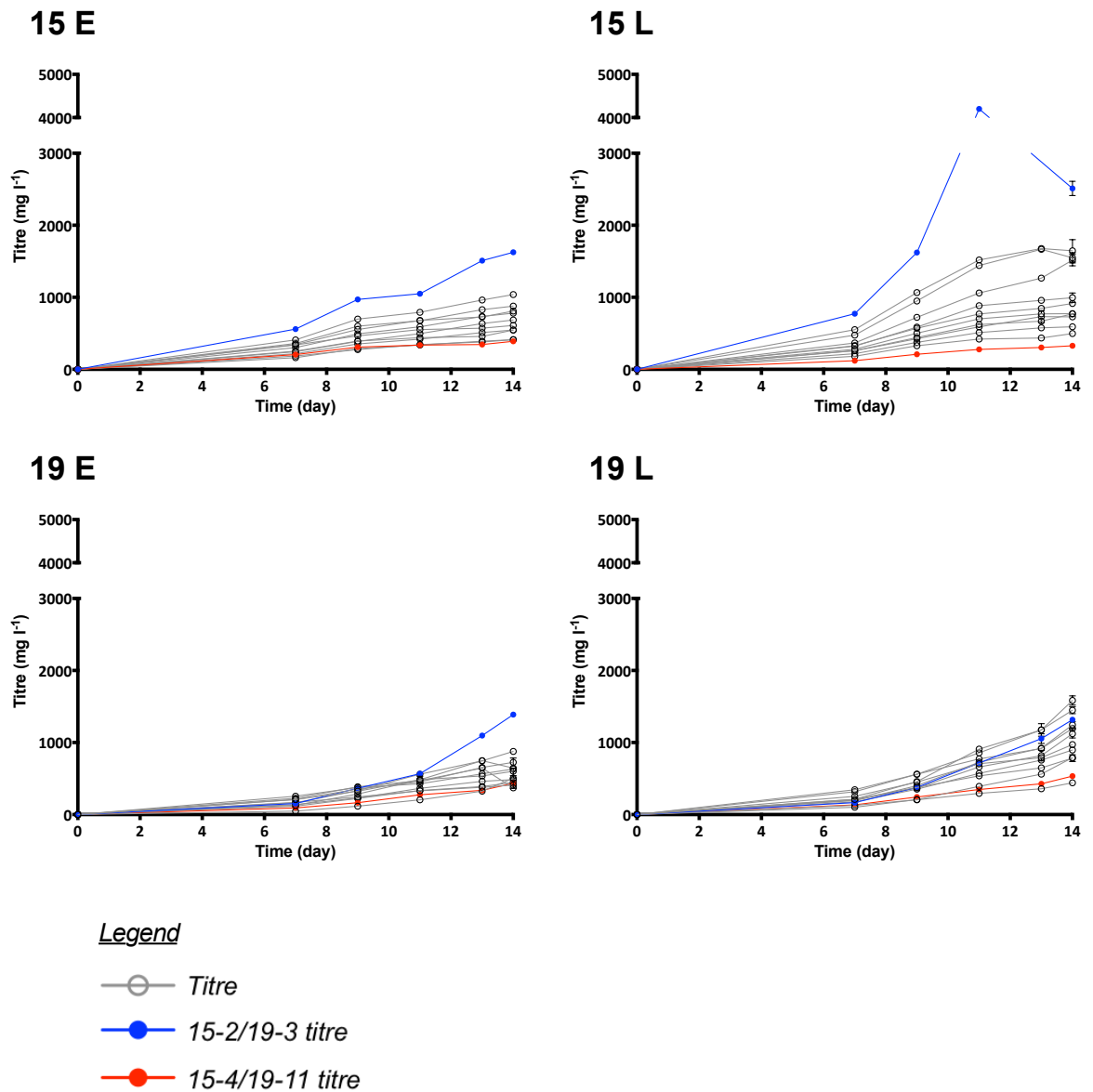


Legend

- Viable cell density
- -○- - Viability
- 15-2/19-3 viable cell density
- -●- - 15-2/19-3 viability
- 15-4/19-11 viable cell density
- -●- - 15-4/19-11 viability

At day 14 (early generation) and day 55 (late generation) during LTC (Section 4.3.1) triplicate fed-batch cultures were created from each maintenance culture. All cultures were initiated and maintained as described in Section 2.3.3. The fed-batch cultures were fed with 3.5 ml of a proprietary feed on days 3, 5, 7, 9 and 11. Cell counts were determined using a Beckman Coulter Vi-CELL XR (Section 2.3.4), this is based on the trypan blue exclusion method. The cultures were monitored for 14 days. The charts show the viable cell densities and viability of cell line 15 early generation transfectants (15 E), cell line 15 late generation transfectants (15 L), cell line 19 early generation transfectants (19 E) and cell line 19 late generation transfectants (19 L). Error bars represent the SEM for three biological replicates. The transfectants highlighted in red and blue were studied further in Chapter 5.

Figure 4.9 Comparison of early and late generation transfectant mAb production in fed-batch culture



At day 14 (early generation) and day 55 (late generation) during LTC (Section 4.3.1) triplicate fed-batch cultures were created from each maintenance culture. All cultures were initiated and maintained as described in Section 2.3.3. The fed-batch cultures were fed with 3.5 ml of a proprietary feed on days 3, 5, 7, 9 and 11. Samples were taken from the cultures for antibody titre analysis as described in Figure 4.4. The cultures were monitored for 14 days. The charts show the antibody titre of cell line 15 early generation transfectants (15 E), cell line 15 late generation transfectants (15 L), cell line 19 early generation transfectants (19 E), cell line 19 late generation transfectants (19 L). Error bars represent the SEM for three biological replicates. The transfectants highlighted in red and blue were studied further in Chapter 5.

Table 4.4 Analysis of early and late generation transfectant growth parameters and specific productivity in fed-batch culture

| Transfectant | Early | | | | | Late | | | | |
|--------------|---|--|-----------------------------|---|---|---|--|-----------------------------|---|---|
| | VCD _{max} (x10 ⁶ cells ml ⁻¹) | CCT (x10 ⁶ cells ml ⁻¹ day ⁻¹) | Doubling time (hours) | Harvest titre (mg l ⁻¹) | Qp (pg cell ⁻¹ day ⁻¹) | VCD _{max} (x10 ⁶ cells ml ⁻¹) | CCT (x10 ⁶ cells ml ⁻¹ day ⁻¹) | Doubling time (hours) | Harvest titre (mg l ⁻¹) | Qp (pg cell ⁻¹ day ⁻¹) |
| 15-1 | 10.2 | 96.3 | 23.9 | 878.1 | 9.0 | 14.9 | 139.5 | 21.7 | 1645.7 | 12.2 |
| 15-2 | 11.7 | 106.1 | 27.1 | 1624.8 | 14.8 | 17.1 | 154.8 | 21.6 | 2510.8 | 17.7 |
| 15-3 | 11.1 | 107.8 | 22.4 | 1037.7 | 9.5 | 12.4 | 117.7 | 22.4 | 1548.2 | 14.3 |
| 15-4 | 10.5 | 90.5 | 23.7 | 388.8 | 4.0 | 11.9 | 111.7 | 20.7 | 327.7 | 2.8 |
| 15-5 | 8.5 | 81.5 | 24.7 | 545.3 | 6.2 | 9.7 | 91.6 | 23.8 | 772.7 | 8.7 |
| 15-6 | 10.8 | 104.1 | 26.2 | 808.2 | 7.4 | 11.6 | 107.5 | 24.5 | 994.5 | 9.5 |
| 15-7 | 12.7 | 118.1 | 20.0 | 609.8 | 4.9 | 12.9 | 119.7 | 21.4 | 914.5 | 7.6 |
| 15-8 | 6.8 | 70.9 | 23.2 | 411.2 | 5.6 | 9.9 | 93.9 | 22.9 | 590.9 | 6.4 |
| 15-9 | 8.2 | 78.2 | 25.7 | 684.9 | 8.8 | 8.3 | 81.7 | 22.2 | 769.4 | 9.2 |
| 15-10 | 12.0 | 112.9 | 22.9 | 780.4 | 6.8 | 14.9 | 137.1 | 20.0 | 1516.6 | 10.7 |
| 15-11 | 9.3 | 86.2 | 26.5 | 546.6 | 6.1 | 11.8 | 116.0 | 20.1 | 728.3 | 6.5 |
| 15-12 | 8.9 | 78.4 | 30.9 | 411.7 | 5.0 | 11.7 | 110.2 | 20.4 | 497.0 | 4.3 |
| 19-1 | 5.4 | 53.9 | 26.6 | 632.4 | 11.4 | 8.6 | 75.3 | 24.2 | 1195.2 | 12.8 |
| 19-2 | 3.9 | 37.0 | 35.3 | 601.8 | 16.2 | 6.0 | 53.3 | 30.6 | 971.7 | 17.4 |
| 19-3 | 12.9 | 101.8 | 31.7 | 1387.3 | 13.5 | 15.8 | 131.2 | 28.0 | 1316.8 | 9.8 |
| 19-4 | 6.5 | 63.4 | 24.8 | 725.3 | 11.4 | 7.8 | 58.2 | 27.0 | 783.4 | 13.1 |
| 19-5 | 9.0 | 75.7 | 29.5 | 504.3 | 6.2 | 11.3 | 99.1 | 28.8 | 790.6 | 7.5 |
| 19-6 | 9.5 | 89.1 | 30.0 | 371.3 | 5.6 | 11.9 | 89.7 | 43.7 | 1244.5 | 12.6 |
| 19-7 | 10.1 | 82.4 | 32.4 | 644.4 | 9.0 | 13.7 | 115.3 | 30.0 | 1583.3 | 13.0 |
| 19-8 | 8.4 | 72.8 | 34.7 | 446.7 | 6.0 | 10.4 | 90.7 | 25.4 | 896.1 | 9.7 |
| 19-9 | 9.9 | 79.0 | 39.2 | 876.8 | 11.4 | 8.9 | 83.7 | 27.3 | 1448.3 | 16.7 |
| 19-10 | 4.9 | 51.1 | 31.6 | 410.2 | 8.3 | 3.7 | 35.6 | 28.6 | 441.2 | 11.9 |
| 19-11 | 8.2 | 73.7 | 28.1 | 433.5 | 5.7 | 8.2 | 71.5 | 31.2 | 533.7 | 7.0 |
| 19-12 | 6.9 | 65.6 | 37.1 | 485.4 | 7.7 | 10.9 | 88.0 | 33.1 | 1121.5 | 11.5 |
| 15 (SD) | 10.1 (1.8)* | 94.3 (15.5)* | 24.8 (2.8)* | 727.3 (347.6) | 7.3 (2.9) | 12.3 (2.5)* | 115.1 (21.1)* | 21.8 (1.4)* | 1068.0 (623.0) | 9.2 (4.2) |
| 19 (SD) | 8.0 (2.6) | 70.5 (17.7) | 31.8 (4.3) | 626.6 (281.0) | 9.4 (3.4) | 9.8 (3.3) | 82.6 (26.4) | 29.8 (5.0) | 1027.2 (353.9) | 11.9 (3.2) |

Twelve transfectants generated from clonal host cell lines 15 and 19 were grown in fed-batch culture as previously described (Figure 4.8 and 4.9). VCD_{max} for each host cell line in batch culture was determined from cell count data. CCT was calculated from the summation of the integral of viable cell density, which was determined between each cell count cell count time point. Doubling time was calculated between day 0 and day 3, this time period falls within the exponential growth phase for all of the transfectants. The harvest titre was determined from the culture supernatant on day 14. The Qp column represents the Qp final and was calculated from the harvest titre and CCT data. Average values are displayed for each group of transfectants in the table footer with the standard deviation (SD). * indicates p<0.05, using independent samples t-test to compare cell line 15 transfectants with the cell line 19 transfectants.

4.3.3 Analysis of recombinant mAb-109 mRNA expression

As described in Section 4.3.2, only 35-60% of the variance in mAb production of the transfectants could be explained by the growth parameters VCD_{max} and CCT, and this only applied to the late generation transfectants. Using recombinant mAb-109 as a model, relationships were examined between expression of mAb-109 at mRNA and protein levels. Correlation analysis of mRNA expression against harvest titre (Figure 4.10 A) suggested that there was a significant correlation between light chain mRNA and harvest titre. The r^2 value of this correlation suggested that only 33% of the variance in light chain mRNA and harvest titre was shared. Significant correlations were observed for both heavy and light chain mRNA against Qp (Figure 4.10 B) The correlation was greater for heavy chain mRNA than light chain mRNA with 67% and 46% of the variance shared with Qp respectively.

Previous reports have associated Qp with mAb mRNA expression (Lattenmayer et al. 2007), with heavy chain transcript being the most strongly associated (Lee et al. 2009). However, post-transcriptional mechanisms in the secretory pathway could limit productivity (Barnes & Dickson 2006). Analysis of the early generation mAb mRNA expression found that transcript expression correlated with Qp (Figure 4.10 B). The relationship was greatest for the heavy chain transcript, in agreement with published findings (Lee et al. 2009; Vishwanathan et al. 2014). Whilst care was taken to ensure the accuracy of mRNA expression analysis, fluctuations in housekeeping gene expression has previously been reported (Bahr et al. 2009). The correlation of mRNA expression to Qp in this study may have been stronger if methods to minimise this variability had been adopted (Vandesompele et al. 2002; Bahr et al. 2009). Differences in recombinant gene copy number of each transfectant could account for variation in mAb-109 mRNA expression. However, gene copy number analysis of high and low producing transfectants (Section 5.2.3) did not show a relationship to mAb-109 mRNA expression.

In addition to the fed-batch cultures described in Section 4.3.2, triplicate early generation unfed flasks were created to allow for day 4 samples to be collected. On day 4, 1.5×10^6 cells were harvested for mRNA extraction (Section 2.6.1.3). The mRNA was used for qRT-PCR to analyse the heavy and light chain mRNA expression in the transfectants (Section 2.6.1.4 and Section 2.6.1.7). mRNA expression data was normalised against a calibrator sample prepared by combining cDNA from several transfectants, the $\beta 2$ microglobulin (B2M) gene was used as an endogenous control. The charts show the relative mRNA expression plotted against the harvest titre (A) and Qp (B) of the corresponding fed-batch cultures described in Section 4.3.2. Error bars, where applicable, represent the SEM for three biological replicates, additionally each biological replicate was assayed as a technical duplicate.

4.3.4 Analysis of nutrient utilisation by early and late generation transfectants

Cell culture supernatant samples were collected throughout the fed-batch cultures (Section 4.3.2) and were used to analyse glucose, lactate, glutamine and glutamate utilisation rates. The average rate of glucose consumption was greater for the cell line 15 transfectants than for cell line 19 transfectants (Figure 4.11 15 A, 19 A). Similarly the average rate of lactate production was greater for the cell line 15 transfectants when compared to the cell line 19 transfectants (Figure 4.11 15 B, 19 B). No statistical difference was observed in average glucose consumption or lactate production rates between the early and late generation transfectants for either cell line. However, statistical differences were observed between rates of metabolite use and production for individual transfectants at early and late generation (Figure 4.11). The average ratio of lactate production to glucose consumption (Table 4.5) suggested that the early generation cell line 15 transfectants produced the least lactate per glucose consumed. The late generation cell line 15 transfectants had a significantly greater average lactate:glucose ratio than the early generation. The average ratio for the cell line 19 transfectants was greater than the ratio of the cell line 15 transfectants at both generations. Additionally, greater variance was observed in the lactate:glucose ratios determined for the cell line 19 transfectants.

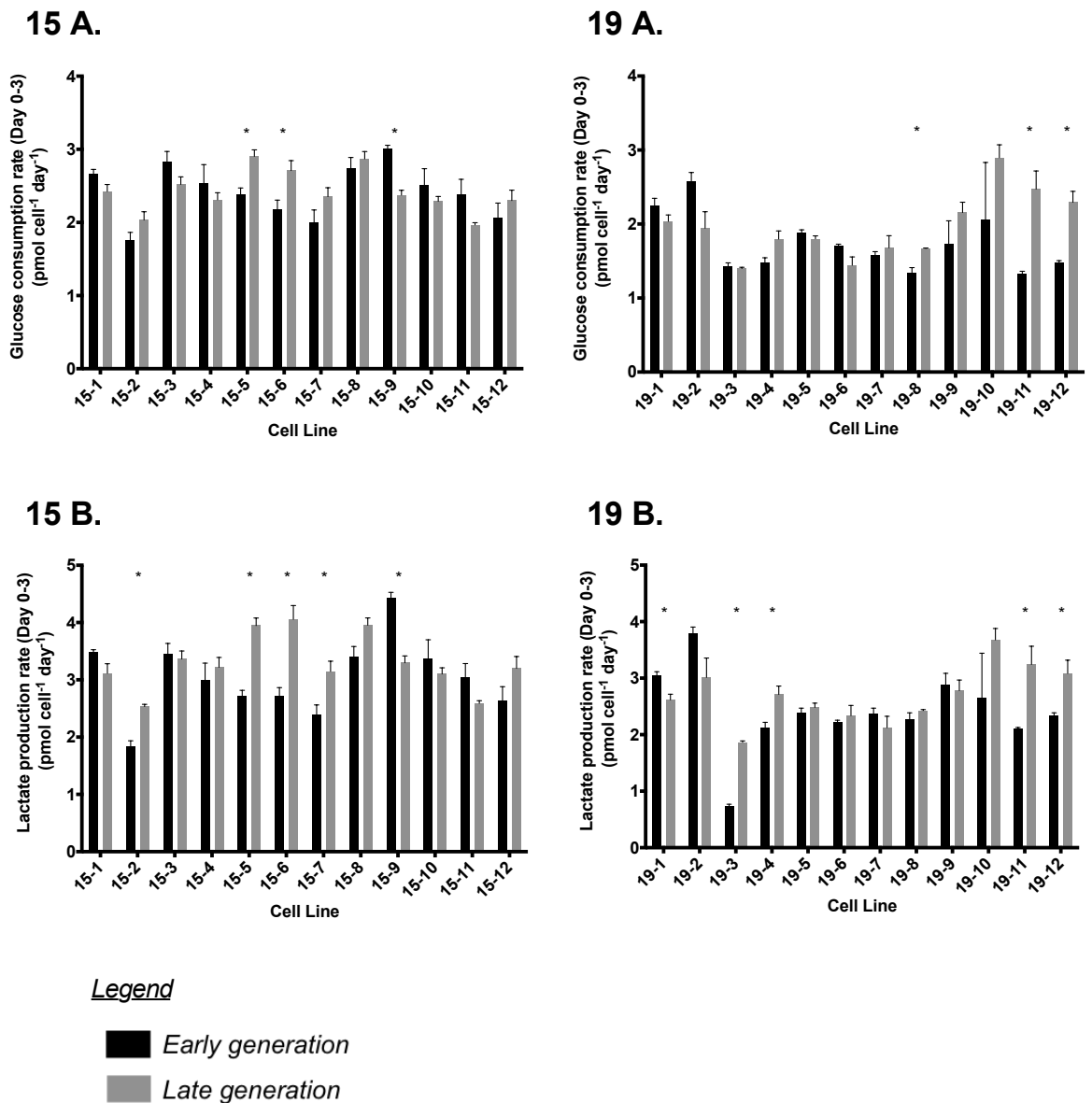
During fed-batch culture, glutamine production was observed (Figure 4.12 15A, 19A). The rate of glutamine production was significantly greater for the cell line 15 transfectants compared to the cell line 19 transfectants for both generations. The concentration of glutamine in the medium at day 3 of culture was low (data not shown) for all transfectants, this could be due to most of the glutamine produced being metabolised by the cells, and not secreted into the medium. Glutamate was consumed by the transfectants in fed-batch culture (Figure 4.12 15B, 19B). The rate of glutamate consumption was significantly less for the cell line 15 transfectants compared to the cell line 19 transfectants for both generations. This contrasted to the glutamate data of the host cell lines, which were observed to produce glutamate (Section 3.3). However, the host cell lines were supplemented with, and consumed, L-glutamine, which can be used for glutamate production.

The cell line 19 transfectants had greater lactate:glucose ratios (Table 4.5) than the cell line 15 transfectants. This pattern was also identified in the host cell lines (Table 3.4) and, as previously discussed (Section 3.3), suggested that host cell line 19 is inefficient in

terms of glucose usage (Section 3.6). The persistence of this pattern in the transfectants suggests heritability of this property. Cultured mammalian cells have been compared to cancer cells in terms of their glucose metabolism in terms of high glucose consumption and lactate production under normal oxygen availability (Warburg 1956; Mulukutla et al. 2010). The lactate:glucose ratio was greater than the ratios observed in the host cell lines, this could be a result of glutamine-free culture and/or the recombinant GS may have altered metabolic flux and nutrient transport in the transfectants (Gòdia & Cairó 2001).

The inefficiency of glucose utilisation in the cell line 19 transfectants may suggest that glucose derived metabolites weren't entering the TCA cycle as effectively as in the cell line 15 transfectants. Greater glutamate consumption rate and lower glutamine production rates were observed in the cell line 19 transfectants compared to the cell line 15 transfectants (Figure 4.11). This suggests that the cell line 19 transfectants are more reliant on glutamine/glutamate to fuel the TCA cycle than the cell line 15 transfectants. This could also explain why host cell line 19 had a lower glutamine production rate than host cell line 15 (Figure 3.7). Metabolic flux analysis of the clonal hosts and transfectants could be used to test these interpretations and provide further insight into the metabolic state of the transfectants (Young 2014).

Figure 4.11 Analysis of glucose and lactate utilisation rates in early and late generation transfectants during fed-batch culture



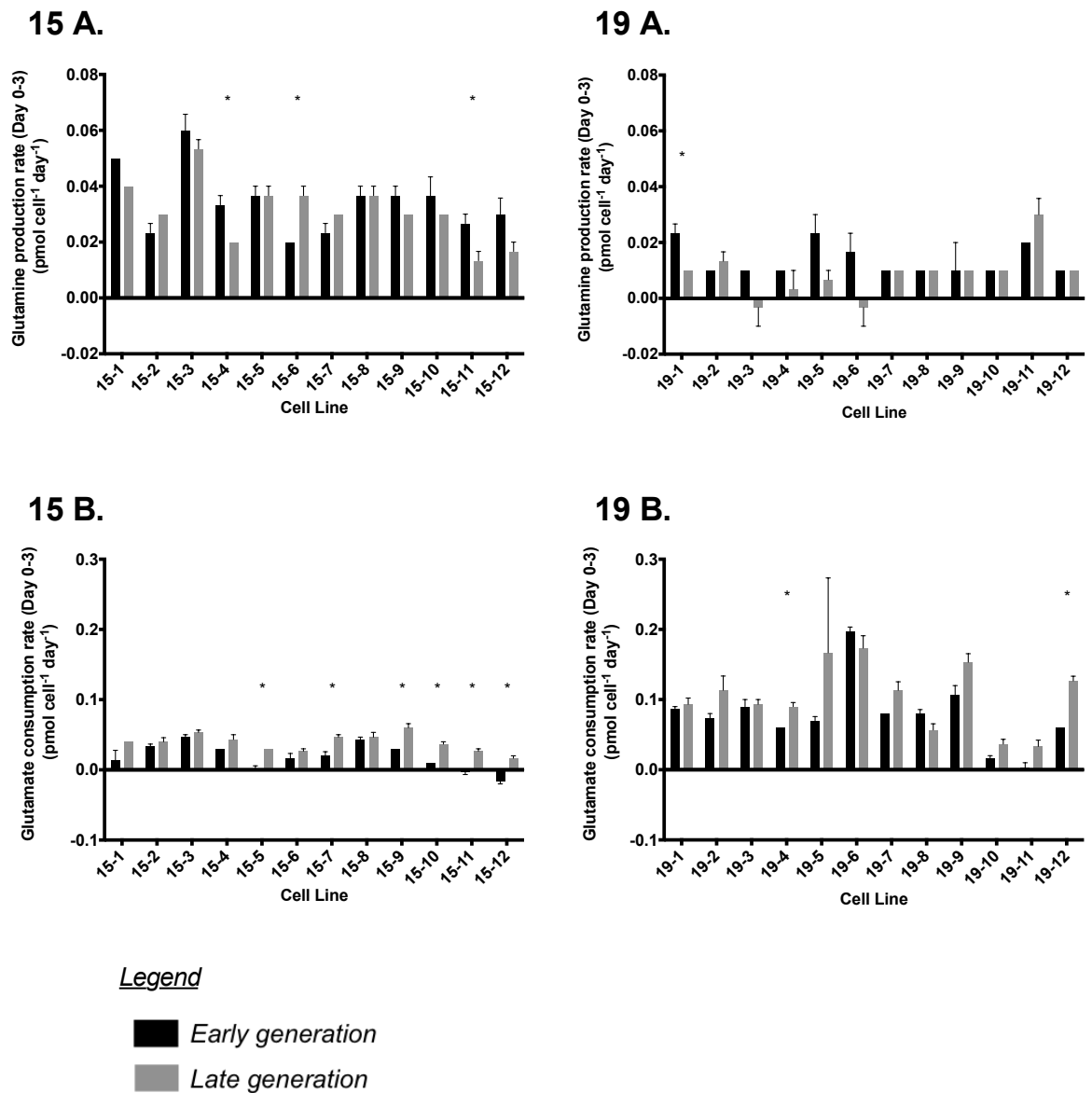
During the fed-batch cultures described in Figure 4.8, cell culture media samples were collected for metabolite analysis. The media samples were analysed using a YSI 2900 Biochemistry Analyzer for glucose and lactate concentration (Section 2.4.1). The cell counts and metabolite analyses were used to determine the rates of utilisation of these metabolites between days 0-3 of culture. Glucose utilisation rates are shown for cell line 15 transfectants (15 A) and cell line 19 transfectants (19 A). Lactate utilisation rates are shown for cell line 15 transfectants (15 B) and cell line 19 transfectants (19 B). Error bars represent SEM for three biological replicates. * indicates $p < 0.05$, using independent samples t -test to compare early and late generation of each transfectant.

Table 4.5 Ratio of lactate production rate to glucose consumption rate in early and late generation transfectants during fed-batch culture

| Transfectant | Lactate:glucose ratio | | | |
|---------------------|-----------------------|--------------------|--------------------|--------------------|
| | Cell line 15 | | Cell line 19 | |
| | Early generation | Late generation | Early generation | Late generation |
| 1 | 1.30 | 1.28 | 1.36 | 1.28 |
| 2 | 1.05 | 1.25 | 1.47 | 1.55 |
| 3 | 1.22 | 1.33 | 0.52 | 1.33 |
| 4 | 1.18 | 1.39 | 1.43 | 1.51 |
| 5 | 1.14 | 1.36 | 1.27 | 1.38 |
| 6 | 1.25 | 1.50 | 1.30 | 1.62 |
| 7 | 1.19 | 1.34 | 1.51 | 1.26 |
| 8 | 1.24 | 1.38 | 1.70 | 1.45 |
| 9 | 1.47 | 1.39 | 1.66 | 1.29 |
| 10 | 1.35 | 1.36 | 1.29 | 1.27 |
| 11 | 1.28 | 1.32 | 1.58 | 1.31 |
| 12 | 1.28 | 1.39 | 1.58 | 1.34 |
| Average (SD) | 1.24 (0.11)* | 1.36 (0.06) | 1.39 (0.31) | 1.38 (0.12) |

*Ratios were calculated from the lactate production rate and glucose consumption rates described in Figure 4.11. A high ratio implies that more lactate is produced per glucose consumed. Average values are displayed for each group of transfectants with the standard deviation (SD). * indicates $p < 0.05$, using independent samples t-test to compare early generation transfectants to the late generation transfectants from the same clonal host cell line.*

Figure 4.11 Analysis of glutamine and glutamate utilisation rates in early and late generation transfectants during fed-batch culture



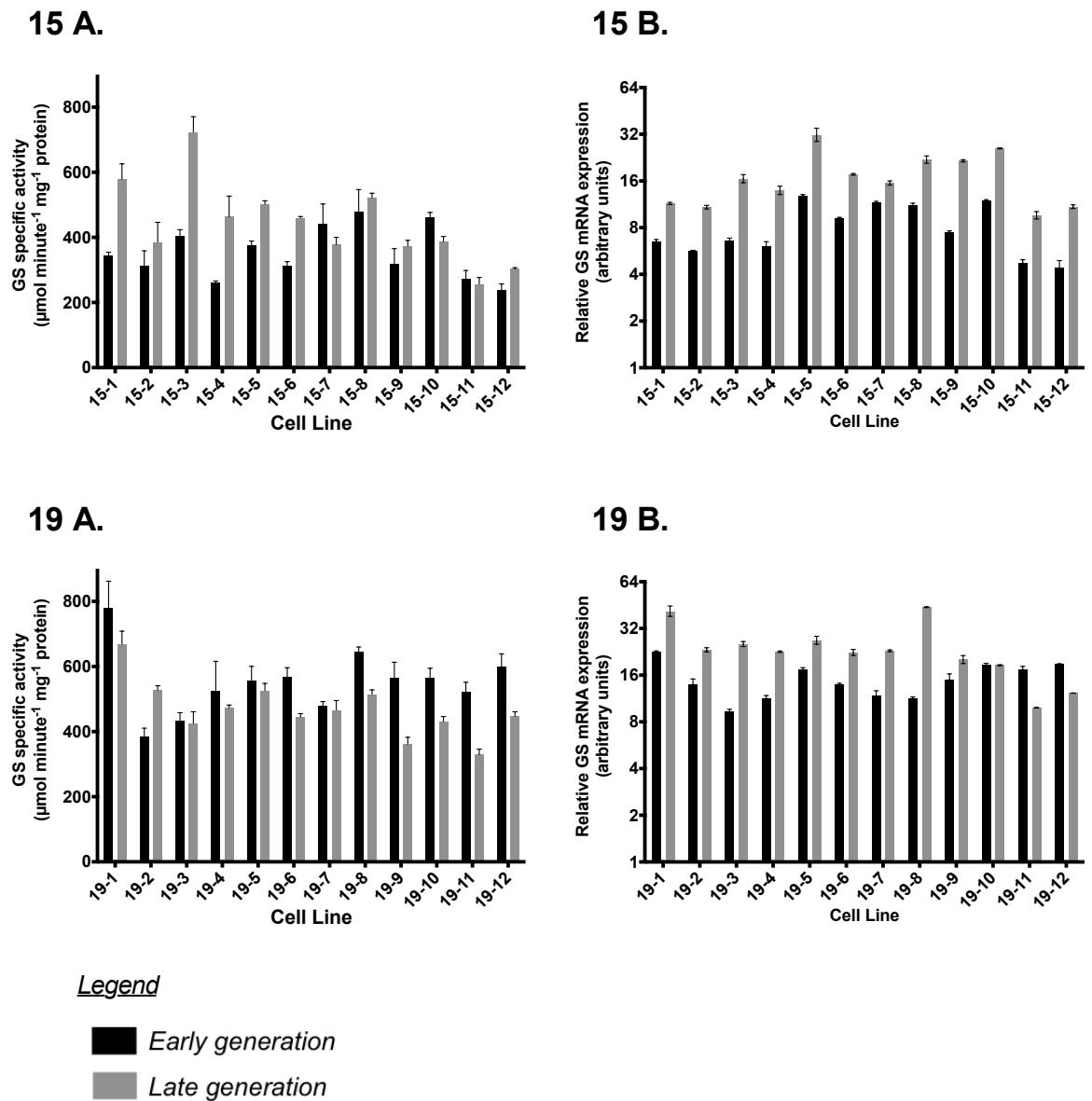
During the fed-batch cultures described in Figure 4.8, cell culture media samples were collected for metabolite analysis. The media samples were analysed using a YSI 2900 Biochemistry Analyzer for glutamine and glutamate concentration (Section 2.4.1). The cell counts and metabolite analyses were used to determine the rates of utilisation of these metabolites between days 0-3 of culture. Glutamine utilisation rates are shown for cell line 15 transfectants (15 A) and cell line 19 transfectants (19 A). Glutamate utilisation rates are shown for cell line 15 transfectants (15 B) and cell line 19 transfectants (19 B). Error bars represent SEM for three biological replicates. * indicates $p < 0.05$, using independent samples t -test to compare early and late generation of each transfectant.

4.3.5 Analysis of early and late generation transfectant glutamine synthetase

Protein and mRNA samples were collected from early and late generation transfectants to assess the activity and mRNA expression of glutamine synthetase (Figure 4.12). The average GS specific activity and mRNA expression was significantly greater in the late generation cell line 15 transfectants than in the early generation (Figure 4.12 15 A, 15 B). In the cell line 19 transfectants, the early generation had significantly greater average GS activity than the late generation cell line 19 transfectants (Figure 4.12 19 A). However, the average mRNA expression was greater in the late generation transfectants than the early generation transfectants. A significant decrease in GS specific activity was also observed for host cell line 19 between early and late generation cultures (Figure 3.8). In support of the host data (Section 3.4.1), a positive correlation was observed between GS mRNA expression and specific activity ($r = 0.50$). Only 25% of the variation was shared, in comparison to 40% variance in the hosts.

The average GS specific activity of the cell line 19 transfectants was greater than the cell line 15 transfectants GS specific activity for both generations, the difference was significant in the early generation. The same observation was made for the average mRNA expression. This does not explain the greater rate of glutamine production observed in the cell line 15 transfectants compared to the cell line 19 transfectants (Figure 4.11). Expression of GS mRNA in the transfectants was greater in comparison to the clonal host cell lines (Figure 4.12 and 3.8). This confirms increased expression in relation to the recombinant GS gene. The qRT-PCR assay for GS mRNA expression does not discriminate between the endogenous and exogenous GS mRNA, thus transcript quantity from both sources were determined. An increase in the average GS specific activity was also observed in comparison to the host cell lines, this could be due to the abundance of mRNA, but also less degradation of the enzyme in the absence of exogenous glutamine (Tiemeier & Milman 1972; Huang et al. 2007). GS mRNA expression and specific activity was greater on average in the cell line 19 transfectants than the cell line 15 transfectants, this pattern was also observed in the host cell lines. Greater GS specific activity in the cell line 19 transfectants could be linked to the greater glutamate consumption rate observed. However, it does not explain the greater production rate of glutamine in the cell line 15 transfectants.

Figure 4.12 Analysis of glutamine synthetase activity and mRNA expression in early and late generation transfectants



In addition to the fed batch cultures described in Section 4.3.2, early and late generation triplicate unfed flasks were created to allow for day 4 samples to be collected. On day 4, cells were harvested for protein extraction (Section 2.5.2.1). The protein extracts were analysed for specific GS activity (Section 2.5.3). Additionally, cells were harvested for mRNA extraction (Section 2.6.1.3). The mRNA was used for qRT-PCR to analyse GS mRNA expression in the transfectants (Section 2.6.1.7). All mRNA expression data was normalised to a calibrator sample, cDNA prepared from host cell line NC early generation (Figure 3.4), 18s ribosomal RNA was used as an endogenous control. Error bars represent SEM for three biological replicates, additionally, each biological replicate was assayed as a technical duplicate in the qRT-PCR assay.

4.4 Summary

This Chapter aimed to address whether the use of clonal host cell lines would give rise to transfectants that display less phenotypic variability than a non-clonal host cell line. It was also hypothesised that transfectants would inherit the characteristics of the host cell line. The data discussed in Chapter 3 suggest that clonal host cell lines can possess phenotypic advantages over non-clonal host cell lines. The ability to produce transfectants with limited variability and desirable phenotypes could have the implication that less transfectants would need to be screened during a cell line development process.

The objectives of this Chapter were:

- To determine the variability of transfectants derived from clonal host cell lines in relation to a non-clonal host cell line.
- To determine the response of transfectants to feed.
- To assess the heritability of host cell line phenotype in transfectant populations.

Variability in growth and productivity was apparent following transfection of all of the host cell lines. The transfection round 1 pools provided some evidence that the use of clonal host cell lines results in less variability than a non-clonal host cell line. However, the data was not strong enough to prove the hypothesis. Previous publications and the experiments in this study found that variability tends to increase during continuous culture. As mentioned in Section 1.5, the hosts were cultured for 40-50 generations before the cell banks were created. The use of clonally derived host cell lines, which had been cultured for a shorter period of time prior to transfection may have resulted in less transfectant variability. The use of batch and fed-batch cultures, following both transfection round 1 and transfection round 2 in this work determined CCT and Qp to increase in response to feed. These observations are in support of published findings. The data discussed in this chapter are generally in support of the hypothesis that transfectants will inherit the host cell line phenotype. This has the implication that host cell line selection plays a determining role in transfectant suitability for a defined production process.

5. Molecular and metabolic profiling to identify indicators of high productivity

5.1 Introductory remarks

The aim of the work presented in this Chapter was to identify metabolic and molecular determinants of a high producing transfectant cell line. A high and a low producing transfectant derived from each of clonal host cell lines 15 and 19 (15-2, 15-4, 19-3, 19-11), were chosen for more detailed analyses based on interpretation of both growth and productivity data and are specifically highlighted in Chapter 4 (Figure 4.8 and 4.9). The transfectants were grown in fed-batch culture to confirm their productivity and to generate parallel samples for analysis. The clonal hosts and transfectants were analysed for chromosome number, recombinant gene copy number and mitochondrial membrane potential to assess relationships to data discussed in the previous chapters. Based on previous publications (Chong et al. 2011; Dietmair et al. 2012; Dean & Reddy 2013; Young 2014), it was hypothesised that high and low producing transfectants would differ metabolically, and that metabolites could be identified that relate to productivity.

5.2 Characterisation of high and low producing transfectants

High producing transfectants (15-2, 19-3) and low producing transfectants (15-4, 19-11), in addition to their early generation, untransfected host cell lines (15, 19), were grown in fed-batch and batch culture, to confirm previous data and for sample collection for subsequent experiments. The host cell lines were cultured in glutamine-free medium for consistency with the transfectants. The main criteria for transfectant selection were Q_p and harvest titre as high and low producers were required for study. However, growth was also considered, as evidence of a relationship between growth and harvest titre had been observed previously (Section 4.3.2). Both early (between generations 8-12) and late (between generations 47-50) generation transfectants were analysed in this Chapter.

5.2.1 Growth and mAb titre analysis of high and low producing transfectants

The growth of host cell line 15 (15 H) and host cell line 19 (19 H) reflected data presented in Chapter 3 (Table 3.3). 15 H achieved greater cell densities and CCT than 19 H at both generations. The VCD_{max} and CCT of the hosts (Table 5.1) was greater than observed in Chapter 3 (Table 3.3), this can be attributed to the greater seeding density, which was used for consistency with the transfectants. The doubling time was also greater than the values observed in Chapter 3; this could be a result of glutamine free-culture as glutamine limitation has been shown to induce the amino acid response pathway, and cause growth suppression via G1 cell cycle arrest in CHO and tumour cell lines (Wasa et al. 1996; Fomina-Yadlin et al. 2014). Additionally, it was observed that glutamine-free culture of the hosts (Figure 3.9) decreased the growth rate of all hosts. 19 H showed the greatest increase in doubling time compared to the data in Table 3.3. Host 15 was observed to downregulate GS expression to a greater extent than host 19 in the presence of 6mM glutamine (Figure 3.10), this could imply that host 15 is more adaptable to glutamine-free culture.

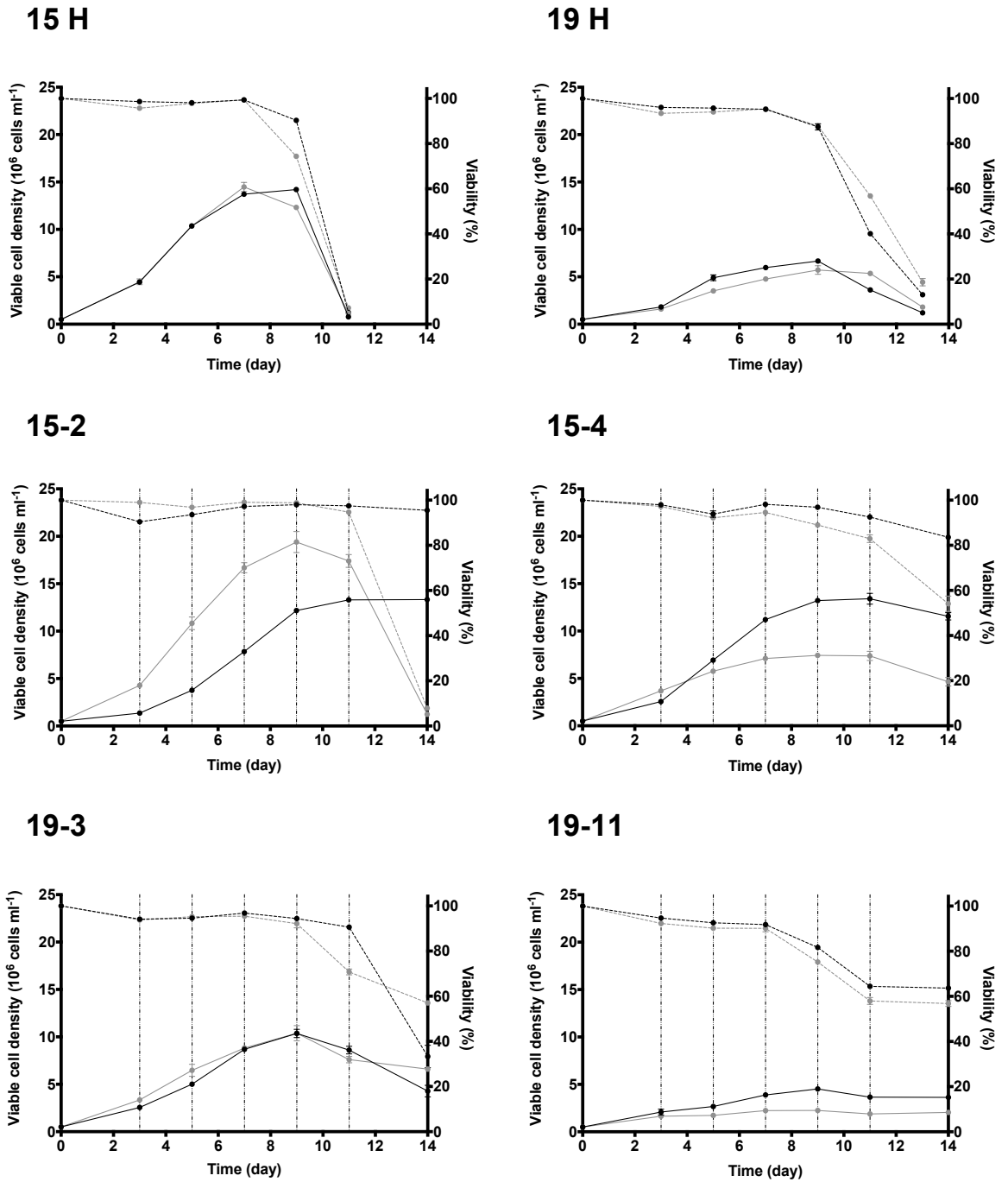
The growth parameters of the transfectants (Figure 5.1, Table 5.1) showed differences when compared with previous fed-batch cultures (Figure 4.8, Table 4.4). The growth curves of transfectants 19-3 and 19-11 were more consistent at the early and late generation, when compared with 15-2 and 15-4 (Figure 5.1). The growth of 19-11 at both generations was poor when compared to previous data for this transfectant. The VCD_{max} was approximately 50% and 25% of the previously observed VCD_{max} at early and late generation, respectively. Published research has also shown evidence of inconsistent growth in clonal transfectants in shake-flask culture following revival of frozen cell stocks

and long-term culture, as these population bottlenecks may select for subpopulations with different phenotypes (Davies et al. 2013).

Analysis of mAb titre confirmed that 15-2 and 19-3 produced the greatest harvest titres (Figure 5.2). However, the harvest titres of 15-4 and 19-3 (early generation) were significantly increased, and the harvest titres of 15-4 and 19-11 (late generation) were significantly decreased, when compared to previous data ($p < 0.05$). 15-2 had a significantly greater Q_p than 15-4 at both generations, whilst 19-3 only had a significantly greater Q_p than 19-11 in the early generation cultures (Table 5.1). The Q_p of 19-11 increased in the late generation cultures and was significantly greater than the decreased Q_p of 19-3.

The differences discussed here, compared to the data presented in Chapter 4 indicate the necessity of confirming this data. The parallel assessment of this data with the metabolomic data discussed in Section 5.3 is important to evaluate the relationships of metabolites to the phenotype of the cells.

Figure 5.1 Analysis of growth of host cell lines, high and low producing transfectants growth parameters in batch and fed-batch culture



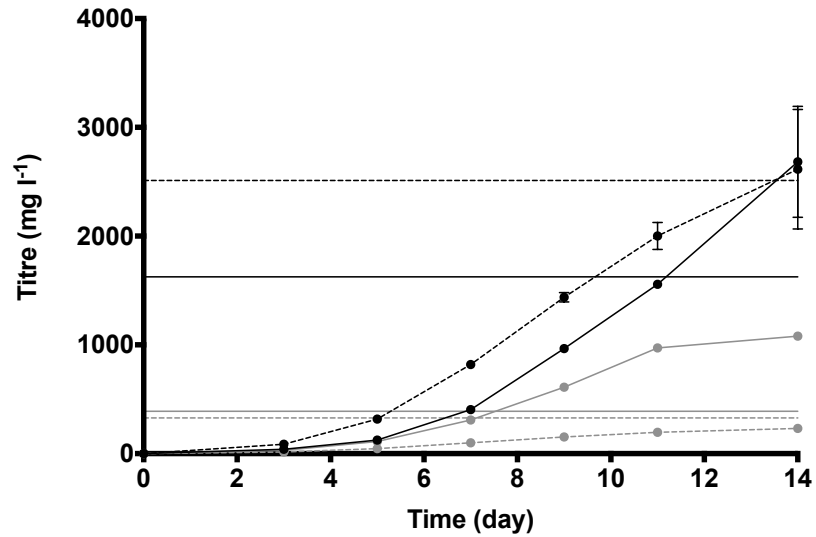
Legend

- Early viable cell density
- Late viable cell density
- -●- - Early viability
- -●- - Late viability

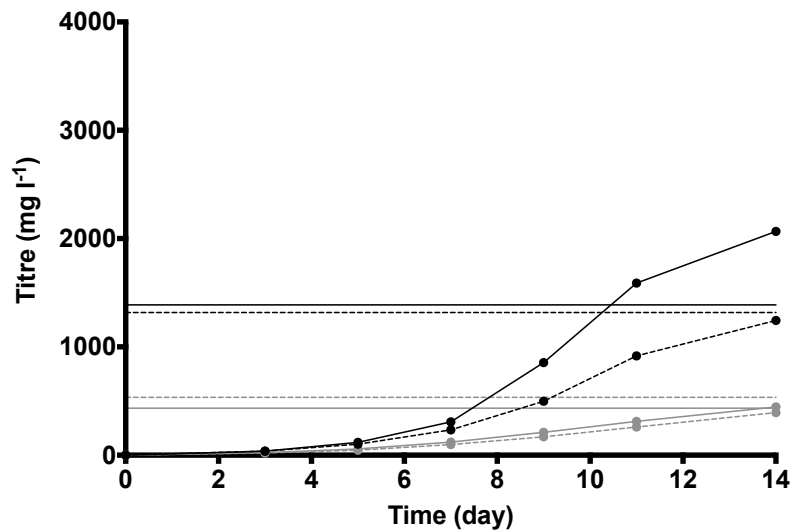
Early and late generation clonal host cell lines 15 and 19, from the host LTC (Section 3.2.1), and early and late generation transfectants 15-2, 15-4, 19-3 and 19-11, from the transfectant LTC (Section 4.3.1) were revived. Triplicate batch (hosts) and fed-batch (transfectants) cultures were initiated as described in Section 2.3.3. The host cell line batch cultures were inoculated at 0.5×10^6 cells mL^{-1} and were grown in the absence of L-glutamine. Cell counts were determined using a Beckman Coulter Vi-CELL XR (Section 2.3.4). The cultures were monitored for up to 14 days. The charts show early and late generation viable cell densities and viabilities of host cell line 15 (15 H), host cell line 19 (19 H), and the transfectant cell lines 15-2, 15-4, 19-3 and 19-11. Error bars represent the SEM for three biological replicates. Vertical dashed lines indicate feed addition, all counts were taken prior to feed addition.

Figure 5.2 Analysis of mAb production from high and low producing transfectants in fed-batch culture

15.



19.



Legend

- 15-2 or 19-3 early titre
- - 15-2 or 19-3 late titre
- 15-4 or 19-11 early titre
- - 15-4 or 19-11 late titre

As described in Figure 5.1, early and late generation transfectants were grown in fed-batch culture for 14 days. Samples were taken from the cultures for antibody titre analysis as described in Section 2.5.1. The charts show the antibody titre of the clonal host cell line 15 transfectants (15) and the clonal host cell line 19 transfectants (19). The horizontal lines represent the harvest titre of the transfectants from Figure 4.9. Error bars represent the SEM for three biological replicates.

Table 5.1 Analysis of growth and specific productivity of host cell lines, high and low producing transfectants in batch and fed-batch culture

| Transfectant | Early | | | | | Late | | | | |
|--------------|--|---|--------------------------|--|--|--|---|--------------------------|--|--|
| | VCD _{max} (x10 ⁶ cells ml ⁻¹) | CCT (x10 ⁶ cells ml ⁻¹ day ⁻¹) | Doubling time (hours) | Harvest titre (mg l ⁻¹) | Qp (pg cell ⁻¹ day ⁻¹) | VCD _{max} (x10 ⁶ cells ml ⁻¹) | CCT (x10 ⁶ cells ml ⁻¹ day ⁻¹) | Doubling time (hours) | Harvest titre (mg l ⁻¹) | Qp (pg cell ⁻¹ day ⁻¹) |
| Host 15 | 14.2 | 89.2 | 22.9 | - | - | 14.5 | 87.3 | 22.9 | - | - |
| 15-2 | 13.4 | 104.9* | 50.4* | 2683.3* | 25.6* | 19.7* | 150.6* | 23.3* | 2615.3* | 17.4* |
| 15-4 | 13.5 | 120.7 | 30.9 | 1080.3 | 9.0 | 7.7 | 76.0 | 25.0 | 232.3 | 3.1 |
| Host 19 | 6.7 | 48.8 | 38.7 | - | - | 5.9 | 45.3 | 42.9 | - | - |
| 19-3 | 10.4* | 83.2* | 30.6 | 2065.7* | 24.8* | 10.4* | 89.3* | 26.3* | 1243.3* | 13.9* |
| 19-11 | 4.5 | 42.7 | 36.6 | 445.3 | 10.5 | 2.3 | 25.0 | 42.1 | 393.3 | 15.7 |

Clonal host cell lines and transfectants were grown in batch and fed-batch culture as previously described (Figure 5.1). VCD_{max} was determined from cell count data. CCT was calculated from the summation of the integral of viable cell density, which was determined between each cell count time point. Doubling time was calculated between day 0 and day 3. The harvest titre was determined from the culture supernatant on day 14. The Qp represents Qp final and was calculated from the harvest titre and CCT data. The data represent average values of three biological replicates. * indicates p<0.05, using independent samples t-test to compare the high producing transfectant (15-2, 19-3) to the low producing transfectant (15-4, 19-11) from the respective host cell line and generation.

5.2.2 Chromosome numbers of high and low producing transfectants

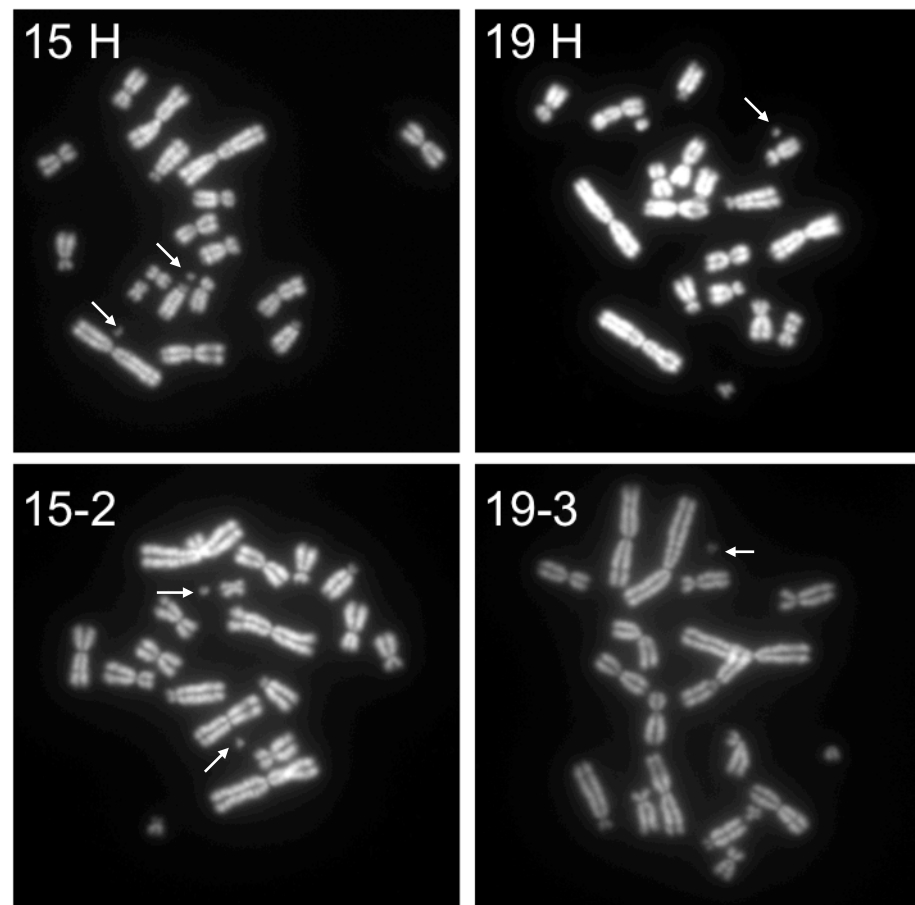
Karyotype analysis of CHO K1, CHO DG44 and CHO pro⁻ cells showed that these lineages had an unstable chromosome structure (Kao & Puck 1969; Deaven & Petersen 1973; Bacsi & Wejksnora 1986; Derouazi et al. 2006). The chromosome numbers of the clonal hosts and transfectants studied in this Chapter, were analysed for chromosome number to assess any relationship to the phenotypic variability observed in the previous Section. Metaphase spreads were prepared from the host cell lines and transfectants (Figure 5.3). The modal number of chromosomes from 50 spreads for each cell type studied are shown in Table 5.2. Modal number of chromosomes for host cell line 15 was 18: for host cell line 19 the number was greater at 19 chromosomes. All transfectants had a modal number of 19 chromosomes, with the exception of late generation transfectant 15-4, which had a modal chromosome number of 18.

In addition to the chromosomes, small “extra-chromosomal” DNA was identified. These could be double minutes or satellite DNA (Sen et al. 1989; Hahn 1993). The modal average of these artefacts was either 1 or 2, for all cell lines including the hosts (Table 5.2).

The modal chromosome numbers observed in this work were relatively consistent, indicating stability in the chromosome structure of the transfectants. The host cell lines used in this work were derived from the heterogeneous CHO-K1 lineage. Previous research showed that CHO-K1 has a modal chromosome number of 21 (Kao & Puck 1969; Deaven & Petersen 1973; Derouazi et al. 2006). The values presented in Table 5.2 suggest that during the development of the clonal host cell lines, a selection process occurred, resulting in lower than expected modal values. Consistent with previous observations (Wurm 2013), the hosts and transfectants analysed had a broad range in chromosome number of 13-22 chromosomes. This shows that the cells are able to survive outside the modal value. Derouazi et al. found chromosomal aberrations in CHO DG44 cells were mostly unbalanced and included deletions and complex rearrangements (Derouazi et al. 2006), however G-banding analysis of CHO-K1 chromosomes, showed that only a few elements of hamster genome structure was not retained in the rearranged chromosomes (Deaven & Petersen 1973). 22% of the host 15 cells analysed had 19 chromosomes, this may account for the early generation cell line 15 transfectants analysed, having a modal value of 19 chromosomes, rather than 18 as observed in the host.

Additionally, the karyotype of host cell lines 15 and 19 had been previously determined on behalf of MedImmune by Chrombios. Hosts 15 and 19 had modal chromosome numbers of 18 and 19, respectively, which supports of the data presented here.

Figure 5.3 Metaphase spreads of host cell lines and transfectants



Clonal host and transfectant cells were fixed in metaphase using 150 ng ml^{-1} [w/v] colcemid. Metaphase spreads were prepared and images collected as described in Section 2.8. The figure shows typical examples of early generation metaphase spreads of clonal host cell line 15 (15 H), clonal host cell line 19 (19 H), transfectant 15-2 and transfectant 19-3. The white arrows indicate what could be double minutes.

Table 5.2 Analysis of chromosome number of host cell lines, high and low producing transfectants

| Transfectant | Chromosome number | |
|--------------|-------------------|-----------------|
| | Early generation | Late generation |
| Host 15 | 18 (2) | - |
| 15-2 | 19 (2) | 19 (2) |
| 15-4 | 19 (2) | 18 (1) |
| Host 19 | 19 (1) | - |
| 19-3 | 19 (1) | 19 (1) |
| 19-11 | 19 (1) | 19 (1) |

Clonal host and transfectant cells were fixed in metaphase using 150 ng ml⁻¹ [w/v] colcemid. Metaphase spreads were prepared and images collected as described in Section 2.8. Images of 50 metaphase spreads were collected from each clonal host/transfectant and counted for chromosome number using ImageJ software. The table shows the modal chromosome number, and the modal number of “extra-chromosomal” DNA in brackets. The modal number of chromosomes remained stable for all transfectants during LTC, with the exception of transfectant 15-4, which showed a decrease in chromosome number from 19 to 18.

5.2.3 Recombinant gene copy number analysis of high and low producing transfectants

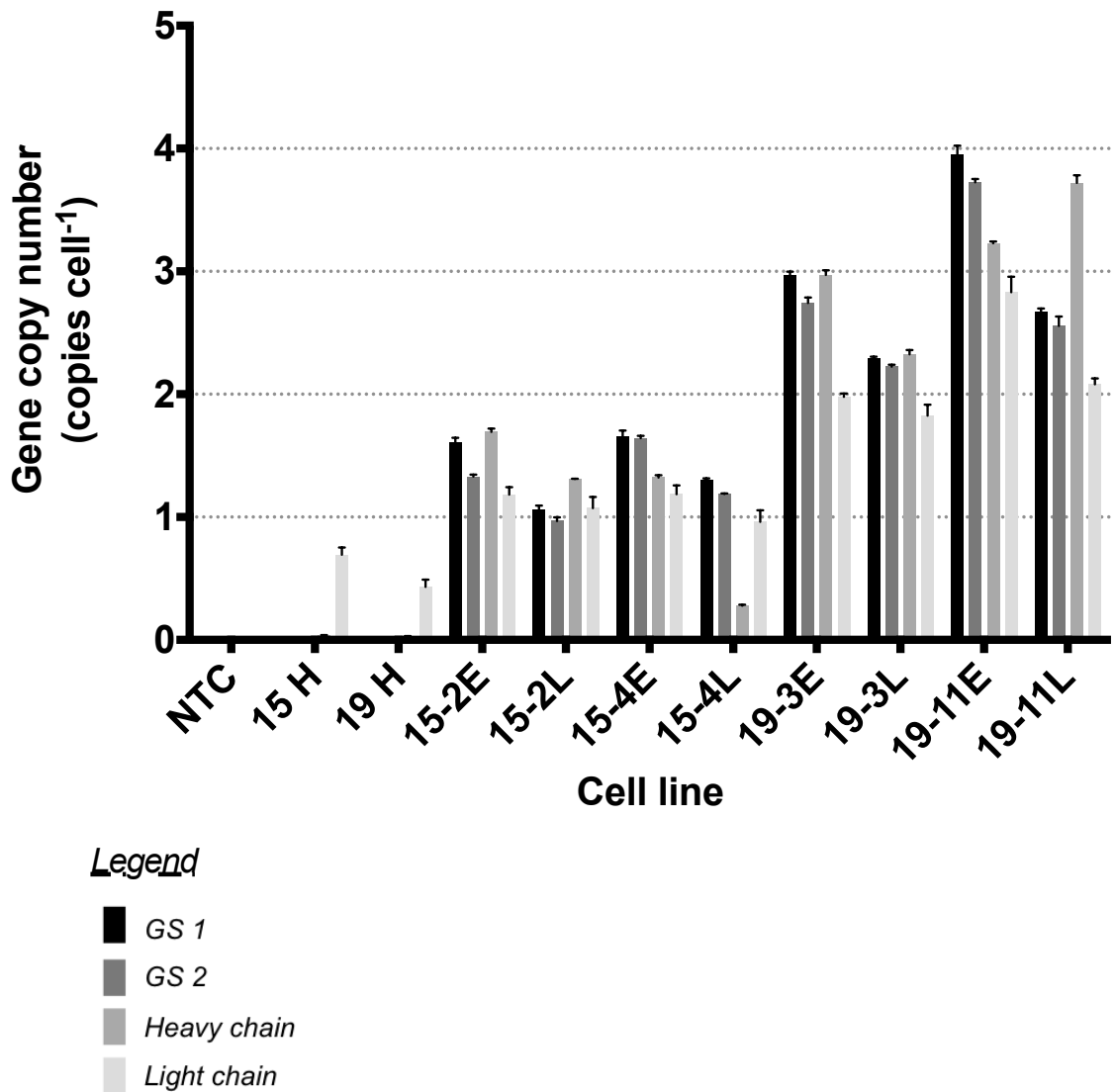
The expression of mAb mRNA was previously found to correlate with Qp (Section 4.3.3). qRT-PCR analysis enabled a determination of recombinant gene copy number for the transfectants. For early generation transfectants, transfectants 15-2 and 15-4 had between 1-2 copies cell⁻¹, transfectant 19-3 had 3 copies cell⁻¹ and transfectant 19-11 had between 3-4 copies cell⁻¹ (Figure 5.4). The gene copy number decreased in DNA isolated from the late generation cells for all transfectants. The decreases corresponding to the GS 1, GS 2 and heavy chain primers were significant ($p < 0.05$), with the exception of the heavy chain copy number for the cell line 19 transfectants, which showed a significant increase in the late generation. The decrease in light chain copy number was only significant in transfectant 19-11. Amplification of DNA was detected, corresponding to the light chain primers in both host cell lines, this was not expected and indicated less than one copy per cell.

The primers used in this experiment, targeted genes contained within one plasmid, it was expected that the copy number of each gene would be the same within a host/transfectant, as both genes were delivered on the same DNA vector. Care was taken to design specific primers with optimal efficiency (Appendix E), however, the variation in copy number by each primer set could be related to amplification efficiency/specificity. The light chain DNA detected in the host samples may be related to primer specificity, although evidence of this was not apparent when the primers were tested (Appendix E). Primer specificity could also have resulted in the low copy number values determined for the cell line 19 transfectants, compared to the other primer sets.

The data show that there was negligible difference in the recombinant gene copy number between the high producing and low producing transfectant from each host cell line. This suggests that gene copy number was not a major determinant of productivity, as the productivities were significantly different (Table 5.1). It is possible that the insertion site of the recombinant DNA may have affected mRNA expression, however the inclusion of UCOE in the vector DNA has been reported to minimise these effects (Zhang et al. 2010). mRNA expression analysis (Section 4.3.3) found greater heavy and light chain expression in the high producing transfectants; this appears to be independent of copy number. The data provides some evidence of recombinant gene copy number loss between the early and late generations. However, the differences (significance) observed between the early and late generations are questionable, the differences are relatively small and the assay

will have an associated error rate. The Qp of transfectants 15-2, 15-4 and 19-3 decreased in the late generation fed-batch cultures (Table 5.1); this could be related to loss of recombinant gene copy number. However, only transfectant 19-11 showed a decrease in GS mRNA expression at the late generation (Figure 4.12) (late generation mAb-109 mRNA expression data was not available). Decreased Qp has been previously linked to copy number loss in CHO DG44 cells (Kim et al. 1998), although changes to the chromosomal location of the recombinant genes (Kim & Lee 1999) and epigenetic regulation (Kim et al. 2011; Osterlehner et al. 2011) have also been found to influence Qp. It is possible that epigenetic regulation of the heavy and light chain DNA could have affected Qp in the transfectants. However, as this information is lost during standard PCR techniques (Kristensen & Hansen 2009), it is not possible to confirm this from the methodology used in this study.

Figure 5.4 Recombinant gene copy number analysis of high and low producing transfectants



DNA was isolated from the clonal hosts and transfectants for recombinant gene copy number analysis as described in Section 2.6.2. Four primer sets were used for analysis; GS1 and GS2 were two independent primer sets targeted against the recombinant GS gene, the heavy and light chains were assayed using one independent primer set each. The chart shows the gene copy number data for the no template control (NTC), clonal host cell line 15 (15 H), clonal host cell line 19 (19 H), transfectants 15-2, 15-4, 19-3 and 19-11. The early (E) and late (L) generation transfectants were analysed in this experiment. Error bars represent the SEM for three biological replicates. Each biological replicate was assayed as a technical triplicate.

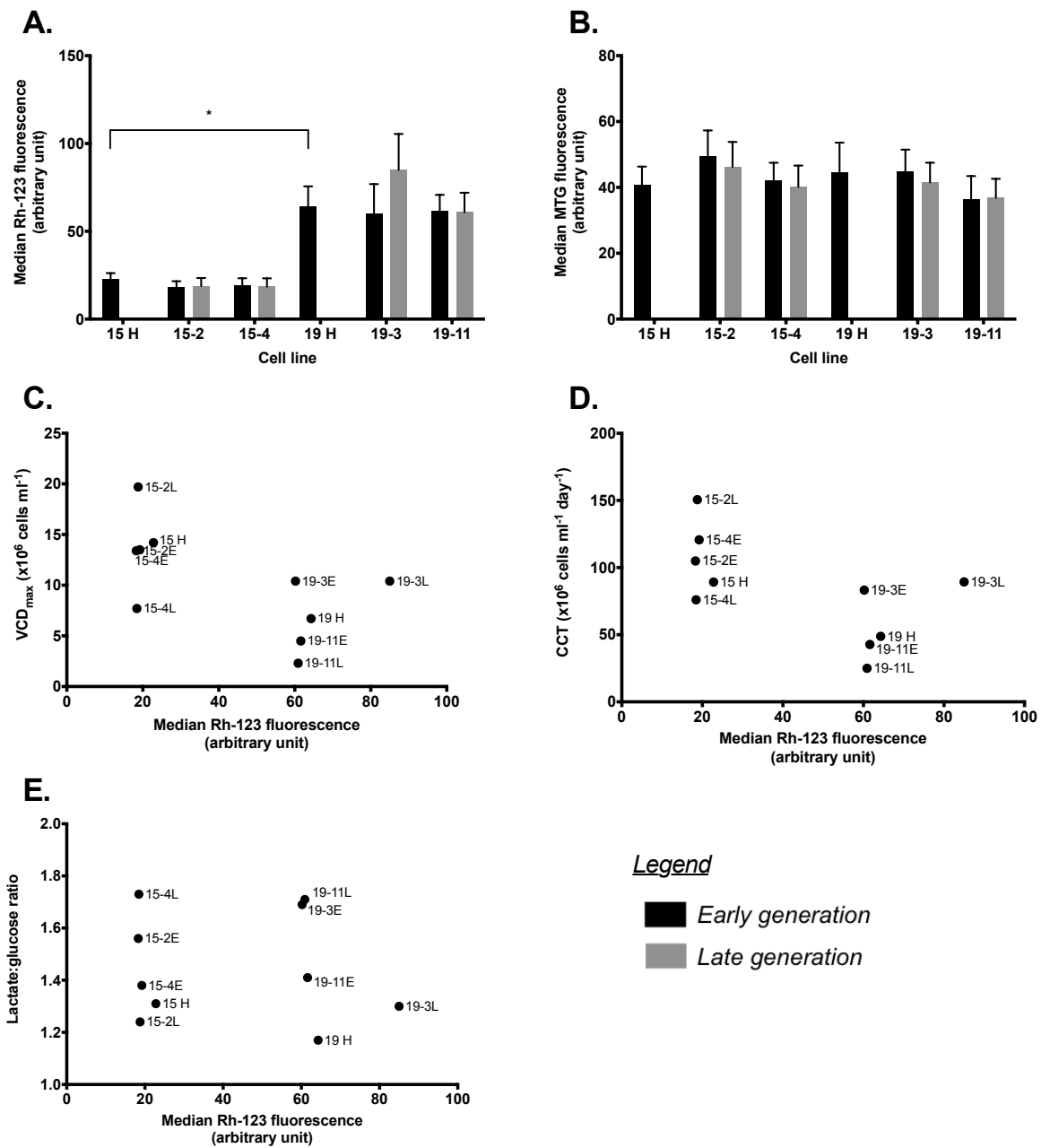
5.2.4 Analysis of mitochondrial membrane potential in high and low producing transfectants

Analysis of mitochondrial membrane potential using Rh-123 showed that host cell line 19 had significantly greater median Rh-123 fluorescence intensity than host cell line 15 (Figure 5.5 A). This was consistent with the observations in Section 3.5, which showed that host cell lines with slower growth rates had greater Rh-123 fluorescence. No significant difference was observed between the transfectants at early or late generation and their parent host cell line. Additionally, no significant difference was observed in MitoTracker Green FM (MTG) fluorescence between the cells, suggesting consistency in the mitochondrial mass (Figure 5.5 B).

Rh-123 analysis of the host cell lines in Section 3.5 identified a relationship between Rh-123 fluorescence and the growth parameters VCD_{max} and CCT. There was no significant correlation between the Rh-123 fluorescence in this experiment to the VCD_{max} and CCT data in Table 5.1 (Figure 5.5 C and D). However, cell line 15 host and transfectants typically achieved greater VCD_{max} and CCT than the cell line 19 host and transfectants. This was coupled with less Rh-123 fluorescence in the cell line 15 cells, which is in support of the observations in Section 3.5.

No significant correlation was observed between the Rh-123 fluorescence and the lactate:glucose ratio of the cells (Figure 5.5 E). Also, the lactate:glucose ratios observed in this experiment (Figure 5.5 E) were greater than the values observed in Chapter 3 (Table 3.4). All of the cells in this experiment were cultured under glutamine-free conditions, whereas the hosts in Chapter 3 were cultured in medium supplemented with 6 mM L-glutamine. It was proposed in Chapter 3 that Rh-123 staining might be a useful tool for the identification of cells with a metabolically efficient phenotype. However, the data presented here, suggest that this is not applicable to cells grown in the absence of L-glutamine, which was shown to influence mitochondrial membrane potential in human epithelial-like lung carcinoma cells (Ahmad et al. 2001). However, as no significant difference in Rh-123 fluorescence was observed between the clonal host cell lines and the transfectants, this suggests that mitochondrial membrane potential may be a heritable phenotype. Heritability of mitochondrial DNA has been observed in human twin studies (Xing et al. 2008), this may contribute to heritability of the mitochondrial phenotype in clonal CHO cell lines.

Figure 5.5 Analysis of mitochondrial membrane potential in high and low producing transfectants



Clonal host cell lines and transfectants were grown as described in Section 2.3.2 in the absence of L-glutamine. Cells were sampled on day 4 of culture from 3 consecutive maintenance flasks and assayed for Rh-123 (A) or MTG (B) fluorescence as described in Section 2.7.1. Error bars represent SEM for three biological replicates. * indicates $p < 0.05$, using independent samples t-test.

Correlation analysis was applied to assess the relationship between Rh-123 fluorescence and the VCD_{max} (C) and CCT (D) data from Table 5.1. Additionally, correlation analysis was applied to lactate:glucose ratio data of the cells (E).

5.3 Metabolite profiling of high and low producing transfectants

Cell culture medium samples were collected from the transfectant fed-batch cultures (Section 5.2.1) for extracellular metabolite analysis using GC-MS (as described in Section 2.4.2). Additionally, CD-CHO medium was analysed as a control and baseline. Intracellular metabolite extracts were prepared (as described in Section 2.4.2) from replicate “sacrifice” cultures that were grown together with the main fed-batch cultures.

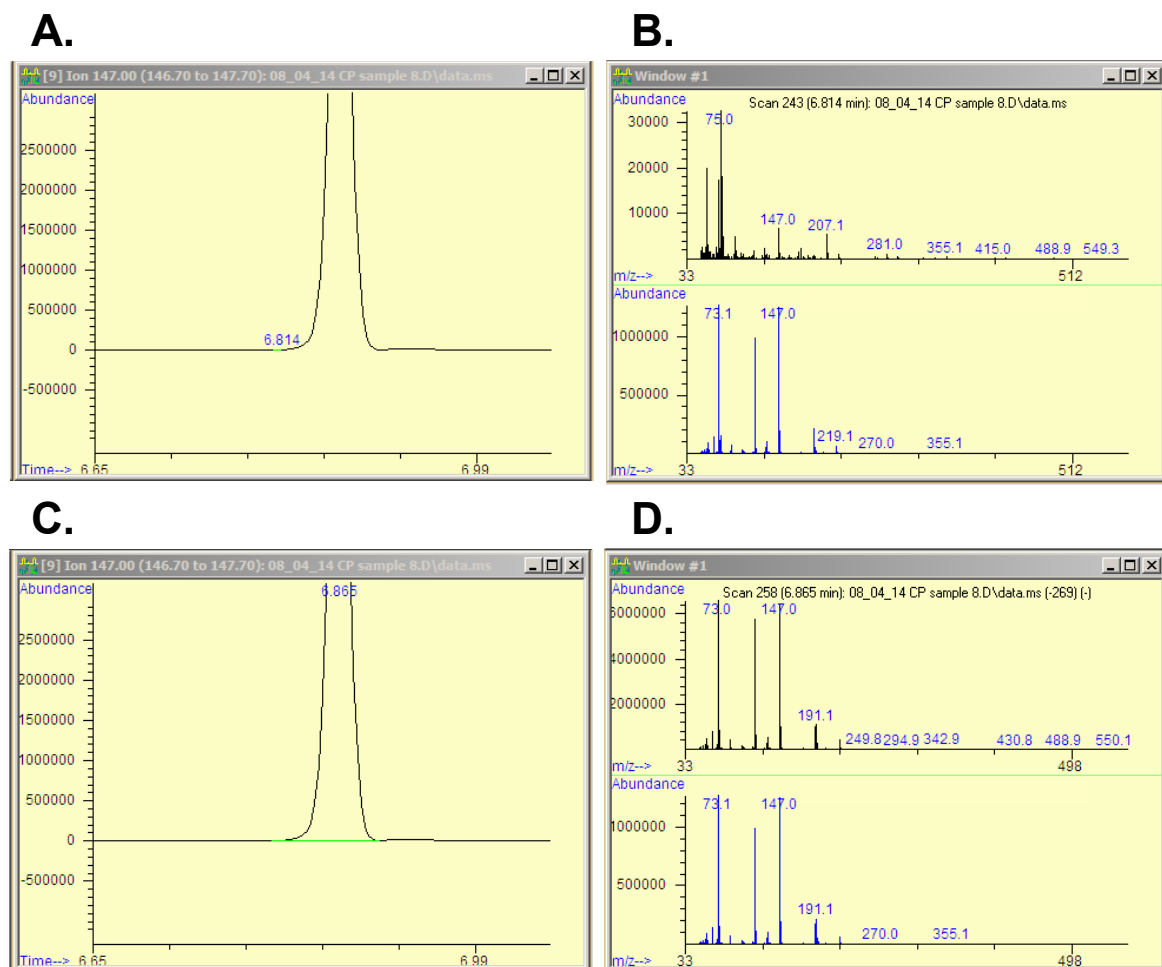
Raw GC-MS data was acquired and quantified using Agilent Technologies Chemstation software in conjunction with the Fiehn mass spectral library. The library contains the mass spectra of over 1000 metabolite derivatives (Kind et al. 2009). A custom report of the data from each sample analysed was generated, listing each metabolite in the Fiehn library for subsequent analysis. For each metabolite the report detailed the quantified amount (response value), retention time, expected retention time, and a quality score (Q value). The Fiehn library includes many metabolites that were not truly identified and/or not considered biologically relevant. The following criteria were applied to the data to screen for successful identifications:

- A response value $\geq 10,000$.
- A retention time within 0.2 minutes of the expected retention time.
- A Q value of ≥ 50 .

In addition to these criteria, manual checks were undertaken on metabolites reported in this work to ensure accurate identification. Some of the samples analysed contained high concentrations of metabolites, e.g. glucose and lactate, which produced large flat peaks that were not identified by Chemstation. In these instances, the peaks were manually selected prior to generation of the custom report (Figure 5.6).

The GC-MS method was considered a semi-quantitative tool for profiling a large number of metabolites. Glucose, lactate, glutamine and glutamate concentrations were determined enzymatically (Section 2.4.1) and compared to the GC-MS data. The trends observed in the enzymatic data complemented the GC-MS data confirming its integrity (Appendix F).

Figure 5.6 Manual correction of compound identification in Chemstation



The Figure shows screenshots from Chemstation of a lactic acid peak obtained from a cell culture medium sample (A). Lactate was highly abundant in this sample and was not accurately identified, thus the reported mass spectra (B. top) does not match the Fiehn library spectra for lactic acid (B. bottom). The peak was manually selected (C) and the mass spectra confirmed the correct identification of the peak (D).

The cell culture medium samples were analysed to compare high producing and low producing transfectants from the same host cell line as follows:

- Transfectant 15-2 and 15-4 (early generation)
- Transfectant 15-2 and 15-4 (late generation)
- Transfectant 19-3 and 19-11 (early generation)

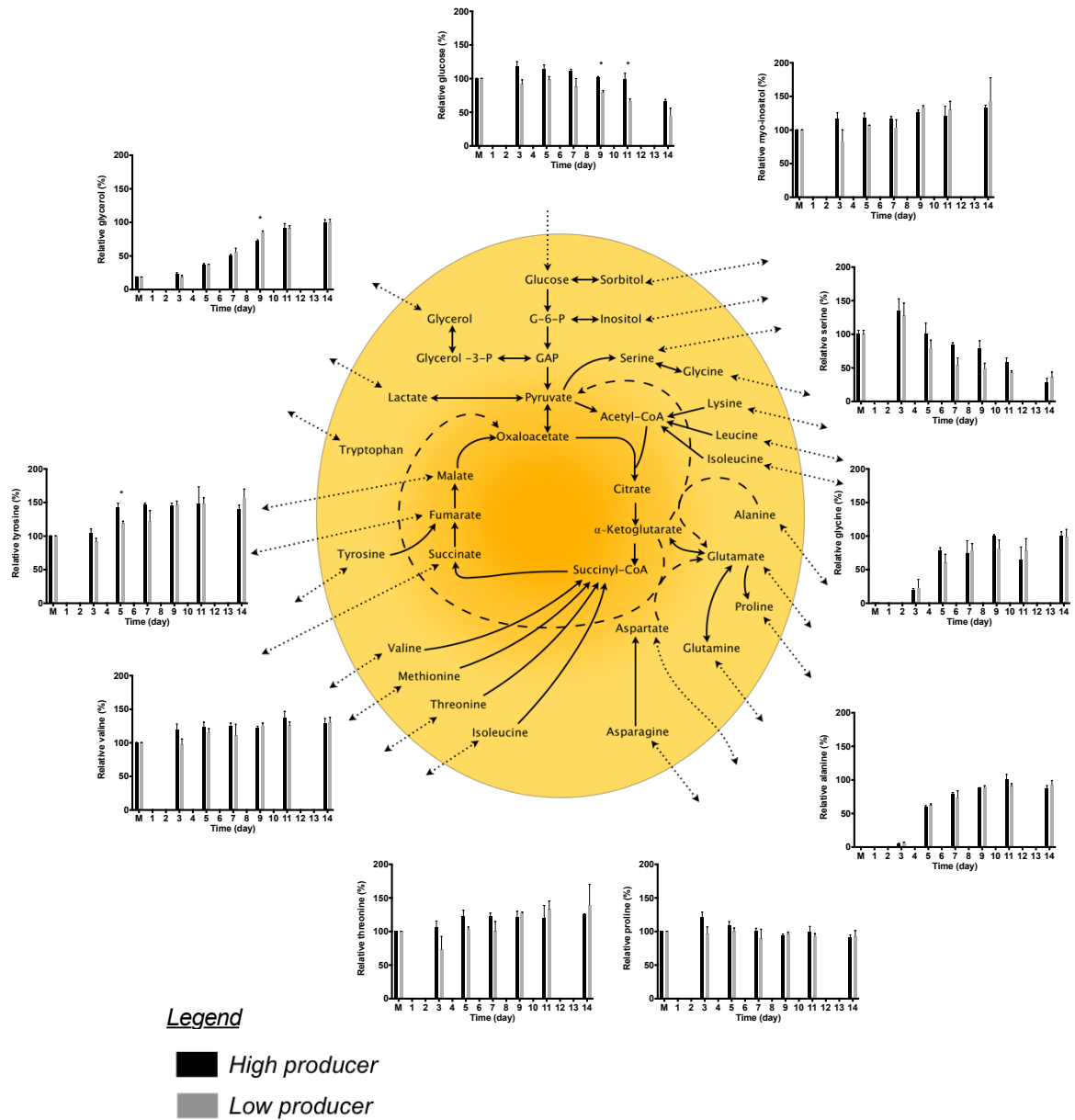
Intracellular metabolite extracts were prepared on day 7 of fed-batch culture, the intracellular data for all transfectants is presented together. Late generation transfectant 19-3 and 19-11 were also included for comparison in the intracellular analysis.

A targeted approach was used for analysis of the data, focussing on metabolites that have been reproducibly identified with this methodology by previous members of the Dickson Lab (Sellick et al. 2009; Sellick et al. 2010; Sellick et al. 2011; Picken 2012). All GC-MS data presented in this Chapter was normalised to the internal standard, myristic-d₂₇ acid, then presented relative to either the baseline response value or maximum response value in each data set. For many of the metabolites that were successfully identified, there was no significant difference (or very little difference) between the high producing and low producing transfectants over the course of fed-batch culture (Figure 5.7). Consequently, much of this data is not shown, as it was not considered to be insightful.

The transfectants used for metabolomic analysis displayed differences in both growth and productivity. Two questions were thus considered during data analysis:

- Which metabolic parameters related to productivity?
- Which metabolic parameters related to growth?

Figure 5.7 Central carbon metabolism of CHO cells



The Figure shows the central carbon metabolism network adapted from Sellick et al (2011). This includes the glycolytic and citric acid cycle pathways and features some of the metabolites that were successfully identified in this study. The data show examples of metabolites that were determined to have no significant difference (or limited difference) over the course of fed-batch culture. All data represents early generation transfectant 15-2 (high producer) and 15-4 (low producer). Error bars represent SEM for three biological replicates. * indicates $p < 0.05$, using independent samples t-test to compare the high producing transfectant to the low producing transfectant.

5.3.1 Glycolysis

Six metabolites (glucose, lactate, sorbitol, threitol, pyruvate and glyceraldehyde 3-phosphate) were successfully identified which relate to the glycolysis pathway. Glucose was detected in both the extracellular and intracellular samples. No significant difference was detected in the extracellular relative glucose response until day 9, for any of the comparisons (Figure 5.8 A, 5.9 A and 5.10 A). On days 9 and 11 of culture, the early generation transfectant 15-2 had a significantly greater relative glucose response than transfectant 15-4 (Figure 5.8 A). In contrast, the late generation 15-2 had a significantly lower relative glucose response than 15-4 from day 9 onwards (Figure 5.9 A). This was reflected by the early generation transfectant 19-3 compared with 19-11 (Figure 5.10 A). The extracellular glucose data provide evidence of glucose utilisation. However, the relative glucose response remained greater than 80% for the duration of the fed-batch culture period for the late generation transfectant 15-4 (Figure 5.9 A) and early generation transfectant 19-11 (Figure 5.10 A). Additionally, no significant differences were observed in the day 7 intracellular glucose response, with the exception of late generation transfectant 19-3 and 19-11 (Figure 5.11 A).

Significant differences in glucose utilisation were observed between the high and low producers. It is probable that these differences are related to growth rather than to productivity. For each pair of transfectants compared, the relative glucose response remained greatest for the transfectant with the poorest growth properties (Table 5.1, Figure 5.8 A, 5.9 A and 5.10 A). The greatest disparity in relative glucose response was observed for the late generation cell line 15 transfectants (Figure 5.9 A) and early generation cell line 19 transfectants (Figure 5.10 A). In these comparisons, the high producers had significantly greater VCD_{max} and CCT than the low producers (Table 5.1) and consumed the most glucose. An undisclosed quantity of glucose was included in the feed added, which could explain why the relative glucose response remained above 80% for two of the low producing transfectants; the rate of glucose addition may have been similar to the rate of glucose consumption for these transfectants.

Lactate was also detected the extracellular and intracellular samples. Consistent with previous findings (Figure 3.4), lactate was not detected in the basal medium samples. By day 3 of culture, lactate had accumulated in the medium of all cultures (Figure 5.8 B, 5.9 B and 5.10 B) and a relative response of between approximately 80-90% was observed. The extracellular data suggest that lactate was consumed by most of the cultures from day 7 of culture onwards. However, the extent of lactate utilisation differed between the

transfectants. The early generation cell line 15 transfectants did consume lactate, but by day 14 of culture the relative lactate response remained greater than 35% for 15-2 and greater than 70% for 15-4 (Figure 5.8 B). In the late generation, transfectant 15-2 consumed almost all of the available lactate by day 14, whilst the lactate response transfectant 15-4 remained at approximately 85% (Figure 5.9 B). The lactate profile of the early generation cell line 19 transfectants followed a similar trend to the late generation cell line 15 transfectants. The high producer consumed the majority of the lactate available by day 14, and although lactate consumption was evident for the low producer, the day 14 response remained above 65% (Figure 5.10 B). For all comparisons, the data showed a significantly greater lactate response for the low producing transfectants in the later stages of culture. The day 7 intracellular data also show a greater lactate response for the low producers, however this was only significant for the late generation cell line 19 transfectants (Figure 5.11 B).

Lactate was produced by all of the transfectants during the early stages of fed-batch culture (Figure 5.8 B, 5.9 B and 5.10 B). This has been observed in the host cell lines (Figure 3.4) and documented in other studies (Tsao et al. 2005; Ma et al. 2009; Luo et al. 2011; Nolan & Lee 2011; Sellick et al. 2011). In the host cell lines (Section 3.3), consumption of lactate occurred following glucose depletion. However, in the transfectants, lactate was consumed in the presence of glucose. Lactate re-utilisation in CHO cells has been identified as an indicator of energy efficient metabolism (Luo et al. 2011). Lactate consumption was less in the low producing transfectants, in the late generation transfectant 15-4 and early generation transfectant 19-11. However, this was linked with poor growth and high extracellular glucose, indicating that lactate consumption is linked to growth rather than productivity. This is supported by Tsao et al, who showed a linear relationship between CCT and combined glucose and lactate consumption (Tsao et al. 2005)

The intracellular glucose and lactate data was supportive of the day 7 extracellular data. However, previous research has suggested intracellular glucose concentration is two orders of magnitude less than extracellular glucose concentration (Ma et al. 2009). The high intracellular glucose responses, compared to the basal medium, in this study (Figure 5.11 A) suggest that there was medium contamination of the intracellular metabolite samples.

The polyols sorbitol and threitol were produced by the transfectants over the duration of fed-batch culture (Figure 5.8 C and D, 5.9 C and D, 5.10 C and D). Neither of these

metabolites were detected in the basal medium samples. In the extracellular metabolite comparisons, significantly greater relative sorbitol responses were detected in the low producing transfectant cultures. A similar trend was observed for the threitol production. However, the threitol response for low producer 19-11 was less than the response for the high producer throughout the culture period (Figure 5.10 D). The intracellular metabolite data supported the greater extracellular sorbitol response in the low producing transfectants (Figure 5.11 C). Intracellular threitol responses were observed to be greater for all low producers, however this was only significant for the cell line 15 transfectants.

Sorbitol accumulation in extracellular medium has been previously reported in CHO K1SV and DUK-XB11 cells (Ma et al. 2009; Sellick et al. 2011; Luo et al. 2011), and high glucose concentrations can lead to an increased production of sorbitol in kidney cells (Tomlinson & Gardiner 2008). This effect was observed by Sellick et al. following administration of a glucose-only feed (Sellick et al. 2011). Luo et al. observed accumulation of sorbitol to be prevalent in low producing CHO cell lines that did not consume lactate (Luo et al. 2011). Here, the low producing transfectants demonstrated significantly greater relative sorbitol responses than the high producing transfectants (Figure 5.8 C, 5.9 C, 5.10 C and 5.11 C), paired with greater relative lactate responses. Increased sorbitol concentrations may therefore also be related to poor productivity. Additionally, sorbitol has been used as an osmotic stressor with CHO-K1 cells, 200 mM caused a half maximal decrease in protein synthesis by the disruption of eukaryotic initiation factor complexes (Patel et al. 2003). However, increased osmolality has also been shown to increase the specific productivity of recombinant CHO cultures (Nasseri et al. 2014). The concentration of sorbitol that accumulated in this study is unknown, however, considering the glucose concentration in the basal medium was approximately 35 mM, it is probable that the sorbitol concentration was significantly lower than 200 mM.

In the cell line 15 transfectants, the relative threitol response was significantly greater for the low producers (Figure 5.8 D and 5.9 D). In the early generation cell line 19 transfectants, the threitol response was greater for the high producer (Figure 5.10 D). However, the VCD_{max} of early generation transfectant 19-3 was more than double that of transfectant 19-11, normalisation to cell density suggests that production of threitol per cell was greater in transfectant 19-11. The intracellular data, in which cell number was controlled, shows a greater threitol response for all of the low producing transfectants. The threitol pathway is not well studied in mammalian organisms, and in humans it is thought to be a product of the glucuronate pathway (Pitkänen 1977; Walters et al. 2009). The data

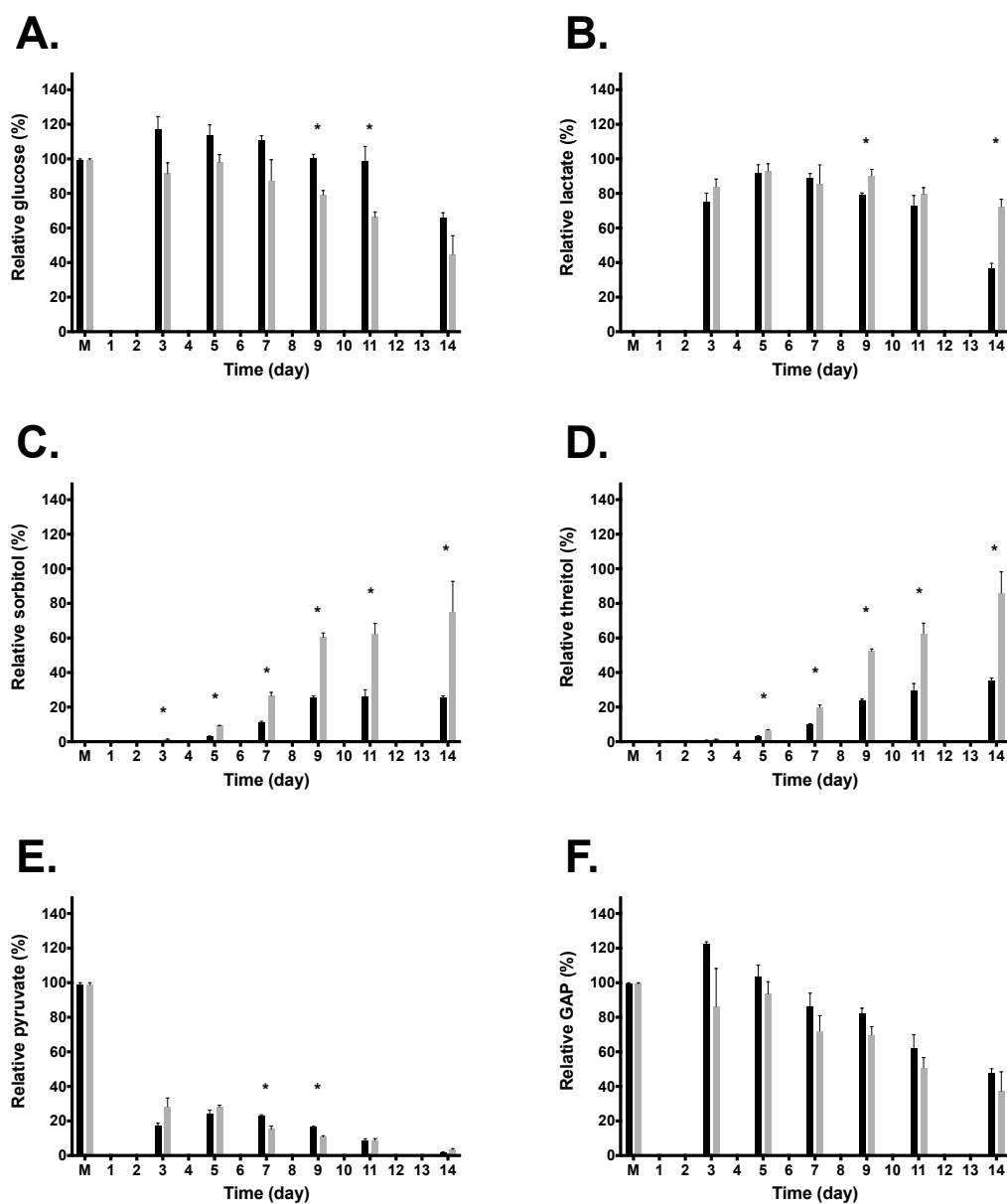
presented here suggest that threitol, similarly to sorbitol, may be linked to poor productivity.

Pyruvate was detected in the basal medium samples and over the duration of fed-batch culture (Figures 5.8 E, 5.9 E and 5.10 E). The extracellular pyruvate response had decreased by at least 45% by day 3 for all cultures. The greatest decrease in pyruvate response by day 3 was observed for the early generation transfectant 15-2 where the response had decreased by more than 80% (Figure 5.8 E). The day 7 intracellular metabolite analysis found very low amounts of intracellular pyruvate in the cell line 15 transfectants (Figure 5.11 E) The actual pyruvate response for the late generation transfectant 15-2 was below the 10,000 response value required for successful identification. The intracellular pyruvate data indicated a significantly greater pyruvate response for transfectant 19-11 when compared to transfectant 19-3 (Figure 5.11 E).

Pyruvate is a key intermediate/metabolic branch point in central carbon metabolism (Figure 5.7). It acts as a major entry point for carbon skeletons from glycolysis into the TCA cycle (Luo et al. 2011; Chen et al. 2012). The sharp decline in extracellular pyruvate between day 0 and day 3 of fed-batch culture, suggests a high demand for metabolite during the growth phase of culture. Pyruvate consumption has been observed in other CHO cell lines derived from CHO-K1 early in fed-batch culture (Sellick et al. 2011). It is also possible that the sharp decline in extracellular pyruvate, could be linked to the accumulation of lactate by day 3 of culture through the action of lactate dehydrogenase, dependent on the catabolic capacity of the citric acid cycle and the cell redox state (Ma et al. 2009; Luo et al. 2011).

Glyceraldehyde 3-phosphate (GAP) was detected in the basal medium samples and at all of the time points analysed during fed-batch culture (Figure 5.8 F, 5.9 F and 5.10 F). A 20% increase in the relative GAP response was observed for the early generation 15-2 and both cell line 19 transfectant cultures (Figure 5.8 F and 5.10 F). Following day 3 the relative GAP response decreased in all of the fed-batch cultures, no significant difference was observed in any of the comparisons. GAP was detected in the intracellular metabolite samples (Figure 5.11 F), the relative response was greater for the cell line 19 low producing transfectant at both generations, however this was only significant for the late generation.

Figure 5.8 Analysis of extracellular glycolysis-associated metabolites for early generation cell line 15 transfectants during fed-batch culture

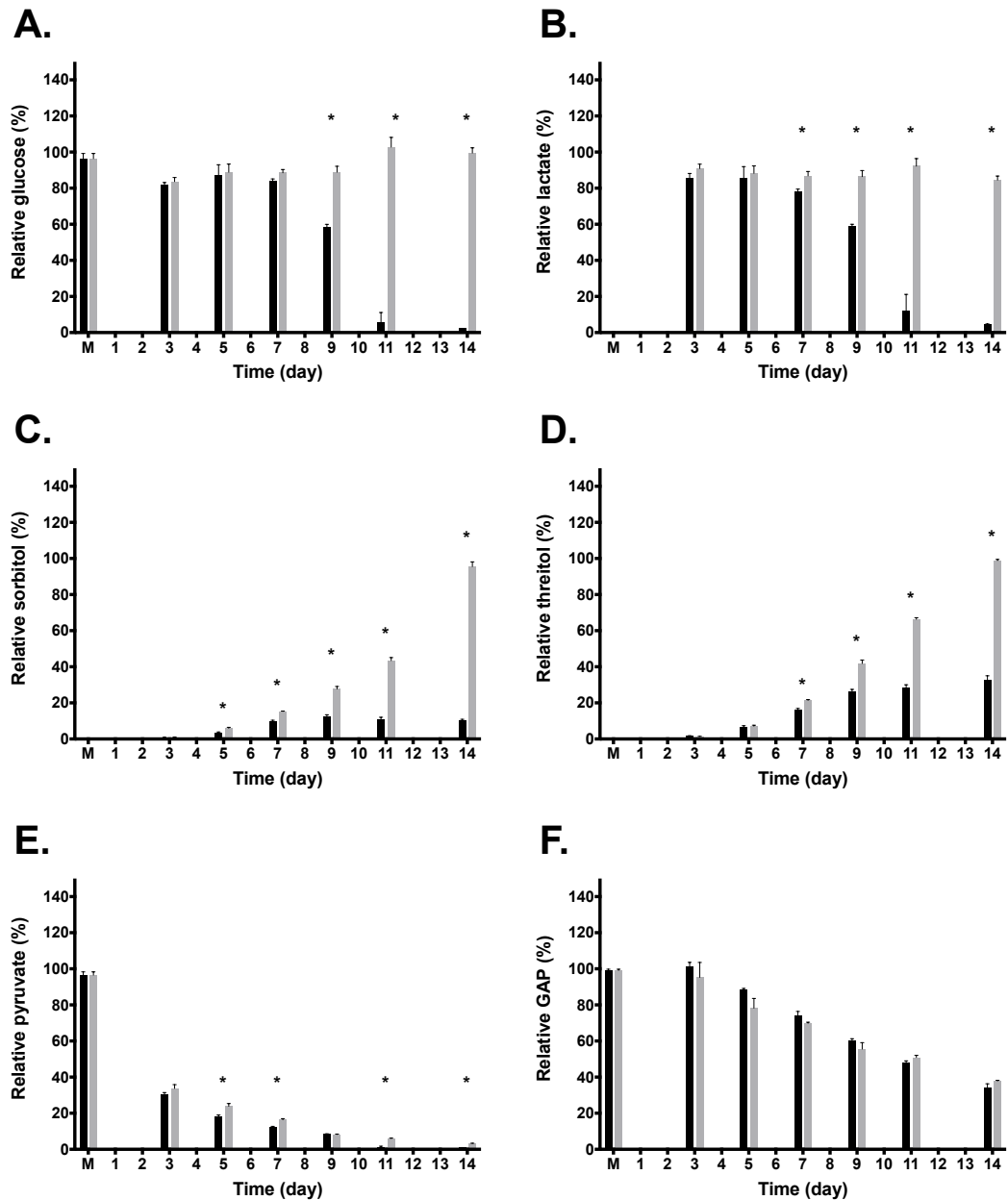


Legend

- High producer
- Low producer

Early generation transfectant 15-2 (high producer) and 15-4 (low producer) were grown in fed-batch culture as previously described (Figure legend 5.1). Medium (M) and cell culture supernatant samples were analysed using GC-MS (Section 2.4.2). The charts show the relative percentage of glucose (A), lactate (B), sorbitol (C), threitol (D), pyruvate (E) and GAP (F). Error bars represent SEM for three biological replicates. * indicates $p < 0.05$, using independent samples t -test to compare the high producing transfectant to the low producing transfectant.

Figure 5.9 Analysis of extracellular glycolysis-associated metabolites for late generation cell line 15 transfectants during fed-batch culture

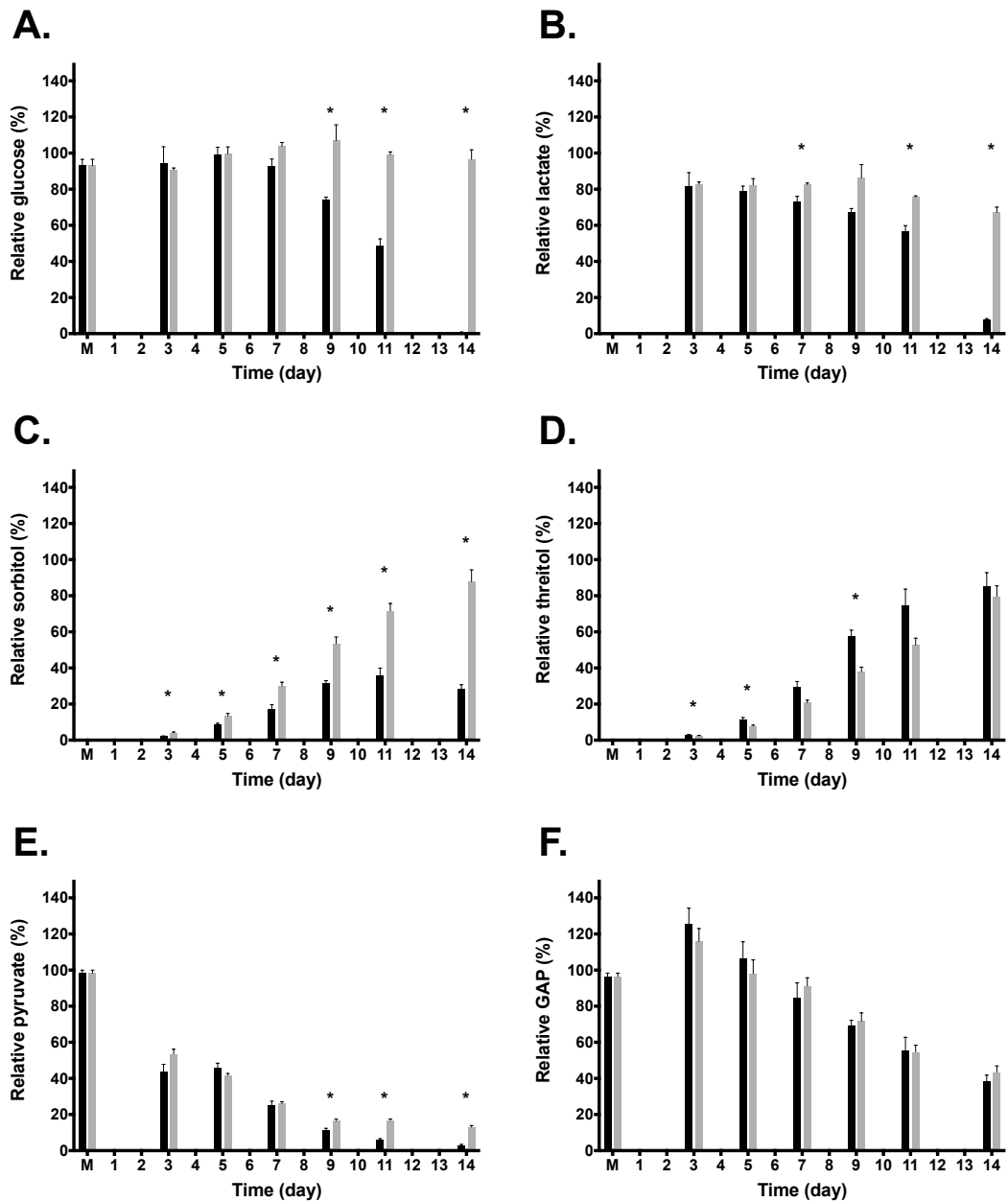


Legend

- High producer
- Low producer

Late generation transfectant 15-2 (high producer) and 15-4 (low producer) were grown in fed-batch culture as previously described (Figure legend 5.1). Medium (M) and cell culture supernatant samples were analysed using GC-MS (Section 2.4.2). The charts show the relative percentage of glucose (A), lactate (B), sorbitol (C), threitol (D), pyruvate (E) and GAP (F). Error bars represent SEM for three biological replicates. * indicates $p < 0.05$, using independent samples t-test to compare the high producing transfectant to the low producing transfectant.

Figure 5.10 Analysis of extracellular glycolysis-associated metabolites for early generation cell line 19 transfectants during fed-batch culture

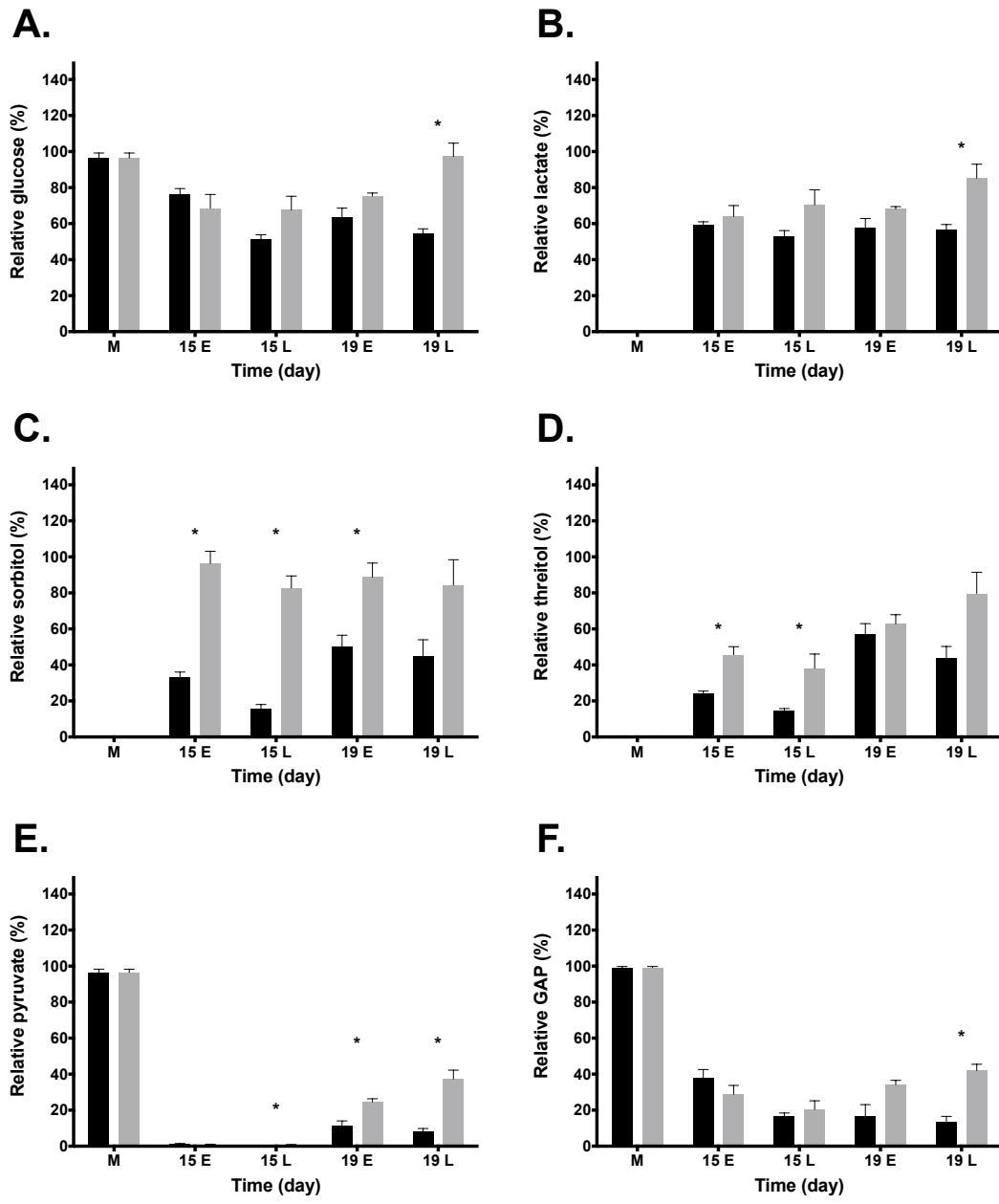


Legend

- High producer
- Low producer

Early generation transfectant 19-3 (high producer) and 19-11 (low producer) were grown in fed-batch culture as previously described (Figure legend 5.1). CD-CHO medium (M) and cell culture supernatant samples were analysed using GC-MS (Section 2.4.2). The charts show the relative percentage of glucose (A), lactate (B), sorbitol (C), threitol (D), pyruvate (E) and GAP (F). Error bars represent SEM for three biological replicates. * indicates $p < 0.05$, using independent samples t -test to compare the high producing transfectant to the low producing transfectant.

Figure 5.11 Analysis of intracellular glycolysis-associated metabolites for early and late generation cell line 15 and 19 transfectants during fed-batch culture



Legend

- High producer
- Low producer

Early generation (E) and late generation (L) transfectants 15-2, 19-3 (high producers) and 15-4, 19-11 (low producers) were grown in fed-batch culture as previously described (Figure legend 5.1). CD-CHO medium (M) and intracellular metabolite extracts were prepared on day 7 of culture and analysed using GC-MS (Section 2.4.2). The charts show the relative percentage of glucose (A), lactate (B), sorbitol (C), threitol (D), pyruvate (E) and GAP (F). Error bars represent SEM for three biological replicates. * indicates $p < 0.05$, using independent samples t-test to compare the high producing transfectant to the low producing transfectant.

5.3.2 Citric acid cycle intermediates

Four metabolites (citrate, succinate, fumarate and malate) associated with the citric acid cycle were successfully identified from the extracellular metabolite samples. Two additional metabolites (oxaloacetate and α -ketobutyrate) were identified from the intracellular metabolite samples. Metabolite peaks were detected for each of the citric acid cycle intermediates in the basal medium samples. However, only fumarate consistently met the criteria for a successful identification in the basal medium.

The relative response for citrate increased over the fed-batch culture period for all cultures (Figure 5.12 A, 5.13 A and 5.14 A). No significant difference in citrate response was observed between the early generation cell line 15 transfectants (Figure 5.12 A). In contrast, the citrate response for the late generation transfectant 15-2 culture was significantly greater than the late generation transfectant 15-4 for all time points analysed (Figure 5.13 A). Consistent with this, the citrate response was greater for the early generation cell line 19 high producer until the day 14 time point (Figure 5.14 A). The high producing late generation cell line 15 and early generation cell line 19 transfectants showed a net utilisation of citrate towards the end of culture. A significantly greater intracellular citrate response was detected in the early generation cell line 19 low producer compared to the high producer (Figure 5.15 A). However, no significant difference in extracellular citrate was observed on day 7 between these transfectants (Figure 5.14 A).

All transfectants produced succinate during fed-batch culture and some of the transfectants showed a net utilisation of succinate towards the end of culture (Figure 5.12 B, 5.13 B, 5.14 B). The succinate response was significantly greater for the transfectant 15-2, compared to transfectant 15-4, at several time points in both generations (Figure 5.12 B and 5.13 B). However, the difference in succinate response was not as exaggerated as that observed for citrate. Additionally, no significant difference was observed in the succinate response of the early generation cell line 19 transfectants succinate response (Figure 5.14 B). Further to this, only the late generation cell line 19 transfectants demonstrated a significant difference in intracellular succinate (Figure 5.15 B).

No significant difference was observed in fumarate relative response, for the early generation cell line 15 transfectants, from the extracellular samples (Figure 5.12 C). The fumarate response was significantly greater for the late generation cell line 15 high producer, compared with the low producing transfectant from day 7 of culture (Figure 5.13

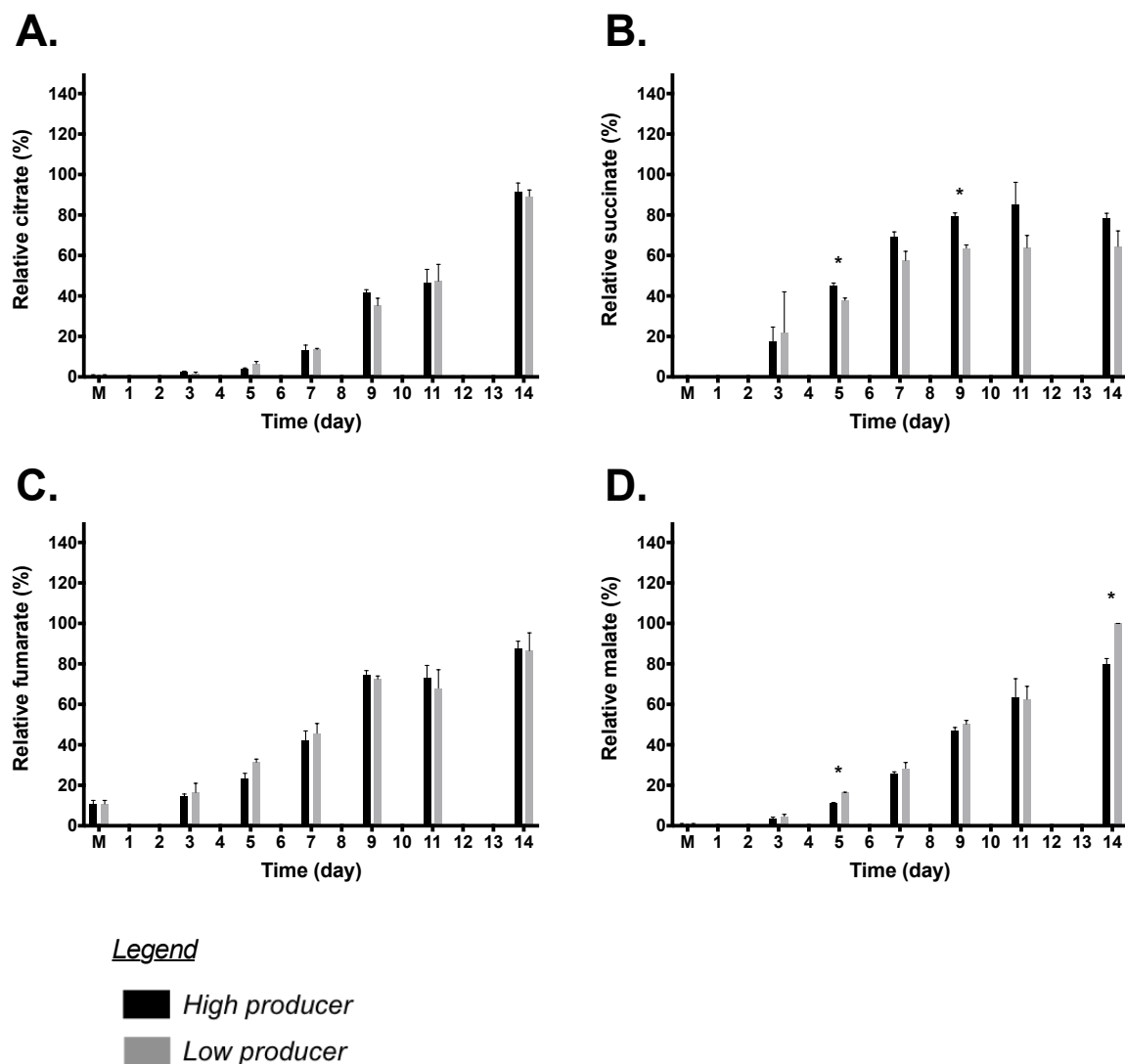
C). Conversely, the fumarate response was significantly greater for the low producer of the early generation, cell line 19 transfectants from day 9 of culture (Figure 5.14 C). The intracellular fumarate data suggest greater quantities of fumarate were present in the high producing cell line 15 transfectant at the early generation (Figure 5.15 C). This observation was not reflected in the late generation despite the high producer having significantly greater extracellular fumarate than the low producing transfectant (Figure 5.13 C). The intracellular data for the cell line 19 transfectants indicated a greater fumarate response in the low producing transfectants (Figure 5.15 C), this reflected the extracellular data (Figure 5.14 C). The patterns observed in the malate data (Figure 5.12 D, 5.13 D, 5.14 D and 5.15 D) very closely mirrored the fumarate data.

Citrate accumulation in the extracellular medium suggested that the cells were transporting citrate out of the mitochondria and across the plasma membrane. Citrate efflux has been observed in other GS-CHO cell systems (Ma et al. 2009; Sellick et al. 2011) and has been identified as a feature of cancer cell lines (linked to a truncated citric acid cycle) (Baggetto 1992; Sengupta et al. 2010). Ma et al. were not able to quantify citrate efflux, but postulated that it must represent a significant drain on the citric acid cycle (Ma et al. 2009). Extracellular citrate was significantly greater in the high producers for the late generation cell line 15 and early generation cell line 19 transfectants (Figure 5.13 A and 5.14 A). Coincidentally, these transfectants had better growth properties than the comparable low producers (Table 5.1) and a greater demand for glucose (Figure 5.9 A and 5.10 A). The efflux of succinate, fumarate and malate from CHO cell lines has been documented in the literature and may result from citric acid cycle inefficiency (Ma et al. 2009; Chong et al. 2010; Sellick et al. 2011). The greater utilisation of glucose and lactate in the high producers, combined with an impaired ability to produce α -ketobutyrate from citrate (Baggetto 1992; Sengupta et al. 2010), may explain the increased extracellular citrate observed in the high producers.

Additional metabolites identified in the intracellular data were oxaloacetate (Figure 5.15 E) and α -ketobutyrate (Figure 5.15 F). No significant difference was observed in the oxaloacetate response for the cell line 15 transfectants. However, at both generations, a significantly greater response was observed for the low producing cell line 19 transfectant compared to the high producer. This could suggest a bottleneck for the production of citrate in transfectant 19-11, however this is not supported by the cell line 15 transfectant data. No significant difference was observed between any of the transfectants in the α -ketobutyrate data. It has been hypothesised that nutrient feeds permit continued synthesis of α -ketobutyrate, despite truncation of the citric acid cycle decreasing the capacity for the

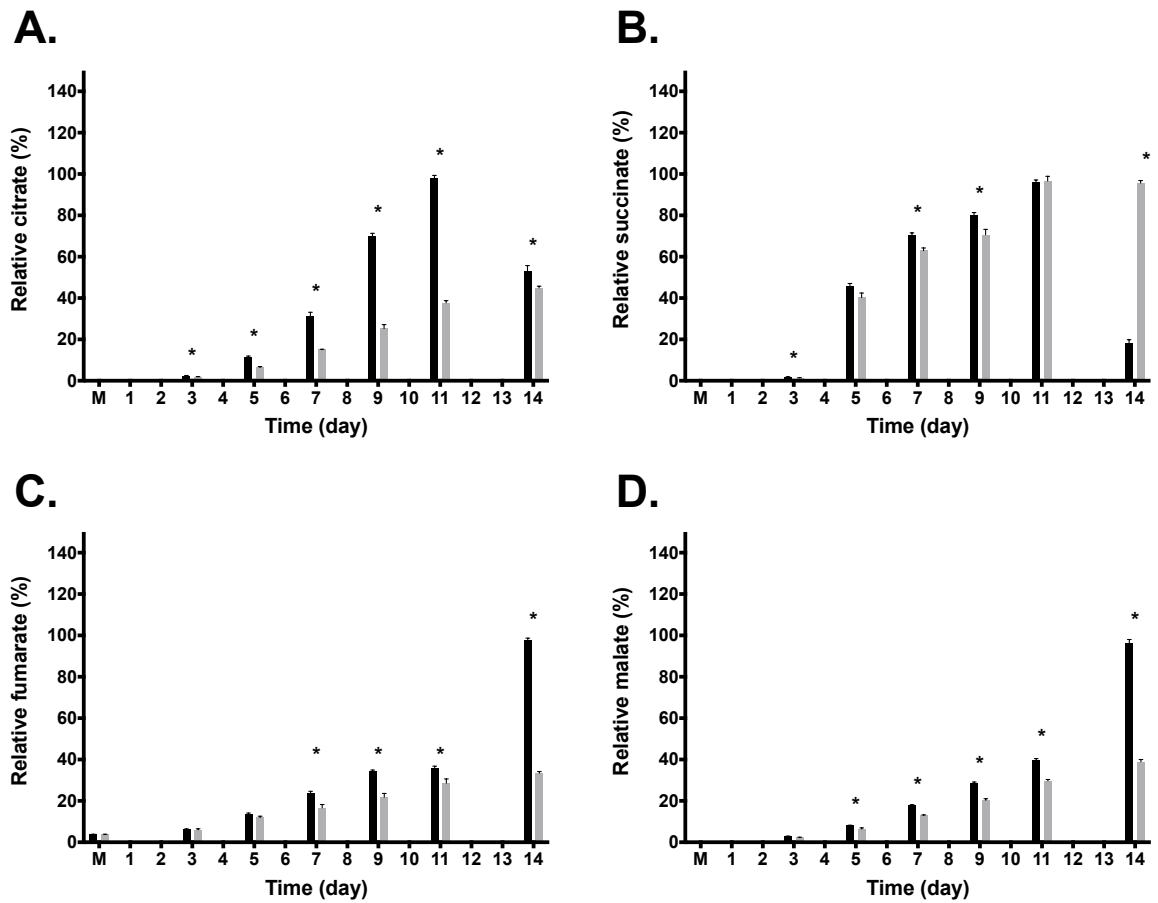
production of α -ketobutyrate from citrate (Baggetto 1992; Sengupta et al. 2010; Sellick et al. 2011).

Figure 5.12 Analysis of extracellular citric acid cycle intermediates for early generation cell line 15 transfectants during fed-batch culture



Early generation transfectant 15-2 (high producer) and 15-4 (low producer) were grown in fed-batch culture as previously described (Figure legend 5.1). Medium (M) and cell culture supernatant samples were analysed using GC-MS (Section 2.4.2). The charts show the relative percentage of citrate (A), succinate (B), fumarate (C) and malate (D). Error bars represent SEM for three biological replicates. * indicates $p < 0.05$, using independent samples t-test to compare the high producing transfectant to the low producing transfectant.

Figure 5.13 Analysis of extracellular citric acid cycle intermediates for late generation cell line 15 transfectants during fed-batch culture

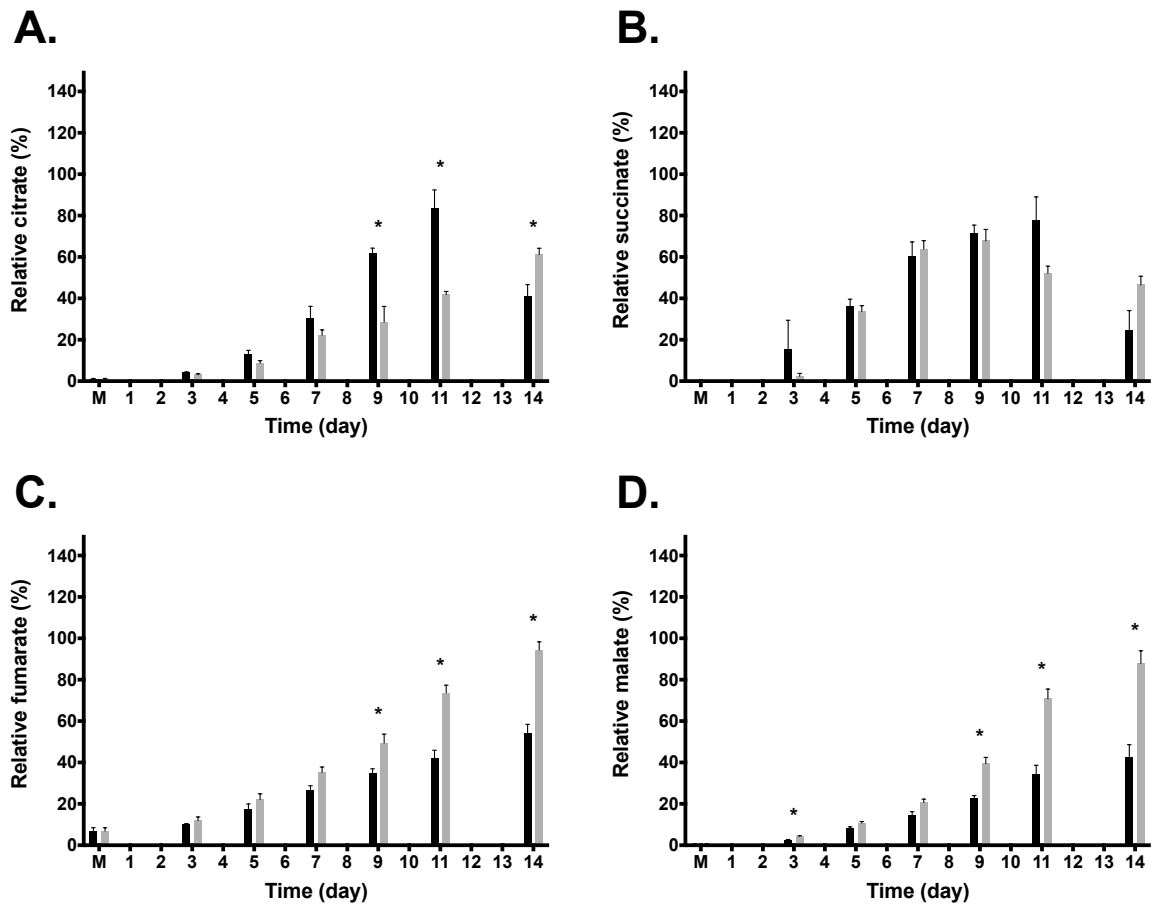


Legend

- High producer
- Low producer

Late generation transfectant 15-2 (high producer) and 15-4 (low producer) were grown in fed-batch culture as previously described (Figure legend 5.1). Medium (M) and cell culture supernatant samples were analysed using GC-MS (Section 2.4.2). The charts show the relative percentage of citrate (A), succinate (B), fumarate (C) and malate (D). Error bars represent SEM for three biological replicates. * indicates $p < 0.05$, using independent samples t-test to compare the high producing transfectant to the low producing transfectant.

Figure 5.14 Analysis of extracellular citric acid cycle intermediates for early generation cell line 19 transfectants during fed-batch culture

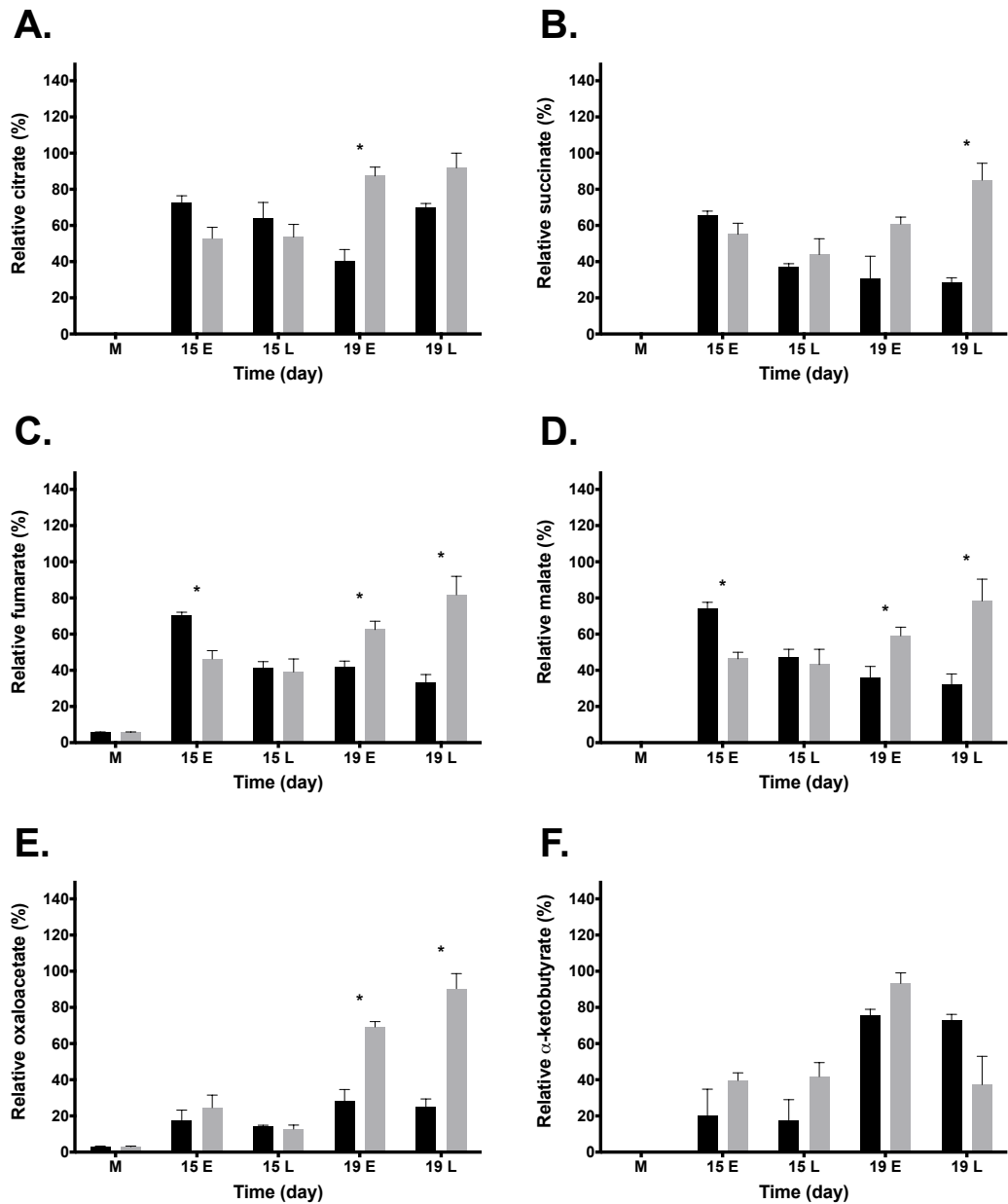


Legend

- High producer
- Low producer

Early generation transfectant 19-3 (high producer) and 19-11 (low producer) were grown in fed-batch culture as previously described (Figure legend 5.1). Medium (M) and cell culture supernatant samples were analysed using GC-MS (Section 2.4.2). The charts show the relative percentage of citrate (A), succinate (B), fumarate (C) and malate (D). Error bars represent SEM for three biological replicates. * indicates $p < 0.05$, using independent samples t-test to compare the high producing transfectant to the low producing transfectant.

Figure 5.15 Analysis of intracellular citric acid cycle intermediates for early and late generation cell line 15 and 19 transfectants during fed-batch culture



Legend

■ High producer
 ■ Low producer

Early generation (E) and late generation (L) transfectants 15-2, 19-3 (high producers) and 15-4, 19-11 (low producers) were grown in fed-batch culture as previously described (Figure legend 5.1). CD-CHO medium (M) and intracellular metabolite extracts were prepared on day 7 of culture and analysed using GC-MS (Section 2.4.2). The charts show the relative percentage of citrate (A), succinate (B), fumarate (C), malate (D), oxaloacetate (E) and α -ketobutyrate (F). Error bars represent SEM for three biological replicates. * indicates $p < 0.05$, using independent samples t-test to compare the high producing transfectant to the low producing transfectant.

5.3.3 Amino acids and derivatives

Many of the amino acids detected in the metabolomic data did not show any significant differences between the transfectants studied. This Section focuses on four amino acids that showed significant differences (aspartate, asparagine, glutamine and glutamate) and the derivatives phenylactic acid and indoleacetic acid.

Aspartate production was observed for all of the transfectants following inoculation of the fed-batch cultures (Figure 5.16 A, 5.17 A and 5.18 A). Aspartate was produced until between day 5 and 9 of culture, after which the aspartate response indicated a net utilisation of the amino acid in the high producing transfectants. No significant differences were observed in the aspartate response for the early generation cell line 15 transfectants (Figure 5.16 A). However, the high producer (15-2) was observed to have significantly greater intracellular aspartate on day 7 of culture (Figure 5.19 A). The data suggest that the late generation transfectant 15-4 and transfectant 19-11, low producers, continued to produce aspartate for the entire culture period (Figure 5.17 A, 5.18 A and 5.19 A). Asparagine was detected in the basal medium samples (Figure 5.16 B, 5.17 B, 5.18 B and 5.19 B). Additionally, an undisclosed quantity of asparagine was present in the nutrient feed (personal communication from Diane Hatton). All of the transfectants consumed asparagine. The relative asparagine response data suggest that most of the transfectants utilised all of the asparagine available in the cell culture medium. However, the asparagine response for the late generation transfectant 15-4 remained above 17% for the duration of the fed-batch culture (Figure 5.17 B).

Aspartate production and consumption has been observed in DXB-11 cells, where aspartate consumption coincided with asparagine depletion (Fomina-Yadlin et al. 2014). Here, aspartate consumption was also observed to coincide with asparagine depletion. The late generation transfectant 15-4, which showed no evidence of aspartate consumption did not deplete all the available asparagine. Dean and Reddy identified that asparagine can fuel the citric acid cycle through conversion to aspartate (Dean & Reddy 2013). They also reported that this process was linked to cellular proliferation. This suggests that the utilisation of aspartate and asparagine observed in the present study was linked to cell growth and not productivity. Further support of this comes from work by Sellick et al. who found VCD_{max} to be greatest in GS-CHO cells that were supplemented with a feed containing aspartate and asparagine (Sellick et al. 2011).

As expected, glutamine was not detected in the basal medium samples; however glutamine was produced during the fed-batch cultures (Figure 5.16 C, 5.17 C and 5.18 C). On days 7 and 9 the relative glutamine response was significantly greater for the early generation transfectant 15-2 compared to 15-4 (Figure 5.16 C and 5.19 C). The relative glutamine responses for the late generation transfectant 15-4 and early generation 19-11 were observed to be greater than for their comparable high producers (Figure 5.17 C, 5.18 C and 5.19 C). These low producing transfectants had poor growth properties compared to the high producers (Table 5.1). Furthermore, the early generation transfectant 15-2 had a significantly greater doubling time than transfectant 15-4 (Table 5.1). Similarly to asparagine, glutamine can be used to fuel the citric acid cycle during proliferation (Dean & Reddy 2013), thus the transfectants with poor growth properties may have utilised less glutamine as a result of decreased citric acid cycle flux. A similar finding was also highlighted in the lactate utilisation data (Section 5.3.1). In Section 4.3.4, the cell line 19 transfectants were observed to have slower rates of glutamine production despite having greater GS activity (Section 4.3.5). It was predicted that the cell line 19 transfectants were more reliant on glutamine than the cell line 15 transfectants. The glutamine GC-MS data suggest that extracellular glutamine accumulates later in fed-batch culture for the cell line 19 transfectants than for the cell line 15 transfectants, thus supporting this hypothesis. The use of stable isotopes would allow further investigation into the metabolic pathways of glutamine utilisation in these transfectants (Dean & Reddy 2013).

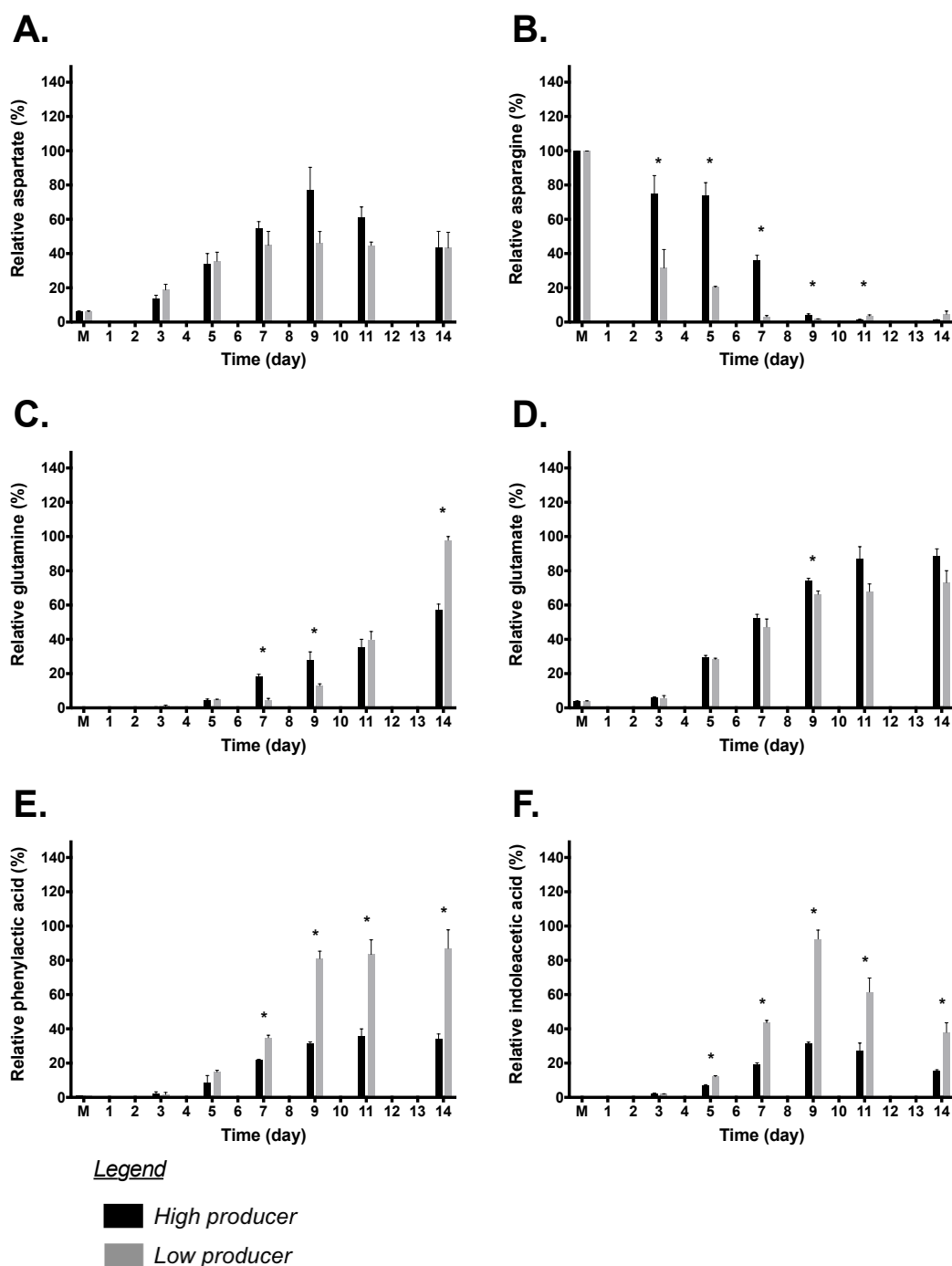
The relative glutamate response increased throughout the fed-batch cultures for all of the transfectants (Figure 5.16 D, 5.17 D and 5.18 D). The majority of the glutamate data analysed shows no significant difference between the transfectants. However, the data indicate that the low producing cell line 19 transfectants had significantly greater intracellular glutamate on day 7 of culture (Figure 5.19 D). The trends observed in the glutamate data were similar for all transfectants. The nutrient feed used in this study contained a source of glutamate (personal communication from Diane Hatton). The accumulation of glutamate observed is likely to be an effect of feed addition; this suggests that the feed can be further optimised to contain a lower concentration of glutamate.

Phenylactic acid and indoleacetic acid were not detected in the basal medium samples and were produced during fed-batch culture for all transfectants (Figure 5.16 E and F, 5.17 E and F, 5.18 E and F). The phenylactic acid relative response was significantly greater in transfectant 15-4 at both generations for the majority of the culture period when compared to transfectant 15-2 (Figure 5.16 E and 5.17 E). This was also reflected in the

intracellular metabolite data (Figure 5.19 E). In contrast to this, the phenylactic acid response was greater in the high producing transfectant 19-3 at the early generation when compared to transfectant 19-11 (Figure 5.18 E). No significant difference was detected in the intracellular phenylactic acid data for the cell line 19 transfectants (Figure 5.19 E). Similarly, a significantly greater response for indoleacetic acid was observed in low producing cell line 15 transfectant, 15-4 when compared to transfectant 15-2 (Figure 5.16 F and 5.17 F). The opposite was observed for the early generation cell line 19 transfectants (Figure 5.18 F). However, the intracellular metabolite data suggested that indoleacetic acid was elevated in all of the low producing transfectants on day 7 of culture (Figure 5.19 F).

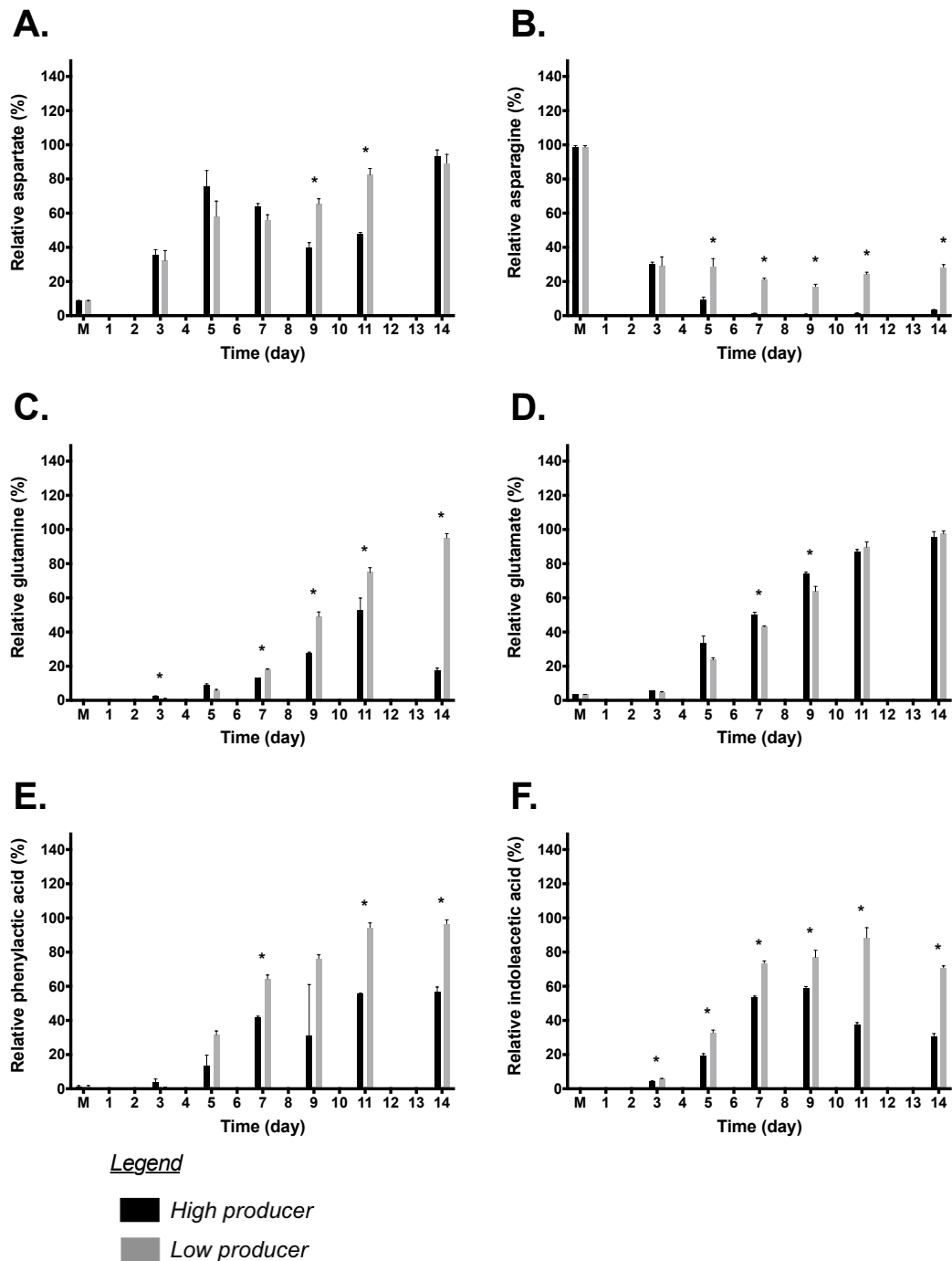
Phenylactic acid is a derivative of phenylalanine that has been identified in the plasma of human patients with phenylketonuria and end-stage renal failure (Clemens et al. 1990; Jankowski et al. 2003). Indoleacetic acid is a derivative of tryptophan and had been reported to accumulate in human patients with chronic kidney disease (Won et al. 2011; Boelaert et al. 2013). Neither of these metabolites have previously been reported to be related to growth or productivity in CHO cells. However in this study, both of these amino acid derivatives were observed to be elevated in the cell line 15 low producing transfectants. The intracellular data indicated that both metabolites were also elevated in the cell line 19 low producing transfectants, however the difference was not significant. The extracellular cell line 19 data showed significantly greater responses for these metabolites in the high producing transfectant samples, however this could be related to the difference in cell number during fed-batch culture. The data in this study suggest that these metabolites could be biomarkers relating to poor productivity.

Figure 5.16 Analysis of extracellular amino acids and derivatives for early generation cell line 15 transfectants during fed-batch culture



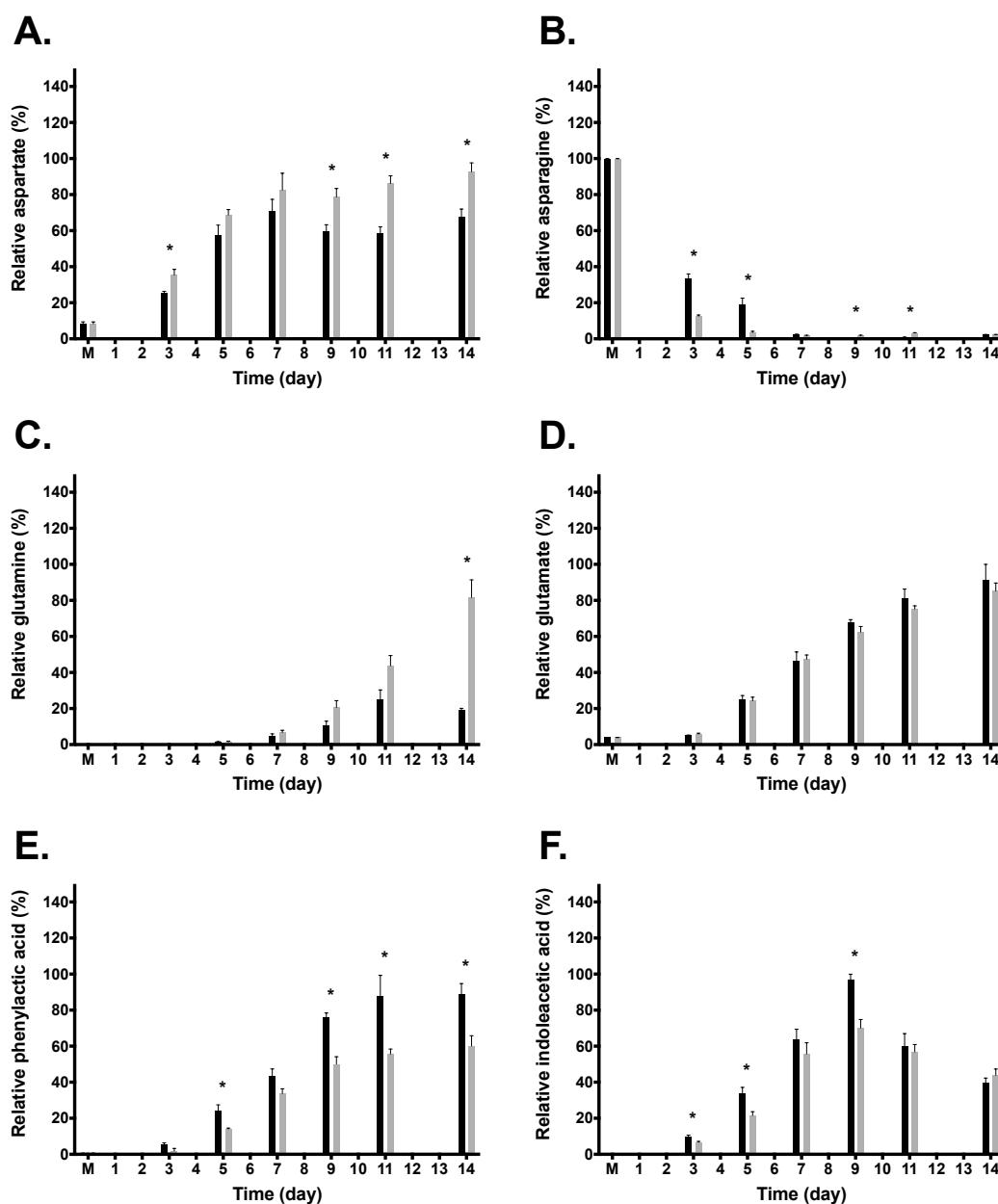
Early generation transfectant 15-2 (high producer) and 15-4 (low producer) were grown in fed-batch culture as previously described (Figure legend 5.1). Medium (M) and cell culture supernatant samples were analysed using GC-MS (Section 2.4.2). The charts show the relative percentage of aspartate (A), asparagine (B), glutamine (C), glutamate (D), phenylactic acid (E) and indoleacetic acid (F). Error bars represent SEM for three biological replicates. * indicates $p < 0.05$, using independent samples t-test to compare the high producing transfectant to the low producing transfectant.

Figure 5.17 Analysis of extracellular amino acids and derivatives for late generation cell line 15 transfectants during fed-batch culture



Late generation transfectant 15-2 (high producer) and 15-4 (low producer) were grown in fed-batch culture as previously described (Figure legend 5.1). Medium (M) and cell culture supernatant samples were analysed using GC-MS (Section 2.4.2). The charts show the relative percentage of aspartate (A), asparagine (B), glutamine (C), glutamate (D), phenylactic acid (E) and indoleacetic acid (F). Error bars represent SEM for three biological replicates. * indicates $p < 0.05$, using independent samples *t*-test to compare the high producing transfectant to the low producing transfectant.

Figure 5.18 Analysis of extracellular amino acids and derivatives for early generation cell line 19 transfectants during fed-batch culture

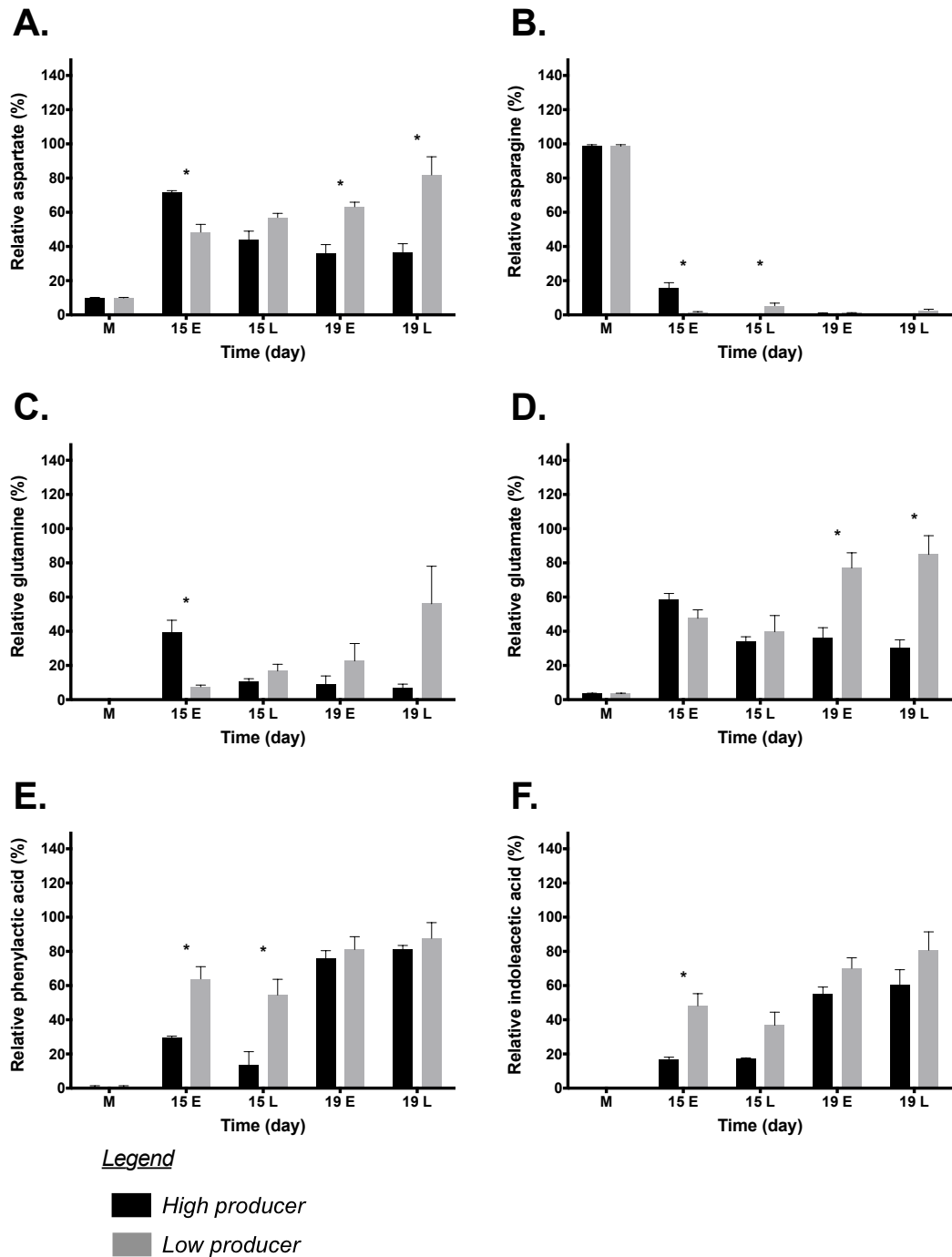


Legend

- High producer
- Low producer

Early generation transfectant 19-3 (high producer) and 19-11 (low producer) were grown in fed-batch culture as previously described (Figure legend 5.1). Medium (M) and cell culture supernatant samples were analysed using GC-MS (Section 2.4.2). The charts show the relative percentage of aspartate (A), asparagine (B), glutamine (C), glutamate (D), phenylactic acid (E) and indoleacetic acid (F). Error bars represent SEM for three biological replicates. * indicates $p < 0.05$, using independent samples t-test to compare the high producing transfectant to the low producing transfectant.

Figure 5.19 Analysis of intracellular amino acids and derivatives for early and late generation cell line 15 and 19 transfectants during fed-batch culture



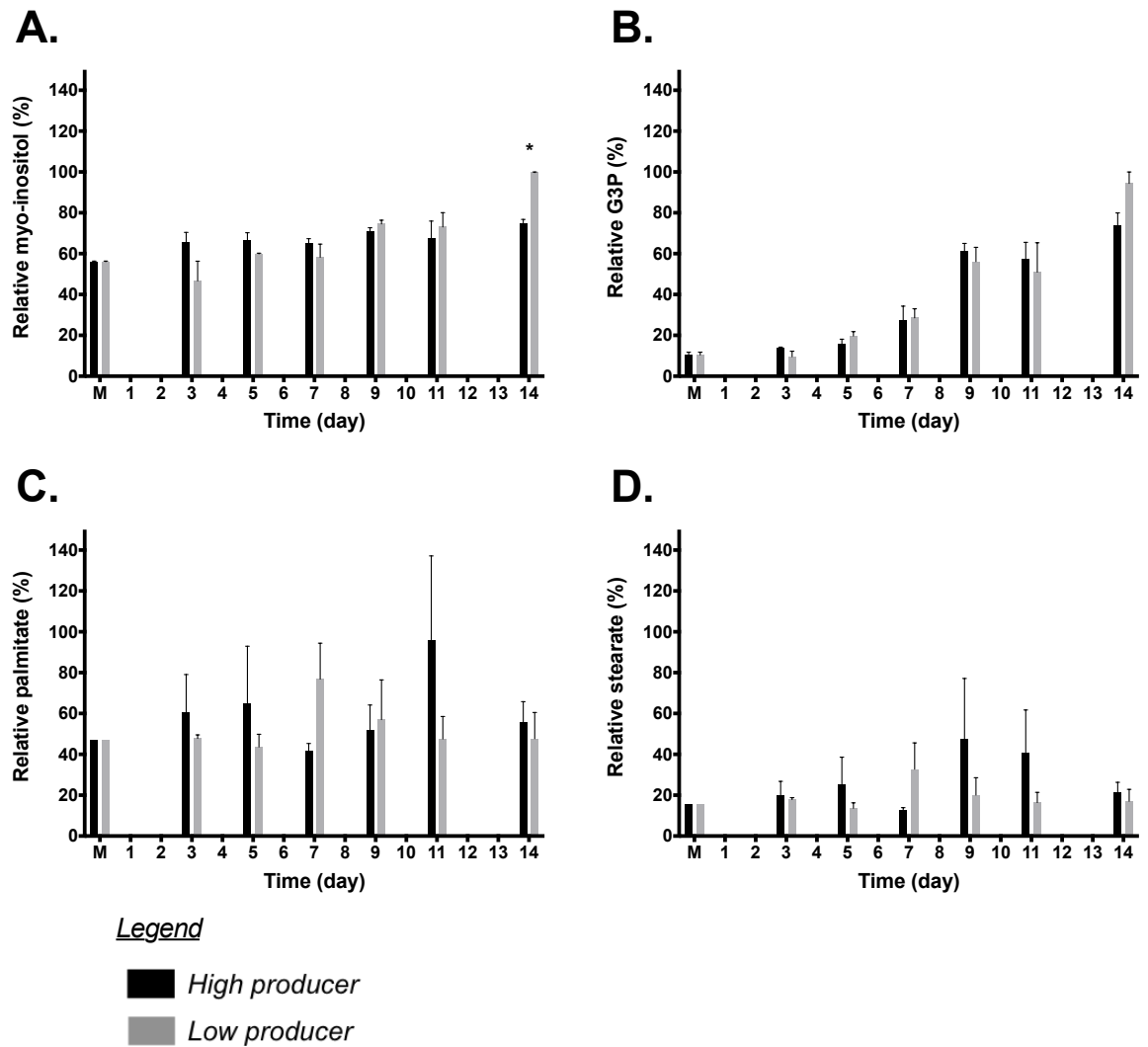
Early generation (E) and late generation (L) transfectants 15-2, 19-3 (high producers) and 15-4, 19-11 (low producers) were grown in fed-batch culture as previously described (Figure legend 5.1). CD-CHO medium (M) and intracellular metabolite extracts were prepared on day 7 of culture and analysed using GC-MS (Section 2.4.2). The charts show the relative percentage of aspartate (A), asparagine (B), glutamine (C), glutamate (D), phenylactic acid (E) and indoleacetic acid (F). Error bars represent SEM for three biological replicates. * indicates $p < 0.05$, using independent samples t -test to compare the high producing transfectant to the low producing transfectant.

5.3.4 Lipid synthesis

Four metabolites were identified which are associated with lipid synthesis (myo-inositol, glycerol 3-phosphate, palmitate and stearate). The relative myo-inositol response was observed to increase over the duration of fed-batch culture for all of the transfectants (Figure 5.20 A, 5.21 A and 5.22 A). A significant difference in extracellular myo-inositol response was only observed for the cell line 15 transfectants on day 14 of culture, the data was conflicting between the early and late generation. The intracellular data (Figure 5.23 A) provided evidence that the transfectants with the poorest growth properties (Table 5.1) had significantly greater amounts of myo-inositol. The glycerol 3-phosphate (G3P) response was also observed to increase during fed-batch culture (Figure 5.20 B, 5.21 B and 5.22 B). The G3P response was significantly greater between days 5-9 of culture for the late generation transfectant 15-2 (Figure 5.21 B), however this was contradicted by the intracellular data (Figure 5.23 B). Similarly to the myo-inositol data, the intracellular G3P data suggest that the transfectants with the poorest growth properties had the greatest amounts of G3P (Figure 5.23 B).

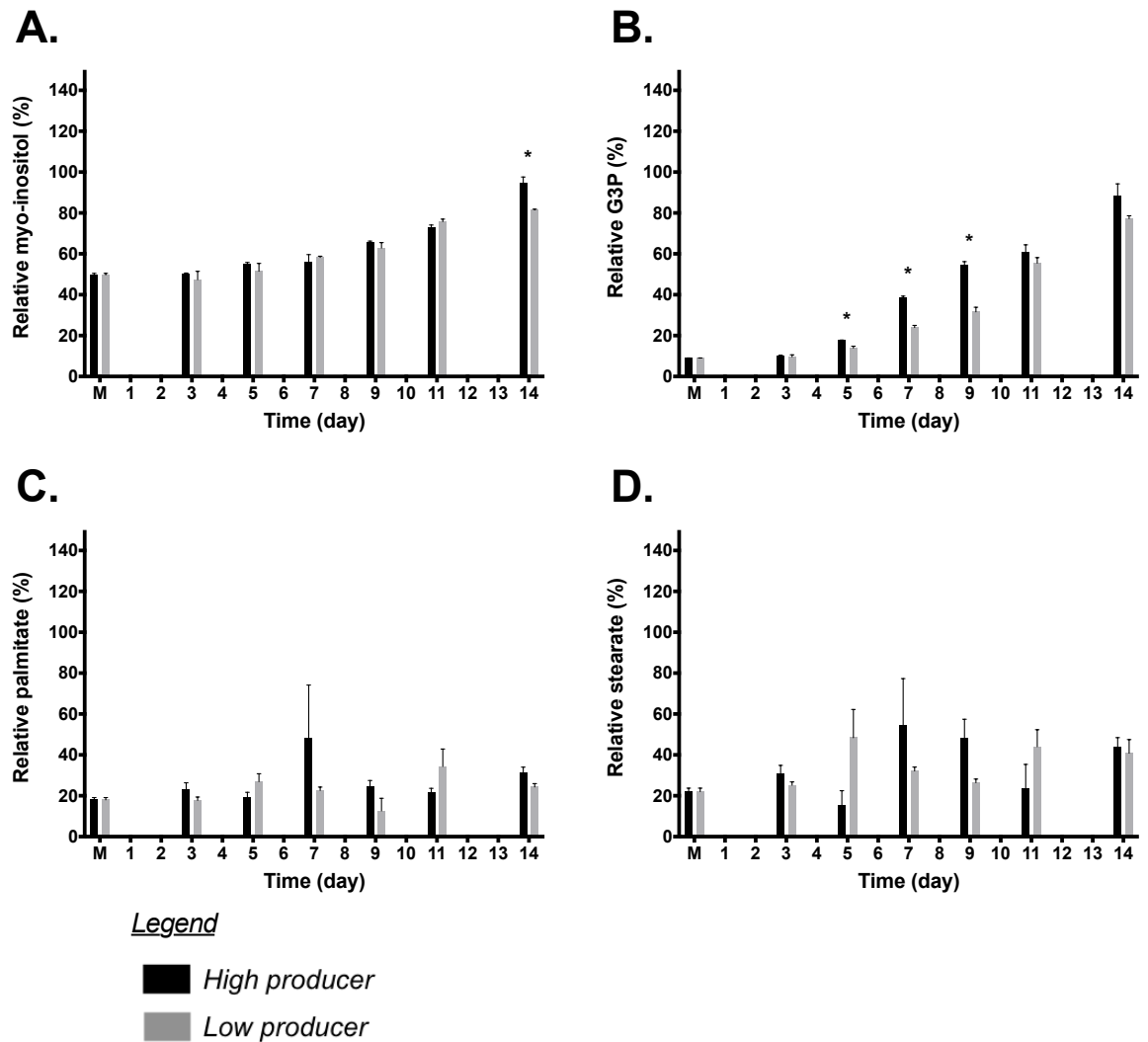
Palmitate and stearate were both detected in the GC-MS data (Figure 5.20 C and D, 5.21 C and D, 5.22 C and D, 5.23 C and D). A large standard error was observed for these metabolites and it is difficult to draw conclusions from the data.

Figure 5.20 Analysis of extracellular lipid-associated metabolites for early generation cell line 15 transfectants during fed-batch culture



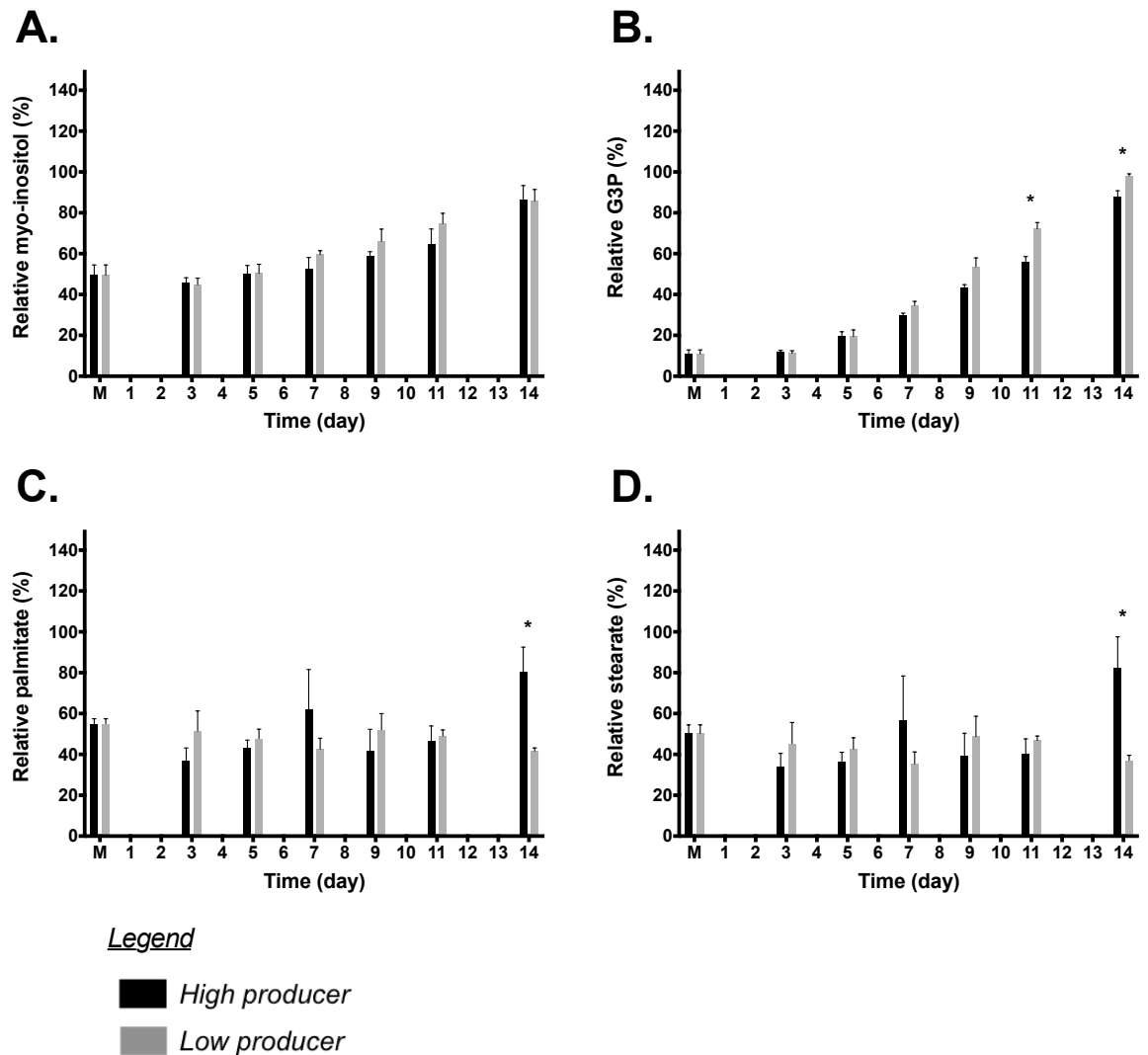
Early generation transfectant 15-2 (high producer) and 15-4 (low producer) were grown in fed-batch culture as previously described (Figure legend 5.1). Medium (M) and cell culture supernatant samples were analysed using GC-MS (Section 2.4.2). The charts show the relative percentage of myo-inositol (A), G3P (B), palmitate (C) and stearate (D). Error bars represent SEM for three biological replicates. * indicates $p < 0.05$, using independent samples t-test to compare the high producing transfectant to the low producing transfectant.

Figure 5.21 Analysis of extracellular lipid-associated metabolites for late generation cell line 15 transfectants during fed-batch culture



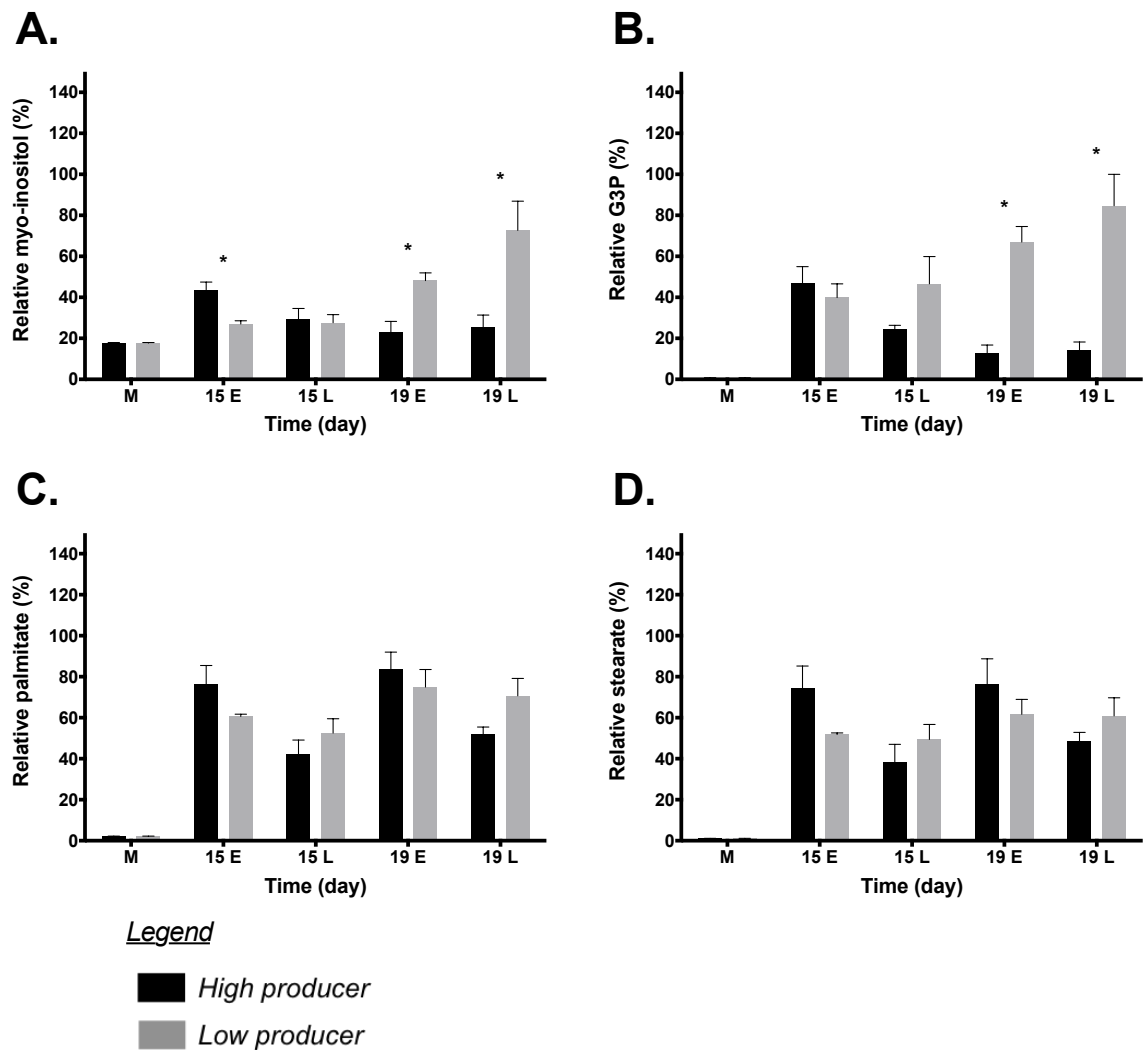
Late generation transfectant 15-2 (high producer) and 15-4 (low producer) were grown in fed-batch culture as previously described (Figure legend 5.1). Medium (M) and cell culture supernatant samples were analysed using GC-MS (Section 2.4.2). The charts show the relative percentage of myo-inositol (A), G3P (B), palmitate (C) and stearate (D). Error bars represent SEM for three biological replicates. * indicates $p < 0.05$, using independent samples t-test to compare the high producing transfectant to the low producing transfectant.

Figure 5.22 Analysis of extracellular lipid-associated metabolites for early generation cell line 19 transfectants during fed-batch culture



Early generation transfectant 19-3 (high producer) and 19-11 (low producer) were grown in fed-batch culture as previously described (Figure legend 5.1). Medium (M) and cell culture supernatant samples were analysed using GC-MS (Section 2.4.2). The charts show the relative percentage of myo-inositol (A), G3P (B), palmitate (C) and stearate (D). Error bars represent SEM for three biological replicates. * indicates $p < 0.05$, using independent samples *t*-test to compare the high producing transfectant to the low producing transfectant.

Figure 5.23 Analysis of intracellular lipid-associated metabolites for early and late generation cell line 15 and 19 transfectants during fed-batch culture



Early generation (E) and late generation (L) transfectants 15-2, 19-3 (high producers) and 15-4, 19-11 (low producers) were grown in fed-batch culture as previously described (Figure legend 5.1). CD-CHO medium (M) and intracellular metabolite extracts were prepared on day 7 of culture and analysed using GC-MS (Section 2.4.2). The charts show the relative percentage of myo-inositol (A), G3P (B), palmitate (C) and stearate (D). Error bars represent SEM for three biological replicates. * indicates $p < 0.05$, using independent samples t-test to compare the high producing transfectant to the low producing transfectant.

5.4 Summary

The objectives of this Chapter were:

- To assess the effect of chromosome number and recombinant gene copy number on productivity
- To identify metabolic markers that related to productivity

The results of this Chapter demonstrate that chromosome number was not linked to productivity. The broad range of chromosome numbers observed was consistent with previous reports and shows that GS-CHO cells survive outside the modal values. Further to this, recombinant gene copy number was not found to be a major determinant of productivity. However, further investigation, such as bisulphite sequencing, into the genomic environment of the recombinant genes could uncover the mechanism of differential mRNA expression observed in Chapter 4. There was evidence (Section 5.2.3) that copy number loss is a factor in decreased specific productivity over time in the non-amplified CHO transfectants; although the genomic environment and epigenetic modification could also be an influence on specific productivity over time.

Metabolomic analysis of the transfectants identified metabolites that were significantly different between the high producers and low producers. Standard curves could be produced for defined metabolites to enable full-quantitation of these metabolites in experimental samples. This would enable data to be analysed in relation to cell density, rather than as relative responses. Differences in the growth properties of the transfectants studied had an impact on the interpretation of the data; a refinement to this experimental approach could be to use an inducible system for mAb expression, although this would not guarantee similar growth rates in the induced and non-induced transfectants (J. Jones et al. 2005). The metabolites sorbitol, threitol, phenylactic acid and indoleacetic acid were identified as being related to productivity; these metabolites were increased in the metabolite profiles of the low producing transfectants.

6. Overall Discussion

6.1 Overall Discussion

The results in this thesis have been presented in three chapters, with discussion alongside. The overall aim of the work presented in this thesis was to gain an improved understanding of CHO cell phenotypic variability and identify metabolic parameters that relate to productivity. Enhancing this area of research could identify tools for the selection of desirable host cell lines and identify new targets for feed optimisation and cell line engineering in biopharmaceutical industry.

The specific objectives of this project were:

1. Analyse phenotypic variability of a panel of clonal host cell lines derived from a non-clonal population.
2. Determine the variability of transfectants derived from clonal host cell lines in relation to a non-clonal host cell line.
3. Determine the response of transfectants to feed.
4. Assess the heritability of host cell line phenotype in transfectant populations.
5. Identify metabolic markers that are related to productivity.

In summary, the key findings of this study were:

Host and transfectant phenotypic variability

- Inter-clonal variability in average growth rate during long-term culture (LTC) was present within a panel of non-clonal host cell lines and their parental population.
- Variability was observed in the VCD_{max} and CCT of the clonal host cell lines in batch culture.
- Inter-clonal variability was observed in the ability of the host cell lines to downregulate GS protein abundance in the presence of L-glutamine.

- No inter-clonal variability was observed in mitochondrial mass. However, there was evidence of variability in the mitochondrial membrane potential.
- The growth rate of the host cell lines decreased during LTC. However, the average VCD_{max} increased by approximately 22% in the late generation clonal transfectants from cell lines 15 and 19. The average doubling time decreased in the late generation transfectants from cell lines 15 and 19, which suggested that the growth rate increased during LTC.

Relationships between phenotypic features

- In clonal hosts, slow growth rates were found to be associated with increased glucose consumption and lactate production rates than hosts with faster growth rates.
- Variability in mitochondrial membrane potential, as determined by Rh-123 fluorescence, correlated with growth rate and lactate production to glucose consumption rate ratios.
- Clonal host cell line GS specific activity was related to GS mRNA expression. However, this only accounted for 40% of the variability observed in specific activity. In the cell line 15 and 19 transfectants, only 25% of the observed GS specific activity variability was accounted for by GS mRNA expression. This suggested that alternative mechanisms, e.g. translation and proteasomal degradation, accounted for up to 75% of the observed variability.
- In fed-batch culture, the late generation transfectants from cell lines 15 and 19 indicated a relationship between VCD_{max} and CCT with harvest titre and Q_p ; however, this was not observed in the early generation. Analysis of early generation mAb-109 mRNA expression suggested shared variation between Q_p and heavy chain mRNA (67%) and light chain mRNA expression (46%).
- Gene copy number and chromosome number were not found to be a major determinant of productivity.
- The following metabolites were identified with potential association to transfectant growth: glucose, lactate, pyruvate, citrate, aspartate, asparagine and glutamine.
- The following metabolites were identified with potential association to transfectant productivity: sorbitol, threitol, phenylactic acid and indoleacetic acid.

Transfectant response to feed

- Fed-batch culture of polyclonal pools prolonged the growth, stationary and decline phases of culture in comparison to batch cultures. This resulted in increased CCT, mAb titre and Qp.
- Feed additions increased the variability of the polyclonal pools (assessed by standard deviation), with respect to VCD_{max} , CCT, doubling time, titre and Qp (Table 4.1).

Heritable features

- Comparison of clonal host cell line and transfectant growth characteristics suggested heritability of growth characteristics.
- Evidence of Qp heritability was observed in the pool and clonal transfectants.
- Correlation between mitochondrial membrane potential and growth/lactate:glucose ratio were not observed for the transfectants in Section 5.2.4. However, there is evidence that mitochondrial membrane potential is a heritable phenotype as discussed in Section 5.2.4.

The findings listed above addressed the main aim and objectives of this thesis and have been discussed in more detail in each results chapter previously. A series of questions were identified during this study, which will be considered in the discussion below.

6.2 Phenotypic variability of clonally derived host cell lines.

It was hypothesised in Section 1.5 that, within a population, there are some cells that would be the 'best' or have the maximum potential in a cell line development process. Whilst there is no universal definition of what constitutes the 'best', cell lines that display a stable phenotype with low variability, robust proliferative capacity and the ability to achieve high recombinant protein titres would certainly be desirable. This thesis investigated the use of clonally derived host cell lines isolated from a non-clonal (heterogeneous) population. The data collected from these clonal host cell lines and subsequently derived transfectants provided insight into the phenotypic variance that occurs from a clonally derived CHO host cell line.

6.2.1 Do clonally derived CHO host cell lines display inter-clonal variability?

Variability between clonally derived host cell lines (interclonal) was both expected and observed in this thesis. As discussed in Section 1.3.2, immortalised mammalian cells display phenotypic drift, and after fairly short periods of culture, clonal CHO cell lines can be considered heterogeneous populations (Barnes et al. 2006; Kim & Lee 2007b; Wurm 2013). Further to this, karyology studies of CHO-K1 have shown a distribution of chromosome numbers per cell (as reviewed by Wurm 2013), which supports the expectation of a variety of distinct phenotypes in a non-clonal population. Despite this inherent variability, only a small number of publications have focused on the host cell phenotype prior to transfection with a gene of interest (Prentice et al. 2007; X. Liu et al. 2010; Davies et al. 2013; O'Callaghan et al. 2015).

The host cell lines studied in this thesis were grown in LTC and growth rates were determined for each host cell line (Section 3.2.1). The growth rate of the non-clonal host was in between the growth rate values of the clonal host cell lines, which displayed both faster and slower rates of growth. Significant differences in average cell diameter were also observed between the clonal host cell lines (Section 3.2.1), however the non-clonal host cell line had the greatest average diameter.

Batch cultures of the clonal and non-clonal host cell lines showed further evidence of inter-clonal variability (Section 3.2.2). A negative correlation was found between the doubling time of the clonal and non-clonal hosts in batch culture (Table 3.3) and the quarter 1 average growth rate during LTC (Table 3.1). Additionally, variation was observed in the VCD_{max} and CCT achieved by each clonal and non-clonal host cell line in batch culture (Table 3.3). This data suggested that clonal host cell lines can be screened to identify new production hosts with desirable growth phenotypes. With reference to the hypothesis in Section 6.2, identifying the 'best' clonal cell line from growth characteristics alone is not a simple task. In Chapter 3, host cell line 21 was observed to achieve the greatest VCD_{max} and CCT. However, the stationary phase of culture for this cell line had a duration of approximately 1 day. Comparatively, host cell line 15, which achieved lower VCD_{max} and CCT, had a stationary phase lasting approximately 4 days. Stationary phase has been associated with high Q_p (Templeton et al. 2013). Considering this, cell lines capable of the greatest cell density and CCT may not result in the greatest recombinant protein yields. In this study, the fed-batch cell line 16 pool (Table 4.2) and cell line 19 pools (Table 4.1 and 4.2) had greater final mAb titres than the fed-batch cell line 21 pools, which had the greatest VCD_{max} and CCT (Table 4.1 and 4.2). This could be associated

nutrient depletion in the cell line 21 pool cultures, as the growth profiles of the cell line 21 pools showed a precipitous decline in viability before the end of the 14 day culture period (Figure 4.3 and 4.5) and shorter stationary phases than the cell line 16 and 19 pools (Figure 4.3 and 4.5).

Interclonal variability was also identified in nutrient utilisation (Section 3.3). Figure 3.4 and 3.6 showed that host cell line 21 batch cultures depleted available glucose and glutamine more rapidly than the other host cell lines. This nutrient limitation may have contributed to the relatively short stationary phase of host cell line 21 (Sellick et al. 2011). In a production process, this could increase costs due to the optimised feed requirements needed to sustain the stationary phase. Additionally, the high VCD_{max} and high nutrient demands of cell line 21, indicate difficulty to control dissolved O_2 , CO_2 and pH in a bioreactor production process, in which process robustness is critical for predicting costs and product supply (Porter et al. 2010). Despite the relatively rapid depletion of these nutrients, host cell line 21 had the lowest utilisation rates of glucose, lactate, glutamine and glutamate $cell^{-1}$ (Section 3.3).

Significant differences in the abundance/specific activity of GS were observed between the host cell lines (Section 3.4.1). This was correlated with endogenous mRNA expression, however mRNA expression only explained 40% of the variation in specific activity. Comparison of the clonal and non-clonal hosts grown in the presence and absence of L-glutamine suggested that the ability to downregulate GS in the presence of L-glutamine was not consistent between them. However in the absence of L-glutamine, the variation in GS protein abundance was decreased. Huang et al. previously reported that proteasomal degradation is involved in the regulation of the GS protein (Huang et al. 2007). Proteasomal degradation is an ATP-dependent process (Haas et al. 1982; Liu et al. 2006). By extension, the ATP synthetic capacity of the clonal host cell lines may influence the regulation of GS protein abundance. Rh-123 analysis of the clonal and non-clonal host cell lines (Section 3.5) suggested that clonal hosts 16 and 19 had the least negative mitochondrial membrane potential thus limiting ATP synthesis (Baracca et al. 2003). This could be linked to the relatively high abundance of GS protein observed in the presence of glutamine. Additionally, in batch culture, clonal hosts 16 and 19 had the longest doubling times, lowest VCD_{max} and lowest CCT. These properties could also be linked to a poor synthetic capacity for ATP production. Clonal host cell line 21 also retained a relatively high GS abundance in the presence of L-glutamine, whilst Rh-123 staining suggested this host had the most negative mitochondrial membrane potential (Section 3.5). This contradicts the interpretation that ATP availability is critical for GS

degradation. However, clonal host 21 was found to have the greatest GS mRNA abundance. Furthermore, the relatively high growth rate (Section 3.2.1) of this host could contribute to a significant drain on available ATP (Mulukutla et al. 2010).

6.2.2 Do clonal host cell lines give rise to transfectants that display less phenotypic variability than the non-clonal host cell line?

Analysis of the clonally derived host cell lines showed that interclonal variability was present across the parameters studied (Chapter 3 and Section 6.2.1). Characterisation of the phenotypic output of these hosts may enable host clone selection based on its suitability for a production process. It may be hypothesized that the use of clonally derived host cell lines will result in transfectants that display less intra-clonal variability than the non-clonal host, however previous studies suggest that clonally derived cell lines rapidly become heterogeneous (Barnes et al. 2006; Kim & Lee 2007b; Davies et al. 2013; Wurm 2013).

The pools generated from transfection round 1 (Section 4.2.1) were analysed in batch and fed-batch culture for VCD_{max} , CCT, doubling time, titre and Q_p . Intra-clonal variability was assessed by the standard deviation of these parameters (Table 4.1). The cell line NC pools showed the greatest intra-clonal variability with respect to harvest titre in batch culture. As discussed in Section 4.2.1, the data suggested that the pools derived from some clonal hosts were less variable than the cell line NC pools in some parameters i.e. VCD_{max} , CCT, harvest titre and Q_p . However, this was not consistent for all of the pools derived from the clonal hosts and the cell line NC pools were the least variable with respect to fed-batch doubling time. The analysis of the transfection round 1 pools did not support the hypothesis that the use of clonal host cell lines results in transfectants that display less intra-clonal variability than the non-clonal host. In addition to the transfection round 1 pool data, the 96-well and 24-well plate static titres of 60 single colony transfectants from transfection round 2 (Figure 4.6) did not support the hypothesis in this discussion. The transfectants derived from host cell line NC showed the least variability at the 24-well plate stage. There are other sources of variation that contribute to the phenotype; these are discussed in the subsequent sections.

6.2.3 What defines the phenotype of a cell line and is it stable?

The phenotype of an organism or cell can be influenced by the genotype, environment and environmental interactions. The cell culture conditions in this study controlled the

environment of the hosts and transfectants by the use of a chemically defined medium, consistent feed formulation, CO₂ and temperature regulated incubator, defined seeding density and a routine subculture schedule. The genotype and environmental interactions were not controlled.

Genomic fluidity in immortalised cell lines has been reported (Hsu 1961; Wurm 2013) and this 'fluidity' is also a feature of CHO cell lines (Deaven & Petersen 1973; Cao et al. 2011). Furthermore, as discussed in Section 1.3.3 the CHO cells have been described as having a mutator phenotype (Davies et al. 2013).

Clonal host cell lines 15 and 19, in addition to high and low producing transfectants, were analysed for chromosome number (Section 5.2.2). The broad range of chromosome numbers observed (13-22) supported previous observations (Deaven & Petersen 1973; Wurm 2013) and suggested that genotype inconsistencies may account for some of the phenotypic variability observed in this study. Karyology analysis of CHO DG44 cells determined that aneuploidy, deletions and complex rearrangements of the chromosomes were prevalent (Derouazi et al. 2006). These chromosomal aberrations are likely ubiquitous amongst all CHO cell lines (Wurm 2013). Whole genome sequencing of the clonal cell lines and transfectants would enable a quantitative analysis of genotype variability that is relatable to the phenotypic output. Whilst this was not practicably feasible within this project, several CHO genomes, including CHO K1, have been recently published (Xu et al. 2011; Lewis et al. 2013). Analysis of this data highlighted 25,711 structural variations, including 13,735 insertions and 11,976 deletions compared to the *C. griseus* genome. However, there was a 99% overlap in the annotated genes (Lewis et al. 2013). This suggested that despite the numerous rearrangements observed in CHO cells, much of the gene content is conserved, suggesting a relatively stable genotype. However, chromosomal aberrations may alter the genomic environment of these genes and further genomic variability was identified between multiple CHO lineages. More than 3 million single nucleotide polymorphisms were identified in addition to indels and copy number variations (Lewis et al. 2013). This genomic variability is likely to impact the host and transfectant phenotype and is likely not stable within a population.

Transfection of a host cell line is another source of genomic variability as recombinant DNA is randomly integrated into the host genome (Section 1.2.2). Random integration has the potential to disrupt endogenous genes causing alterations in the phenotype of the transfectant (Derouazi et al. 2006). Gene expression can be further regulated by epigenetic modification, a process that is crucial for development, differentiation and

imprinting in wild-type organisms (Jones & Baylin 2007; Kouzarides 2007). However in cancer cells, epigenetic modification (DNA methylation and covalent histone modification) could become deregulated, silencing genes which alter the phenotype and causing a disease state (Jones & Baylin 2007). Epigenetics have been shown to affect phenotypic diversification in both clonal human cell lines (Neildez-Nguyen et al. 2008) and clonal CHO cell lines (Kim et al. 2011) and may contribute to a continuous phenotypic drift. Epigenetic modifications have been linked with mAb production instability in recombinant CHO cell lines (Chusainow et al. 2009; Kim et al. 2011). Kim et al. identified a CpG island within the CMV promoter sequence, commonly used in recombinant CHO cell lines which may enhance transgene silencing (Kim et al. 2011) in combination with histone modification (Meilinger et al. 2009). In Chapter 4, the average Qp of the clonal cell line 15 and 19 transfectants increased between the early and late generation (Table 4.4), whilst in Chapter 5 decreased Qp was observed. Whilst it is unlikely that changes in gene copy number are causal to observed differences (Section 5.2.3), chromosomal aberrations (Section 5.2.2) and epigenetic modification may be associated with phenotypic drift.

6.3 Are phenotypic features of the host cell line heritable?

Heritability summarises how much variation is due to genetic factors (Wray & Visscher 2008). In light of research focused on phenotypic drift (Section 1.3.2 and 1.3.3) and the genetic fluidity of immortalised cell lines (Section 6.2.3), the question arises whether phenotype features of host cell lines are heritable? Phenotype heritability, would allow the development of a host cell line 'toolbox', in which each distinct host may possess desirable advantages amenable to a production process or format of recombinant protein (Davies et al. 2013; O'Callaghan et al. 2015).

Inter-clonal variability with respect to growth was observed between clonal and non-clonal hosts and transfectants at all stages of this study. However, evidence of heritability in growth characteristics was also observed. In batch culture, clonal host cell lines 15, 20 and 21 achieved the greatest VCD_{max} , whilst clonal host cell lines 16 and 19 achieved the lowest VCD_{max} and host cell line NC had a relatively average VCD_{max} (Table 3.3). This trend in VCD_{max} was also observed in the transfection round 1 pool data (Table 4.1). The cell line NC pools achieved greater than expected VCD_{max} and were an exception to this trend. However, as host cell line NC is non-clonal, this cell line would be assumed to have the greatest genetic diversity and population bottlenecks (sampling of the population i.e. subculture and cryopreservation) may have selected for cells with rapid proliferation rates (Campos & Wahl 2009; Davies et al. 2013). Similarities were also observed in the data

trends between the clonal and non-clonal hosts (Table 3.3) and transfection round 1 pools (Table 4.1) for CCT and doubling time. Relationships between the hosts (Table 3.3) were also observed when comparing to the transfection round 2 pools (Section 4.2.2). These relationships were assessed by correlation analysis; the results showed positive correlations but were not significant. As discussed in Section 4.2.2 and Section 5.2.1, the transfectants were cultured in the absence of L-glutamine which is likely to have had an influence on the growth rate of the transfectants, also the seeding density of transfectant (fed-) batch cultures was greater than the hosts. Also, the addition of feed can influence cell growth (Section 4.2) (Ma et al. 2009; Sellick et al. 2011). These key differences between host and transfectant cultures may explain the absence of significant growth parameter correlations. Long-term culture of the clonal transfectants derived from cell lines 15 and 19 (Section 4.3.2) also suggested that growth characteristics are heritable. Although variability was observed between the transfectants from each clonal host, the average growth rate (Figure 4.7), VCD_{max} , CCT and doubling time (Table 4.4) were inline with the previously discussed trends for the host cell lines. These observations are further supported by published findings of growth characteristic heritability in CHO cell lines (Konrad et al. 1977; Davies et al. 2013). Together, these findings suggested that a clonal host cell line 'toolbox' could be generated to enhance the probability of isolating transfectant cell lines with desired growth characteristics.

Clonal host cell lines that give rise to transfectants with predictable Q_p would be another advantage in a 'toolbox' of host cell lines. Q_p has previously been determined not to be heritable (Davies et al. 2013) and subject to stochastic variation (Pilbrough et al. 2009). Here, the average fed-batch Q_p observed in the transfection round 1 pools (Section 4.2.1) correlated significantly ($p < 0.05$) against the Q_p observed in the transfection round 2 pools (Section 4.2.2). This suggests that Q_p is heritable in early generation transfectants, however variation in this parameter was observed (Table 4.1). The conclusions of Davies et al, were based on the mAb titre of transiently transfected clonal host cell lines over a period of LTC, during this process population bottlenecks and (epi)genetic variations may have influenced the productivity of the cells (Davies et al. 2013); furthermore transient transfection may have influenced the productivity (e.g. differences in gene copy number taken up by the cells during the multiple transfections). More recent work, using a subset of the clonal hosts studied by Davies et al, found that stable transfection identified clones that consistently and significantly outperformed the non-clonal population at an early generation with respect to mAb product titre (O'Callaghan et al. 2015). In this study, analysis of clonal transfectants found the cell line 19 transfectants had a greater average Q_p when compared to the cell line 15 transfectants. This inter-clonal difference was also

observed in the pool transfectants and again supports the conclusion that specific productivity is heritable from a clonal host cell line. However, variability in Qp was observed between early generation and late generation clonal transfectants (Table 4.4 and Table 5.1). Thus, the data suggest that whilst the use of clonal hosts can enhance the probability of isolating transfectants with desirable Qp, the stability of this parameter over LTC may still be influenced by (epi)genetic drift (Neildez-Nguyen et al. 2008; Pilbrough et al. 2009; Pichler et al. 2010; Davies et al. 2013; Wurm 2013). In this study, gene copy number was not found to be a major determinant of Qp between early and late generation fed-batch cultures (Section 5.2.3). However, significant correlations were observed between mAb mRNA expression and Qp in early generation transfectants (Section 4.3.3). Analysis of late generation transfectant mAb mRNA expression would provide further evidence of epigenetic silencing of the transgene (Kim et al. 2011; Osterlehner et al. 2011).

The mitochondrial membrane potential was found to correlate with the lactate:glucose ratio and growth rate of the clonal and non-clonal host cell lines (Section 3.5), and has been found to report on specific glucose and lactate rates in hybridoma and CHO DG44 cell lines (Borth et al. 1993; Hinterk rner et al. 2007). These findings suggest that Rh-123 staining could be a useful tool for identifying metabolically efficient (with respect to glucose and lactate) clonal cell lines that are capable of rapid proliferation. However in Section 5.2.4, Rh-123 fluorescence in the transfectants did not correlate with growth properties (VCD_{max} and CCT) or the lactate:glucose ratios (Figure 5.5). It is possible that glutamine-free culture (Ahmad et al. 2001) and overexpression of the GS gene may have influenced the mitochondrial membrane potential, however the data also suggest that the membrane potential could be heritable. Mitochondria are semi-autonomous, containing their own genome (mtDNA); this encodes 13 polypeptides crucial for the electron transport chain and 24 RNA molecules necessary for intra-mitochondrial protein synthesis (Capps et al. 2003; Xing et al. 2008). Variations in mtDNA copy number has shown in human cancer and leukocyte cells (Lee et al. 2006; Gemma et al. 2006; Tiao et al. 2007; Mizumachi et al. 2008; Xing et al. 2008), and the copy number can be related to the energy demands of the cell (Capps et al. 2003; Lee et al. 2006). Xing et al, conducted studies on human twins and concluded the heritability of mtDNA to be 65% (Xing et al. 2008). Instability and decreased mtDNA copy number in human cancer cell lines has been linked to impaired oxidative phosphorylation (Lee et al. 2006). Impaired mitochondrial function in cancer cells can cause increased rates of glycolysis, known as the Warburg effect (Warburg 1956), and this may explain the relatively high rates of cell specific glucose consumption and lactate production observed in hosts 16 and 19 (Section 3.3).

Analysis of clone specific mtDNA copy number may further support this, and the use of Rh-123 assays as a tool for host clone selection.

6.4 Can metabolic markers be identified that relate to productivity?

Significant differences were determined in the metabolite profiles (Section 5.3) of high and low producing (Table 5.1) transfectants derived from two clonal host cell lines. As discussed in Section 5.3, the metabolites glucose, lactate, pyruvate, citrate, aspartate, asparagine and glutamine were all determined to be most strongly associated with transfectant growth. These interpretations are supported by previous studies (Tsao et al. 2005; Sellick et al. 2011; Dietmair et al. 2012; Dean & Reddy 2013; Templeton et al. 2013; Young 2014).

Sorbitol, threitol, phenylactic acid and indoleacetic acid were all identified to have an increased relative concentration in low producing transfectants (Section 5.3). However, the differences in the growth and cell densities of the transfectants used in this study (Figure 5.1) are a confounding factor to interpretation of the data. As mentioned in Section 6.2.3, environmental interactions are a contributing factor to phenotype; it is reasonable to assume that the environmental interactions will differ between clonal transfectants that grow to high cell densities compared to clonal transfectants that grow to low cell densities, and that this may affect the metabolic phenotype. It is therefore not surprising that sorbitol has previously been associated with cell line growth rate (Dietmair et al. 2012), however in the study by Dietmair et al. productivity data was not reported.

To the best of my knowledge, threitol has not previously been associated with low productivity in CHO cells. The biosynthetic pathway for the production of this metabolite is not well studied in mammalian organisms, however a proposed pathway in *U. ceramboides* involves glucose-6-phosphate, ribulose-derivative and erythritol-derivative intermediates (Walters et al. 2009). These intermediates were not identified in the GC-MS data, potentially due to low concentration and rapid turnover. Stable isotope studies and metabolic flux analysis could further validate the pathway of threitol synthesis and its association with CHO cell phenotype (Young 2014; Dickson 2014).

Both phenylactic acid and indoleacetic acid were identified as having a greater relative concentration in the low producing phenotype. As discussed in Section 5.3.3, these metabolites have not previously been reported to be associated with growth or productivity. Chong et al. found the phenylalanine derivatives acetylphenylalanine and

glutamylphenylalanine were positively correlated with caspase activity, however addition of acetylphenylalanine to CHO cells did not cause an increase in caspase activation (Chong et al. 2011). They concluded that the detrimental effects could be cell line specific or limited to long-term exposure. Quantitation and further investigation into the effects of these metabolites would enable an enhanced understanding of their role in productivity and/or growth. The incidence of these metabolites in organisms with genetic diseases supports their abundance in the low producing clonal transfectants (Clemens et al. 1990; Jankowski et al. 2003; Won et al. 2011; Boelaert et al. 2013), however they could be a result of overfeeding phenylalanine and tryptophan which are supplied in the medium and feed (Chong et al. 2011).

The metabolites identified here which significantly differ in abundance in relation to growth and productivity add to a growing list of potential metabolic markers (Tsao et al. 2005; Sellick et al. 2011; Dietmair et al. 2012; Dean & Reddy 2013; Templeton et al. 2013; Ma et al. 2009; Young 2014). However, previous publications vary in the CHO clone, medium, feed, culture conditions and phenotype studied. Furthermore, a number of publications have failed to define the growth rate (Chong et al. 2012) or specific productivity (Dietmair et al. 2012) of the transfectants studied. Stringent control over extraneous parameters and increased application of metabolic flux analysis and bioinformatics modelling will enable novel engineering and culture optimisation strategies that may build upon currently achieved productivities (Dickson 2014; Young 2014).

6.5 Future work

Whilst addressing the questions in this Chapter some future investigations have been suggested.

Rh-123 staining was suggested as a tool for identifying metabolically efficient host cell lines, with an improved capacity for oxidative phosphorylation (Section 6.3). Further investigations to confirm this, would involve sequencing and copy number determination of clonal host cell line mtDNA. This may identify deleterious mutations in mitochondrial genes involved in the electron transport chain (Lee et al. 2006). This approach could be extended to early and late generation clonal transfectants to further define the heritability of mitochondrial phenotype and membrane potential. It would also be of interest to investigate the concentration of the energy intermediates ATP/ADP and NAD^+/NADH , to determine their relationship to mitochondrial function. As reviewed by Yoon et al. several approaches have been explored to engineer mitochondrial genomes as therapy for

heritable human mitochondrial metabolic diseases (Yoon et al. 2010). The group have shown potential for using non-replicating, invasive *E. coli* strains to introduce engineered mtDNA into the mitochondrial of living cells through bacterial conjugation *in vitro* (Yoon 2005; Yoon et al. 2010). This technology could be explored as a method for mitochondrial engineering in clonal CHO cell line.

Analysis of late generation mAb mRNA expression would help to determine the stability of the transgene expression during LTC. Further to this, it would be of interest to use bisulfite sequencing to determine DNA methylation of the recombinant genes. This would enable a determination of epigenetic silencing of the transgenes, and the effectiveness of the associated UCOE elements (Kristensen & Hansen 2009; M. Kim et al. 2011; Saunders et al. 2015).

The mAb produced by the transfectants in this thesis, represents an 'easy-to-express' molecule. As the variety of recombinant molecular formats expands (Section 1.1.1.3), some molecules have been observed as 'difficult-to-express' (Pybus et al. 2014; O'Callaghan et al. 2015). This represents challenges for product yield and product quality with respect to the ability of a clone to produce molecules with the correct glycosylation profile (O'Callaghan et al. 2015). It has been suggested that the ability of clonal transfectants to perform these post-translational modifications is highly variable and clone-specific (Davies et al. 2013; O'Callaghan et al. 2015), however these functional traits may be heritable (Davies et al. 2013; O'Callaghan et al. 2015). Extension of the work presented in this thesis, to include 'difficult-to-express' molecules and analyse product quality, could further define criteria for a clonal host cell line 'toolbox'.

Further metabolomic analysis of high and low producing transfectants is also suggested. Further investigations should include clones that exhibit similar growth characteristics; this would enable better extrapolation of metabolites that are related to cell specific productivity. The use of fully quantitative methodology would be of further benefit, and allow cell specific rates of metabolite utilisation to be determined. Finally, metabolic flux analysis and bioinformatics approaches to data analysis would enable the production of models that may allow for further feed optimisations and the identification targets for cell line engineering (Dickson 2014; Young 2014).

References

- Ahmad, S., White, C.W., Chang, L.Y., Schneider, B.K. & Allen, C.B. 2001. Glutamine protects mitochondrial structure and function in oxygen toxicity. *American journal of physiology. Lung cellular and molecular physiology*, 280(4), pp.L779–91.
- Ahn, W.S. & Antoniewicz, M.R. 2013. Parallel labeling experiments with [1,2-13C]glucose and [U-13C]glutamine provide new insights into CHO cell metabolism. *Metabolic Engineering*, 15, pp.34–47.
- Al-Rubeai, M. & Singh, R. 1998. Apoptosis in cell culture. *Current Opinion in Biotechnology*, 9(2), pp.152–156.
- Aranibar, N., Borys, M., Mackin, N.A., Ly, V., Abu-Absi, S., Neimitz, M., Schilling, B., Li, Z.J., Brock, B., Russell, R.J., Tymiak, A. & Reily, M.D. 2011. NMR-based metabolomics of mammalian cell and tissue cultures. *Journal of Biomolecular NMR*, 49, pp.195–206.
- Araten, D.J., Golde, D.W., Zhang, R.H., Thaler, H.T., Gargiulo, L., Notaro, R. & Luzzatto, L. 2005. A Quantitative Measurement of the Human Somatic Mutation Rate. *Cancer Research*, 65(18), pp.8111–8117.
- Arden, N. & Betenbaugh, M.J. 2006. Regulating apoptosis in mammalian cell cultures. *Cytotechnology*, 50(1-3), pp.77–92.
- Attolini, C.S.O. & Michor, F. 2009. Evolutionary Theory of Cancer. *Annals of the New York Academy of Sciences*, 1168(1), pp.23–51.
- Bacsi, S.G. & Wejksnora, P.J. 1986. Effect of increase in ploidy on the activation of nucleolar organizer regions in Chinese hamster ovary (CHO) cells. *Experimental cell research*, 165(1), pp.283–289.
- Baggetto, L.G. 1992. Deviant Energetic Metabolism of Glycolytic Cancer-Cells. *Biochimie*, 74(11), pp.959–974.
- Bahr, S.M., Borgschulte, T., Kayser, K.J. & Lin, N. 2009. Using microarray technology to select housekeeping genes in Chinese hamster ovary cells. *Biotechnology and Bioengineering*, 104(5), pp.1041–1046.
- Bailey, L.A., Hatton, D., Field, R. & Dickson, A.J. 2012. Determination of Chinese hamster ovary cell line stability and recombinant antibody expression during long-term culture. *Biotechnology and Bioengineering*, 109(8), pp.2093–2103.
- Baracca, A., Sgarbi, G., Solaini, G. & Lenaz, G. 2003. Rhodamine 123 as a probe of mitochondrial membrane potential: evaluation of proton flux through F₀ during ATP synthesis. *Biochimica et Biophysica Acta (BBA) - Bioenergetics*, 1606(1), pp.137–146.
- Barnes, L.M. & Dickson, A.J. 2006. Mammalian cell factories for efficient and stable protein expression. *Current Opinion in Biotechnology*, 17(4), pp.381–386.
- Barnes, L.M., Moy, N. & Dickson, A.J. 2006. Phenotypic variation during cloning procedures: Analysis of the growth behavior of clonal cell lines. *Biotechnology and Bioengineering*, 94(3), pp.530–537.

- Bebbington, C.R., Renner, G., Thomson, S., King, D., Abrams, D. & Yarranton, G.T. 1992. High-level expression of a recombinant antibody from myeloma cells using a glutamine synthetase gene as an amplifiable selectable marker. *Bio-Technology*, 10(2), pp.169–175.
- Beck, A., Cochet, O. & Wurch, T. 2010. GlycoFi's technology to control the glycosylation of recombinant therapeutic proteins. *Expert Opinion on Drug Discovery*, 5(1), pp.95–111.
- Beckman, R.A. & Loeb, L.A. 2005. Negative clonal selection in tumor evolution. *Genetics*, 171(4), pp.2123–2131.
- Beckmann, T.F., Krämer, O., Klausning, S., Heinrich, C., Thüte, T., Bütemeyer, H., Hoffrogge, R. & Noll, T. 2012. Effects of high passage cultivation on CHO cells: a global analysis. *Applied Microbiology and Biotechnology*, 94(3), pp.659–671.
- Bell, S., Bebbington, C.R., Scott, M.F., Wardell, N., Spier, R.E., Bushell, M.E. & Sanders, P.G. 1995. Genetic-Engineering of Hybridoma Glutamine-Metabolism. *Enzyme and Microbial Technology*, 17(2), pp.98–106.
- Betts, Z. & Dickson, A.J. 2015. Assessment of UCOE on Recombinant EPO Production and Expression Stability in Amplified Chinese Hamster Ovary Cells. *Molecular biotechnology*, 57(9), pp.846–858.
- Bhopale, G. & Nanda, R. 2005. Recombinant DNA expression products for human therapeutic use. *Current Science*, 89(4), pp.614–622.
- Birch, J.R. & Racher, A.J. 2006. Antibody production. *Advanced Drug Delivery Reviews*, 58, pp.671–685.
- Boelaert, J., Lynen, F., Glorieux, G., Eloot, S., Landschoot, M.V., Waterloos, M.A., Sandra, P. & Vanholder, R. 2013. A novel UPLC–MS–MS method for simultaneous determination of seven uremic retention toxins with cardiovascular relevance in chronic kidney disease patients. *Analytical and Bioanalytical Chemistry*, 405(6), pp.1937–1947.
- Borth, N., Kral, G. & Katinger, H. 1993. Rhodamine 123 fluorescence of immortal hybridoma cell lines as a function of glucose concentration. *Cytometry*, 14(1), pp.70–73.
- Boulianne, G.L., Hozumi, N. & Shulman, M.J. 1984. Production of functional chimaeric mouse/human antibody. *Nature*, 312(5995), pp.643–646.
- Brannigan, J.A. & Wilkinson, A.J. 2002. Protein engineering 20 years on. *Nature Reviews Molecular Cell Biology*, 3(12), pp.964–970.
- Brekke, O.H. & Sandlie, I. 2003. Therapeutic antibodies for human diseases at the dawn of the twenty-first century. *Nature Reviews Drug Discovery*, 2(1), pp.52–62.
- Brinkrolf, K. et al. 2013. Chinese hamster genome sequenced from sorted chromosomes. *Nature Biotechnology*, 31(8), pp.694–695.
- Brown, M.E., Renner, G., Field, R. & Hassell, T. 1992. Process development for the production of recombinant antibodies using the glutamine synthetase (GS) system. *Cytotechnology*, 9(1), pp.231–236.

- Büscher, J.M., Czernik, D., Ewald, J.C., Sauer, U. & Zamboni, N. 2009. Cross-platform comparison of methods for quantitative metabolomics of primary metabolism. *Analytical Chemistry*, 81(6), pp.2135–2143.
- Campos, P.R.A. & Wahl, L.M. 2009. The effects of population bottlenecks on clonal interference, and the adaptation effective population size. *Evolution; international journal of organic evolution*, 63(4), pp.950–958.
- Canatella, P.J., Karr, J.F., Petros, J.A. & Prausnitz, M.R. 2001. Quantitative Study of Electroporation-Mediated Molecular Uptake and Cell Viability. *Biophysical Journal*, 80(2), pp.755–764.
- Cao, Y., Kimura, S., Itoi, T., Honda, K., Ohtake, H. & Omasa, T. 2011. Construction of BAC-based physical map and analysis of chromosome rearrangement in chinese hamster ovary cell lines. *Biotechnology and Bioengineering*, 109(6), pp.1357–1367.
- Capps, G.J., Samuels, D.C. & Chinnery, P.F. 2003. A Model of the Nuclear Control of Mitochondrial DNA Replication. *Journal of Theoretical Biology*, 221(4), pp.565–583.
- Castro, P.M.L., Hayter, P.M., Ison, A.P. & Bull, A. 1992. Application of a Statistical Design to the Optimization of Culture-Medium for Recombinant Interferon-Gamma Production by Chinese-Hamster Ovary Cells. *Applied Microbiology and Biotechnology*, 38(1), pp.84–90.
- Chen, F., Kou, T., Fan, L., Zhou, Y., Ye, Z., Liang, Z. & Wen-Song, T. 2012. Correlation of antibody production rate with glucose and lactate metabolism in Chinese hamster ovary cells. *Biotechnology letters*, 34(3), pp.425–432.
- Chiang, G.G. & Sisk, W.P. 2005. Bcl-x(L) mediates increased production of humanized monoclonal antibodies in Chinese hamster ovary cells. *Biotechnology and Bioengineering*, 91(7), pp.779–792.
- Chong, W.P.K., Thng, S.H., Hiu, A.P., Lee, D.Y., Chan, E.C.Y. & Ho, Y.S. 2012. LC-MS-based metabolic characterization of high monoclonal antibody-producing Chinese hamster ovary cells. *Biotechnology and Bioengineering*, 109(12), pp.3103–3111.
- Chong, W.P.K., Yusufi, F.N.K., Lee, D.Y., Reddy, S.G., Wong, N.S.C., Heng, C.K., Yap, M.G.S. & Ho, Y.S. 2011. Metabolomics-based identification of apoptosis-inducing metabolites in recombinant fed-batch CHO culture media. *Journal of Biotechnology*, 151(2), pp.218–224.
- Chong, W.P.K., Reddy, S.G., Yusufi, F.N.K., Lee, D.Y., Wong, N.S.C., Heng, C.K., Yap, M.G.S. & Ho, S.y. 2010. Metabolomics-driven approach for the improvement of Chinese hamster ovary cell growth: Overexpression of malate dehydrogenase II. *Journal of Biotechnology*, 147(2), pp.116–121.
- Chusainow, J., Yang, Y.S., Yeo, J.H.M., Toh, P.C., Asvadi, P., Wong, N.S.C. & Yap, M.G.S. 2009. A study of monoclonal antibody-producing CHO cell lines: What makes a stable high producer? *Biotechnology and Bioengineering*, 102(4), pp.1182–1196.
- Clemens, P.C., Schünemann, M.H., Hoffmann, G.F. & Kohlschütter, A. 1990. Plasma concentrations of phenyllactic acid in phenylketonuria. *Journal of inherited metabolic disease*, 13(2), pp.227–228.
- Clynes, R.A., Towers, T.L., Presta, L.G. & Ravetch, J.V. 2000. Inhibitory Fc receptors

- modulate in vivo cytotoxicity against tumor targets. *Nature medicine*, 6(4), pp.443–446.
- Costa, A.R., Rodrigues, E., Henriques, M., Azeredo, J. & Oliveira, R. 2010. Guidelines to cell engineering for monoclonal antibody production. *European Journal of Pharmaceutics and Biopharmaceutics*, 74(2), pp.127–138.
- D'Anna, J.A. et al., 1996. Synchronization of mammalian cells in S phase by sequential use of isoleucine-deprivation G1- or serum-withdrawal G0-arrest and aphidicolin block. *Methods in Cell Science*, 18(2), pp.115–125.
- Davies, S.L., Lovelady, C.S., Grainger, R.K., Racher, A.J., Young, R.J. & James, D.C. 2013. Functional heterogeneity and heritability in CHO cell populations. *Biotechnology and Bioengineering*, 110(1), pp.260–274.
- Dean, J. & Reddy, P. 2013. Metabolic analysis of antibody producing CHO cells in fed-batch production. *Biotechnology and Bioengineering*, 110(6), pp.1735–1747.
- Deaven, L.L. & Petersen, D.F. 1973. The chromosomes of CHO, an aneuploid Chinese hamster cell line: G-band, C-band, and autoradiographic analyses. *Chromosoma*, 41(2), pp.129–144.
- Derouazi, M., Martinet, D., Schmutz, N.B., Flaction, R., Wicht, M., Bertschinger, M., Hacker, D.L., Beckmann, J.S. & Wurn, F.M. 2006. Genetic characterization of CHO production host DG44 and derivative recombinant cell lines. *Biochemical and Biophysical Research Communications*, 340(4), pp.1069–1077.
- Dickson, A.J. 2014. Enhancement of production of protein biopharmaceuticals by mammalian cell cultures: the metabolomics perspective. *Current Opinion in Biotechnology*, 30, pp.73–79.
- Dietmair, S., Hodson, M.P., Quek, L., Timmins, N.E., Chrysanthopoulos, P., Jacob, S.S., Gray, P. & Nielsen, L.K. 2012. Metabolite profiling of CHO cells with different growth characteristics. *Biotechnology and Bioengineering*, 109(6), pp.1404–1414.
- Dietmair, S., Nielsen, L.K. & Timmins, N.E. 2011. Engineering a mammalian super producer. *Journal of Chemical Technology & Biotechnology*, 86(7), pp.905–914.
- Dorai, H., Corisdeo, S., Ellis, D., Kinney, C., Chomo, M., Hawley-Nelson, P., Moore, G., Betenbaugh, M.J. & Ganguly, S. 2012. Early prediction of instability of chinese hamster ovary cell lines expressing recombinant antibodies and antibody-fusion proteins. *Biotechnology and Bioengineering*, 109(4), pp.1016–1030.
- Dreesen, I.A.J. & Fussenegger, M. 2011. Ectopic expression of human mTOR increases viability, robustness, cell size, proliferation, and antibody production of chinese hamster ovary cells. *Biotechnology and Bioengineering*, 108(4), pp.853–866.
- Dundar, Y. 2003. Comparative efficacy of thrombolytics in acute myocardial infarction: a systematic review. *QJM*, 96(2), pp.103–113.
- Edmonds, M.C. de L.C., Tellers, M., Chan, C., Salmon, P., Robinson, D.K. & Markusen, J. 2006. Development of transfection and high-producer screening protocols for the CHOK1SV cell system. *Molecular Biotechnology*, 34, pp. 179–190.
- EKR Therapeutics. 2009. Retavase Full Prescribing Information. pp.1–2.

- Fan, L., Kadura, I., Krebs, L.E., Hatfield, C.C., Shaw, M.M. & Frye, C.C. 2011. Improving the efficiency of CHO cell line generation using glutamine synthetase gene knockout cells. *Biotechnology and Bioengineering*, 109(4), pp.1007–1015.
- Fann, C.H., Guirgis, F., Chen, G., Lao, M.S. & Piret, J.M. 2000. Limitations to the amplification and stability of human tissue-type plasminogen activator expression by Chinese hamster ovary cells. *Biotechnology and Bioengineering*, 69(2), pp.204–212.
- Ferrer-Miralles, N., Domingo-Espín, J., Corchero, J.L., Vázquez, E. & Villaverde, A. 2009. Microbial factories for recombinant pharmaceuticals. *Microbial cell factories*, 8(17), p.1–8.
- Fiehn, O., Kopka, J., Trethewey, R.N. & Willmitzer, L. 2000. Identification of Uncommon Plant Metabolites Based on Calculation of Elemental Compositions Using Gas Chromatography and Quadrupole Mass Spectrometry. *Analytical Chemistry*, 72(15), pp.3573–3580.
- Flintoff, W.F., Davidson, S.V., Siminovitch, L. 1976. Isolation and partial characterization of three methotrexate-resistant phenotypes from Chinese Hamster Ovary cells. *Somatic Cell Genetics*, 2, pp.245–261.
- Fomina-Yadlin, D., Gosink, J.J., McCoy, R., Follstad, B., Morris, A., Russell, C.B. & McGrew, J.T. 2014. Cellular responses to individual amino-acid depletion in antibody-expressing and parental CHO cell lines. *Biotechnology and Bioengineering*, 111(5), pp.965–979.
- Frame, K.K. & Hu, W.S. 1990. The loss of antibody productivity in continuous culture of hybridoma cells. *Biotechnology and Bioengineering*, 35(5), pp.469–476.
- Fussenegger, M. & Betenbaugh, M.J. 2002. Metabolic engineering II. Eukaryotic systems. *Biotechnology and Bioengineering*, 79(5), pp.509–531.
- Gassmann, M., Grenacher, B., Rohde, B. & Vogel, J. 2009. Quantifying Western blots: Pitfalls of densitometry. *Electrophoresis*, 30(11), pp.1845–1855.
- Gemma, C., Sookoian, S., Alvariñas, J., García, S.I., Quintana, L., Kanevsky, D., González, C.D. & Pirola, C.J. 2006. Mitochondrial DNA depletion in small- and large-for-gestational-age newborns. *Obesity*, 14(12), pp.2193–2199.
- Genentech, Inc, 2015. *Activase Full Prescribing Information*,
- Genentech, Inc, 2011. *TNKase Full Prescribing Information*. pp.1–17.
- Gilbert, A., McElearney, K., Kshirsagar, R., Sinacor, M.S. & Ryll, T. 2013. Investigation of metabolic variability observed in extended fed batch cell culture. *Biotechnology Progress*, 29(6), pp.1519–1527.
- Godbey, W.T., Wu, K.K. & Mikos, A.G. 1999. Tracking the Intracellular Path of Poly(ethylenimine)/DNA Complexes for Gene Delivery. *Proceedings of the National Academy of Sciences of the United States of America*, 96(9), pp.5177–5181.
- Gòdia, F. & Cairó, J.J. 2001. Metabolic engineering of animal cells. *Bioprocess and Biosystems Engineering*, 24(5), pp.289–298.
- Gregory, T.R. Animal Genome Size Database. *Animal Genome Size Database*. Available

at: http://www.genomesize.com/result_species.php?id=4570 [Accessed August 2014].

- Haas, A.L., Warms, J.V.B., Hershko, A. & Rose, I.A. 1982. Ubiquitin-activating enzyme. Mechanism and role in protein-ubiquitin conjugation. *The Journal of biological chemistry*, 257(5), pp.2543–2548.
- Hahn, P.J. 1993. Molecular-Biology of Double-Minute Chromosomes. *Bioessays*, 15(7), pp.477–484.
- Hamilton, W.G. & Ham, R.G. 1977. Clonal growth of Chinese hamster cell lines in protein-free media. *In Vitro*, 13(9), pp.537–547.
- Hinterkörner, G., Brugger, G., Müller, D., Hesse, F., Kunert, R., Katinger, H. & Borth, N. 2007. Improvement of the energy metabolism of recombinant CHO cells by cell sorting for reduced mitochondrial membrane potential. *Journal of Biotechnology*, 129(4), pp.651–657.
- Hsu, T.C. 1961. Chromosomal Evolution in Cell Populations. *International Review of Cytology-a Survey of Cell Biology*, 12, pp.69–161.
- Huang, Y.-F., Wang, Y. & Watford, M. 2007. Glutamine directly downregulates glutamine synthetase protein levels in mouse C2C12 skeletal muscle myotubes. *The Journal of nutrition*, 137(6), pp.1357–1362.
- Hui, S.W., Langner, M., Zhao, Y., Ross, P., Hurley, E. & Chan, K. 1996. The role of helper lipids in cationic liposome-mediated gene transfer. *Biophysical Journal*, 71(2), pp.590–599.
- Hwang, W.Y.K. & Foote, J. 2005. Immunogenicity of engineered antibodies. *Methods*, 36(1), pp.3–10.
- Ifandi, V. & Al-Rubeai, M. 2005. Regulation of cell proliferation and apoptosis in CHO-K1 cells by the coexpression of c-Myc and Bcl-2. *Biotechnology Progress*, 21(3), pp.671–677.
- Ifandi, V. & Al-Rubeai, M. 2003. Stable transfection of CHO cells with the c-myc gene results in increased proliferation rates, reduces serum dependency, and induces anchorage independence. *Cytotechnology*, 41(1), pp.1–10.
- Jankowski, J., Giet, M., Jankowski, V., Schmidt, S., Hemeier, M., Mahn, B., Giebing, G., Tölle, M., Luftmann, H., Schlüter, H., Zidek, W. & Tepel, M. 2003. Increased plasma phenylacetic acid in patients with end-stage renal failure inhibits iNOS expression. *Journal of Clinical Investigation*, 112(2), pp.256–264.
- Jayapal, K.P., Wlaschin, K.F., Hu, W. & Yap, M.G.S. 2007. Recombinant protein therapeutics from CHO cells-20 years and counting. *Chemical Engineering Progress*, 103(10), p.40.
- Jefferis, R. 2007. Antibody therapeutics: isotype and glycoform selection. *Expert opinion on biological therapy*, 7(9), pp.1401–1413.
- Jefferis, R. 2009. Glycosylation as a strategy to improve antibody-based therapeutics. *Nature Reviews Drug Discovery*, 8(3), pp.226–234.
- Johnson, I.S. 1983. Human insulin from recombinant DNA technology. *Science*,

219(4585), pp.632–637.

- Jones, J., Nivitchanyong, T., Giblin, C., Ciccarone, V., Judd, D., Gorfien, S., Krag, S.S. & Betenbaugh, M.J. 2005. Optimization of tetracycline-responsive recombinant protein production and effect on cell growth and ER stress in mammalian cells. *Biotechnology and Bioengineering*, 91(6), pp.722–732.
- Jones, P.A. & Baylin, S.B. 2007. The epigenomics of cancer. *Cell*, 128(4), pp.683–692.
- Jones, P.T., Dear, P.H., Foote, J., Neuberger, M.S. & Winter, G. 1986. Replacing the complementarity-determining regions in a human antibody with those from a mouse. *Nature*, 321(6069), pp.522–525.
- Jordan, M., Schallhorn, A. & Wurm, F.M. 1996. Transfecting mammalian cells: optimization of critical parameters affecting calcium-phosphate precipitate formation. *Nucleic Acids Research*, 24(4), pp.596–601.
- Kao, F.T. & Puck, T.T. 1967. Genetics of somatic mammalian cells. IV. Properties of Chinese hamster cell mutants with respect to the requirement for proline. *Genetics*, 55(3), pp.513–524.
- Kao, F.T. & Puck, T.T. 1969. Genetics of somatic mammalian cells. IX. Quantitation of mutagenesis by physical and chemical agents. *Journal of cellular physiology*, 74(3), pp.245–258.
- Kaufman, R.J., Wasley, L.C., Spiliotes, A.J., Gossels, S.D., Latt, S.A., Larsen, G.R. & Kay, R.M. 1985. Coamplification and Coexpression of Human Tissue-Type Plasminogen-Activator and Murine Dihydrofolate-Reductase Sequences in Chinese-Hamster Ovary Cells. *Molecular and Cellular Biology*, 5(7), pp.1750–1759.
- Kennard, M.L., Goosney, D.L., Monteith, D., Roe, S., Fischer, D. & Mott, J. 2009. Auditioning of CHO host cell lines using the artificial chromosome expression (ACE) technology. *Biotechnology and Bioengineering*, 104(3), pp.526–539.
- Khoo, S.H.G. & Al-Rubeai, M. 2009. Detailed understanding of enhanced specific antibody productivity in NS0 myeloma cells. *Biotechnology and Bioengineering*, 102(1), pp.188–199.
- Kim, M., O'Callaghan, P.M., Droms, K.A., James, D.C. 2011. A mechanistic understanding of production instability in CHO cell lines expressing recombinant monoclonal antibodies. *Biotechnology and Bioengineering*, 108(10), pp.2434–2446.
- Kim, N.S., Kim, S.J. & Lee, G.M. 1998. Clonal variability within dihydrofolate reductase-mediated gene amplified Chinese hamster ovary cells: stability in the absence of selective pressure. *Biotechnology and Bioengineering*, 60(6), pp.679–688.
- Kim, S., Park, Y. & Hong, H. 2005. Antibody engineering for the development of therapeutic antibodies. *Molecules and Cells*, 20(1), pp.17–29.
- Kim, S.H. & Lee, G.M. 2009. Development of serum-free medium supplemented with hydrolysates for the production of therapeutic antibodies in CHO cell cultures using design of experiments. *Applied Microbiology and Biotechnology*, 83(4), pp.639–648.
- Kim, S.H. & Lee, G.M. 2007a. Down-regulation of lactate dehydrogenase-A by siRNAs for reduced lactic acid formation of Chinese hamster ovary cells producing

- thrombopoietin. *Applied Microbiology and Biotechnology*, 74(1), pp.152–159.
- Kim, S.H. & Lee, G.M. 2007b. Functional expression of human pyruvate carboxylase for reduced lactic acid formation of Chinese hamster ovary cells (DG44). *Applied Microbiology and Biotechnology*, 76(3), pp.659–665.
- Kim, S.J. & Lee, G.M. 1999. Cytogenetic analysis of chimeric antibody-producing CHO cells in the course of dihydrofolate reductase-mediated gene amplification and their stability in the absence of selective pressure. *Biotechnology and Bioengineering*, 64(6), pp.741–749.
- Kim, T.K., Chung, J.Y., Sung, Y.H. & Lee, G.M. 2001. Relationship between cell size and specific thrombopoietin productivity in chinese hamster ovary cells during dihydrofolate reductase-mediated gene amplification. *Biotechnology and Bioprocess Engineering*, 6(5), pp.332–336.
- Kind, T., Wohlgemuth, G., Lee, D.Y., Lu, Y., Palazoglu, M., Shahbaz, S. & Fiehn, O. 2009. FiehnLib: Mass Spectral and Retention Index Libraries for Metabolomics Based on Quadrupole and Time-of-Flight Gas Chromatography/Mass Spectrometry. *Analytical Chemistry*, 81(24), pp.10038–10048.
- Konrad, M.W., Storrie, B., Glaser, D.A. & Thompson, L.H. 1977. Clonal variation in colony morphology and growth of CHO cells cultured on agar. *Cell*, 10(2), pp.305–312.
- Koressaar, T. & Remm, M. 2007. Enhancements and modifications of primer design program Primer3. *Bioinformatics (Oxford, England)*, 23(10), pp.1289–1291.
- Kotsopoulou, E., Bosteels, H., Chim, Y., Pegman, P., Stephen, G., Thornhill, S.I., Faulkner, J.D. Uden, M. 2010. Optimised mammalian expression through the coupling of codon adaptation with gene amplification: Maximum yields with minimum effort. *Journal of Biotechnology*, 146(4), pp.186–193.
- Kouzarides, T. 2007. Chromatin modifications and their function. *Cell*, 128(4), pp.693–705.
- Kristensen, L.S. & Hansen, L.L. 2009. PCR-based methods for detecting single-locus DNA methylation biomarkers in cancer diagnostics, prognostics, and response to treatment. *Clinical Chemistry*, 55(8), pp.1471–1483.
- Krueger, G. & Callis, K. 2003. Development and use of alefacept to treat psoriasis. *Journal of the American Academy of Dermatology*, 49(2), pp.S87–S97.
- Kuystermans, D. & Al-Rubeai, M. 2009. cMyc increases cell number through uncoupling of cell division from cell size in CHO cells. *BMC Biotechnology*, 9(1), p.76.
- Kuystermans, D., Dunn, M.J. & Al-Rubeai, M. 2010. A proteomic study of cMyc improvement of CHO culture. *BMC Biotechnology*, 10, pp.1–13.
- Labow, B.I., Souba, W.W. & Abcouwer, S.F. 2001. Mechanisms governing the expression of the enzymes of glutamine metabolism - Glutaminase and glutamine synthetase. *The Journal of nutrition*, 131(9), pp.2467S–2474S.
- Lapchak, P. 2002. Development of thrombolytic therapy for stroke: a perspective. *Expert Opinion on Investigational Drugs*, 11(11), pp.1623–1632.

- Lattenmayer, C., Trummer, E., Schreibl, K., Vorauer-Uhl, K., Mueller, D., Katinger, H. & Kunert, R. 2007. Characterisation of recombinant CHO cell lines by investigation of protein productivities and genetic parameters. *Journal of Biotechnology*, 128(4), pp.716–725.
- Lee, C.J., Seth, G., Tsukuda, J. & Hamilton, R.W. 2009. A clone screening method using mRNA levels to determine specific productivity and product quality for monoclonal antibodies. *Biotechnology and Bioengineering*, 102(4), pp.1107–1118.
- Lee, G.M., Kim, E.J., Kim, N.S., Yoon, S.K., Ahn, Y.H. & Song, J.Y. 1999. Development of a serum-free medium for the production of erythropoietin by suspension culture of recombinant Chinese hamster ovary cells using a statistical design. *Journal of Biotechnology*, 69(2-3), pp.85–93.
- Lee, H.C., Yin, P., Lin, J., Wu, C., Chen, C., Wu, C., Chi, C., Tam, T. & Wei, Y. 2006. Mitochondrial Genome Instability and mtDNA Depletion in Human Cancers. *Annals of the New York Academy of Sciences*, 1042(1), pp.109–122.
- Lee, Y.Y., Wong, K.T.K., Tan, J., Toh, P.C., Mao, Y., Brusic, V. & Yap, M.G.S. 2009. Overexpression of heat shock proteins (HSPs) in CHO cells for extended culture viability and improved recombinant protein production. *Journal of Biotechnology*, 143(1), pp.34–43.
- Lewis, N.E. et al. 2013. Genomic landscapes of Chinese hamster ovary cell lines as revealed by the *Cricetulus griseus* draft genome. *Nature Biotechnology*, 31(8), pp.759–765.
- Litzinger, M.T., Fernando, R., Curiel, T.J., Grosenbach, D.W., Schlön, J. & Palena, C. 2007. IL-2 immunotoxin denileukin diftotox reduces regulatory T cells and enhances vaccine-mediated T-cell immunity. *Blood*, 110(9), pp.3192–3201.
- Liu, C., Li, X., Thompson, D., Wooding, K., Chang, T., Tang, Z., Yu, H., Thomas, P.J. & DeMartino, G.N. 2006. ATP Binding and ATP Hydrolysis Play Distinct Roles in the Function of 26S Proteasome. *Molecular Cell*, 24(1), pp.39–50.
- Liu, X., Liu, J., Wright, T.W., Lee, J., Lio, P., Donahue-Hjelle, L., Ravnkar, P. & Wu, F. 2010. Isolation of novel high-osmolarity resistant CHO DG44 cells after suspension of DNA mismatch repair. *BioProcess International*, 8, pp.68–76.
- Livak, K.J. & Schmittgen, T.D. 2001. Analysis of Relative Gene Expression Data Using Real-Time Quantitative PCR and the $2^{-\Delta\Delta CT}$ Method. *Methods*, 25(4), pp.402–408.
- Llavadot, J., Giugliano, R. & Antman, E. 2001. Bolus fibrinolytic therapy in acute myocardial infarction. *Jama-Journal of the American Medical Association*, 286(4), pp.442–449.
- Loeb, L.A. 2001. A Mutator Phenotype in Cancer. *Cancer Research*, 61(8), pp.3230–3239.
- Loeb, L.A. 1991. Mutator phenotype may be required for multistage carcinogenesis. *Cancer Research*, 51(12), pp.3075–3079.
- Loeb, L.A., Springgate, C.F. & Battula, N. 1974. Errors in DNA Replication as a Basis of Malignant Changes. *Cancer Research*, 34(9), pp.2311–2321.

- Lonza Group Ltd. Advantages of the GS System. Available at: <http://www.lonza.com/custom-manufacturing/development-technologies/gs-gene-expression-system.aspx> [Accessed March 21, 2015].
- Luo, J., Vijayasankaran, N., Autsen, J., Santuray, R., Hudson, T., Amanullah, A. & Li F. 2011. Comparative metabolite analysis to understand lactate metabolism shift in Chinese hamster ovary cell culture process. *Biotechnology and Bioengineering*, 109(1), pp.146–156.
- Ma, N., Ellet, J., Okediadi, C., Hermes, P., McCormick, E. & Casnocha, S. 2009. A single nutrient feed supports both chemically defined NS0 and CHO fed-batch processes: Improved productivity and lactate metabolism. *Biotechnology Progress*, 25(5), pp.1353–1363.
- Mahboudi, F., Abolhassan, M.R., Azarpanah, A., Aghajani-Lazarjani, H., Sadeghi-Haskoo, M.A., Maleknia, S. & Vaziri, B. 2013. The Role of Different Supplements in Expression Level of Monoclonal Antibody against Human CD20. *Avicenna journal of medical biotechnology*, 5(3), pp.140–147.
- Maier, U., Losen, M. & Buchs, J. 2004. Advances in understanding and modeling the gas-liquid mass transfer in shake flasks. *Biochemical Engineering Journal*, 17(3), pp.155–167.
- Majors, B.S., Arden, N., Oyler, G.A., Chiang, G.G., Pederson, N.E. & Betenbaugh, M.J. 2008. E2F-1 overexpression increases viable cell density in batch cultures of Chinese hamster ovary cells. *Journal of Biotechnology*, 138(3-4), pp.103–106.
- Martin, U., Sponer, G. & Strein, K. 1992. Evaluation of Thrombolytic and Systemic Effects of the Novel Recombinant Plasminogen-Activator Bm-06.022 Compared with Alteplase, Anistreplase, Streptokinase and Urokinase in a Canine Model of Coronary-Artery Thrombosis. *Journal of the American College of Cardiology*, 19(2), pp.433–440.
- Mastrangelo, A.J., Hardwick, J.M., Bex, F. & Betenbaugh, M.J. 2000. Part I. Bcl-2 and bcl-xL limit apoptosis upon infection with alphavirus vectors. *Biotechnology and Bioengineering*, 67(5), pp.544–554.
- Matasci, M., Baldi, L., Hacker, D.L. & Wurm, F.M. 2011. The PiggyBac transposon enhances the frequency of CHO stable cell line generation and yields recombinant lines with superior productivity and stability. *Biotechnology and Bioengineering*, 108(9), pp.2141–2150.
- McCafferty, J., Griffiths, A.D., Winter, G. & Chiswell, D.J. 1990. Phage antibodies: filamentous phage displaying antibody variable domains. *Nature*, 348(6301), pp.552–554.
- Meilinger, D., Fellingner, K., Bultmann, S., Rothbauer, U., Bonapace, I.M., Kilnkert, W.E.F., Spada, F. & Leonhardt, H. 2009. Np95 interacts with de novo DNA methyltransferases, Dnmt3a and Dnmt3b, and mediates epigenetic silencing of the viral CMV promoter in embryonic stem cells. *EMBO reports*, 10(11), pp.1259–1264.
- Mizumachi, T., Muskhelishvili, L., Naito, A., Furusawa, J., Fan, C., Siegel, E.R., Kadlubar, F.F., Kumar, U. & Higuchi, M. 2008. Increased distributional variance of mitochondrial DNA content associated with prostate cancer cells as compared with normal prostate cells. *Prostate*, 68(4), pp.408–417.

- Moreland, L. et al. 1997. Treatment of rheumatoid arthritis with a recombinant human tumor necrosis factor receptor (p75)-Fc fusion protein. *New England Journal of Medicine*, 337(3), pp.141–147.
- Mulukutla, B.C., Khan, S., Lange, A. & Hu, W. 2010. Glucose metabolism in mammalian cell culture: new insights for tweaking vintage pathways. *Trends in Biotechnology*, 28(9), pp.476–484.
- Nasseri, S.S., Ghaffari, N., Braasch, K., Jardon, M.A., Butler, M., Kennard, M., Gopaluni, B. & Piret, J.M. 2014. Increased CHO cell fed-batch monoclonal antibody production using the autophagy inhibitor 3-MA or gradually increasing osmolality. *Biochemical Engineering Journal*, 91, pp.37–45.
- Neildez-Nguyen, T.M.A., Parisot, A., Vignal, C., Rameau, P., Stockholm, D., Picot, J., Allo, V., Le Bec, C., Laplace, C. & Paldi, A. 2008. Epigenetic gene expression noise and phenotypic diversification of clonal cell populations. *Differentiation; research in biological diversity*, 76(1), pp.33–40.
- Nelson, A.L. & Reichert, J.M. 2009. Development trends for therapeutic antibody fragments. *Nature Biotechnology*, 27(4), pp.331–337.
- Neuberger, M.S., Williams, G.T. & Fox, R.O. 1984. Recombinant Antibodies Possessing Novel Effector Functions. *Nature*, 312(5995), pp.604–608.
- Nicolaides, N.C., Sass, P.M. & Grasso, L. 2010. Advances in targeted therapeutic agents. *Expert Opinion on Drug Discovery*, 5(11), pp.1123–1140.
- Nolan, R.P. & Lee, K. 2011. Dynamic model of CHO cell metabolism. *Metabolic Engineering*, 13(1), pp.108–124.
- O'Callaghan, P.M., McLeod, J., Pybus, L.P., Lovelady, C.S., Wilkinson, S.J., Racher, A.J., Porter, A. & James, D.C. 2010. Cell line-specific control of recombinant monoclonal antibody production by CHO cells. *Biotechnology and Bioengineering*, 106(6), pp.938–951.
- O'Callaghan, P.M., Berthelot, M.E., Young, R.J., Graham, J.W.A., Racher, A.J. & Aldana, D. 2015. Diversity in host clone performance within a Chinese hamster ovary cell line. *Biotechnology Progress*, pp.n/a–n/a.
- Olinger, G.G. et al. 2012. Delayed treatment of Ebola virus infection with plant-derived monoclonal antibodies provides protection in rhesus macaques. *Proceedings of the National Academy of Sciences of the United States of America*, 109(44), pp.18030–18035.
- Osterlehner, A., Simmeth, S. & Göpfert, U. 2011. Promoter methylation and transgene copy numbers predict unstable protein production in recombinant chinese hamster ovary cell lines. *Biotechnology and Bioengineering*, 108(11), pp.2670–2681.
- Pan, Z. & Raftery, D. 2006. Comparing and combining NMR spectroscopy and mass spectrometry in metabolomics. *Analytical and Bioanalytical Chemistry*, 387(2), pp.525–527.
- Park, H., Kim, I.K., Kim, I.Y., Kim, K.H & Kim, H.J. 2000. Expression of carbamoyl phosphate synthetase I and ornithine transcarbamoylase genes in Chinese hamster ovary dhfr-cells decreases accumulation of ammonium ion in culture media. *Journal of*

- Biotechnology*, 81(2-3), pp.129–140.
- Patel, J., McLeod, L.E., Vries, R.G.J., Flynn, A., Wang, X. & Proud, C.G. 2003. Cellular stresses profoundly inhibit protein synthesis and modulate the states of phosphorylation of multiple translation factors. *European Journal of Biochemistry*, 269(12), pp.3076–3085.
- Perry, S., Norman, J.P., Barbieri, J., Brown, E.B. & Gelbard, H. 2011. Mitochondrial membrane potential probes and the proton gradient: a practical usage guide. *BioTechniques*, 50(2), pp.98–115.
- Pichler, J., Galosy, S., Mott, J. & Borth, N. 2010. Selection of CHO host cell subclones with increased specific antibody production rates by repeated cycles of transient transfection and cell sorting. *Biotechnology and Bioengineering*, 108(2), pp.386–394.
- Picken, A. 2012. Metabolic profiling to understand the productivity enhancing effects of a Yeastolate on IgG-producing CHO cells. *Ph.D Thesis*, pp.1–318.
- Pikaart, M.J., Recillas-Targa, F. & Felsenfeld, G. 1998. Loss of transcriptional activity of a transgene is accompanied by DNA methylation and histone deacetylation and is prevented by insulators. *Genes & Development*, 12(18), pp.2852–2862.
- Pilbrough, W., Munro, T.P. & Gray, P. 2009. Intraclonal protein expression heterogeneity in recombinant CHO cells. *PloS one*, 4(12), p.e8432.
- Pitkänen, E. 1977. The conversion of d-xylose into d-threitol in patients without liver disease and in patients with portal liver cirrhosis. *Clinica Chimica Acta*, 80, pp.49–54.
- Porter, A.J., Dickson, A.J. & Racher, A.J. 2010. Strategies for selecting Recombinant CHO cell lines for cGMP manufacturing: Realizing the potential in bioreactors. *Biotechnology Progress*, 26(5), pp.1446–1454.
- Porter, A.J., Racher, A.J., Preziosi, R. & Dickson, A.J. 2010. Strategies for selecting recombinant CHO cell lines for cGMP manufacturing: Improving the efficiency of cell line generation. *Biotechnology Progress*, 26(5), pp.1455–1464.
- Prentice, H.L., Ehrenfels, B.N. & Sisk, W.P. 2007. Improving Performance of Mammalian Cells in Fed-Batch Processes through “Bioreactor Evolution.” *Biotechnology Progress*, 23(2), pp.458–464.
- Prindle, M.J., Fox, E.J. & Loeb, L.A. 2010. The Mutator Phenotype in Cancer: Molecular Mechanisms and Targeting Strategies. *Current Drug Targets*, 11(10), pp.1296–1303.
- Puck, T.T., Cieciura, S.J. & Robinson, A. 1958. Genetics of Somatic Mammalian Cells .3. Long-Term Cultivation of Euploid Cells From Human and Animal Subjects. *Journal of Experimental Medicine*, 108(6), pp.945–959.
- Kao, F.T. & Puck, T.T., 1966. Genetics of somatic mammalian cells. IV. Properties of Chinese hamster cell mutants with respect to the requirement for proline. *Genetics*, 55(3), pp.513–524.
- Kao, F.T. & Puck, T.T., 1968. Genetics of somatic mammalian cells, VII. Induction and isolation of nutritional mutants in Chinese hamster cells. *Proceedings of the National Academy of Sciences of the United States of America*, 60(4), pp.1275–1281.

- Pybus, L.P. Dean, G., West, N.R., Smith, A., Daramola, O., Field, R., Wilkinson, S.J. & James, D.C. 2014. Model-directed engineering of “difficult-to-express” monoclonal antibody production by Chinese hamster ovary cells. *Biotechnology and Bioengineering*, 111(2), pp.372–385.
- Qiu, X. et al. 2014. Reversion of advanced Ebola virus disease in nonhuman primates with ZMapp. *Nature*, 514(7520), pp.47–53.
- Regis Technologies. 2000. GC Derivatization. *Chromspec.com*, pp.1–15. Available at: https://www.chromspec.com/pdf/gc_derivativization_methods.pdf [Accessed March 29, 2015].
- Saunders, F., Sweeney, B., Antoniou, M.N., Stephens, P. & Cain, K. 2015. Chromatin function modifying elements in an industrial antibody production platform--comparison of UCOE, MAR, STAR and cHS4 elements. *PLoS one*, 10(4), p.e0120096.
- Schneider, C.A., Rasband, W.S. & Eliceiri, K.W. 2012. NIH Image to ImageJ: 25 years of image analysis. *Nature Methods*, 9(7), pp.671–675.
- Sekhon, B.S. 2010. Biopharmaceuticals: an overview. *Thai J. Pharm. Sci*, 34, pp.1–19.
- Sellick, C.A., Hansen, R., Maqsood, A.R., Dunn, W.B., Stephens, G.M., Goodacre, R. & Dickson, A.J. 2009. Effective Quenching Processes for Physiologically Valid Metabolite Profiling of Suspension Cultured Mammalian Cells. *Analytical Chemistry*, 81(1), pp.174–183.
- Sellick, C.A., Knight, D., Croxford, A.S., Maqsood, A.R., Stephens, G.M., Goodacre, R. & Dickson, A.J. 2010. Evaluation of extraction processes for intracellular metabolite profiling of mammalian cells: matching extraction approaches to cell type and metabolite targets. *Metabolomics*, 6(3), pp.427–438.
- Sellick, C.A., Croxford, A.S., Maqsood, A.R., Stephens, G.M., Westerhoff, H.V., Goodacre, R. & Dickson, A.J. 2011. Metabolite profiling of recombinant CHO cells: Designing tailored feeding regimes that enhance recombinant antibody production. *Biotechnology and Bioengineering*, 108(12), pp.3025–3031.
- Sellick, C.A., Hansen, R., Stephens, G.M., Goodacre, R. & Dickson, A.J. 2011. Metabolite extraction from suspension-cultured mammalian cells for global metabolite profiling. *Nature Protocols*, 6(8), pp.1241–1249.
- Selvarasu, S., Ho, Y.S., Chong, W.P.K., Wong, N.S.C., Yusufi, F.N.K., Lee, Y.Y., Yap, M.G.S. & Lee, D. 2012. Combined in silico modeling and metabolomics analysis to characterize fed-batch CHO cell culture. *Biotechnology and Bioengineering*, 109(6), pp.1415–1429.
- Sen, S., Hittelman, W.N., Teeter, L.D. & Kuo, M.T. 1989. Model for the Formation of Double Minutes from Prematurely Condensed Chromosomes of Replicating Micronuclei in Drug-treated Chinese Hamster Ovary Cells Undergoing DNA Amplification. *Cancer Research*, 49(23), pp.6731–6737.
- Sengupta, N., Rose, S.T. & Morgan, J.A. 2010. Metabolic flux analysis of CHO cell metabolism in the late non-growth phase. *Biotechnology and Bioengineering*, 108(1), pp.82–92.
- Shin, S., 1991. Chimeric antibody: Potential applications for drug delivery and

- immunotherapy. *Biotherapy*, 3(1), pp.43–53.
- Shukla, A.A. & Thömmes, J. 2010. Recent advances in large-scale production of monoclonal antibodies and related proteins. *Trends in Biotechnology*, 28(5), pp.253–261.
- Siegall, C.B., Chaudhary, V.K., FitzGerald, D.J. & Pastan, I. 1988. Cytotoxic activity of an interleukin 6-Pseudomonas exotoxin fusion protein on human myeloma cells. *Proceedings of the National Academy of Sciences of the United States of America*, 85(24), pp.9738–9742.
- Sinacore, M.S., Drapeau, D. & Adamson, S.R. 2000. Adaptation of mammalian cells to growth in serum-free media. *Molecular biotechnology*, 15(3), pp.249–257.
- Singh, R.P., Al-Rubeai, M., Gregory, C.D. & Emery, A.N. 1994. Cell-Death in Bioreactors - A Role for Apoptosis. *Biotechnology and Bioengineering*, 44(6), pp.720–726.
- Tcheng, J. et al. 2001. Abciximab readministration - Results of the ReoPro readministration registry. *Circulation*, 104(8), pp.870–875.
- Templeton, N., Dean, J. & Reddy, P. 2013. Peak antibody production is associated with increased oxidative metabolism in an industrially relevant fed-batch CHO cell culture. *Biotechnology and Bioengineering*, 110(7), pp.2013–2024
- Terpe, K. 2006. Overview of bacterial expression systems for heterologous protein production: from molecular and biochemical fundamentals to commercial systems. *Applied Microbiology and Biotechnology*, 72(2), pp.211–222.
- Tiao, M., Lin, T., Kuo, F., Huang, C., Du, Y., Chen, C. & Chuang, J. 2007. Early stage of biliary atresia is associated with significant changes in 8-hydroxydeoxyguanosine and mitochondrial copy number. *Journal of Pediatric Gastroenterology and Nutrition*, 45(3), pp.329–334.
- Tiemeier, D.C. & Milman, G. 1972. Regulation of glutamine synthetase in cultured Chinese hamster cells, induction and repression by glutamine. *The Journal of biological chemistry*, 247(18), pp.5722–5727.
- Tomlinson, D.R. & Gardiner, N.J. 2008. Glucose neurotoxicity. *Nature Reviews Neuroscience*, 9(1), pp.36–45.
- Tsao, Y.S., Cardoso, A.G., Condon, R.G.G., Voloch, M., Lio P., Lagos, J.C., Kearns, B.G. & Liu, Z. 2005. Monitoring Chinese hamster ovary cell culture by the analysis of glucose and lactate metabolism. *Journal of Biotechnology*, 118(3), pp.316–327.
- Untergasser, A., Cutcutache, I., Koressaar, T., Ye, J., Faircloth, B.C., Remm, M. & Rozen, S.G. 2012. Primer3--new capabilities and interfaces. *Nucleic Acids Research*, 40(15), pp.e115–e115.
- Urlaub, G. & Chasin, L.A. 1980. Isolation of Chinese hamster cell mutants deficient in dihydrofolate reductase activity. *Proceedings of the National Academy of Sciences of the United States of America*, 77(7), pp.4216–4220.
- Urlaub, G., Käs, E., Corothers, A.M. & Chasin, L.A. 1983. Deletion of the diploid dihydrofolate reductase locus from cultured mammalian cells. *Cell*, 33(2), pp.405–412.

- Vandesompele, J., De Preter, K., Pattyn, F., Poppe, B., Van Roy, N., De Paepe, A. & Speleman, F. 2002. Accurate normalization of real-time quantitative RT-PCR data by geometric averaging of multiple internal control genes. *Genome Biology*, 3(7), pp.1–12.
- Venkatesan, R.N., Treuting, P.M., Fuller, E.D., Goldsby, R.E., Norwood, T.H., Gooley, T.A., Ladiges, W.C., Preston, B.D. & Loeb, L. 2007. Mutation at the Polymerase Active Site of Mouse DNA Polymerase Increases Genomic Instability and Accelerates Tumorigenesis. *Molecular and Cellular Biology*, 27(21), pp.7669–7682.
- Verma, R., Boleti, E. & George, A.J. 1998. Antibody engineering: comparison of bacterial, yeast, insect and mammalian expression systems. *Journal of Immunological Methods*, 216(1), pp.165–181.
- Vishwanathan, N., Le, H., Jacob, N.M., Tsao, Y.S., Ng, S., Loo, B., Liu, Z., Kantardjieff, A. & Hu, W. 2014. Transcriptome Dynamics of Transgene Amplification in Chinese Hamster Ovary Cells. *Biotechnology and Bioengineering*, 111(3), pp.518–528.
- Vitetta, E.S., Krolick, K.A., Miyama-Inaba, M., Cushley, W., Uhr, J.W. 1983. Immunotoxins: A New Approach to Cancer Therapy. *Science*, 219(4585), pp.644–650.
- Walsh, G. 2010. Biopharmaceutical benchmarks 2010. *Nature Biotechnology*, 28(9), pp.917–924.
- Walsh, G. 2014. Biopharmaceutical benchmarks 2014. *Nature Biotechnology*, 32(10), pp.992–1000.
- Walsh, G. 2002. Biopharmaceuticals and biotechnology medicines: an issue of nomenclature. *European Journal of Pharmaceutical Sciences*, 15(2), pp.135–138.
- Walsh, G. 2005. Biopharmaceuticals: recent approvals and likely directions. *Trends in Biotechnology*, 23(11), pp.553–558.
- Walsh, G. 2004. Second-generation biopharmaceuticals. *European Journal of Pharmaceutics and Biopharmaceutics*, 58(2), pp.185–196.
- Walters, K.R., Pan, Q., Serianni, A.S. & Duman, J.G. 2009. Cryoprotectant Biosynthesis and the Selective Accumulation of Threitol in the Freeze-tolerant Alaskan Beetle, *Upis ceramboides*. *Journal of Biological Chemistry*, 284(25), pp.16822–16831.
- Wang, X., Xie, Y., Gao, P., Zhang, S., Tan, H., Yang, F., Lian, R., Tian, J. & Xu, G. 2014. A metabolomics-based method for studying the effect of yfcC gene in *Escherichia coli* on metabolism. *Analytical Biochemistry*, 451, pp.48–55.
- Warburg, O. 1956. On the origin of cancer cells. *Science*, 123(3191), pp.309–314.
- Wasa, M., Bode, B.P., Abcouwer, S.F., Collins, C.L., Tanabe, K.K. & Souba, W.W. 1996. Glutamine as a regulator of DNA and protein biosynthesis in human solid tumor cell lines. *Annals of surgery*, 224(2), pp.189–197.
- Weibel, K.E., Mor, J.R. & Fiechter, A. 1974. Rapid Sampling of Yeast-Cells and Automated Assays of Adenylate, Citrate, Pyruvate and Glucose-6-Phosphate Pools. *Analytical Biochemistry*, 58(1), pp.208–216.

- Wilkins, C.A. & Gerdtzen, Z.P. 2011. Engineering CHO cells for improved central carbon and energy metabolism. *BMC Proceedings*, 5(Suppl 8), p.P120.
- Winter, G., Fersht, A.R., Wilkinson, A.J., Zoller, M. & Smith, M. 1982. Redesigning Enzyme Structure by Site-Directed Mutagenesis - Tyrosyl Transfer-Rna Synthetase and Atp Binding. *Nature*, 299(5885), pp.756–758.
- Witzig, T.E. 2002. Randomized Controlled Trial of Yttrium-90-Labeled Ibritumomab Tiuxetan Radioimmunotherapy Versus Rituximab Immunotherapy for Patients With Relapsed or Refractory Low-Grade, Follicular, or Transformed B-Cell Non-Hodgkin's Lymphoma. *Journal of Clinical Oncology*, 20(10), pp.2453–2463.
- Won, C., Shen, X. & Mashiguchi, K. 2011. Conversion of tryptophan to indole-3-acetic acid by tryptophan aminotransferases of arabidopsis and yuccas in Arabidopsis. In *Proceedings of the National Academy of Sciences* pp. 18518–18523.
- Wood, P. 2001. *Understanding Immunology*, Essex: Pearson Education Limited.
- Wray, N. & Visscher, P. 2008. Estimating trait heritability. *Nature Education*, 1(1), p29.
- Wurm, F.M. 2013. CHO Quasispecies—Implications for Manufacturing Processes. *Processes*, 1(3), pp.296–311.
- Wurm, F.M. 2004. Production of recombinant protein therapeutics in cultivated mammalian cells. *Nature Biotechnology*, 22(11), pp.1393–1398.
- Wurm, F.M. & Hacker, D. 2011. First CHO genome. *Nature Biotechnology*, 29(8), pp.718–720.
- Wurm, F.M., Gwinn, K.A. & Kingston, R.E. 1986. Inducible Overproduction of the Mouse C-Myc Protein in Mammalian-Cells. *Proceedings of the National Academy of Sciences of the United States of America*, 83(15), pp.5414–5418.
- Xing, J., Chen, M., Wood, C.G., Lin, J., Spitz, M.R., Ma, J., Amos, C.L., Shields, P.G., Benowitz, N.L., Gu, J., Andrade, M., Swan, G.E. & Wu, X. 2008. Mitochondrial DNA Content: Its Genetic Heritability and Association With Renal Cell Carcinoma. *JNCI Journal of the National Cancer Institute*, 100(15), pp.1104–1112.
- Xu, X. et al. 2011. The genomic sequence of the Chinese hamster ovary (CHO)-K1 cell line. *Nature Biotechnology*, 29(8) pp.735–742.
- Yoon, S., Kim, Y., Shim, H. & Chung, J. 2010. Current perspectives on therapeutic antibodies. *Biotechnology and Bioprocess Engineering*, 15, pp.709–715.
- Yoon, S.K., Kim, S.H., Song, J.Y. & Lee, G.M. 2006. Biphasic culture strategy for enhancing volumetric erythropoietin productivity of Chinese hamster ovary cells. *Enzyme and Microbial Technology*, 39(3), pp.362–365.
- Yoon, Y.G. & Koob, M.D. 2005. Transformation of isolated mammalian mitochondria by bacterial conjugation. *Nucleic Acids Research*, 33(16), pp.e139–e139.
- Yoon, Y.G., Koob, M.D. & Yoo, Y.H. 2010. Re-engineering the mitochondrial genomes in mammalian cells. *Anatomy & Cell Biology*, 43(2), pp.97–13.
- Yoshikawa, T., Nakanishi, F., Ogura, Y., Oi, D., Omasa, T., Katakura, Y., Kishimoto, M. &

Suga, K. 2000. Amplified Gene Location in Chromosomal DNA Affects Recombinant Protein Production and Stability of Amplified Genes. *Biotechnology Progress*, 16(5), pp.710–715.

Young, J.D. 2014. ¹³C metabolic flux analysis of recombinant expression hosts. *Current Opinion in Biotechnology*, 30, pp.238–245.

Zhang, F., Frost, A.R., Blundell, M.P., Bales, O., Antoniou, M.N. & Thrasher, A.J. 2010. A ubiquitous chromatin opening element (UCOE) confers resistance to DNA methylation-mediated silencing of lentiviral vectors. *Molecular therapy : the journal of the American Society of Gene Therapy*, 18(9), pp.1640–1649.

Appendices

Appendix A – List of materials, equipment and suppliers

Bacterial cell lines

MedImmune, UK

Z-competent DH5 α *E. coli* cells

Mammalian cell lines

MedImmune, UK

Host cell line NC, host cell line 10, host cell line 15, host cell line 16, host cell line 19, host cell line 20, host cell line 21

Medium and supplements

Life Technologies, USA

CD CHO medium without glutamine, hypoxanthine, or thymidine (Gibco)

L-glutamine, 200 mM (Gibco)

MedImmune, UK

Proprietary feed

Melford Laboratories Ltd., UK

Agar

Tryptone

Yeast extract

Sigma-Aldrich Company Ltd., UK

Ampicillin sodium salt

Dimethyl sulphoxide, Hybri-Max (DMSO)

L-methionine sulfoximine

Sodium chloride

Plasmids

Recombinant IgG – recombinant glutamine synthetase plasmid

Chemicals and reagents

5 PRIME

Phase Lock Gel Heavy 2 ml

Agilent Technologies, UK

Perfluorotributylamine

Bio-Rad Laboratories Inc., USA

Protein Assay Dye Reagent Concentrate

Bioline, UK

Agarose powder

BIOTAQ™ DNA polymerase (kit)

dNTP Set

HyperLadder 25bp

SensiFast™ SYBR® probe Hi-ROX (kit)

Tetro cDNA synthesis kit

BOC Industrial, UK

Helium (GC grade)

Eurofins MWG operon, Germany

Oligonucleotide primers

LI-COR Biosciences, USA

IRDye 800CW donkey anti-mouse

IRDye 800CW donkey anti-mouse

Life technologies, USA

18s ribosomal TaqMan probe/primers (VIC)

KaryoMAX colcemid solution in PBS

MitoTracker Green FM

NuPAGE Novex 4-12% Bis-Tris Protein Gels, 1.0 mm, 15 well

NuPAGE MES SDS Running Buffer (20X)

ProLong Gold Antifade Mountant (with DAPI)

PureLink Genomic DNA (kit)

Rhodamine-123

SuperScript VILO MasterMix

TaqMan Gene Expression MasterMix

TRizol reagent

MedImmune, UK

GS TaqMan probe/primers (FAM)

NBS Biologicals, UK

SafeView nucleic acid stain

New England Biolabs, UK

Prestained Protein Marker, Broad Range (7-175 kDa)

Qiagen Ltd., UK

Buffer RLT Plus

HiSpeed Plasmid Maxi kit

RNeasy Plus Mini Kit

Roche, Switzerland

Buffer H

Pvu1 restriction endonuclease

Santa Cruz Biotechnology Inc., USA

Mouse monoclonal anti-ERK2 (6H3)

Sigma-Aldrich Company Ltd., UK

Adenosine 5'-diphosphate sodium salt

Ammonium bicarbonate

Anti-Glutamine Synthetase antibody produced in rabbit (G2781)

β -mercaptoethanol

Boric acid

Bovine serum albumin

Bromophenol blue

Diethyl pyrocarbonate (DEPC)

DNase I, amplification grade (Kit)

Glycerol, BioReagent

Hydrochloric acid, reagent grade, 37%

Hydroxylamine hydrochloride

Imidazole buffer solution, 1 M

L-glutamic acid monohydroxamate

L-glutamine

Manganese (II) chloride solution, 1 M

Myristic-d₂₇ acid

Phosphate buffered saline tablets (PBS)

Ponceau-S

Potassium chloride

Propidium iodide

Pyridine

Sodium acetate 3 M

Sodium arsenate dibasic heptahydrate

Sodium dodecyl sulfate (SDS)

Sodium hydroxide, reagent grade pellets

Trichloroacetic acid, 1 M

Tris base

Tris-HCL

Trypan blue

Tween-20

Water, TC grade

Thermo Fisher Scientific, USA

Chloroform

Ethylenediaminetetraacetic acid (EDTA)

Glacial acetic acid

Glycine

Halt protease inhibitor

Isopropanol, Optima

Methanol, Optima

MPER mammalian protein extraction reagent

N-methyl-N-(trimethylsilyl)trifluoroacetamide + 1% (v/v) trichloromethylsilane
(MSTFA + 1% TCMS)

Water, Optima

VWR International, UK

Ethanol, absolute

Ferric (III) chloride, anhydrous

Hydrochloric acid, 1 M

Isopropanol

Marvel™ non-fat milk powder is available at all major supermarket chains.

Equipment, Consumables and Software

Acros Organics, Belgium

Methoxyamine hydrochloride

Agilent Technologies, UK

10 µl gold standard syringe

7890A gas chromatograph

5975C Inert XL MSD mass spectrometer with triple-axis detector

7683B series autosampler

7683B series sample injector

Chemstation

DB-5ms (30 m, 0.25 mm, 0.25 µm) + DuraGuard (10 m) column

BD Biosciences, USA

BD Accuri C6 flow cytometer

BD Plastipak™ 10 ml syringes

Beckman Coulter, USA

Vi-CELL XR

Bibby Scientific Ltd., UK

Digital tube roller SRT6D

TC-3000 Personal 48-well Thermal Cycler

Binder, Germany

BD Series incubator

Bio-Rad Laboratories Inc., USA

ChemiDoc MP System

Clear plastic PCR caps, 8-strip

Trans-Blot SD Semi-Dry Transfer Cell

Mini-Sub Cell GT Systems

Wide Mini-Sub Cell GT Systems

BioTek Instruments Inc., USA

Gen5 Data Analysis Software

PowerWave microplate spectrophotometer

BMG Labtech, Germany

Polarstar OPTIMA plate reader

Boeco, Germany

Table top Centrifuge (U-32)

Corning Inc. Life Sciences, USA

Assorted DeckWorks pipette filter tips

15 ml centrifuge tubes

50 ml centrifuge tubes

125 ml Erlenmeyer flask, vented caps

250 ml Erlenmeyer flask, vented caps

Costar 24-well microplates

Costar 96-well microplates

Costar UV 96-well plates

Round bottom test tubes

Serological pipettes (1 ml, 5 ml, 10 ml, 25 ml 50 ml)

T25 TC treated flasks, vented caps

Thermowell 96-well PCR plates

Eppendorf, Germany

Concentrator Plus, vacuum centrifuge

Mastercycler Pro thermal cycler

New Brunswick U700 ultra-low temperature freezer

FluidX, UK

2ml cryo tube with 2D barcode, internal thread screw cap

Grant Instruments, UK

SUB 6 waterbath

QBT2 heat block

GraphPad Software, USA

GraphPad Prism Version 6.02

GE Healthcare, UK

Whatman 3mm filter paper

Greiner Bio-One Ltd., UK

MASTERBLOCK 96-deep well plate

Infors HT, UK

Multitron shaking incubator

<<Sticky Stuff>> adhesive matting

Kuhner, Switzerland

LT-X shaking incubator

Labcaire Systems LTD, UK

Recirculating class II microbiological safety cabinet

Labnet International Inc., USA

Prism Mini microcentrifuge

LI-COR Biosciences, USA

Odyssey Classic Imager System

Life Technologies™, USA

ABI7000MBI Real-Time PCR System

Countess Automated Cell Counter

StepOnePlus™ Real-Time PCR system

XCell SureLock Mini-Cell

Lonza, Switzerland

Amaxa Nucleofector 2b Device

Cell Line Nucleofector Kit V (non cGMP)

Mettler Toledo, UK

SevenEasy pH meter

Microsoft, USA

Excel, 2011

Millipore, UK

Milliex 0.22 µm syringe filter units

Elix water purification system

Molecular Devices, USA

MetaVue software

National Scientific, USA

1.5 ml target silanized glass vials

NIH, USA

ImageJ software

Olympus, UK

BX51 upright microscope

Pall Life Sciences, USA

BioTrace NT nitrocellulose blotting membrane

FortéBIO Octet 384QK

Photometrics, USA

Coolsnap HQ camera

Prestige Medical, UK

Classic Media autoclave (210048)

Qiagen Ltd, UK

QIAcube

Roche, Switzerland

Innovatis Cedex cell counter

SciQuip Ltd., UK

Microfuge 24-place (Sigma, 1-14)

Serial Basics

Serial Cloner 2.6 Software

STARLAB, UK

Assorted pipette tips

0.2 ml thin-wall PCR tubes

0.5 ml microcentrifuge tubes

1.5 ml microcentrifuge tubes

2.0 ml microcentrifuge tubes

TAP Biosystems, UK

Sonata

Thermo Scientific , USA

90 mm Petri dish, Sterilin

Cryobox, System 100

Cryo 400 Storage System

CryoTubes 1.8 ml, Nunc

HERAcell CO₂ incubator

Heraeus Fresco 17 microcentrifuge

Holten Safe class II microbiological safety cabinet

Mr Frosty freezing container, Nalgene

Nanodrop ND-1000 UV/Vis spectrophotometer

Racks for cryogenic vials, Nunc

Sorvall Legend X1R centrifuge

VWR International, UK

Bijou containers, 7 ml

Cover glass, square

Microscope slides

Spreaders, L-shaped

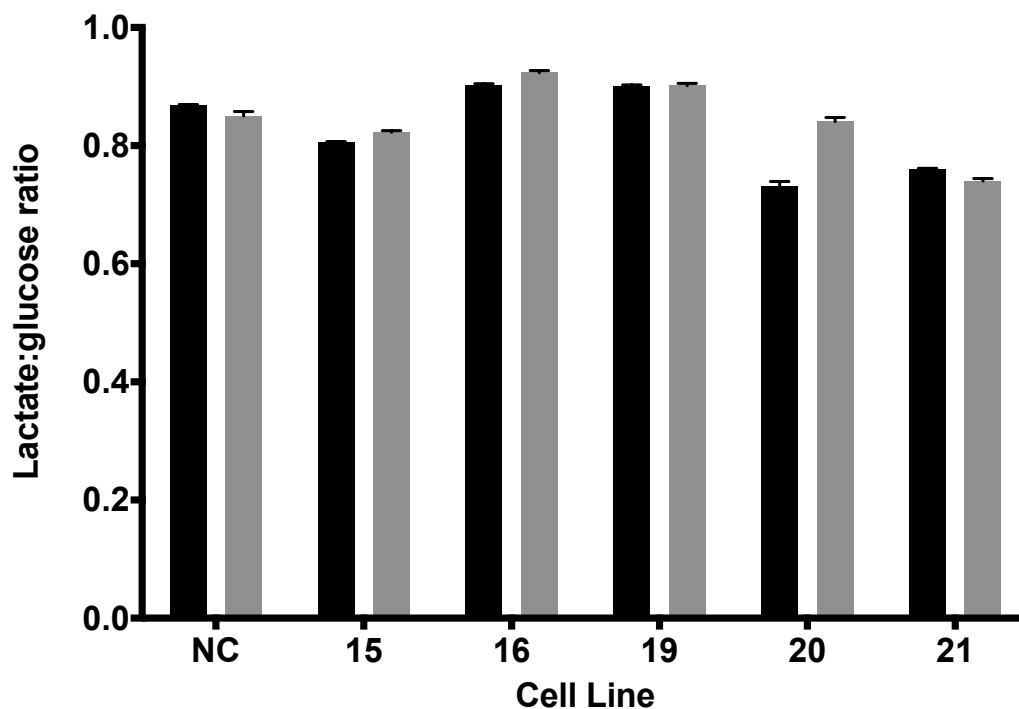
Universal containers, 30 ml

YSI Inc., USA

2900 Biochemistry Analyzer

Appendix B – Host cell line lactate:glucose ratio

Figure AB.1 – Ratio of lactate production rate to glucose consumption rate during batch culture in response to LTC



Legend

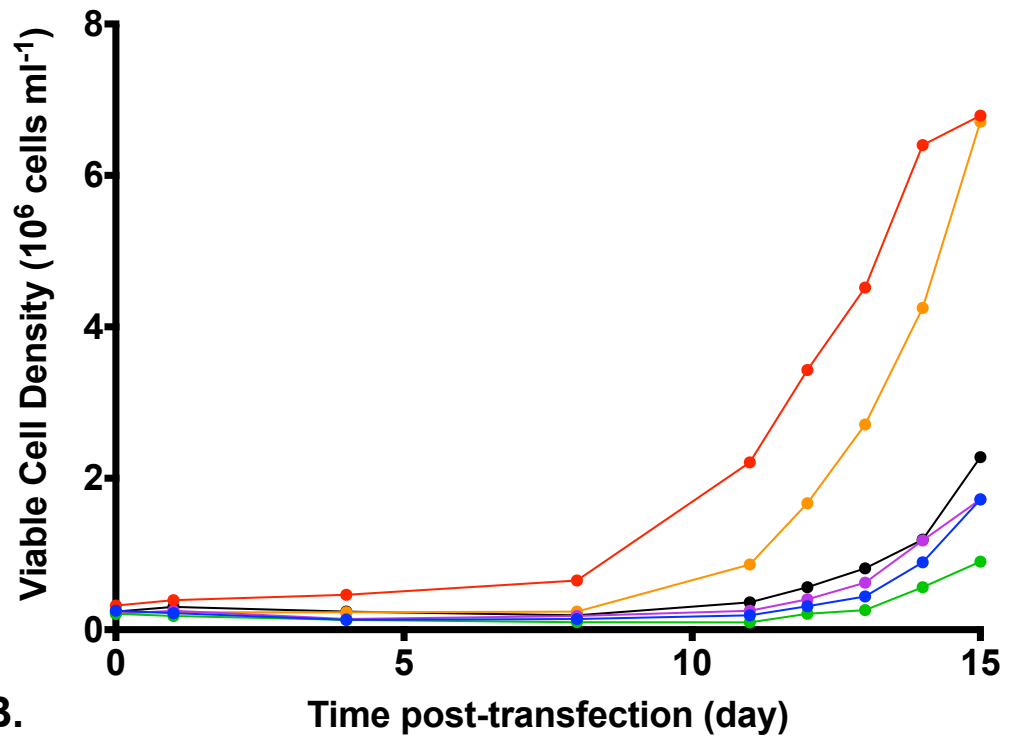
- Early generation
- Late generation

Ratios were calculated from the lactate production rate and glucose consumption rates described in Figure 3.5. Considering an approximate molar exchange that 1 glucose molecule can be converted into 2 lactate molecules, a ratio of 1 would imply that 50% of the glucose consumed was converted to lactate. Lower ratio values imply that more carbon enters the citric acid cycle as pyruvate, this represents a more efficient metabolic state.

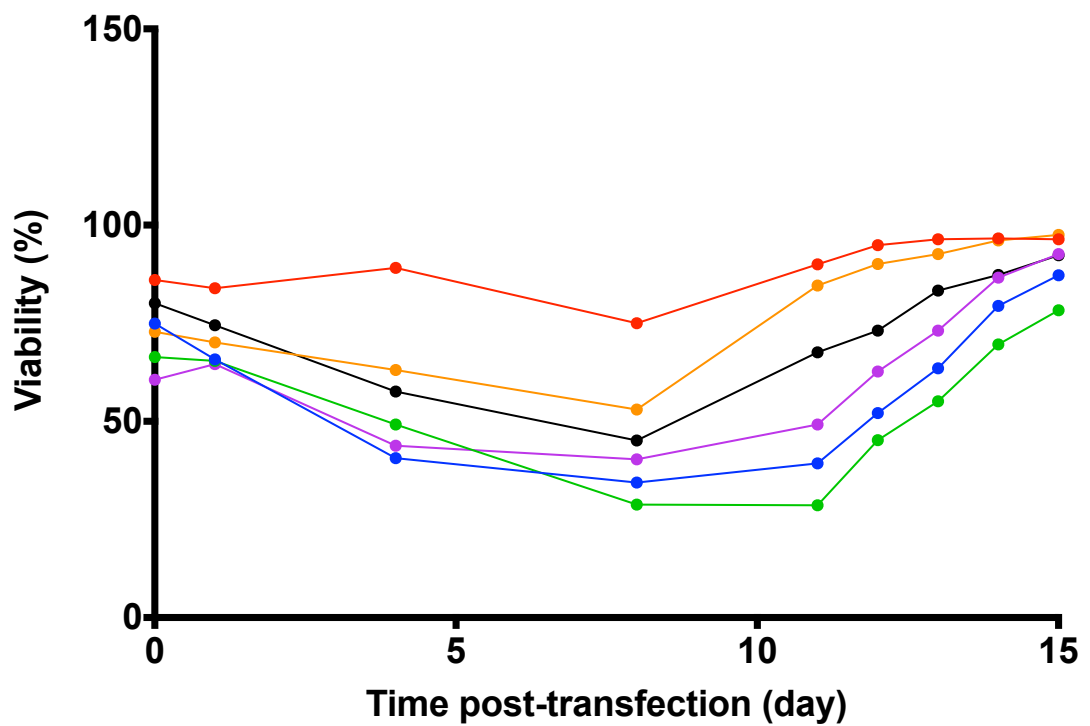
Appendix C – Analysis of transfection round 2 pool kill curves

Figure AC.1 Analysis of transfection round 2 pool kill curves

A.









B.



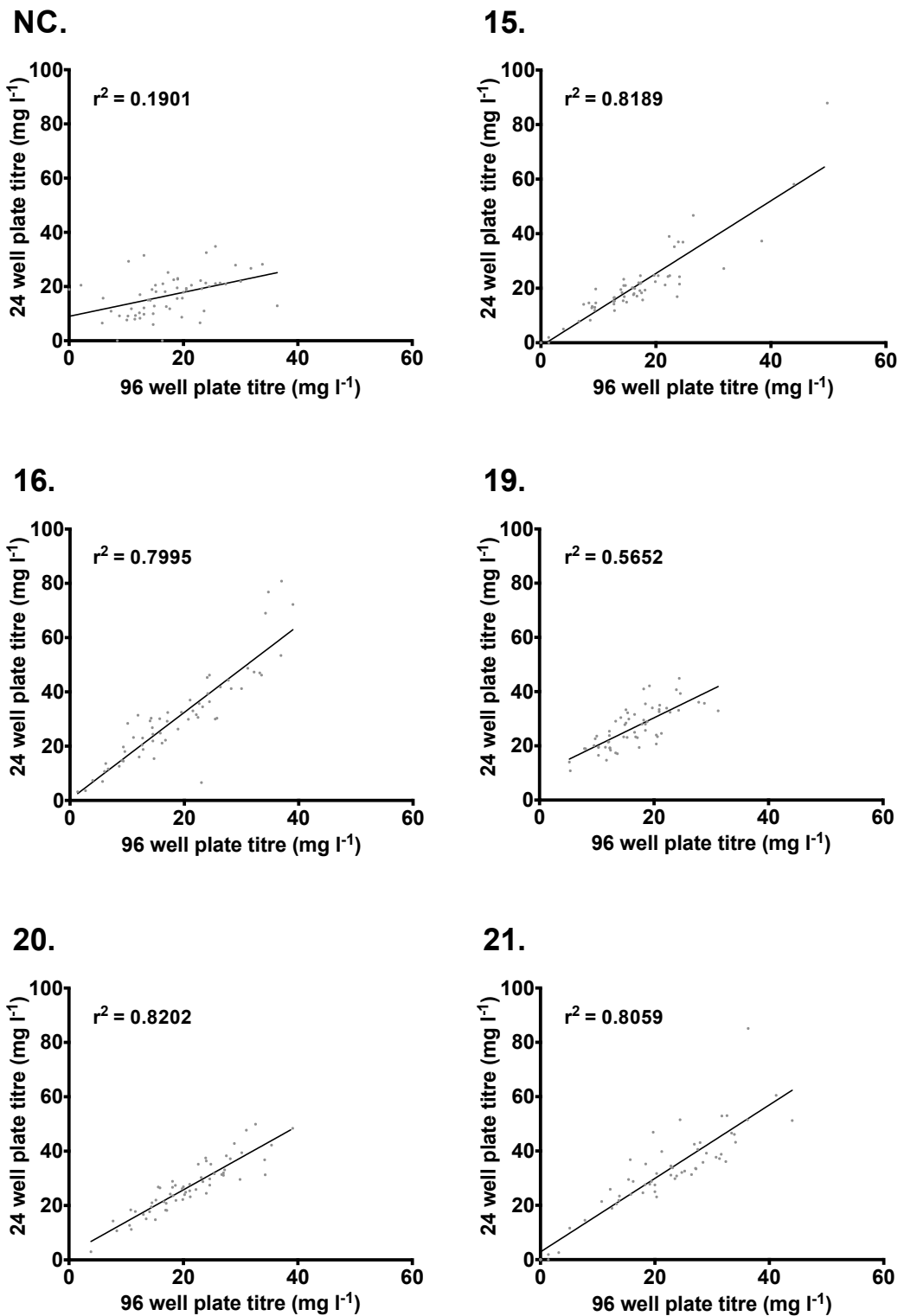
One pool was created for each host cell line during transfection round 2 (Section 2.3.8). Following transfection the pools were maintained at 37 °C, 140 rpm with 5% CO₂ in a 70% humidity incubator. MSX to a final concentration of 50 µM was added on day 1 post-transfection. Cell counts were taken until 15 days post-transfection whilst the pools recovered, a Beckman Coulter Vi-CELL XR, this is based on the trypan blue exclusion method. The charts show the viable cell densities (A) and viability (B) of the pools.

Legend

-  Pool NC
-  Pool 15
-  Pool 16
-  Pool 19
-  Pool 20
-  Pool 21

Appendix D – Linear regression analysis of clonal transfectant mAb production from 96-well and 24-well static plate culture

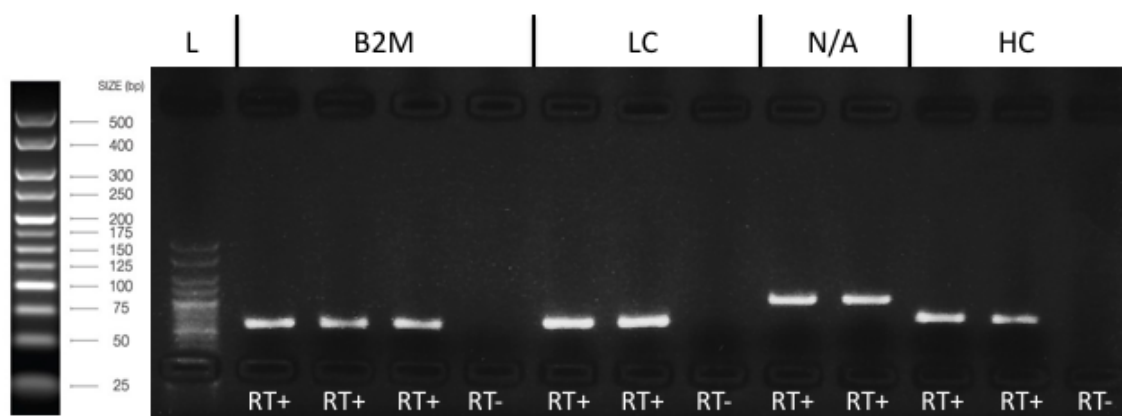
Figure AD.1 Linear regression analysis of clonal transfectant mAb production from 96-well and 24-well static plate culture



As described in Section 4.2.3 and Section 2.5.1, cell culture media from clonal transfectants was harvested from 96- and 24-well plates and analysed for antibody titre. The titre of these samples was used to perform linear regression analysis to determine any relationship between the values. The charts show the results of the linear regression for the transfectants from cell line NC (NC), cell line 15 (15), cell line 16 (16), cell line 19 (19), cell line 20 (20) and cell line 21 (21).

Appendix E – Verification of primer specificity and efficiency

Figure AE.1 Agarose gel electrophoresis of PCR products from mAb-109 primers



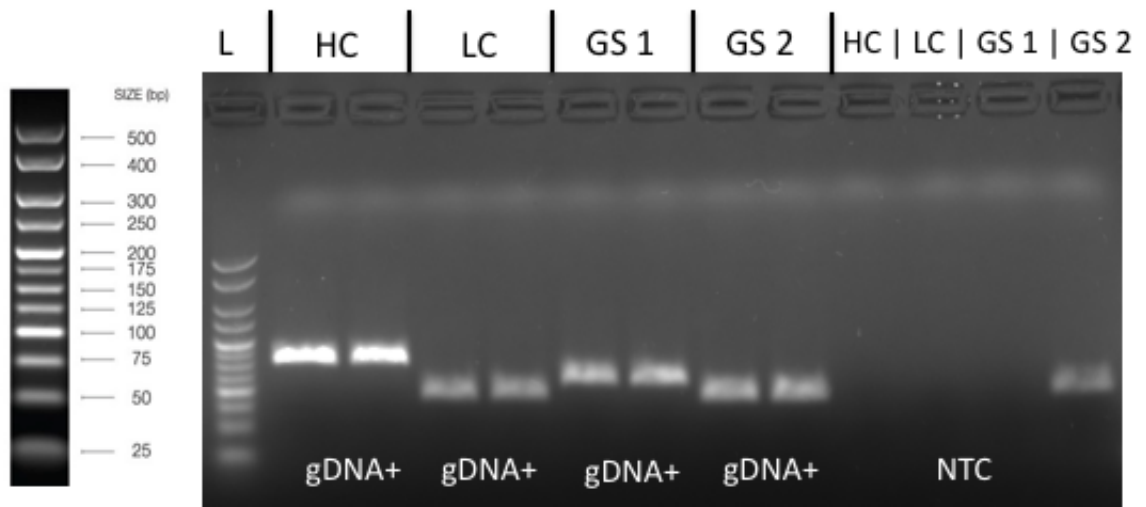
As described in Section 2.6.1.5 and Section 2.6.1.6, PCR and agarose gel electrophoresis was used to verify the specificity of the primers used for the qRT-PCR analysis of mAb-109 mRNA expression. The figure shows the fragments amplified by the β_2 microglobulin (B2M) primers, mAb-109 light chain primers (LC) and the mAb-109 heavy chain primers (HC). Both reverse transcriptase positive (RT+) and reverse transcriptase negative (RT-) cDNA samples were amplified. The labelled HyperLadder 25bp molecular weight marker (L) is also shown to the left of the figure. N/A represents an amplicon for polyadenylate-binding nuclear protein 1 primers, which were not otherwise used in this study.

Table AE.1 Efficiency of PCR primers for qRT-PCR analysis of mAb-109 mRNA expression

| Target gene | Amplicon size (base pairs) | Slope | Efficiency |
|-------------|----------------------------|--------|------------|
| B2M | 119 | -3.363 | 98.3% |
| LC | 137 | -3.379 | 97.7% |
| HC | 138 | -3.489 | 93.5% |

The table shows the amplicon size of the primers used for mAb-109 mRNA analysis. The efficiency of the primers was tested as an additional verification step, to ensure suitability of the primers for data analysis by the $\Delta\Delta C_t$ method. A 5 point standard curve was prepared by 1:10 serial dilutions of cDNA, this was used for qRT-PCR as described in Section 2.6.1.7. The table shows the slope and efficiency determined from the C_T values. An efficiency between 90-110% was determined acceptable, providing the efficiency of the primer sets were within 10% of each other.

Figure AE.2 Agarose gel electrophoresis of PCR products from gene copy number analysis primers



As described in Section 2.6.1.5 and Section 2.6.1.6, PCR and agarose gel electrophoresis was used to verify the specificity of the primers used for the qRT-PCR analysis of gene copy number. The figure shows the fragments amplified by the mAb-109 heavy chain primers (HC), mAb-109 light chain primers (LC), GS primer set 1 primers (GS 1) and the GS primer set 2 primers (GS 2). Both gDNA positive (gDNA+) and no template control (NTC) samples were amplified. The labelled HyperLadder 25bp molecular weight marker (L) is also shown to the left of the figure. The positive result for GS 2 NTC was determined to be a result of contamination; further tests were performed on this primer set to confirm specificity (not shown).

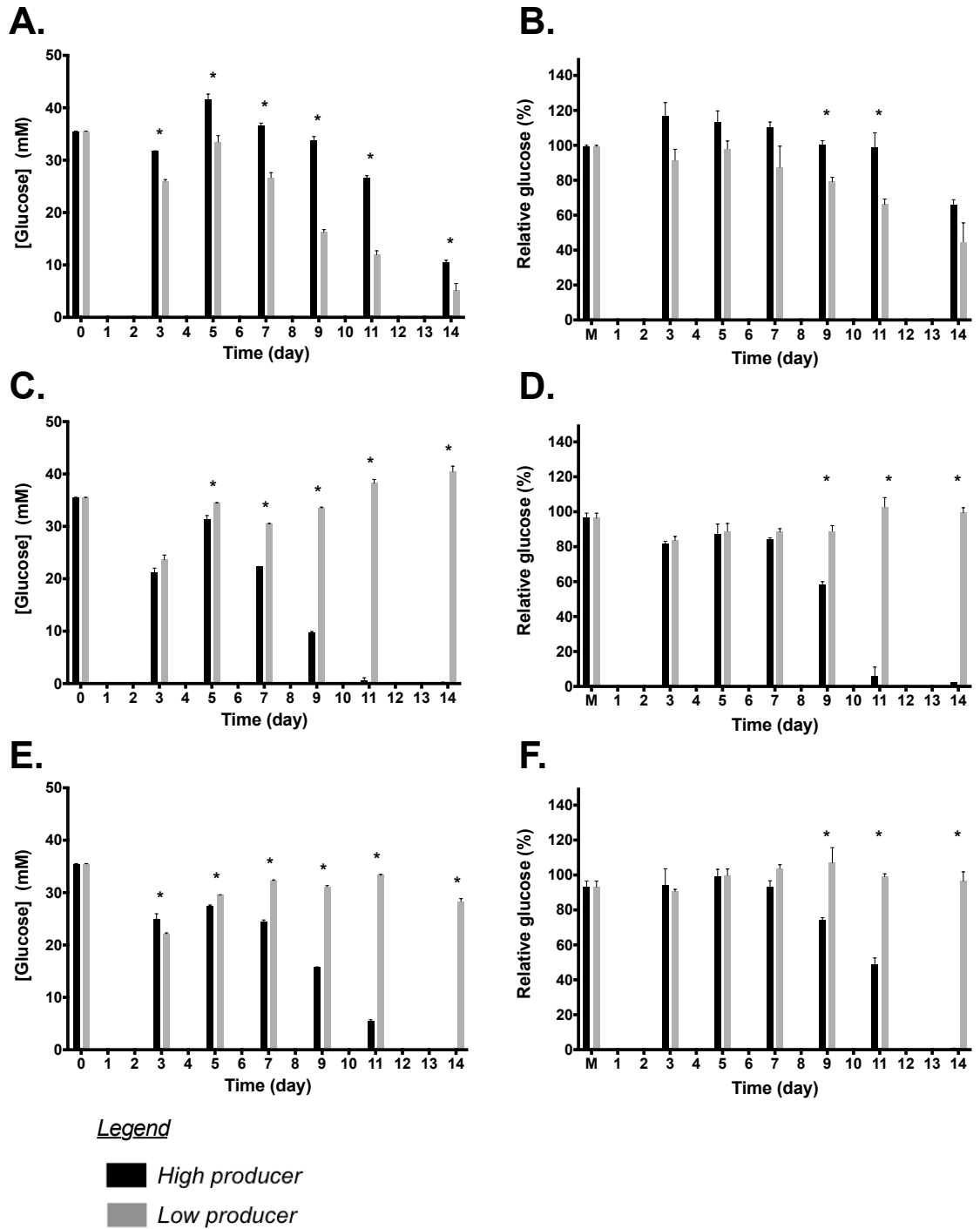
Table AE.2 Efficiency of PCR primers for qRT-PCR analysis of gene copy number

| Target gene | Amplicon size (base pairs) | Slope | Efficiency |
|--------------------|-----------------------------------|---------------|-------------------|
| HC | 168 | -3.386 | 97.4% |
| LC | 101 | -3.204 | 105.2% |
| GS 1 | 126 | -3.257 | 102.8% |
| GS 2 | 102 | -3.355 | 98.6% |

The table shows the amplicon size of the primers used for mAb-109 mRNA analysis. The efficiency of the primers was tested as an additional verification step, to ensure suitability of the primers for data analysis by the $\Delta\Delta C_t$ method. A 5-point standard curve was prepared by 1:10 serial dilutions of cDNA, this was used for qRT-PCR as described in Section 2.6.2.2. The table shows the slope and efficiency determined from the C_T values. Efficiency between 90-110% was determined acceptable, providing the efficiency of the primer sets were within 10% of each other.

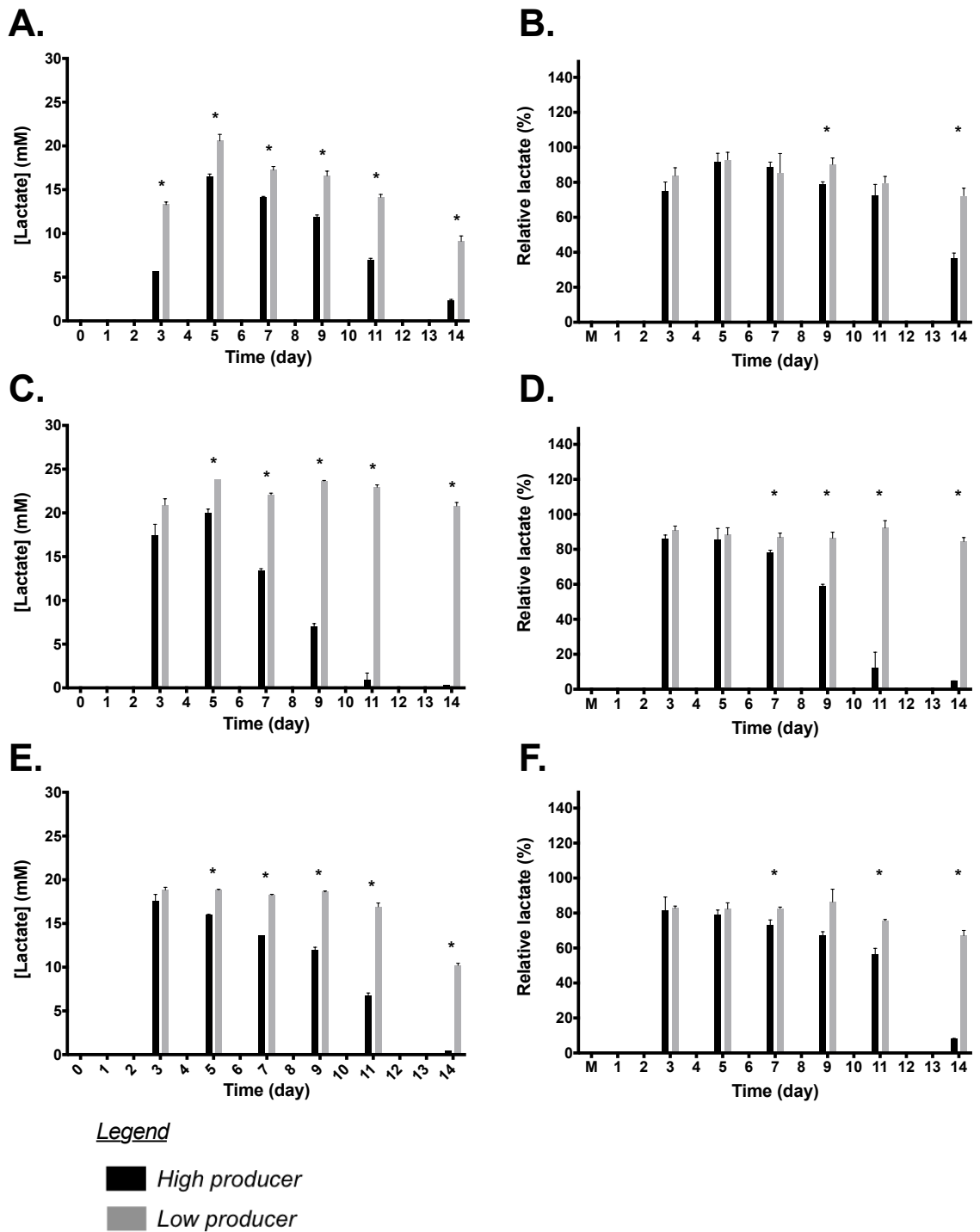
Appendix F – Comparison of enzymatic and GC-MS metabolite data

Figure AF.1 Comparison of enzymatic and GC-MS glucose data from high and low producing transfectants



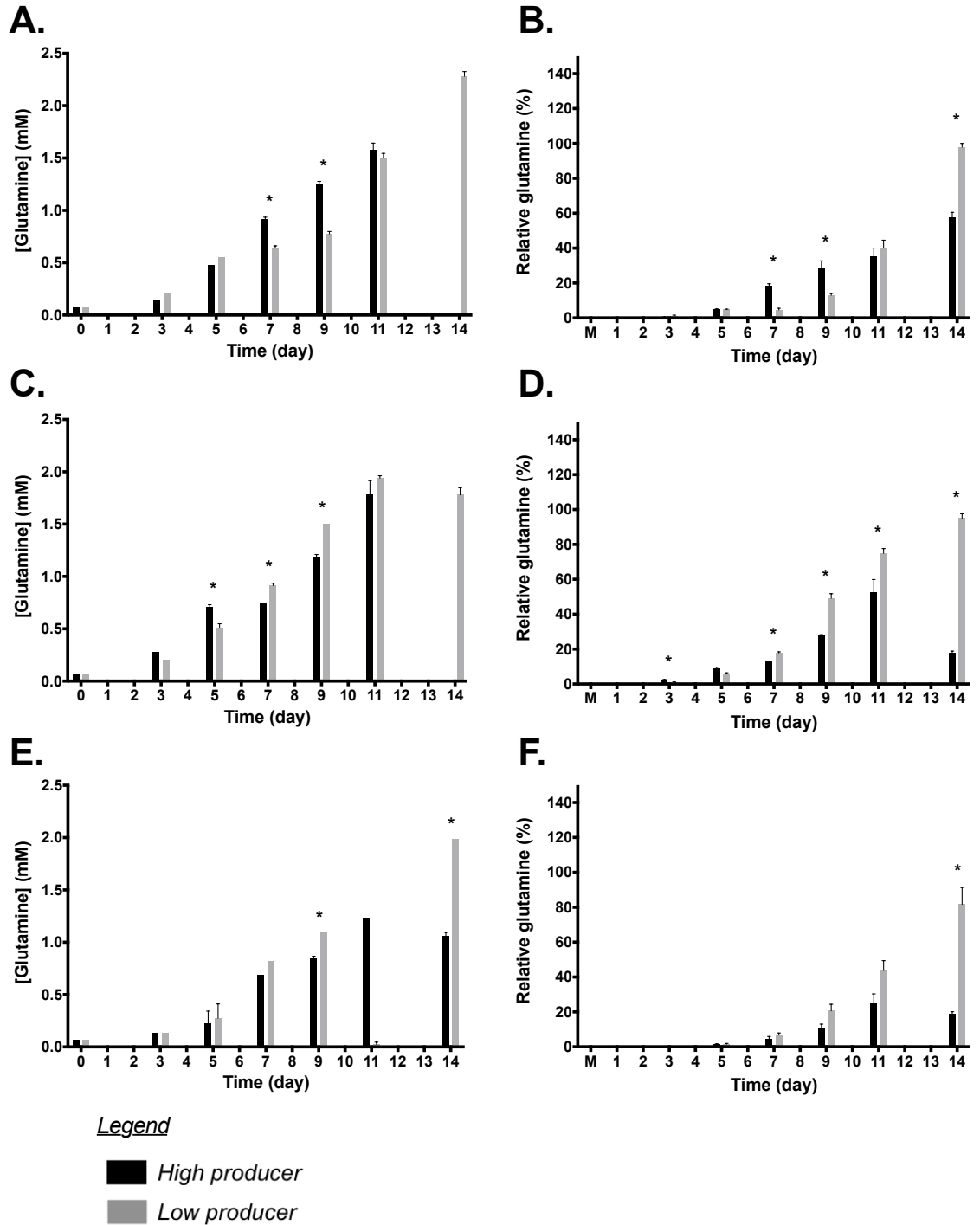
*High producing transfectants (15-2 (early and late generation) and 19-3 (early generation)) and low producing transfectants (15-4 (early and late generation) and 19-11 (early generation)) were grown in fed-batch culture as previously described (Figure legend 5.1). Medium (M) and cell culture supernatant samples were analysed enzymatically (Section 2.4.1) and by GC-MS (Section 2.4.2). The charts show the enzymatically determined glucose concentration of the early generation 15-2 and 15-4 (A). Late generation 15-2 and 15-4 (C). Early generation 19-3 and 19-11 (E). The relative glucose response (determined by GC-MS) of the early generation 15-2 and 15-4 (B). Late generation 15-2 and 15-4 (D). Early generation 19-3 and 19-11 (F). Error bars represent SEM for three biological replicates. * indicates $p < 0.05$, using independent samples t-test to compare the high producing transfectant to the low producing transfectant.*

Figure AF.2 Comparison of enzymatic and GC-MS lactate data from high and low producing transfectants



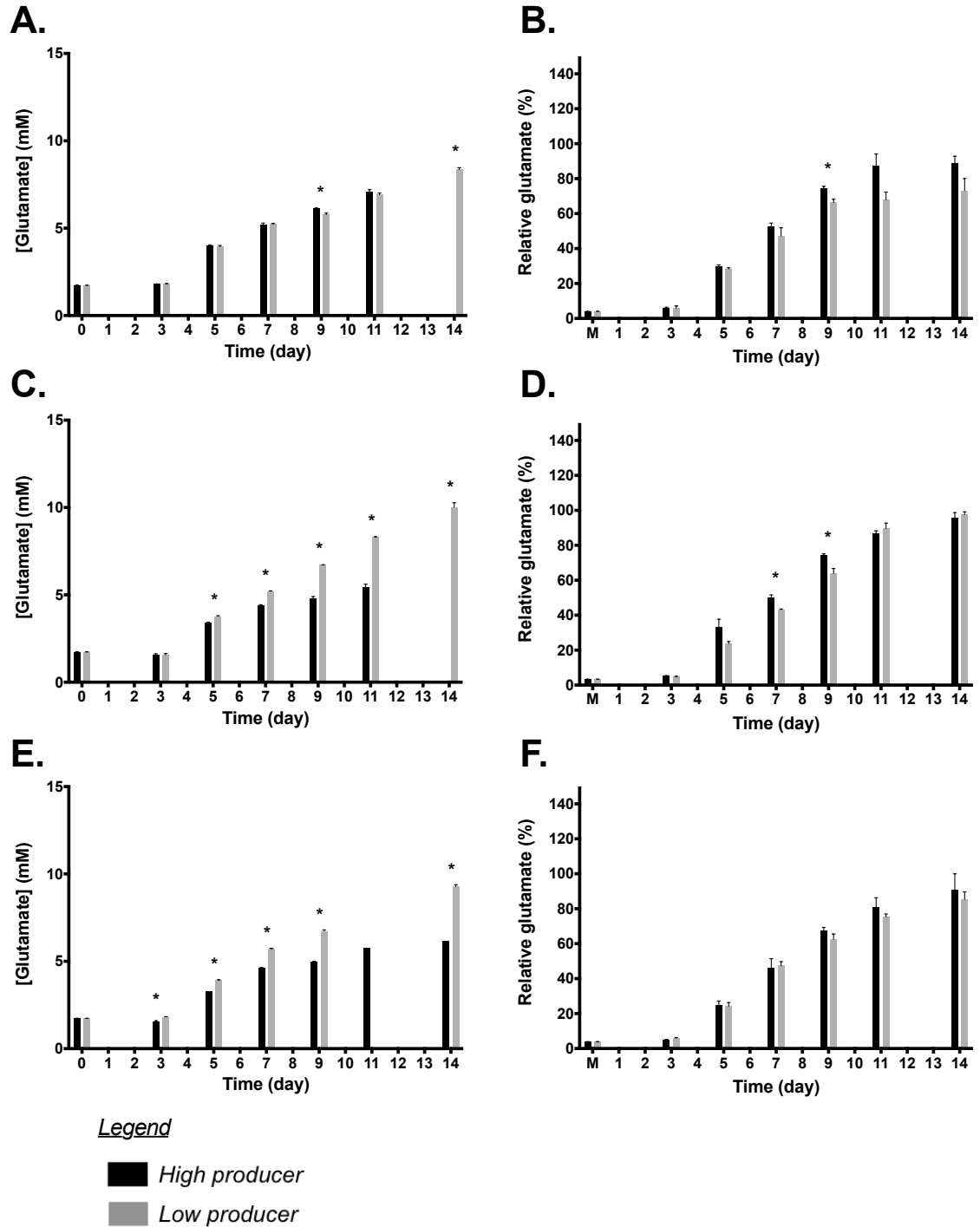
*High producing transfectants (15-2 (early and late generation) and 19-3 (early generation)) and low producing transfectants (15-4 (early and late generation) and 19-11 (early generation)) were grown in fed-batch culture as previously described (Figure legend 5.1). Medium (M) and cell culture supernatant samples were analysed enzymatically (Section 2.4.1) and by GC-MS (Section 2.4.2). The charts show the enzymatically determined lactate concentration of the early generation 15-2 and 15-4 (A). Late generation 15-2 and 15-4 (C). Early generation 19-3 and 19-11 (E). The relative lactate response (determined by GC-MS) of the early generation 15-2 and 15-4 (B). Late generation 15-2 and 15-4 (D). Early generation 19-3 and 19-11 (F). Error bars represent SEM for three biological replicates. * indicates $p < 0.05$, using independent samples t-test to compare the high producing transfectant to the low producing transfectant.*

Figure AF.3 Comparison of enzymatic and GC-MS glutamine data from high and low producing transfectants



*High producing transfectants (15-2 (early and late generation) and 19-3 (early generation)) and low producing transfectants (15-4 (early and late generation) and 19-11 (early generation)) were grown in fed-batch culture as previously described (Figure legend 5.1). Medium (M) and cell culture supernatant samples were analysed enzymatically (Section 2.4.1) and by GC-MS (Section 2.4.2). The charts show the enzymatically determined glutamine concentration of the early generation 15-2 and 15-4 (A). Late generation 15-2 and 15-4 (C). Early generation 19-3 and 19-11 (E). The relative glutamine response (determined by GC-MS) of the early generation 15-2 and 15-4 (B). Late generation 15-2 and 15-4 (D). Early generation 19-3 and 19-11 (F). Error bars represent SEM for three biological replicates. * indicates $p < 0.05$, using independent samples t-test to compare the high producing transfectant to the low producing transfectant.*

Figure AF.4 Comparison of enzymatic and GC-MS glutamate data from high and low producing transfectants



*High producing transfectants (15-2 (early and late generation) and 19-3 (early generation)) and low producing transfectants (15-4 (early and late generation) and 19-11 (early generation)) were grown in fed-batch culture as previously described (Figure legend 5.1). Medium (M) and cell culture supernatant samples were analysed enzymatically (Section 2.4.1) and by GC-MS (Section 2.4.2). The charts show the enzymatically determined glutamate concentration of the early generation 15-2 and 15-4 (A). Late generation 15-2 and 15-4 (C). Early generation 19-3 and 19-11 (E). The relative glutamate response (determined by GC-MS) of the early generation 15-2 and 15-4 (B). Late generation 15-2 and 15-4 (D). Early generation 19-3 and 19-11 (F). Error bars represent SEM for three biological replicates. * indicates $p < 0.05$, using independent samples t-test to compare the high producing transfectant to the low producing transfectant.*